
Design and manufacture of an electrochemical flow
reactor, and its application in organic
electrosynthesis



A Thesis Submitted to Cardiff University
in Fulfilment of the Requirements for the
Degree of Doctor of Philosophy
by **Ana Alicia Folgueiras Amador**

PhD Thesis November 2017

Cardiff University

DECLARATION

This work has not been submitted in substance for any other degree or award at this or any other university or place of learning, nor is being submitted concurrently in candidature for any degree or other award.

Signed (Ana Alicia Folgueiras Amador) Date

STATEMENT 1

This thesis is being submitted in partial fulfillment of the requirements for the degree of (insert MCh, MD, MPhil, PhD etc, as appropriate)

Signed (Ana Alicia Folgueiras Amador) Date

STATEMENT 2

This thesis is the result of my own independent work/investigation, except where otherwise stated, and the thesis has not been edited by a third party beyond what is permitted by Cardiff University's Policy on the Use of Third Party Editors by Research Degree Students. Other sources are acknowledged by explicit references. The views expressed are my own.

Signed (Ana Alicia Folgueiras Amador) Date

STATEMENT 3

I hereby give consent for my thesis, if accepted, to be available online in the University's Open Access repository and for inter-library loan, and for the title and summary to be made available to outside organisations.

Signed (Ana Alicia Folgueiras Amador) Date

STATEMENT 4: PREVIOUSLY APPROVED BAR ON ACCESS

I hereby give consent for my thesis, if accepted, to be available online in the University's Open Access repository and for inter-library loans **after expiry of a bar on access previously approved by the Academic Standards & Quality Committee.**

Signed (Ana Alicia Folgueiras Amador) Date

ACKNOWLEDGEMENTS

I am thankful to many people for their help and support over the duration of this research project. There are no words that can fully express how thankful I am for the time these persons dedicated to me. I will mention a few of the people who I feel deserve a specific mention for their positive impact on my research project and life during my studies.

First, I would like to thank Professor Thomas Wirth, my supervisor, for giving me the opportunity to join his research group and work on such an exciting project. I am grateful for his knowledge guidance during my studies, and also for the freedom he gave me to make my own decisions and mistakes; it has really helped me to learn and grow as a scientist over the last few years.

Next, I want to express my gratitude more specifically to the students who worked with me. Seb, Kai, Rosaria, Anaïs and Adam, thanks for all your hard work and contributions to my thesis! Everyone than has been part of the Wirth research group, attended the group meetings and shared the office needs to be thanked for their suggestions, advice, support and company. Pushpak, Mike, Nida, Baker, Rich, Matt, Rhodri, Simon, Florence, Ravi, Anaïs, Anne, Céline, Daniel, James S., James M., Adam, Jon, Seb, Kai, Rosaria, Agatha, Alex, Svenja, Tomohiro, Wilke, Xiaoping, Yuri, Micol, Tobi, Filipa, Jihan, Haifa, Mekhman, Ziyue, Mohamed, Marina, Tom, Rossana, Adele, Alena, Saira, Guilherme, Frauke, Nasser, Wenchao, Xiang-Yang, Abdul, Niklas, Taifur, Jarno, Paulina, Chrissi, Joey and James, it's been a pleasure.

My special gratitude to Flo, Baker, Rich, Chrissi and Mohamed for proof-reading parts of my thesis. Special thanks to Mohamed for being a great support during the last year of my PhD, mil gracias.

I would like to acknowledge all the workshop staff, who were of great help in manufacturing the reactor. Alan, Steve, Lee and Julian, thanks a lot. I would also like to thank all the technical and non-technical staff at the school of chemistry, specially to Dr Rob Jenkins. My acknowledgements also have to be extended to Prof. Waldvogel and everyone in his group for welcoming me in their lab. I also need to say thank to Stefano for his help and guidance with the 3D printer, and to the staff at the EPSRC National Mass Spectrometry Service Centre for their excellent service providing spectrometric data.

Finally, I would like to thank all my family and friends in Cardiff and in Spain for their support, it would have never been the same without them. Special thanks to my parents Pepa y Joaquín, my sister Laura and my brother David, and the sweet Carlota, Álex, Álvaro and Nacho. Also to my friends, that I can consider my family, Luisa, Martina, Azahara and María (and very soon Leo). To María and Pablo, huge thanks for their invaluable support from the distance.

Ana Folgueiras

Dedicated to David, gracias por haber existido

LIST OF ABBREVIATIONS

°C	Degree Celsius
µL	Microlitre
Ac	Acetyl
AcOH	Acetic acid
A	Amperes
aq.	Aqueous
APCI	Atmospheric pressure chemical ionisation
Ar	Aryl
BPR	Back-pressure regulator
C	Concentration
Cat.	Catalytic
Conv.	Conversion
CV	Cyclic voltammetry
<i>d.r.</i>	Diastereomeric ratio
DBU	1,8-Diazabicycloundec-7-ene
DIB	(Diacetoxyiodo)benzene
DCE	1,2-Dichloroethane
DME	1,2-Dimethoxyethane
DMF	<i>N,N</i> -Dimethylformamide
DMP	Dess-Martin periodinane
DMSO	Dimethylsulfoxide
EDG	Electron donating group
<i>ee</i>	Enantiomeric excess
EI	Electron ionisation
eq.	Equivalent(s)
ESI	Electrospray ionisation
Et	Ethyl
EWG	Electron withdrawing group
F mol ⁻¹	Faraday per mole
FEP	Fluorinated ethylene propylene
g	Gram

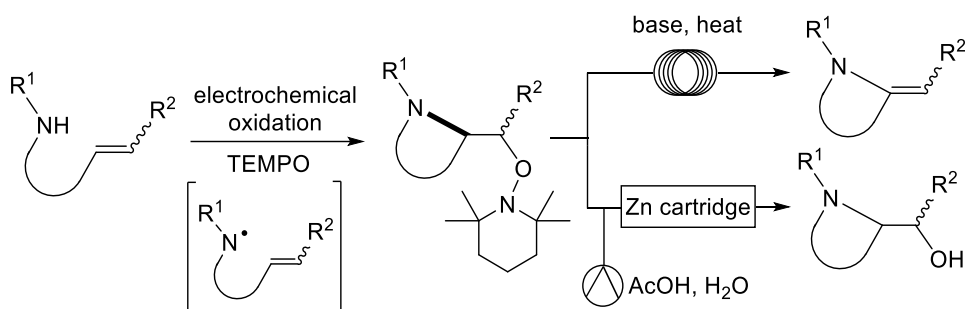
GP	General procedure
GC	Gas chromatography
h	Hour(s)
HFIP	1,1,1,3,3,3-Hexafluoro-2-propanol
HOMO	Highest occupied molecular orbital
HPLC	High pressure liquid chromatography
HRMS	High resolution mass spectroscopy
Hz	Hertz
<i>i</i> -Pr	Iso-Propyl
IR	Infrared
J	Coupling constant
L	Ligand
LDA	Lithium diisopropylamide
LUMO	Lowest unoccupied molecular orbital
M	Molarity [mol/l]
mA	milliamperes
m.p.	Melting point
m/z	Mass over charge ratio
<i>m</i> -CPBA	<i>m</i> -chloroperbenzoic acid
Me	Methyl
Mes	Mesityl
MHz	Megahertz
min	Minute(s)
mL	Millilitre
mmol	Millimole
mol%	Mole percentage
N	Normality
nm	nanometre
<i>n</i> -BuLi	<i>n</i> -butyllithium
NMR	Nuclear magnetic resonance
psi	Pounds per square inch
<i>p</i> -TsOH	<i>p</i> -Toluenesulfonic acid

PEEK	Polyether ether ketone
PTFE	Polytetrafluoroethylene
Rf	Retention factor (TLC)
rt	Room temperature
sat.	Saturated
<i>t</i> -Bu	tert-butyl
TEMPO	2,2,6,6-Tetramethylpiperidine 1-oxyl
Tf	Trifluoromethanesulfonate
TFA	Trifluoroacetic acid
TFE	2,2,2-Trifluoroethanol
TfOH	Trifluoromethanesulfonic acid
THF	Tetrahydrofuran
TLC	Thin layer chromatography
TMSOTf	Trimethylsilyl trifluoromethanesulfonate
r.t.	Residence time (Flow system)
Ts	<i>p</i> -toluenesulfonyl
<i>vs</i>	versus
V	Volts

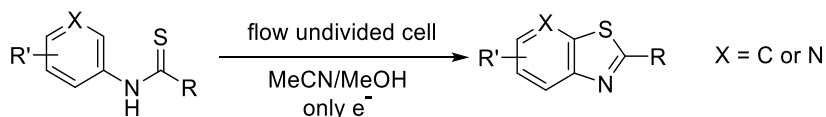
ABSTRACT

Organic electrochemistry is recognised as a green enabling methodology to perform reactions in an efficient and straightforward way. Electrons are used as the reagent to form anion and cation radical species from neutral organic molecules achieving oxidations and reductions by replacing toxic and dangerous reagents. Within this field, the use of microreactors in continuous flow is also concurrent with electrochemistry because of its convenient advantages over batch, such as: i) low loading or no supporting electrolyte at all, due to the small distance between electrodes, providing significant advantages in downstream processing; ii) high electrode surface-to-reactor volume ratio; iii) short residence time; iv) improved mixing effect.

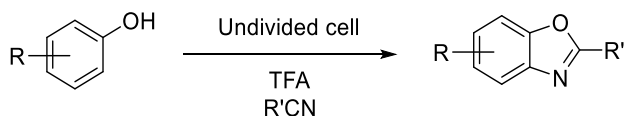
In this thesis, a novel easy-to-machine flow electrochemical reactor has been designed and fabricated. This reactor can be made either of aluminium or polymers, if additive manufacturing employed. The efficiency of the reactor has been shown in the electrochemical synthesis of nitrogen-containing heterocycles. The products obtained have been further functionalised in a single two-step flow system connected to the electrochemical reactor:



For the electrochemical synthesis of benzothiazoles from *N*-arylthioamides in flow a catalyst- and supporting electrolyte-free method has been developed. A library of benzothiazoles was synthesised only in the presence of solvent and electricity:



Finally, a new synthetic method for the electrochemical formation of benzoxazoles from easily accessible and inexpensive resorcinol and nitriles was discovered:



In conclusion, flow electrochemistry has shown to be a promising tool for electroorganic synthesis, improving the outcome of standard batch cells.

TABLE OF CONTENTS

CHAPTER 1: Introduction	1
1.1. Organic electrochemistry	4
1.1.1. General introduction.....	4
1.1.2. History of organic electrochemistry	5
1.1.3. Industrial applications of organic electrosynthesis.....	6
1.1.4. Fundamental aspects of organic electrosynthesis.....	8
1.1.5. Methods of electrolysis.....	11
1.1.5.1. Controlled potential electrosynthesis	11
1.1.5.2. Controlled current electrosynthesis.....	12
1.1.5.3. Direct and indirect electrolysis.....	13
1.1.6. Types of cells.....	15
1.1.6.1. Batch cells	15
1.1.6.2. Flow through cells.....	17
1.1.7. Electrode materials	17
1.1.7.1. Anode materials	18
1.1.7.2. Cathode materials.....	18
1.1.7.3. Reference electrodes	19
1.1.7.4. Other types of electrodes.....	19
1.1.8. Solvents	20
1.1.9. Supporting electrolytes.....	21
1.2. Organic electrochemistry in continuous flow	22
1.2.1. Fundamental aspects of flow electrochemistry	22
1.2.1.1. Principles of preparative flow electrosynthesis.....	23

1.2.2. Organic synthesis with electrochemical flow reactors	24
1.2.2.1. Divided cells.....	24
1.2.2.2. Undivided cells.....	26
1.2.2.3. Paired electrosynthesis	40
1.2.2.4. Indirect electrosynthesis.....	43
1.3. References	45
CHAPTER 2: Flow electrochemical reactor design and manufacture.....	51
2.1. Introduction	53
2.1.1. Flow electrochemical cells.....	53
2.1.2. Stereolithography (SLA) printers	63
2.2. Reactor design.....	64
2.2.1. Aluminium electrochemical reactor.....	68
2.2.2. 3D printed flow electrochemical reactor	69
2.3. Conclusions	71
2.4. References	72
CHAPTER 3: Electrosynthesis of nitrogen-containing heterocycles in flow	74
3.1. Introduction	77
3.1.1. Nitrogen-centred radicals.....	77
3.1.2. Different methods for the synthesis of isoindolinones	79
3.2. Electrochemical addition of nitrogen-centred radicals to double bonds.....	81
3.2.1. Electrode screening.....	81
3.2.2. Solvent screening.....	85
3.2.3. Base screening	86
3.3. Isoindolinone derivatives synthesis.....	90

3.3.1.	Synthesis of substrates	90
3.3.2.	Inline Mass Spectrometry analysis for optimisation of reaction conditions 94	
3.3.3.	Base effect study for amides as substrates	97
3.3.4.	Effect of different spacers	100
3.3.5.	Scope of the reaction	101
3.3.6.	Tandem cyclisation attempt	107
3.3.7.	Proposed mechanism	109
3.4.	Two-step flow approach: Electrochemical cyclisation and elimination of TEMPO to form alkenes	113
3.5.	Two-step flow approach: Electrochemical cyclisation and N–O bond reductive cleavage to form alcohols	116
3.6.	Two-step flow approach: Synthesis of carbamates in flow and subsequent electrochemical cyclisation	118
3.7.	Conclusions	123
3.8.	References	124
CHAPTER 4: Electrosynthesis of benzothiazoles from <i>N</i>-arylthioamides		126
4.1.	Introduction	128
4.1.1.	C–H and X–H cross-coupling reactions	128
4.1.2.	Different methods for the synthesis of benzothiazoles from <i>N</i> -arylthioamides	128
4.2.	Synthesis of substrates	132
4.3.	Flow electrochemical synthesis of benzothiazoles	136
4.3.1.	Optimisation of the reaction conditions	136
4.3.2.	Scope of substrates	138

4.3.3.	Gram-scale reaction	141
4.3.4.	Proposed mechanism	141
4.4.	Conclusions	143
4.5.	References	144
CHAPTER 5: Electrochemical synthesis of benzoxazoles		146
5.1.	Introduction	148
5.1.1.	Typical methods for the synthesis of benzoxazoles.....	148
5.1.2.	Electrochemical methods for the synthesis of benzoxazoles.....	151
5.2.	Trifluoromethylation of resorcinol.....	153
5.3.	Electrochemical synthesis of benzoxazoles from phenol derivatives and nitriles 155	
5.3.1.	Acid screening	156
5.3.2.	Electrode screening.....	156
5.3.3.	Other conditions screening	157
5.3.4.	Scope of substrates.....	159
5.3.5.	Proposed mechanism	161
5.4.	Conclusions and outlook	162
5.5.	References	163
CHAPTER 6: Experimental Part.....		165
6.1.	General methods.....	167
6.2.	Experimental data for Chapter 2: Flow electrochemical reactor design	169
6.2.1.	Reactor design.....	169
6.2.2.	Schematic representation of the aluminium reactor	171
6.2.3.	Schematic representation of the 3D-printed Río reactor	173

6.3. Experimental data for Chapter 3: Electrochemical synthesis of isoindolinones and its functionalisation in flow.....	175
6.3.1. Cyclic voltammetry.....	175
6.3.2. Synthesis of substrates.....	177
6.3.3. Electrochemical synthesis of isoindolinones.....	196
6.3.4. Elimination products.....	210
6.3.5. Reduction products.....	214
6.4. Experimental data for Chapter 4: Electrochemical synthesis of Benzothiazoles from <i>N</i> -arylthioamides in flow.....	218
6.4.1. Cyclovoltammetric measurements.....	218
6.4.2. Synthesis of substrates.....	219
6.4.3. Electrochemical synthesis of benzothiazoles.....	224
6.5. Experimental data for Chapter 5: Electrochemical synthesis of benzoxazoles in flow from resorcinol and nitriles.....	231
6.6. References.....	233

CHAPTER 1: Introduction

CHAPTER 1: Introduction	1
1.1. Organic electrochemistry	4
1.1.1. General introduction	4
1.1.2. History of organic electrochemistry	5
1.1.3. Industrial applications of organic electrosynthesis.....	6
1.1.4. Fundamental aspects or organic electrosynthesis.....	8
1.1.5. Methods of electrolysis.....	11
1.1.5.1. Controlled potential electrosynthesis	11
1.1.5.2. Controlled current electrosynthesis.....	12
1.1.5.3. Direct and indirect electrolysis.....	13
1.1.6. Types of cells.....	15
1.1.6.1. Batch cells	15
1.1.6.2. Flow through cells.....	17
1.1.7. Electrode materials	17
1.1.7.1. Anode materials	18
1.1.7.2. Cathode materials.....	18
1.1.7.3. Reference electrodes	19
1.1.7.4. Other types of electrodes.....	19
1.1.8. Solvents	20
1.1.9. Supporting electrolytes.....	21
1.2. Organic electrochemistry in continuous flow	22
1.2.1. Fundamental aspects of flow electrochemistry	22
1.2.1.1. Principles of preparative flow electrosynthesis.....	23

1.2.2. Organic synthesis with electrochemical flow reactors	24
1.2.2.1. Divided cells.....	24
1.2.2.2. Undivided cells.....	26
1.2.2.3. Paired electrosynthesis	40
1.2.2.4. Indirect electrosynthesis.....	43
1.3. References	45

1.1. Organic electrochemistry

1.1.1. General introduction

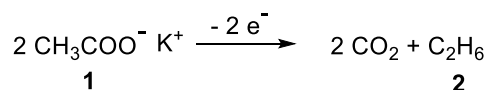
Organic electrosynthesis is recognised as a methodology to perform oxidations and reductions of compounds in an environmentally friendly process, as toxic and/or dangerous oxidants and reductants are replaced by electricity.^[1-3] Unstable and hazardous reagents can be produced *in situ* and directly reacted.^[4,5] Therefore, organic electrosynthesis can be considered as a versatile method, with a big number of applications on the laboratory scale,^[6-12] and also several applications in industry.^[13,14] This methodology has some clear advantages to alternative methods,^[1] such as reaction selectivity, which can be controlled by the nature of the electrode, the potential applied at the working electrode, or the composition of the electrolyte used. The degree of transformation of a molecule can also be controlled, as in classical organic chemistry, by regulating the consumption of electrons. In general, the reaction conditions for an electrochemical transformation are described as mild, since they are usually performed at atmospheric pressure and ambient temperature. However, electrosynthesis also has some drawbacks. As the reaction only proceeds at the electrode surface, the area for electron transfer is limited. The scale-up can also be problematic, since handling of a large cell can be more challenging and create problems of overheating due to the increased electricity demand. In addition, supporting electrolytes are typically required to transport the charge through the solution, making the process less cost-efficient and more time-consuming, as the supporting electrolyte will have to be removed from the product.

Some limitations of conventional electrosynthesis^[15] can be overcome by the use of electrochemical flow cells,^[6,16] which typically have a small gap separating the electrodes. Therefore, lower concentrations of supporting electrolytes are possible, or even devoid of external supporting electrolyte entirely. A number of microfluidic electrochemical cells have been developed and their performance has been studied.^[17-22]

In this thesis, the design and manufacture of a new flow electrochemical reactor and its application in different organic transformations is presented.

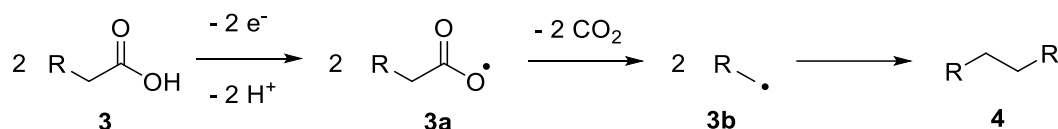
1.1.2. History of organic electrochemistry

Electrochemistry is known as early as the year 1800 when Alessandro Volta invented the first electric battery using zinc and copper electrodes, which is considered the first electrochemical cell.^[23] In this same year William Nicholson and Anthony Carlisle discovered the electrolysis as a chemical reaction, after observing the decomposition of water into hydrogen and oxygen.^[24] However, the first experiments of organic electrosynthesis date back to the middle of 19th century, when Faraday reported the generation of carbon dioxide and a hydrocarbon (ethane, **2**) after performing the electrolysis of potassium acetate (**1**, Scheme 1.1).^[25,26]



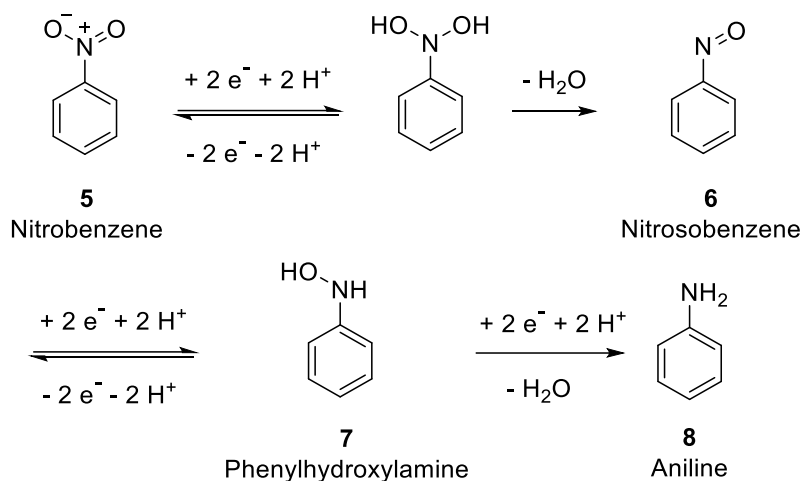
Scheme 1.1: First electroorganic synthesis by Faraday.

In 1848 Kolbe studied the reaction above in more detail. He investigated and established the synthesis of dimeric alkanes (**4**) by anodic oxidation of fatty acids and organic carboxylic acids (**3**), which undergo decarboxylation to give alkyl radicals (**3b**) that then dimerise. C–C bond formation is therefore achieved in a relatively easy way (Scheme 1.2).^[27] This is probably the best known electroorganic reaction which also bears Kolbe's name.



Scheme 1.2: Kolbe Electrolysis reaction.

In 1898 Haber reduced nitrobenzene (**5**) to form nitrosobenzene (**6**), phenylhydroxylamine (**7**) and aniline (**8**), which were all subsequently isolated. He studied how the use of different potential values could lead to different product compositions, and concluded that the selectivity towards the product obtained depends on the potential applied to the working electrode (Scheme 1.3).^[28]



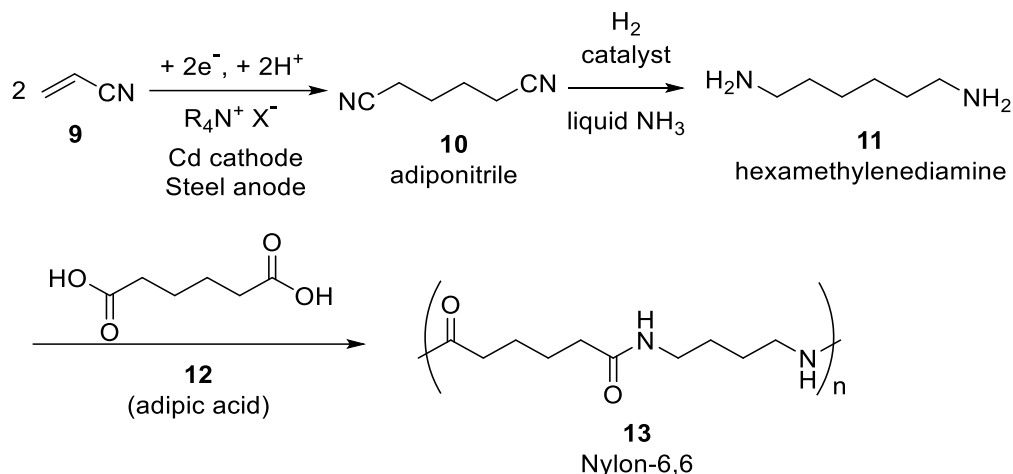
Scheme 1.3: Haber's cathodic reduction of nitrobenzene.

1.1.3. Industrial applications of organic electrosynthesis

There are three large scale electroorganic industrial processes that stand out:

- The “Monsanto” process for the production of adiponitrile:

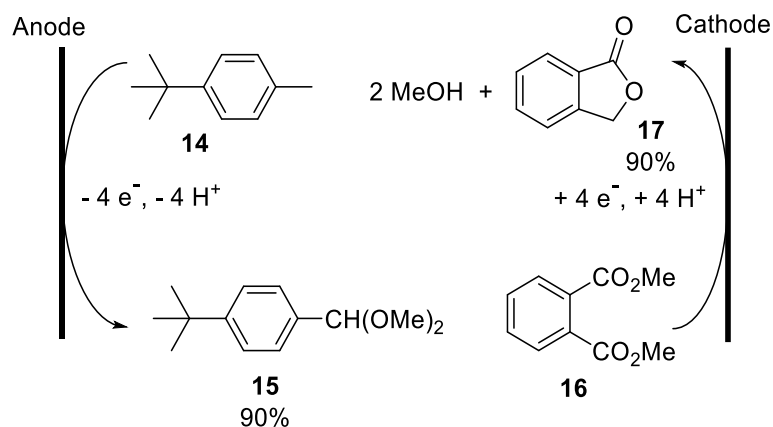
Hydrodimerisation of acrylonitrile (**9**) to form adiponitrile (**10**) was discovered by Baizer in 1960,^[29] and it is nowadays used to produce over 300 000 tons p.a. It consists of a paired electrosynthesis process employing a two-phase reaction mixture in an undivided cell, which was discovered to give higher current efficiency than the divided cell.^[30] The use of a quaternary ammonium salt is essential for the reaction selectivity (> 90% yield of the desired product), and it is important that the cation is not reduced at the cathode so that the solubility of adiponitrile in the solution is enhanced by the salt.^[31] This process is almost exclusively used to produce hexamethylenediamine (**11**), the precursor for nylon 6-6 (**13**), which is formed after the reduction of adiponitrile with hydrogen, a metal catalyst and liquid ammonia (pressurised system) (Scheme 1.4).



Scheme 1.4: The "Monsanto" process: Electrosynthesis of adiponitrile and production of Nylon-6,6.

- BASF paired electrosynthesis of phthalide and 4-(*t*-butyl)benzaldehyde dimethylacetal:

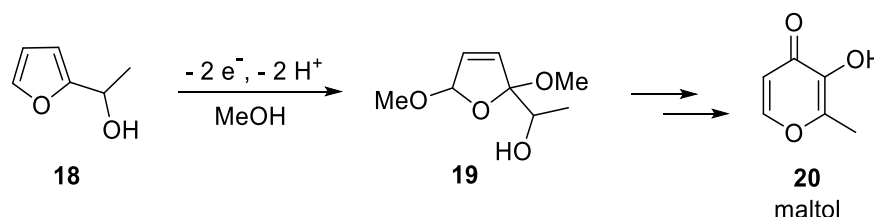
In 1999 BASF introduced a commercial paired electrosynthesis for the simultaneous synthesis of phthalide (**17**) and 4-(*t*-butyl)benzaldehyde (**15**). Starting from methyl phthalate (**16**) and 4-(*t*-butyl)toluene (**14**), the former is reduced at the cathode producing phthalide, and the latter is oxidised at the anode producing 4-(*t*-butyl)benzaldehyde, both in 90% yield. The process is carried out in an undivided cell and methanol is used as both solvent and reagent. Protons are simultaneously generated at the anode and consumed at the cathode, as a result hydrogen gas is not formed during the reaction, increasing the process safety. This process is used to produce 1000 tons per year (Scheme 1.5).^[32]



Scheme 1.5: BASF paired electrosynthesis of phthalide and 4-(*t*-butyl)benzaldehyde.

- Methoxylation process (Otsuka, Japan):

A commercial methoxylation process for the methoxylation of 1-(furan-2-yl)ethan-1-ol (**18**) was established by Otsuka in Japan. The methoxylated product obtained (**19**) is produced in approximately 150 tons per year and it is a precursor for the production of the food additive maltol (**20**). The process is conducted using a carbon cylinder anode and steel pipe cathode (Scheme 1.6).^[32]



Scheme 1.6: Methoxylation process (Otsuka).

1.1.4. Fundamental aspects of organic electrosynthesis

In the course of an electrochemical reaction, the molecules are activated by the addition or removal of electrons. In a simplistic electrolysis cell, a solid anode (positive) and cathode (negative) are introduced into a solution containing the substrate and a supporting electrolyte, in order to carry the current through the cell (Figure 1.1). The electrical current, measured in amperes, passes through the solution from the cathode to the anode to complete the circuit. The substrate can either be oxidised at the anode (losing electrons), or reduced at the cathode (gaining electrons). This process takes place at the surface of the electrode, making it a heterogeneous process (Figure 1.1). The electrode where the desired reaction takes place is known as the “working” electrode, while the other is referred to as the “counter” or “auxiliary” electrode.^[9,33] The electrically charged species are known as radicals.

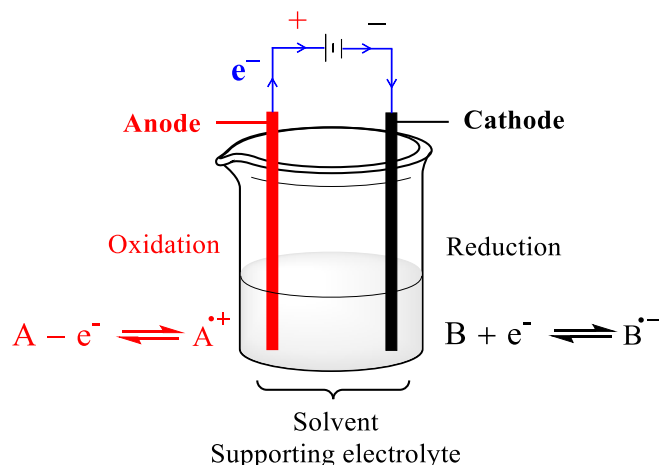
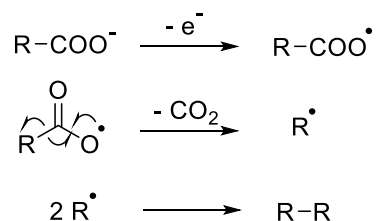


Figure 1.1: Electrolysis cell.

Both anodic oxidations and cathodic reductions are reversible processes until a chemical reaction occurs from the radicals that have been formed electrochemically, giving place to a more stable compound. Using the Kolbe reaction as an example, the first step is the electrochemical formation of a carboxyl radical. This intermediate quickly decarboxylates to generate an alkyl radical, which dimerises with another alkyl radical to complete the synthesis (Scheme 1.7).



Scheme 1.7: Kolbe electrolysis mechanism.

The formation of an electrosynthesis product **P** from substrate **S** *via* intermediate **I** is illustrated in Figure 1.2 showing each elementary reaction step.^[33]

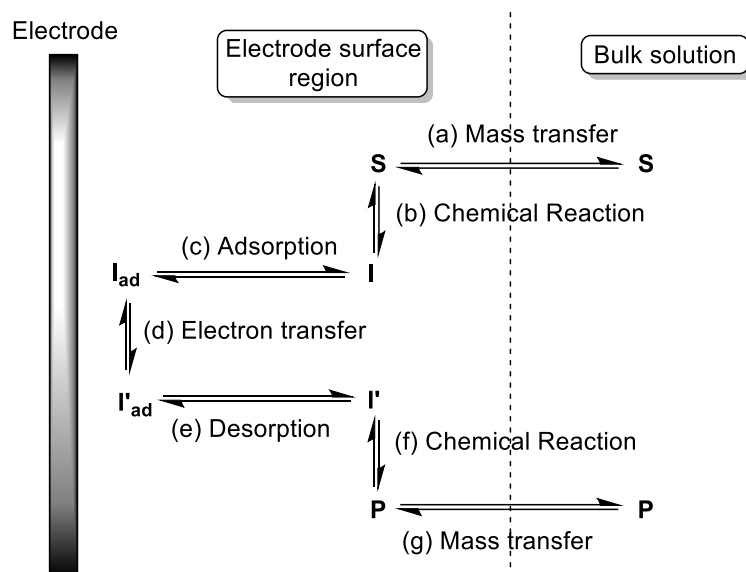


Figure 1.2: Elementary reaction steps of electrode reactions.

- Step (a): mass transport of **S** from the bulk to the electrode surface. This mass transport can take place by diffusion, migration or convection.
- Step (b): chemical reactions such as deprotonation or dissociation of **S** may take place to generate intermediate **I**, although these reactions do not always happen.
- Step (c): adsorption of **I** on the electrode surface to form the intermediate **I_{ad}**.
- Step (d): electron transfer between the electrode and **I_{ad}** forms the oxidised/reduced intermediate **I'_{ad}**.
- Step (e): desorption of **I'_{ad}**.
- Step (f): Possible chemical reaction to form product **P**.
- Step (g): Diffusion of the product from the electrode surface region to the bulk solution.

The order of steps (e) and (f) may be inverted, the chemical reaction may take place on the electrode surface region, and then desorption occurs.

In terms of molecular orbitals, a reduction is described as the transfer of an electron from the cathode to the lowest unoccupied molecular orbital (LUMO) of the substrate. An oxidation process is the transfer of an electron from the highest occupied molecular orbital (HOMO) of the substrate to the anode (Figure 1.3).^[6,33]

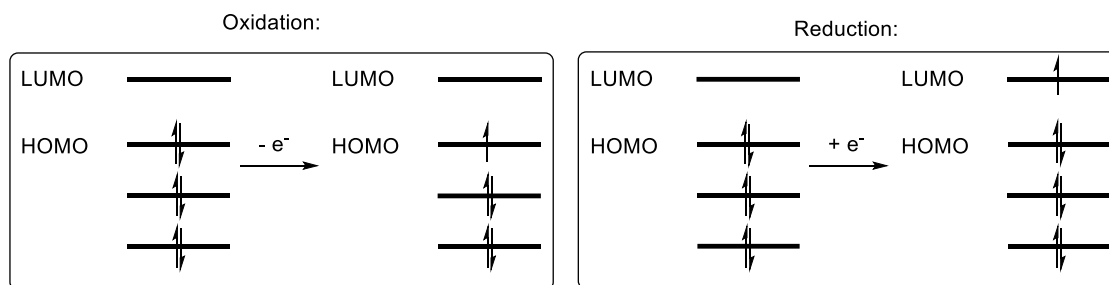


Figure 1.3: Molecular-orbital diagram for oxidation/reduction electron transfer.

1.1.5. Methods of electrolysis

In electrochemistry, the amount of electricity that is used in a reaction can be controlled in two different modes: using either constant current or constant potential.

1.1.5.1. Controlled potential electrosynthesis

Constant potential electrolysis was first introduced by Haber in 1898, when he selectively reduced nitrobenzene stepwise to phenylhydroxylamine or aniline, by controlling the potential applied to the electrolytic cell. This example was explained in Section 1.1.2 of this chapter.

Constant potential electrosynthesis is less prevalent than constant current electrolysis. However, with the constant potential higher selectivity or mechanistic information can be obtained. When carrying out a constant potential electrolysis, the oxidation or reduction potential of the substrate of interest should be known in advance, therefore it must be measured before executing the reaction.^[33] This way the reactivity can be controlled, for instance, if a substrate once oxidised or reduced, can be subject to further oxidation or reduction, one can control whether this second transformation will occur or not just by controlling the potential applied. The same principle can be applied to molecules containing two or more functional groups subject to react, setting the potential accurately can control the desired reaction.

Constant potential electrolysis requires a third electrode, which is known as reference electrode. In this three-electrode configuration, the current is passed through the working and counter electrodes, while the potential is measured with respect to the reference electrode, which is currentless (Figure 1.4).^[13,33,34] In some cases, this reference electrode can be omitted.

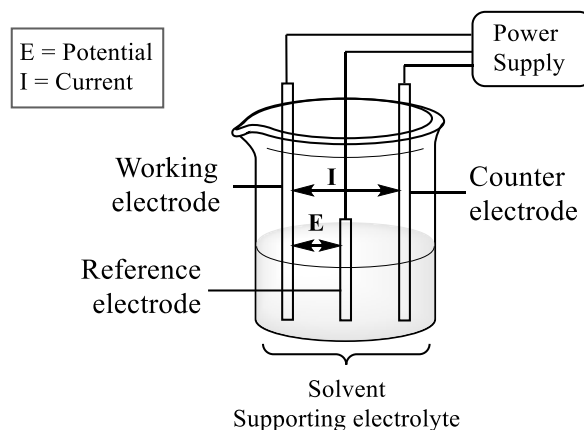


Figure 1.4: Schematic experimental set-up of a three-electrode cell for constant potential electrolysis.

This constant potential technique has some disadvantages, such as a slow rate of the reaction. The current of the reaction will depend on the concentration of the substrate. Therefore, as the substrate is consumed, the current will decrease becoming very low, and this will slow down the reaction.^[13]

1.1.5.2. Controlled current electrosynthesis

In controlled current electrosynthesis, the current is kept constant and the voltage will vary in order to keep this current at the desired constant value. This technique is more commonly used, since the electrolytic system and instruments are simpler than compared to controlled potential electrolysis, as there is no feedback from the reference electrode to the power supply. A schematic representation is shown in Figure 1.1.

Within this sort of set-up the product selectivity can sometimes be controlled by regulating the current density (amperes per square decimetre) and the amount of electricity passed through the cell. The concentration of the substrate must also be considered when choosing the current density applied. A low concentration of the starting substrate will need low current density and *vice versa*.^[33] The theoretical amount of electricity needed in a reaction can be calculated by Faraday's law:

$$Q_{\text{theory}} = z \cdot N \cdot F$$

Where Q_{theory} is measured in coulombs (C, 1 C = 1 A·s), z is the number of electrons involved in the reaction, N is the number of moles of the compound being transformed,

and F is the Faraday's constant ($96\,485\text{ C mol}^{-1}$). When this calculated electricity (Q) is divided by the applied current (A), the time of reaction can be calculated.

This theoretical amount of electricity is not enough during actual experiments; therefore a higher amount of charge is needed in order to complete the reaction of interest. The current efficiency can be easily calculated, a parameter that is highly important in industrial processes:^[35]

$$\text{Current efficiency} = X \cdot Q_{\text{theory}} / Q$$

Where X is the yield of the transformation, Q_{theory} is the calculated amount of charge, and Q is the real charge passed through the cell.

1.1.5.3. Direct and indirect electrolysis

The electrochemical transformation can be done as direct or indirect electrolysis. The former involves an electron transfer to the substrate from the electrode, and this occurs at the surface of the electrode. In an indirect electrolysis, a homogeneous redox reaction of the substrate occurs in the solution in the presence of a mediator, instead of the heterogeneous electron transfer between the electrode and the substrate. This mediator is an electrochemically activated species that will be part of a reversible redox couple starting at the electrode and then performing the reaction of interest (Figure 1.5).^[36]

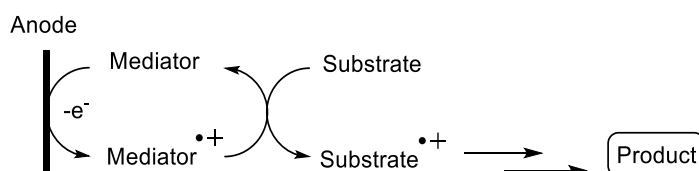


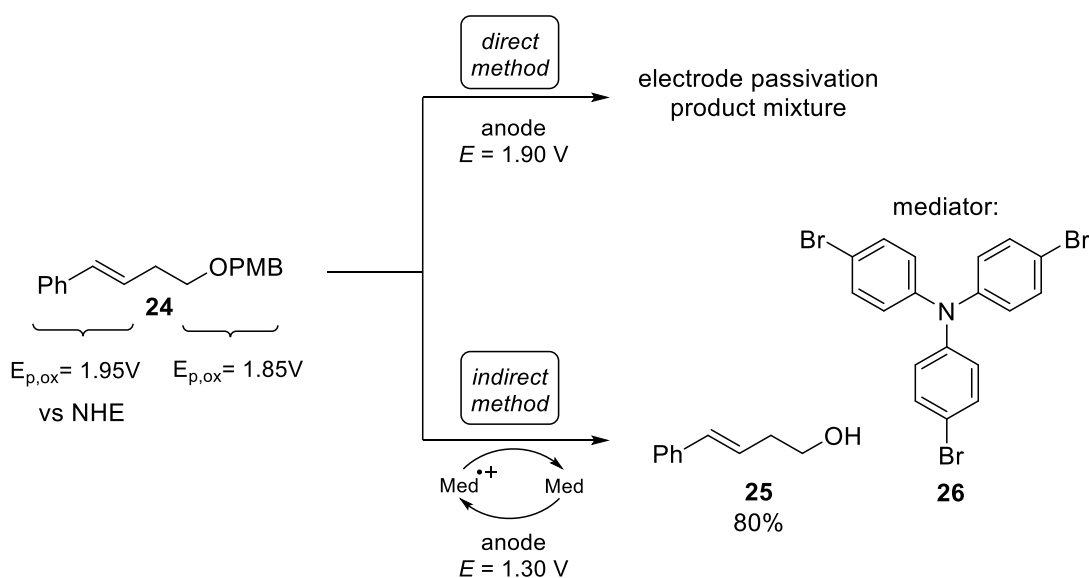
Figure 1.5: Indirect electrolysis.

Indirect electrolysis can also be performed using two different types of cells: in-cell and ex-cell. When the electrolysis is done in the presence of the substrate and the mediator, it is called in-cell. In this case, the redox potential of the mediator must be lower than that of the substrate, and it can be used in catalytic amounts. This use of lower potentials would permit the reaction to be carried out under milder conditions, and the formation of side products can be avoided. This can be very beneficial when other functional groups are present in the molecule and they want to be preserved. When the electrolysis is carried out only for the regeneration of the mediator, it is called ex-cell. This technique is

employed when the redox potential of the substrate is lower than that of the mediator, and a quantitative amount or excess of the mediator should be used.^[33]

There are many types of mediators available, and their redox potentials can be modified by tuning the molecular design, according to the need of the desired transformation.^[33] Furthermore, asymmetric synthesis can be achieved electrochemically by the use of some mediators with chiral nature.^[37,38]

The use of mediators can induce higher or totally different selectivity in the reaction. A common problem in electrosynthesis is the passivation of the electrodes, which can occur when a compound is produced and accumulated at the surface of the electrode. This accumulation can partially or totally block the electrode surface. When passivation of the electrode occurs due to direct electrochemical conversion on the surface of the electrode, the use of a mediator can negate this problem, since there is no direct interaction of the substrate with the surface of the electrode. An example is shown in Scheme 1.8,^[39] where deprotection of *p*-methoxybenzyl ether (PMB) is carried out by anodic oxidation. When the reaction is performed by direct electrolysis, passivation occurs and a mixture of products is observed, while using indirect electrolysis gives the desired product (**25**) in good selectivity and without passivation of the electrode.^[40]



Scheme 1.8: Indirect electrolysis for selective deprotection of PMB ethers.

Another example will be shown in Section 1.2.2.4, where electrochemical transformations carried out in flow cells are discussed.

1.1.6. Types of cells

When performing an electrochemical reaction, there are several cells available. Each of them will offer different advantages depending on the type of transformation to be carried out.

1.1.6.1. Batch cells

In batch cells, the reactor contains a solution of the substrates and reagents and it is operating for the time needed to complete the desired reaction until all the starting material is consumed. Ideally, the reaction mixture is stirred to have a homogeneous concentration throughout the cell.

1.1.6.1.1. Undivided cells

The simplest type of cell consists in an undivided cell, which is a container with a solution of the substrate and two electrodes (working and counter electrode) connected to the power supply (Figure 1.6). The vessel is usually constructed from some rigid inert material, such as glass or PTFE, although in some cases the inner wall of the container can be made of some conducting material that is used as one of the electrodes. The distance between the working and the counter electrode must be maintained as short as possible in order to reduce the ohmic resistance of the cell. Several electrodes can be set in parallel if a larger electrode surface is needed.

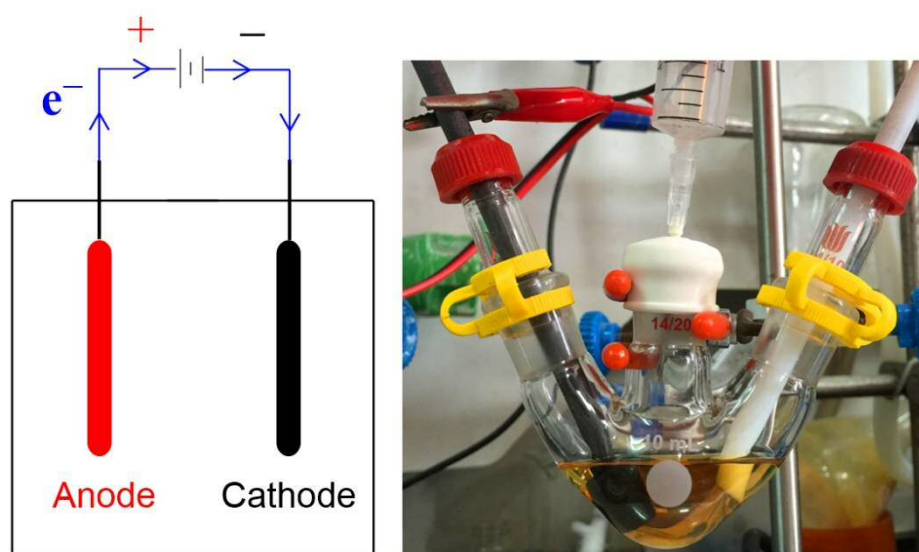


Figure 1.6: A simple undivided cell.

An undivided cell can be used when the substrate and product formed cannot react at the counter electrode, or with the products produced as a counter reaction. These cells can be heated up or cooled down according to the requirements of the reaction.^[9,13,34]

1.1.6.1.2. Divided cells

In some cases, it is not possible to avoid undesired reactions at the counter electrode, being necessary to separate the anolyte and catholyte. The anolyte is the part of electrolyte to be oxidised on the anode side of the cell, and the catholyte is the electrolyte present in the cathodic side of the cell to be reduced. This separation of anolyte and catholyte can be achieved by using divided cells. They consist of two parts separated by a membrane or diaphragm, where only ions can diffuse from one to the other chamber (Figure 1.7). This set-up makes their initial and maintenance cost higher, since the separator should have some thermal, chemical, mechanical and dimensional stability.^[13,34]

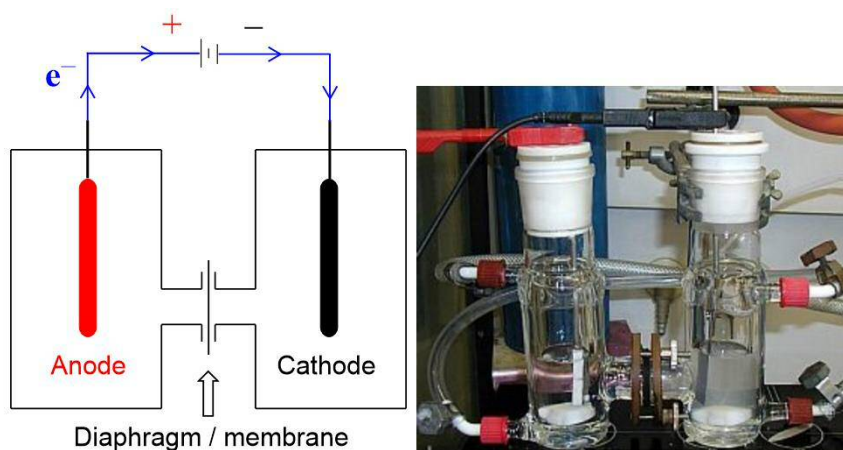


Figure 1.7: A divided cell.

There are mainly two different types of cell separators:^[13,34]

- “Ion exchange membranes”, where cations or anions are transported selectively. The most common one is the cation-exchange membrane (H^+ form). In some cases, the ion exchange membrane acts as both separator and as electrolyte.
- Porous separators, where the ion transport is not selective. They are normally used when ion exchange membranes are not suitable to use, such as aprotic media. The most common porous materials are sintered glass and ceramic refractories. They can vary in shape, size and porosity as needed. A drawback is related to the wall

thickness of the material, since thicker separators are essential to have an acceptable mechanical strength, but that will add more resistance to the system.

1.1.6.2. Flow through cells

Continuous processes are achieved using a flow cell in steady state operation. A solution with the substrate is contained in a reservoir and it is pumped through the cell. An example of important industrial application is the Monsanto process for the production of adiponitrile, described in Section 1.1.3.

This topic, flow organic electrosynthesis, is to be the main subject of this thesis, and it will be discussed in more detail in the following sections.

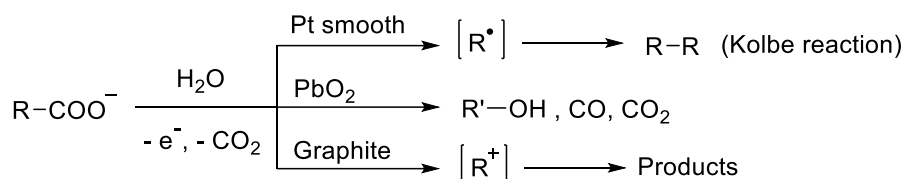
1.1.7. Electrode materials

The electrodes are the most crucial elements of an electrochemical cell, which usually control the outcome of the electrochemical synthesis. A wide review on different electrode materials and their reactivity has been published by Pletcher.^[41] The electrode of choice must meet the following conditions:

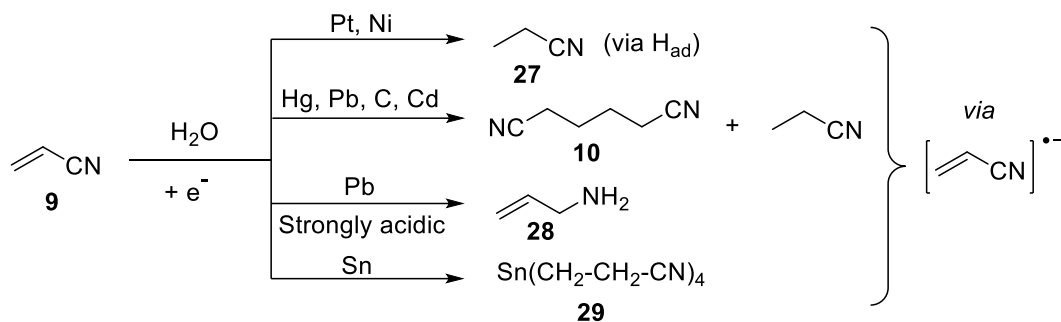
- Electrical conductivity, for the current to pass through the circuit.
- Chemical stability, being inert to the solvent used, substrates and intermediates formed in the course of the reaction.
- Physical stability, to avoid any damage during the construction and use of the electrochemical cell.
- Selective electrocatalytic activity, to favour the desired transformation.
- Cost/durability, having a good life-time to avoid increase of the cost of the process.

The two examples shown in Scheme 1.9 demonstrate the clear influence of the electrode material on the product obtained from the same substrate and reaction conditions.

- Anodic oxidation of carboxylic acids in aqueous solution via decarboxylation



- Cathodic reduction of acrylonitrile in water



Scheme 1.9: Examples of the influence of the electrode material in the outcome of an electrochemical reaction.^[34]

1.1.7.1. Anode materials

Corrosion is a main factor to take into account when deciding the anode material of choice. However, this effect can be harnessed when a “sacrificial anode” is used, where the dissolution of the metal is desired.

Common materials for anode electrodes are noble metals such as platinum, platinum metals or their alloys, and gold. Carbon anodes are also very typical in different forms, such as graphite, reticulated vitreous carbon (RVC) or glassy carbon. Recently diamond coating (boron doped) electrodes have been used, since it has the highest known overvoltage for oxygen evolution, giving a broader potential window to work with. Other anode materials can be nickel, lead or lead oxide.^[9,34]

1.1.7.2. Cathode materials

Corrosive effects are not common in cathode materials, therefore there is a wider variety of materials to choose. In the early beginning of electrochemistry, mercury was a cathode material often used as a dropping mercury electrode (DME), but its use is decreasing significantly due to its acute toxicity. As mentioned for anode materials, diamond coating (boron doped) electrodes have the highest known overvoltage for hydrogen evolution,

therefore they have been used recently, since they offer a broader potential window to work with. Other typical materials to be used as cathode electrode include copper, platinum, nickel, stainless steel, lead and tin.

Platinum and palladium offer the lowest overvoltage for hydrogen formation, therefore they are commonly used for hydrogenation reactions.^[9,34]

1.1.7.3. Reference electrodes

The reference electrode is very important when carrying out controlled potential electrochemical reactions or analytical experiments. A reference electrode should offer a known potential between the electrolyte and its electric connector, and for the potential to remain practically unchanged during reactions. Normally a metal and a salt of this metal (slightly soluble) is used. The electrolyte in the electrode is connected to the electrolyte in the cell through a diaphragm. A very common reference electrode is the saturated calomel electrode, SCE (Hg/Hg₂Cl₂/saturated KCl in H₂O). The potential is determined by the concentration of Cl⁻ anion when it forms an insoluble salt with the metal cation Hg⁺. The potential of the SCE electrode is $E = +242$ mV (vs SHE). Due to the toxic nature of mercury, the use of these electrodes is decreasing and others such as Ag/AgCl reference electrodes are replacing SCE reference electrodes.^[9,34,42]

1.1.7.4. Other types of electrodes

There are other types of electrodes from those already described above:

- Sacrificial electrodes – they are consumed during the electrolytic reaction and incorporated in the product, and can be used as the anode or the cathode.
- Coated electrodes – they normally consist of an inexpensive metal coated with an expensive metal, the one of interest to use as electrode. For instance, platinum coated carbon or titanium are less costly than a solid platinum piece of electrode.
- Porous electrodes – they can be used to increase the working surface area.
- Gas evolving electrodes – oxygen, hydrogen or carbon dioxide can be often evolved at the electrode surface, and this gas formation can be either of interest in the reaction or used as sacrificial counter reaction. These bubbles can also improve the mass transfer within the electrolyte.

1.1.8. Solvents

As in organic chemistry, the solvent of choice can have a major effect on the result of a reaction. General properties to take into account when considering which solvent to use are temperature range, toxicity, viscosity and price. In the case of organic electrochemistry, there are other factors that can severely influence in the efficiency of the reaction,^[9,34] such as:

- Dielectric constant – The dielectric constant of a solvent is of importance in electrochemistry because it will have an influence in the ohmic resistance of the solution. They are preferred to be high, because this will help in the dissociation of the salts in the medium, lowering the resistance.
- Proton activity – The availability of protons is an important characteristic of a solvent medium. In electrochemistry, the presence of protons is more important in reductions than in oxidations, but it can also help to stabilise cation radicals in anodic oxidations. In cathodic reductions, if there is high proton activity in the medium the substrate can be protonated prior to the electron transfer, making the molecule reduction easier.
- Ability to dissolve electrolytes and substrates – It is necessary to find a compromise solvent capable of dissolving organic substrates and inorganic salts. This is not easy, that is the reason why it is very common to use a solvent mixture, where water can dissolve inorganic supporting electrolytes, and it is mixed with an organic solvent such as acetonitrile or methanol, which will dissolve the organic compounds. Tetraalkylammonium salts, commonly used as supporting electrolytes, are soluble in polar organic solvents and in some non-polar solvents such as acetonitrile; this prevents the need to use water just for solubility issues. Moreover, not only the dissolving power of a solvent is important, but also the ability to solvate ions, dissociated as cations and anions. This will improve the conductivity of the electrolyte, and it is often related to the polarity of the solvent.
- Usable potential window – The usable potential range of the solvent of choice should be broad enough so the solvent itself does not react at the electrode surface. The solvent must also be inert on the electrode reactions, such as adsorption at the electrode surface, and not able to interact with the intermediates formed such as radical ions.

1.1.9. Supporting electrolytes

Common organic solvents are not conductive enough and a supporting electrolyte is needed to conduct the charge in the reaction medium. If an acid or a base is necessary to enhance the desired transformation, this can sometimes be sufficient to increase the conductivity of the solution. The process is less costly and easier, since a simple neutralisation is enough to remove the acid or base from the mixture. However, an acidic or basic reaction medium will be used only in specific circumstances. Therefore, an external supporting electrolyte will be usually needed. There are several factors for the selection of the appropriate supporting electrolyte:^[9,34]

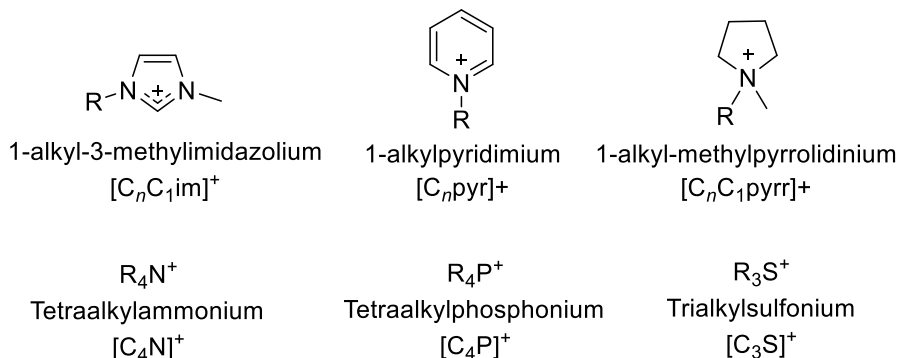
- Good solubility and conductivity in the reaction solvent.
- High stability against reduction and oxidation, it must be inert towards electrochemical transformations and not reactive with the intermediates formed during the reaction.
- Low price and toxicity.
- Easy separation from the crude mixture or product of interest, and if possible, it should be easily recyclable.

The supporting electrolyte usually consists of a salt, where the anion and cation must be chosen carefully. The selection of the anion is more relevant in anodic oxidations, and it needs to be unreactive in the potential range of the reaction. Common anions used as supporting electrolyte are perchlorates, hexafluorophosphates, tetrafluoroborates or nitrates, since they have high discharge potential (the potential at which the anion will be oxidised at the electrode). As for the cation, their choice becomes more important when a cathodic reduction will be performed. Very common cationic parts are tetraalkylammonium ions. Lithium, sodium and magnesium ions are also occasionally used.

The use of room temperature ionic liquids (RTIL) in organic electrochemistry has increased significantly in the last decades. RTILs consist of an ion pair material that exists as a liquid at room temperature.^[43,44] They present inherent ionic conductivity, low volatility, and the broad structural variety available permits the tuning of their physical properties, such as solubility and water miscibility. Mismatched ion pairs with low symmetry are often used to create ionic liquids at room temperature. In general, this can

be achieved using asymmetric bulky organic cations and practically any anion. Some examples of common RTIL ions are shown in Figure 1.8.

a) Common RTIL cations:



b) Common RTIL anions:

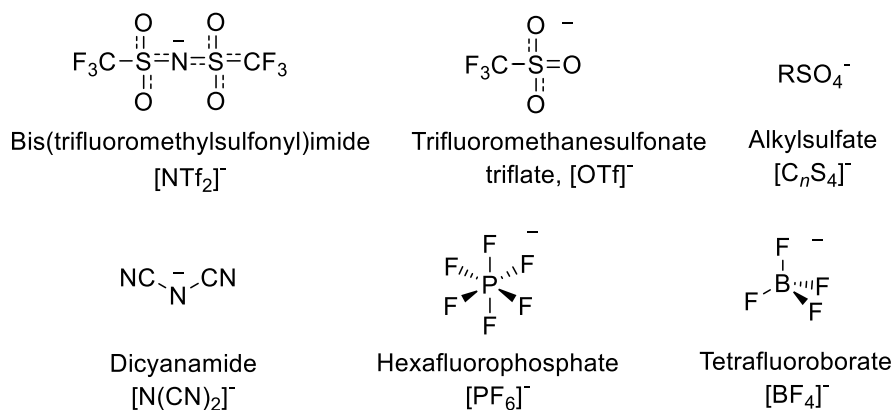


Figure 1.8: Examples for common RTIL molecular structures.^[44]

Although RTILs are good conductors due to their ionic nature, they usually have high viscosity, which can lead to poor mass transport and sometimes even to limited ionic conductivity when compared to some organic solvents. To overcome this problem, cosolvents or dissolved gasses have been employed, providing a higher rate of diffusion.

1.2. Organic electrochemistry in continuous flow

1.2.1. Fundamental aspects of flow electrochemistry

Flow electrochemistry is presented as an established methodology in the synthetic organic laboratory, having convenient advantages over conventional batch electrochemistry, such as very high electrode surface-to-reactor volume ratio, short residence time, no or low concentration of supporting electrolyte, and easier scale-up.^[16,45,46]

The electrode gap in flow electrochemical reactors is very small, normally below 500 μm , which significantly reduces the ohmic resistance and avoids the presence of large current gradients compared to conventional cells, leading to a uniform current distribution.^[30] Therefore, electrochemical reactions can be carried out in very low concentrations or in the absence of a supporting electrolyte, since the two diffusion layers of anode and cathode overlap. Figure 1.9 shows a comparison of conventional stirred-tank-reactor (STR) type and electrochemical microreactors for current distribution, mass transfer and heat transfer.^[47]

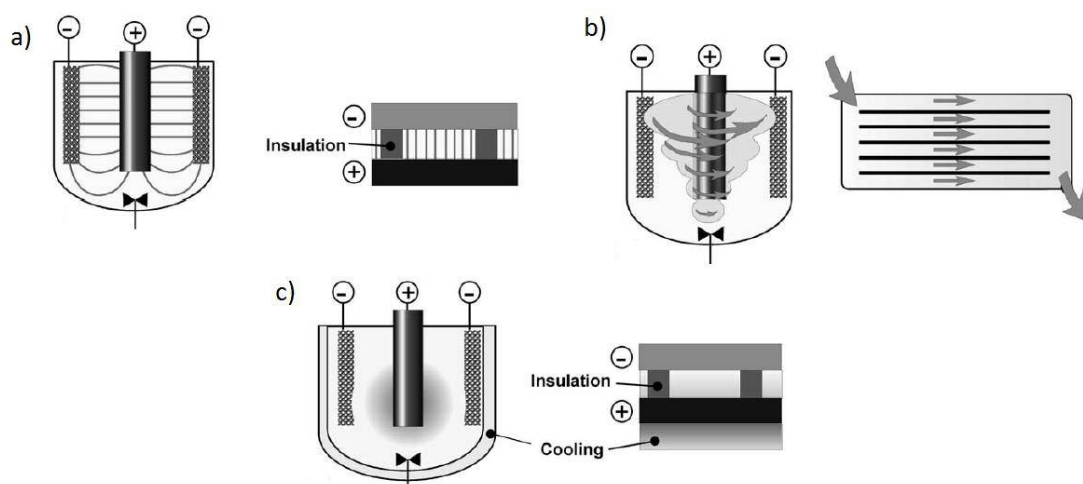


Figure 1.9: Comparison between STR and micro electrochemical reactors: a) current distribution; b) mass transfer; c) heat transfer.^[47] (Reproduced from ref.^[47] with kind permission from Elsevier).

1.2.1.1. Principles of preparative flow electrosynthesis

In flow electrochemical cells, as in conventional chemical processes, the aim is to obtain full conversion of the reactant to the desired product. In order to achieve that, it is important to apply the right amount of charge to the cell, and this is usually done *via* galvanostatic electrolysis (constant current), controlling the number of electron equivalents (measured as Faradays per mole, F mol^{-1}) given to the reaction medium, which is one of the most important parameters in electrosynthesis. In theory, one mole of product needs 96 485 A s (Faraday constant $F =$ charge of 1 mole of electrons), multiplied by the stoichiometric number of electrons required in the reaction.^[48] The theoretical current I (A) needed for a reaction performed in continuous-flow can be calculated using the following equation:^[35]

where n is the number of electrons required in the electrochemical transformation; F is the Faraday constant (A s mol^{-1}); Q_v is the volumetric flow rate of the reaction solution (mL s^{-1}); and C is the concentration of the reaction solution (mol mL^{-1}). As in conventional synthesis, in an electrolytical process a higher current than that calculated (theoretical) might be needed, therefore using a number of electron equivalents ($F \text{ mol}^{-1}$) $> n$.

1.2.2. Organic synthesis with electrochemical flow reactors

Some reactors and their synthetic applications will be explained in the next chapter, which will cover the reactor design.

1.2.2.1. Divided cells

As it has been already discussed in Section 1.1.6.1.2, it is sometimes necessary to separate both compartments of the cell, the anodic and the cathodic chamber, since the electrode reaction or the products at the counter electrode could interfere or compete with the desired product or reaction at the working electrode. Usually diaphragms or porous material is used for this purpose. This allows the current to pass through the anodic and cathodic compartments, but will repress mixing of catholyte and anolyte. This type of cells are called “divided cells”.^[49]

Yoshida and coworkers developed a procedure for the generation and accumulation of highly reactive carbocations (“cation pool”) by electrolysis at low temperature, which is an interesting method to achieve direct oxidative C–C bond formation.^[50,51] Usually the carbocations generated are not very stable, which makes this process challenging. Microflow systems serve as a convenient tool to overcome this problem, since the temperature can be controlled in a very efficient manner, and the residence time of the reactants in the reactor is very short.

A divided cell electrochemical microflow reactor has been used to perform the “cation flow” method.^[52,53] The cell consists of two compartments, one with a carbon felt anode and the other with a platinum wire coil as cathode. The two compartments are divided by a polytetrafluoroethylene (PTFE) membrane (Figure 1.10).

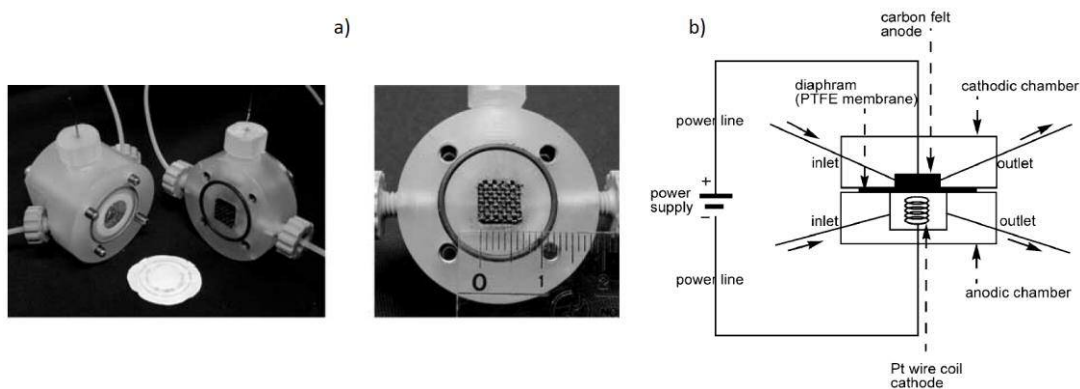
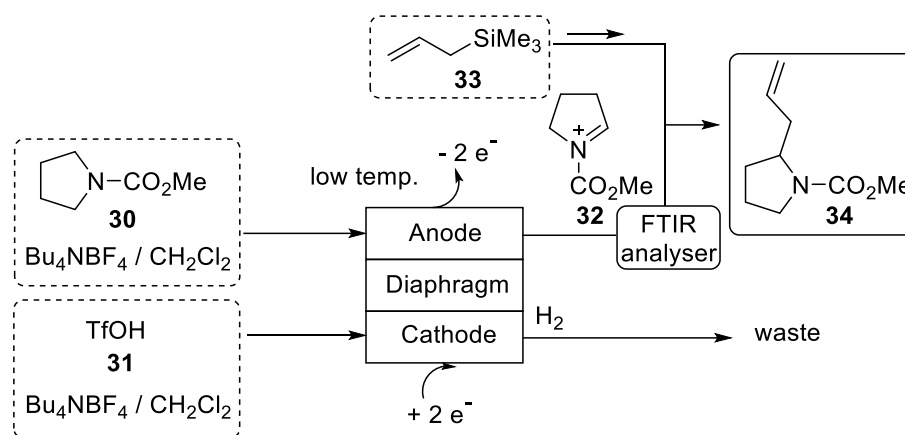


Figure 1.10: a) Photograph of the electrochemical microflow reactor. b) Schematic diagram of the flow electrochemical cell.^[52] (Reproduced from ref.^[52] with kind permission from Wiley-VCH).

Carbamates (**30**) are used as precursors of the cations that are formed by oxidation at the anode. This transformation is performed at low temperature by inserting the reactor in a dry-ice bath. The formation of the acyliminium cation (**32**) is analysed inline by FTIR spectrometry, and is then transferred to a reservoir with nucleophile (**33**), where the coupling reaction takes place to give the final product (**34**). A schematic diagram of the semi-flow process is shown in Scheme 1.10. Trifluoromethanesulfonic acid (**31**) is used in the cathodic chamber as a sacrificial compound, to generate hydrogen gas from protons.



Scheme 1.10: Schematic diagram of a cation flow system for a model reaction.^[52,53]

A number of substrates and nucleophiles have been used for the oxidative C–C bond formation using the cation flow method, affording up to 69% conversion and up to 98% yield based on the reacted starting material. These reactions are carried out at $-72\text{ }^\circ\text{C}$ to deal with the instability of the carbocations formed in the anodic chamber.

In 2015 Waldvogel *et al.* developed a divided flow cell to perform electrochemical dehalogenation,^[54] and more recently (2017) they published another flow cell for a domino oxidation reduction to synthesise nitriles from aldoximes.^[55] These reactors will be explained in Chapter 2 (reactor design).

1.2.2.2. Undivided cells

While in divided cells the anolyte and catholyte are separated in different chambers, in undivided cells both working and counter reactions media are in contact and mixing, there is no separation between them.

1.2.2.2.1. Anodic oxidations

1.2.2.2.1.1. Supporting electrolyte-free anodic oxidations

Yoshida *et al.* reported the anodic methoxylation of organic compounds performed in the electrochemical reactor shown in Figure 1.11.^[56] The reactor consists of two carbon fiber electrodes that are separated from each other by a hydrophobic porous PTFE membrane (75 μm thick, 3 μm pore size). The carbon felt electrodes filled the whole electrochemical chamber, so there is no empty space between anode and cathode. The results of the anodic methoxylation of *p*-methoxytoluene (**35**), *N*-methoxycarbonyl pyrrolidine (**30**) and acenaphthalene (**39**) are shown in Scheme 1.11.

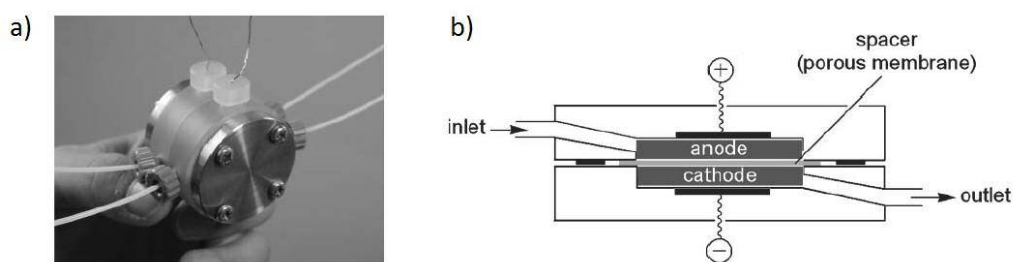
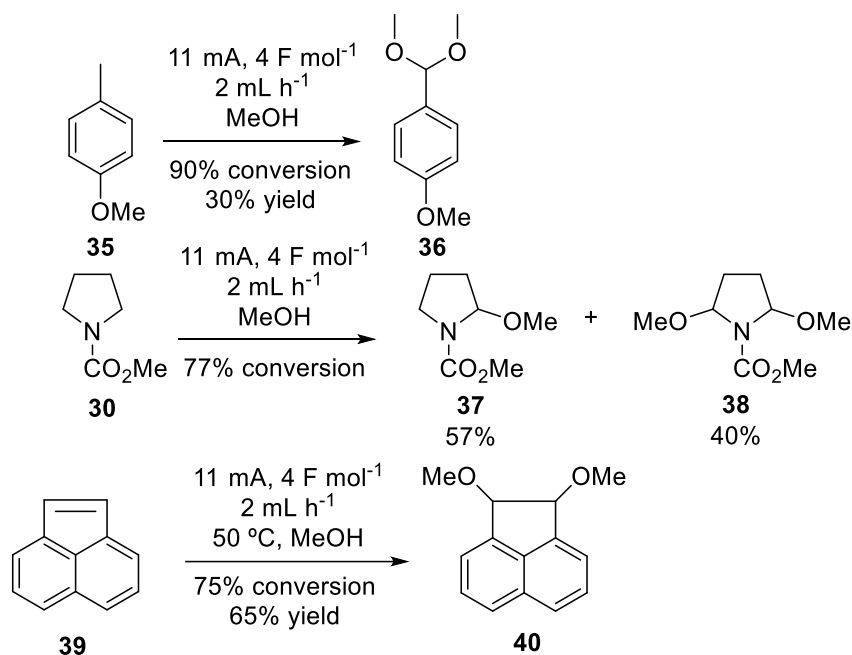
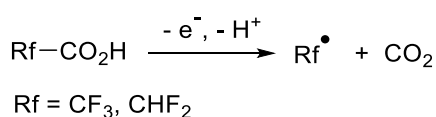


Figure 1.11: Microflow electrochemical reactor: a) photograph of the reactor, b) schematic diagram.^[56] (Reproduced from ref.^[56] with kind permission from the Royal Society of Chemistry).



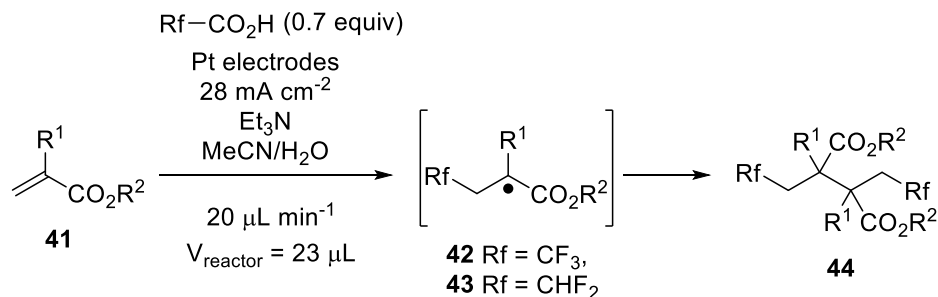
Scheme 1.11: Anodic methoxylation of p-methoxytoluene, N-methoxycarbonyl pyrrolidine and acenaphthalene.^[56]

Wirth and coworkers used the Kolbe electrolysis as a useful method to generate active radical species from carboxylic acids.^[57–59] Di- and trifluoroacetic acid were used as inexpensive reactants to form CF_2H and CF_3 radicals, respectively, that can react in an efficient manner with different electron-deficient alkenes (Scheme 1.12).^[60] This transformation is performed in a reactor developed by Wirth *et al.*, that will be reported in Chapter 2, using platinum electrodes.^[61]



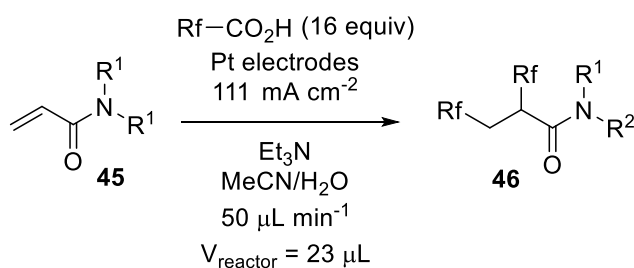
Scheme 1.12: Kolbe electrolysis.

Di- and trifluoromethylation of acrylates take place under electrochemical conditions to give the dimer (**44**), with yields up to 52% (Scheme 1.13).



Scheme 1.13: Di- and trifluoromethylation of acrylates.

Acrylamides (**45**) serve also as suitable substrates for this electrochemical di- and trifluoromethylation. To obtain the double addition of the corresponding tri- or difluoromethyl radical to the alkene instead of the dimerisation product, a large excess (16 equiv) of the corresponding acid had to be used, giving the product in up to 67% yield (Scheme 1.14).



Scheme 1.14: Di- and trifluoromethylation of acrylamides.

1.2.2.2.1.2. Anodic oxidations using supporting electrolyte

Waldvogel *et al.* have contributed extensively in the development of electrochemical aryl-aryl coupling. Non-symmetric aryl-aryl coupling has been of great interest in the past decades to generate biaryl motifs, which are very important in catalysis,^[62] natural product synthesis,^[63] pharmaceutical chemistry^[64,65] and polymer science.^[66,67] Transition metals are commonly used for this transformation, but it is always desirable to find an alternative route to toxic and costly catalysts. Atobe and Waldvogel developed a phenol-aryl coupling performed electrochemically by the oxidation of phenol on a boron-doped diamond (BDD) anode in a batch type reactor using 1,1,1,3,3,3-hexafluoroisopropanol (HFIP) as the solvent,^[68–70] because it can stabilise the anodically generated species.^[71–79] To avoid the use of HFIP as an expensive and non-biodegradable solvent, the phenol-arene cross-coupling reactions were performed in a flow electrochemical microreactor,^[80] which also enables a fast screening of reaction conditions. The flow cell consists of a

BDD anode and a nickel cathode, divided by a spacer with a rectangular channel for the reaction as shown in Figure 1.12.

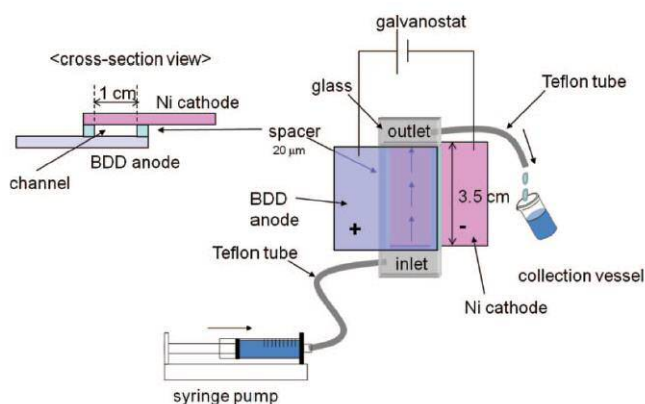
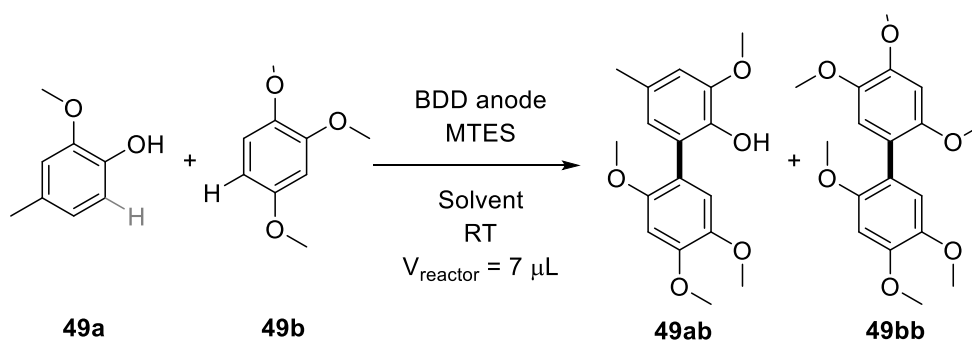


Figure 1.12: Schematic representation of the flow electrochemical microreactor.^[80]
(Reproduced from ref.^[80] with kind permission from the Electrochemical Society).

The phenol derivative (**49a**) is oxidised at the cathode to form the phenoxyl radical or the respective radical cation, and these reactive species are trapped by the coupling aryl moiety (**49b**) to afford the biaryl motif (**49ab**, Scheme 1.15).



Scheme 1.15: Phenol-arene cross coupling electrochemical reaction.^[80]

The homo-coupling reaction of the aryl motif (**49bb**) competes with the desired non-symmetric aryl-aryl coupling, because the oxidation potential of the arene (**49b**) is lower than the oxidation potential of the phenol. Addition of methanol to the solvent mixture used in the reaction can overcome this problem, as the oxidation potential of the phenol (**49a**) is lowered when the concentration of methanol increases, as shown in Figure 1.13. Upon addition of methanol, the phenolic O–H bond of (**49a**) could be split, as methanol can act as a weak base. The deprotonated form of the phenol would then present a lower oxidation potential. Under these conditions, the desired cross coupling product can be obtained in yields up to 44%, with more than 80% selectivity.

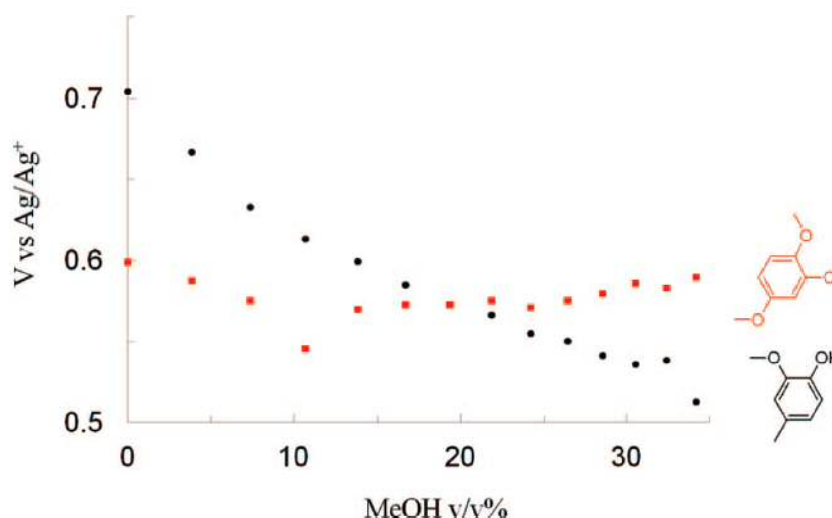


Figure 1.13: Oxidation potential variation of phenol derivative (49a) and arene (49b) by addition of methanol. (Reproduced from ref.^[80] with kind permission from the Electrochemical Society).

Atobe and coworkers reported the use of parallel laminar flow to perform an anodic substitution reaction in a micro-flow reactor. The “cation flow” method to generate highly active carbocations at low temperature electrolysis is described in Section 1.2.2.1, where the carbocation generated is reacted with a nucleophile at the outlet of the reactor to form the coupling product. As the microreactor is very small, it can ensure a laminar flow in the reactor. In the method reported by Atobe, two inlet solutions are introduced separately into the reactor which form a stable liquid-liquid interface. The mass transfer between both streams occurs only *via* diffusion. This concept can be applied to a parallel laminar flow reaction in an electrochemical cell, where carbocations are formed at the anode, and then will react with the nucleophile contained in another solution pumped in parallel to the anodic solution. Using a laminar flow in this process is essential, as generally the oxidation potentials of nucleophiles are lower than the oxidation potential of organic substrates, and will be therefore oxidised easier at the anode.^[81] Figure 1.14 illustrates the electrochemical microreactor with parallel laminar flow. This system allows nucleophilic reactions to overcome the limitations described above, such as the stability of carbocations and the low oxidation potential of nucleophiles.^[82]

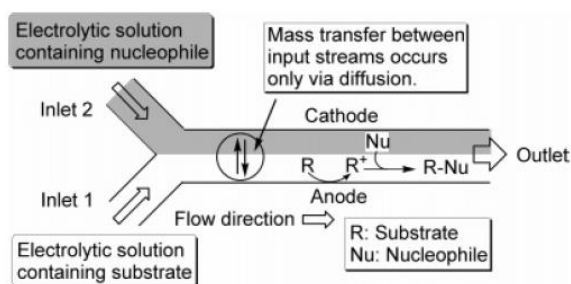
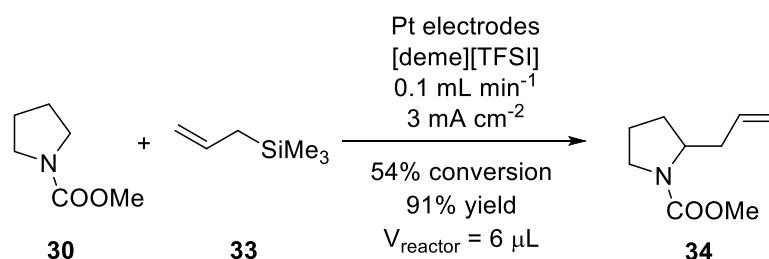


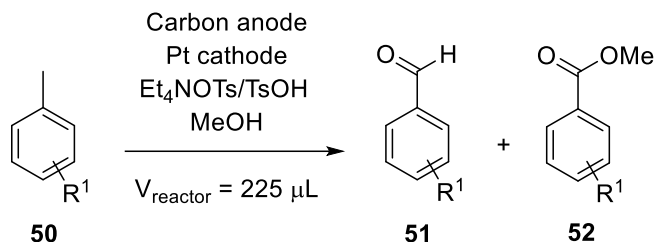
Figure 1.14: Microreactor with parallel laminar flow.^[82] (Reproduced with permission from ref.^[82] Copyright (2007) American Chemical Society).

N-(Methoxycarbonyl)pyrrolidine (**30**) is oxidised on a platinum electrode to form the carbocation intermediate that reacts with allyltrimethylsilane (**33**), as shown in Scheme 1.16. The reaction gives excellent yield of the C–C coupling products (**34**), even if not full conversion, when ionic liquids are used as reaction media such as *N,N*-diethyl-*N*-methyl-*N*-(2-methoxyethyl)ammonium bis(trifluoromethanesulfonyl)imide ([deme][TFSI]). This result suggests that ionic liquids can efficiently stabilise the carbocation formed, so it can react before decomposition.



Scheme 1.16: Parallel laminar flow oxidation reaction of 30 with 33.

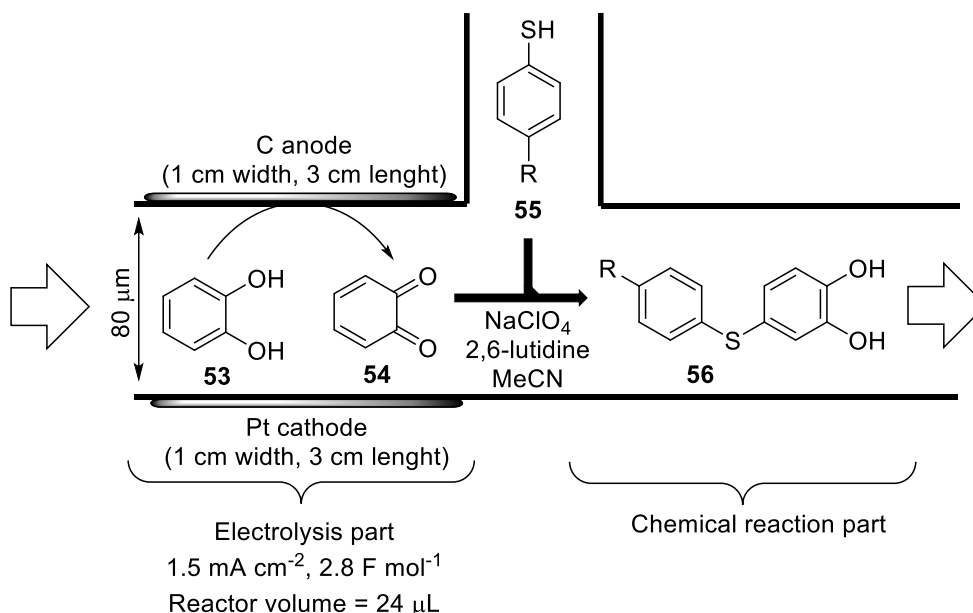
The anodic methoxylation of *p*-methoxytoluene is reported in Section 1.2.2.2.1.1 to give the dimethylacetal by a 4-electron oxidation. A similar method is used by Djuric *et al.* to obtain the ester (6-electron oxidation product **52**).^[83] In this case, the Syrris Flux Module (which will be explained in Chapter 2) is used for these transformations. The selectivity towards the production of the aldehyde (**51**) or the ester (**52**, Scheme 1.17) can be controlled by the electrode material used in the electrochemical reaction. When carbon is used as both anode and cathode, the aldehyde is obtained as major product (6.8:1 ratio). Using carbon as anode and platinum as cathode changes this selectivity favouring ester formation and, depending on the supporting electrolyte used, selectivities up to 31:1 can be obtained.



Scheme 1.17: Toly-based substrates benzylic oxidation.^[83]

Different toluene derivatives (**50**) have been used to obtain the respective aldehydes (**51**) or esters (**52**) in up to 62% yield towards the ester, and 38% yield towards the aldehyde. The *para*-nitro and *para*-cyanotoluene did not form any oxidation product, probably because of the high oxidation potential, which may make the oxidation unfeasible within the potential window used in this process.

Atobe and coworkers developed a flow methodology to prepare the highly reactive *ortho*-quinones *in situ* electrochemically. *Ortho*-quinones (**54**) are important and useful building blocks in organic synthesis,^[84] but they are too unstable and reactive to store. Therefore, they are usually prepared *in situ* by the oxidation of the corresponding catechol (**53**),^[85–87] and used directly in the desired reaction to react with the reaction partner as convenient.



Scheme 1.18: Representation of the electrochemically generated *ortho*-benzoquinone and the subsequent reaction with a benzenethiol in a microflow reactor.^[89]

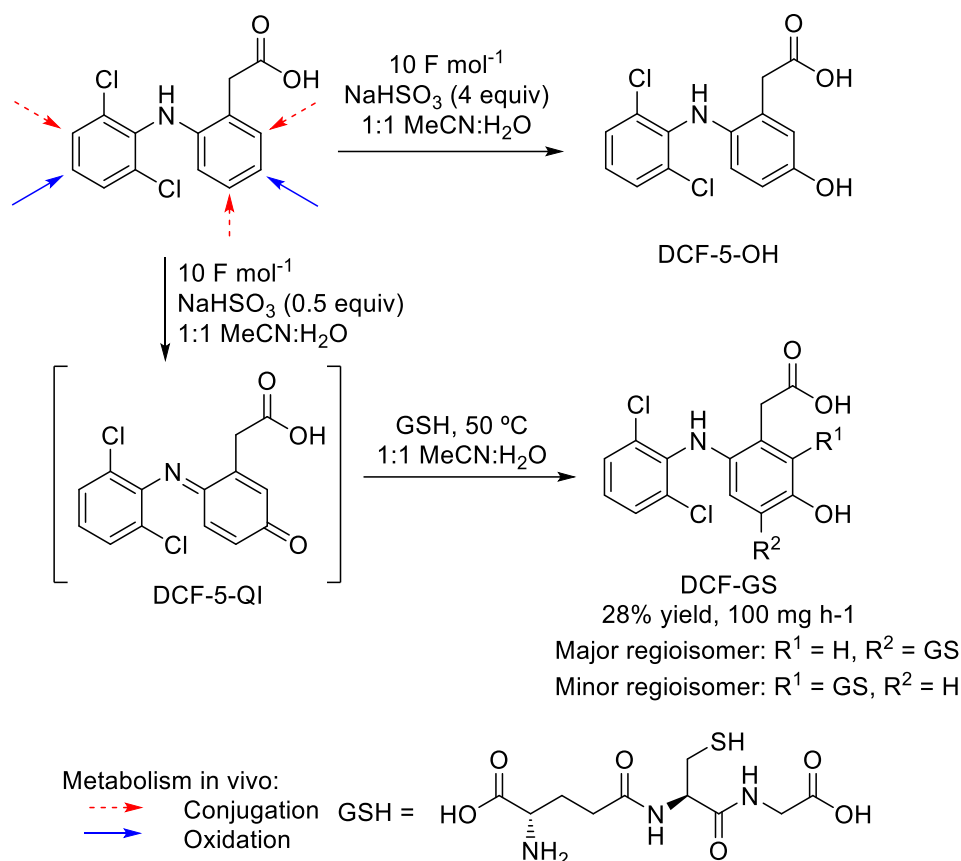
The oxidation potentials of nucleophiles (or reaction partners) are often lower than the oxidation potential of the corresponding catechols,^[88] and will be therefore oxidised

easier at the anode. The flow reactor used for this type of reactions is the same as described in Section 1.2.2.3 (Figure 1.16), but in this case, the second syringe pump containing benzenethiol (**55**) and base is connected to the outlet of the electrochemical reactor.^[89] A schematic representation of the process is shown in Scheme 1.18.

Diphenyl sulfide (**56**) derivatives have been synthesised using this method from catechol (**53**) and the benzenethiol derivative (**55**). The yields were increased up to 88% using the microflow electrochemical reactor, while in a batch type reactor the product can be obtained only in 13% yield. This improvement in the yield is due to the competitive anodic oxidation reaction of the thiol nucleophile being avoided in the microflow system.

Flow electrosynthesis can also be used to complement biosynthetic studies. Roth and coworkers have synthesised drug metabolites electrochemically on the preparative scale. In the liver, a drug molecule experiences its first chemical transformation *via* CYP450-catalysed oxidation.^[90] The chemical result of the first pass hepatic oxidation is very important information to any drug development process. The electrosynthesis in continuous flow of the phase I metabolites of five commercial drugs has been performed in the Asia Flux cell supplied by Syrris LTD (see Chapter 2 for more information about the reactor).

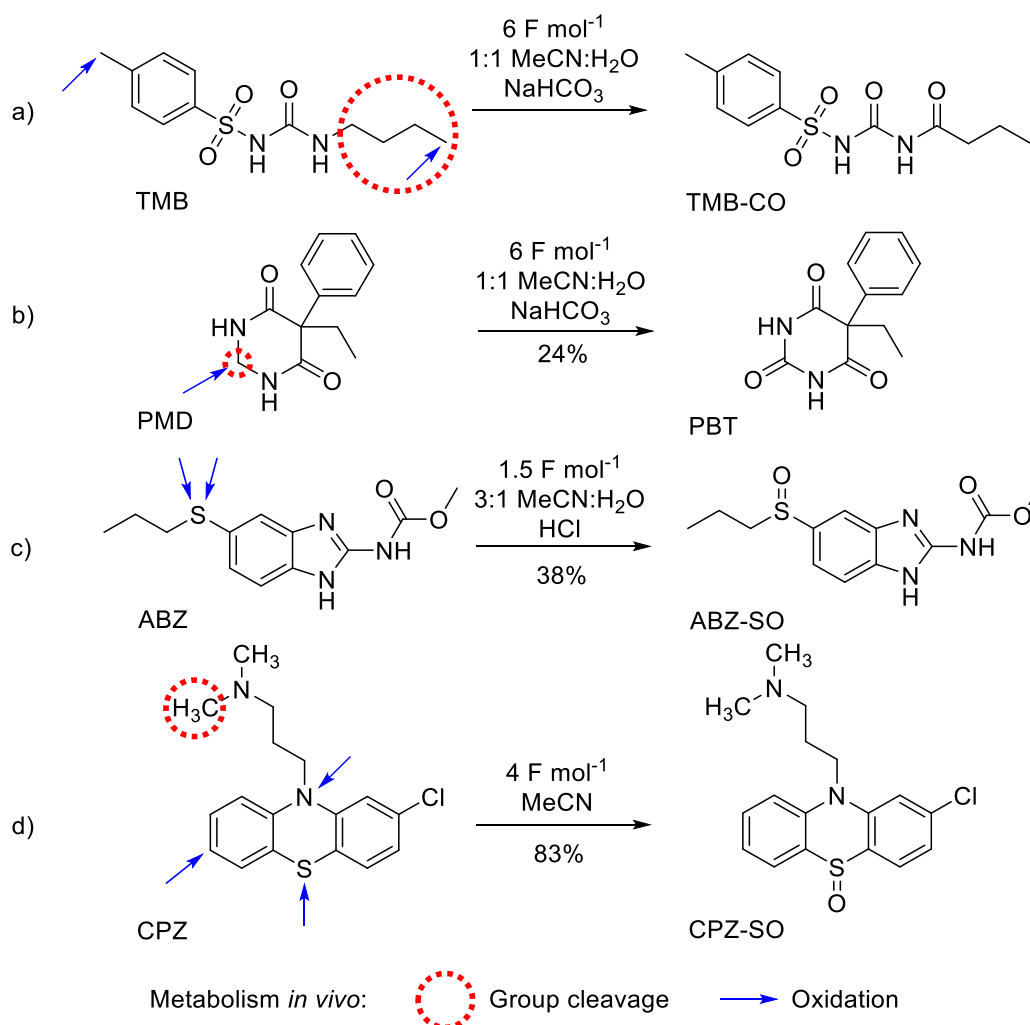
Scheme 1.19 shows the result when diclofenac (DCF), an anti-inflammatory drug metabolised in the liver by aromatic hydroxylation, is treated under electrochemical conditions. Depending on the concentration of sodium bisulfite used, the product obtained is DCF-5-OH^[91] or the quinone imine DCF-5-QI. Quinone imines are known to be first hepatic metabolites, but they are considered toxic because of their electrophilicity.^[92] Therefore, DCF-5-QI is reacted with glutathione to form DCF-GS, which are known conjugation metabolites of diclofenac.^[93] This second transformation is also performed using continuous-flow technology, just by attaching the output of the electrolysis cell to a microfluidic reactor, where the output is mixed with a solution of glutathione.



Scheme 1.19: Phase I metabolite of Diclofenac (DCF-5-OH) obtained by electrosynthesis and its glutathione Phase II adduct (DCF-GS) obtained from the quinone imine (DCF-5-QI).^[94]

The drug tolbutamide (TMB) is metabolised *in vivo* by benzylic oxidation. When the drug is subjected to the electrochemical conditions, no oxidation of the benzyl ring is observed, but the carbon in *alpha* position to the urea is oxidised to the carbonyl to give TMB-CO (Scheme 1.20a, which is not a known metabolite of TBM. Primidone (PMD) is a drug which is known to have a metabolite resulting from alkyl oxidation (phenobarbital, PBT, Scheme 1.20b^[95] which was successfully synthesised in 24% yield in the flow electrochemical cell. Albendazole (ABZ) is an anthelmintic drug that has two metabolites reported *in vivo*, corresponding to the *S*-oxidation of the thioether, to form the sulfoxide (ABZ-SO) or the sulfone (ABZ-SO₂). The synthesis of the corresponding sulfoxide or sulfone could be controlled by the equivalents of electrons taken in the cell. In Scheme 1.20c is shown how the sulfoxide ABZ-SO is formed by using only 1.5 F mol⁻¹, which is not sufficient if the sulfone would be the desired product as the use of a higher charge would be needed. Chlorpromazine (CPZ) is an antipsychotic drug that is also

known to undergo *S*-oxidation in the liver. The sulfoxide metabolite (CPZ-SO)^[96] is synthesised electrochemically in 83% yield.

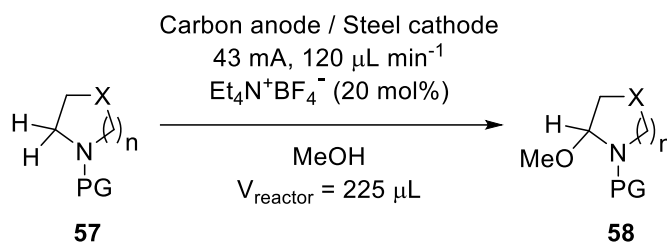


Scheme 1.20: Anodic oxidation products of the drugs Tolbutamide (TBM), Primidone (PMD), Albendazole (ABZ) and Chlorpromazine (CPZ).^[94]

This demonstrates that flow electrochemistry can complement biosynthetic studies, since different drug oxidation products, which are important for their *in vivo* metabolism, can be easily synthesised at a much higher productivity rate than the conventional production rate using typical electroanalytical techniques.^[97,98]

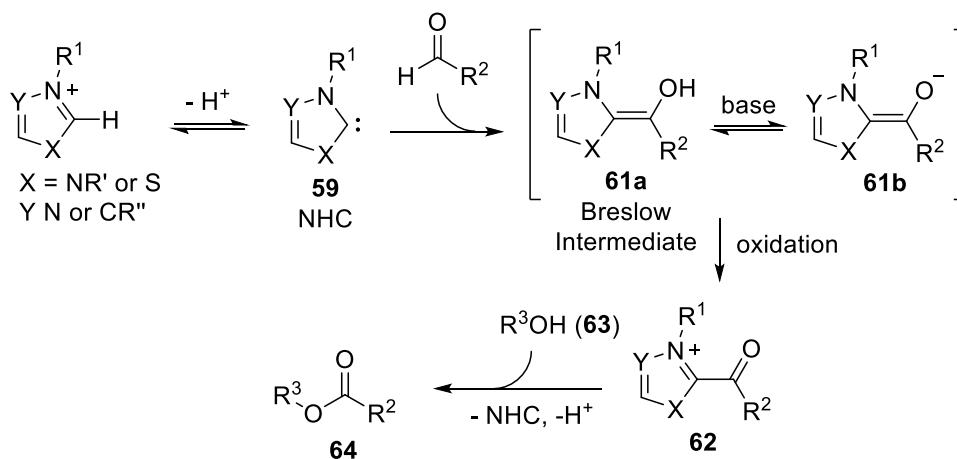
Ley *et al.* developed a method in flow to perform the electrochemical α -methoxylation of *N*-protected cyclic amines (**57**). The use of a flow electrochemistry device to effect the Shono oxidation of *N*-protected cyclic amines is an attractive method to methoxylate such compounds in the α -position,^[99,100] which leads to precursors of a number of natural and unnatural analogues of nazlinine, a naturally occurring biologically active indole

alkaloid.^[101] α -Methoxyamine building blocks (**58**) were synthesised electrochemically from commercially available cyclic amines (**57**)^[102] (in their protected form) in methanol using the Asia Flux electrosynthesis module from Syrris Ltd. In the electrochemical cell, the cyclic amine is oxidised at the anode to form an iminium cation, which can undergo a nucleophilic attack by methanol to form the α -methoxyamine in up to 98% yield (Scheme 1.21).



Scheme 1.21: α -Methoxylation of *N*-protected cyclic amines.^[102]

Brown *et al.* developed a method to synthesise esters *via* anodic oxidation mediated by *N*-heterocyclic carbenes using the Syrris Flux electrochemical flow cell.^[103] *N*-heterocyclic carbenes (NHCs) are powerful organocatalysts for a number of reactions.^[104–107] A general mechanism for this transformation is shown in Scheme 1.22.

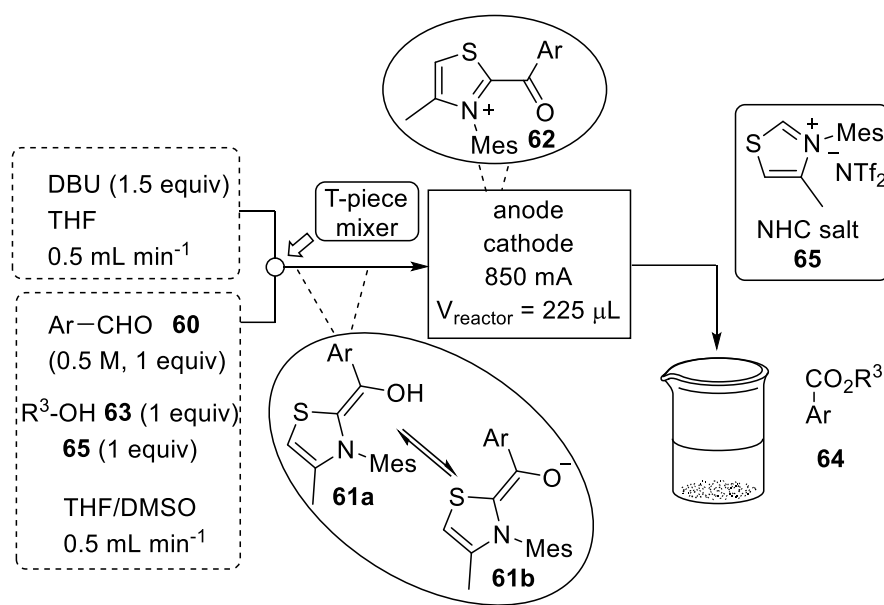


Scheme 1.22: NHC-Mediated oxidative conversion of aldehydes to esters.^[103]

The reactive Breslow intermediates (**61**) are generated by mixing in-flow two different streams: one containing the aldehyde (**60**), methanol, the thiazolium salt (**65**) and dimethyl sulfoxide in tetrahydrofuran; the other containing 1,8-diazabicyclo[5.4.0]undec-7-ene (DBU) in tetrahydrofuran. Scheme 1.23 shows the flow set-up. Both streams are mixed using a T-piece and introduced in the undivided electrochemical cell where the oxidation takes place to afford acylthiazolium (**62**), which then reacts with the alcohol

(**63**) to give the corresponding ester (**64**) in good to excellent yields at a high productivity rate.

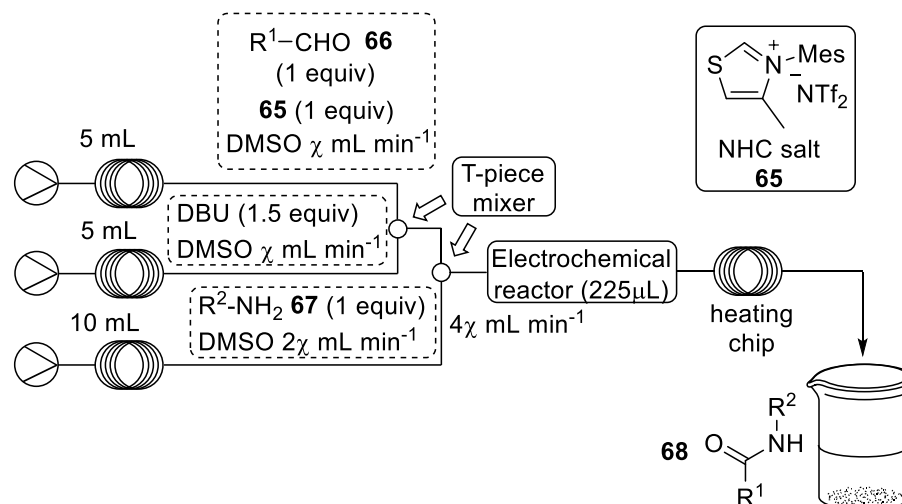
This method has been applied to a range of alcohols and aldehydes to give the desired esters, with productivities from 1.5 up to 4 grams per hour, current efficiencies in the range of 80 to 100% and yields up to 99%.



Scheme 1.23: Flow set-up for the oxidative synthesis of esters from aldehydes.^[103]

The use of *N*-heterocyclic carbenes to form Breslow intermediates (Scheme 1.22) can also be applied for the synthesis of amides from aldehydes, using amines instead of alcohols. Brown and coworkers developed a method using the Syrris Flux electrochemical flow cell, and the flow set-up is described in Scheme 1.24.

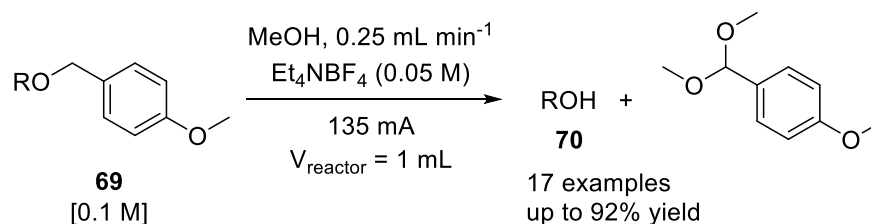
The flow set-up described in Scheme 1.23 was slightly modified, since condensation of aldehyde and amine will occur if they are pumped together in the same mixture. To overcome this problem, three different solutions are prepared in dimethyl sulfoxide: the first one contains the aldehyde (**66**) and the thiazolium salt (**65**); the second one 1,8-diazabicyclo[5.4.0]undec-7-ene (DBU); and the third one the amine (**67**). Solutions one and two are mixed together to form the Breslow intermediate, and this is mixed with the third stream containing the amine. The final mixture is introduced in the electrochemical reactor to perform the anodic oxidation, and the outlet of the electrochemical cell is connected to a heating chip, where the amide formation is accelerated by increased temperature.



Scheme 1.24: General flow set-up for NHC-mediated electrochemical synthesis of amides from aldehydes.^[108]

This method is applied to a range of amines and aldehydes to give the desired amides (**68**) in good to excellent yields (up to 99%). Furthermore, chemically oxidisable functionalities are tolerated in the process such as furan, phenol and indole.

Very recently in 2017 Brown *et al.* published the electrochemical deprotection of *para*-methoxy benzyl ethers (PMB) (**69**) to form the free alcohol (**70**). The reaction was performed in the Ammonite 8 electrochemical flow cell (explained in Chapter 2), with stainless steel cathode and C/PVDF anode (Scheme 1.25). They reported 17 examples with yields up to 92%. The reaction could be scaled up to 7.6 grams per hour, using a 0.3 M concentration and a flow rate of 4 mL min⁻¹. The supporting electrolyte used (Et₄NBF₄) could be recovered and reused. Some other common alcohol protecting groups tolerated these electrochemical conditions, and only the PMB group was removed.^[109]

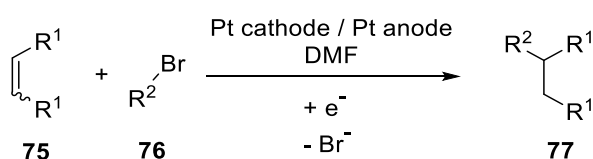


Scheme 1.25: PMB electrochemical deprotection.

1.2.2.2.2. Cathodic reductions

Haswell *et al.* developed a method for cathodic coupling of activated olefins with benzyl bromide derivatives. C–C bond formation is an important process in synthetic chemistry.

Activated olefins (**75**) and benzyl bromide derivatives (**76**) were used as reactants to perform reductive coupling electrochemically, thus forming the new C–C bond (**77**).^[110,111] The products obtained with this method, such as 2-benzyl succinic acid dimethyl ester, can be used as intermediates in the synthesis of important target molecules like pyrrolidines,^[112] natural antibiotics^[113] and monoesters of alkylated succinic acids.^[114] This process has been developed in a flow microreactor performing a one-step cathodic reductive coupling, generating the desired products in higher yields when compared to conventional synthetic methods. The general reaction is shown in Scheme 1.26.



Scheme 1.26: C–C coupling reaction.^[111]

The reaction can be scaled out using a multiple channel version of the reported electrochemical microreactor. There are two different types of configuration; the first one consists of a single set of electrodes used with a multiple flow manifold to give two and four separate flow channels (Figure 1.15a), while the second one contains independent electrodes which are used with the same flow manifolds (Figure 1.15b).

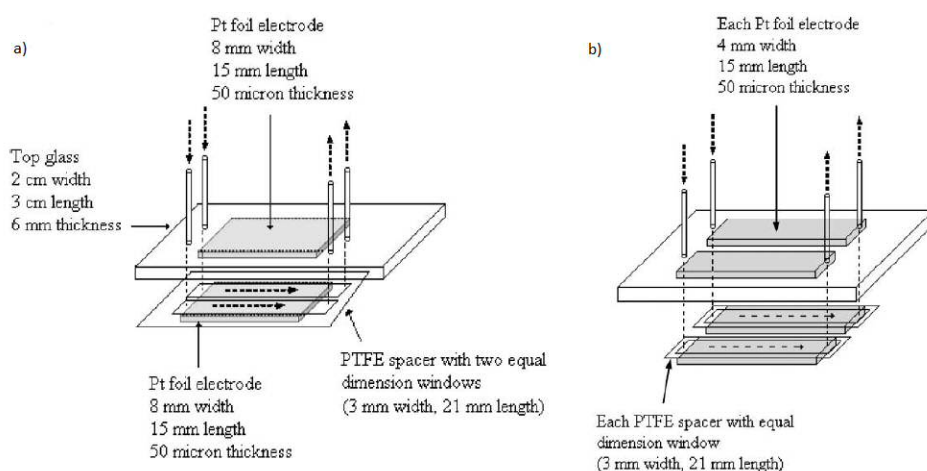


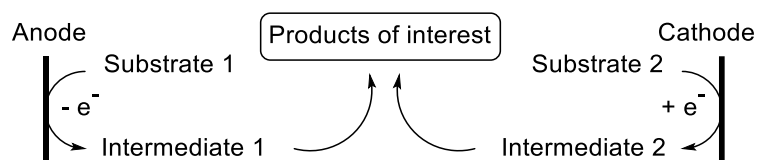
Figure 1.15: Scale out of the electrochemical cell a) with a single pair of electrodes, b) with independent electrode configuration.^[111] (Reproduced from ref.^[111] with kind permission from the Royal Society of Chemistry).

The same coupling reaction described in Scheme 1.26 can be used with the new version of the reactor. The output gives very similar yields (94 – 99%), but when using two

separated electrodes and two flow channels, the flow rate could be increased to 20 $\mu\text{L min}^{-1}$ (4 electrodes / 4 flow channels would allow a flow rate up to 40 $\mu\text{L min}^{-1}$), instead of 10 $\mu\text{L min}^{-1}$, that was the flow rate used in the single reactor. Therefore, the scale-out reactor can be used to achieve the same product yield with higher productivity (up to 4x) with no loss of performance compared to that obtained for a single cell.

1.2.2.3. Paired electrosynthesis

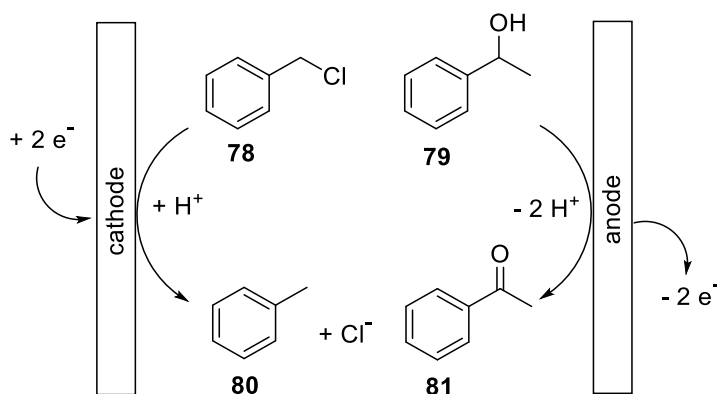
In an electrochemical cell, there are always two reactions taking place simultaneously, one at the anode and one at the cathode. In most cases, only one of these reactions is desired, and the so-called counter reaction would be called the sacrificial one. It is possible to “pair” the two processes and form valuable compounds or intermediates at both electrodes, leading to a higher combined electrochemical yield, and this is called “paired electrolysis” (Scheme 1.27).^[30]



Scheme 1.27: Paired electrolysis.

Willians and coworkers developed a method and a new electrochemical flow reactor for the synthesis of copper-*N*-heterocyclic carbene complexes, where both anodic and cathodic reactions are used for the desired final product.^[115] This reactor and transformation will be described in Chapter 2.

Atobe *et al.* reported the paired electrosynthesis of toluene and acetophenone.^[116] Two starting compounds, benzyl halides (**78**) and 1-phenylethyl alcohol derivatives (**79**), are reduced and oxidised respectively in a paired electrosynthesis microflow reactor to give the two product, toluene (**80**) and acetophenone (**81**, Scheme 1.28).^[116] This transformation is performed using a silver cathode and an indium tin oxide (ITO) anode without the use of any supporting electrolyte. The chloride ions formed at the cathode serve as a main charge carrier.



Scheme 1.28: Paired electrochemical reaction of benzyl halides and secondary alcohols.^[116]

When using a single inlet in the reactor with both substrates (Figure 1.16a), the yield obtained of the desired product is very low. This is due to the electrochemical reactions at each counter electrode of the products generated and substrates, which compete with the desired reaction. In order to avoid this problem, a different set-up of the reactor is used with two separate inlets (Figure 1-16b, volume of the channel exposed to electrolysis: 24 μ L.), where a parallel laminar flow mode is achieved, creating a stable liquid-liquid interface and avoiding the anodic and cathodic solution to mix and interfere with each other. This parallel laminar flow electrolysis was previously explained in Section 1.2.2.2.1.2.^[82]

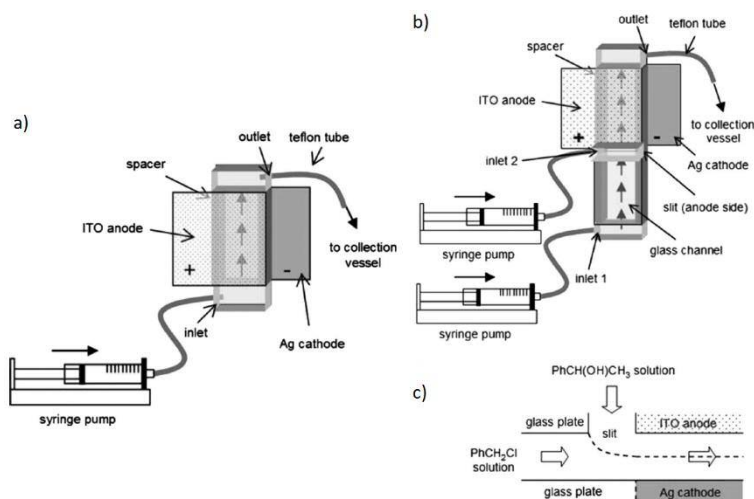
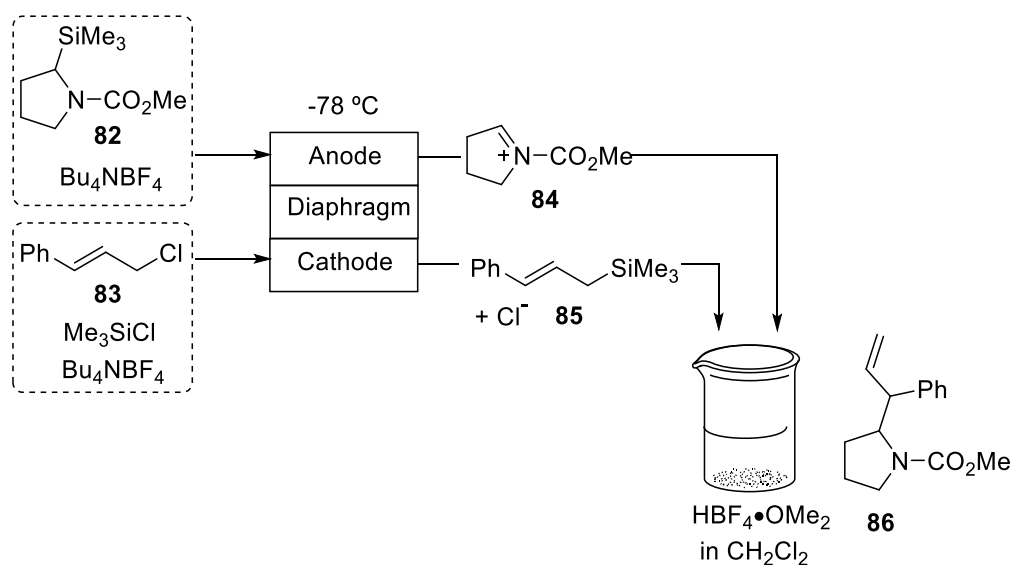


Figure 1.16: Schematic of the microflow reactor: a) one inlet with both substrates b) two inlets to inject each substrate separately and form a liquid-liquid interface c) cross-section of the reactor with two inlets.^[116] (Reproduced from ref.^[116] with kind permission from the Electrochemical Society).

Yoshida and coworkers developed a variation of the “cation flow” method, where both the catholyte and the anolyte are useful intermediates for the formation of the final

product. In the “cation flow” method described in Section 1.2.2.1, only the oxidised compound formed at the anode is used for the synthesis, and the cathodic counterpart was the sacrificial reduction of trifluoromethanesulfonic acid to generate hydrogen. This variation is performed in a microflow system where both the cathodic reduction and the anodic oxidation contribute to the generation of the final product.^[52] The divided cell described in Section 1.2.2.1 (Figure 1.10)^[52] with some modifications, is used for this transformations. A carbocation is generated at the anode and a carbon nucleophile is generated at the cathode. A schematic diagram of this paired electrochemical microflow system is shown in Scheme 1.29. When the anolyte and catholyte products are mixed directly after the electrochemical reaction, no product is obtained. This is due to the presence of chloride ions generated at the cathode. To overcome this problem, both outlets from the anodic and cathodic reactions are added simultaneously to a vessel containing a solution of tetrafluoroboric acid dimethyl ether complex as a strong acid to trap the chloride ions generated in the cathodic reduction and therefore giving place to the desired coupling reaction in good yields.



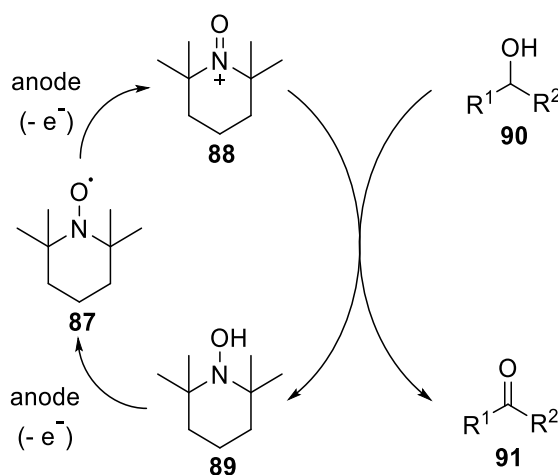
Scheme 1.29: Paired electrolysis by the direct coupling of cathodic and anodic products.^[52]

A number of substrates have been used in the paired electrosynthesis for C–C bond formation using the cation flow method to afford the desired product in up to 88% conversion and up to 79% yield. These reactions are carried out at -78°C to deal with the instability of the carbocations formed in the anodic chamber.

1.2.2.4. Indirect electrosynthesis

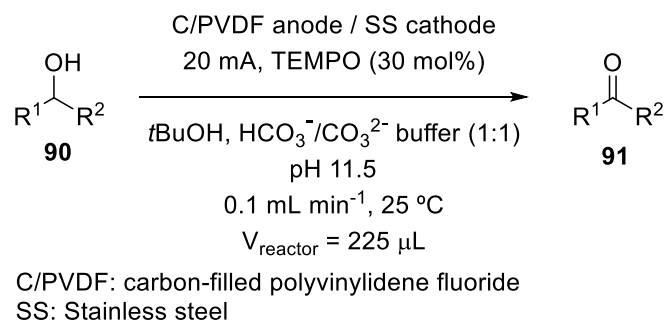
The principle of indirect electrolysis was described in Section 1.1.5.3.

Brown *et al.* reported a flow method to electrochemically oxidise primary and secondary alcohols (**90**), to form aldehydes and ketones (**91**).^[117] The free radical 2,2,6,6-tetramethylpiperidine-1-oxyl (TEMPO **87**)^[118-121] is used as a mediator for this transformation. TEMPO **87** is oxidised at the anode to give the oxoammonium ion (**88**), which then oxidises the alcohol to form the corresponding aldehyde or ketone, and the hydroxylamine by-product (**89**). Compound **89** is rapidly oxidised at the anode through a single electrode transfer to regenerate the TEMPO radical **87** (Scheme 1.30).



Scheme 1.30: Electrochemical TEMPO-mediated alcohol oxidation.^[122]

This transformation is done in the Flux electrolytical cell supplied by Syrris LTD using a carbon-filled polyvinylidene fluoride anode and stainless steel cathode. A number of primary and secondary alcohols are transformed to the corresponding aldehydes or ketones in yields up to 87%, tolerating various functional groups in the molecule (Scheme 1.31).



Scheme 1.31: Electrochemical TEMPO-mediated oxidation of primary and secondary alcohols.^[117]

1.3. References

- [1] B. A. Frontana-Urbe, R. D. Little, J. G. Ibanez, A. Palma, R. Vasquez-Medrano, *Green Chem.* **2010**, *12*, 2099–2119.
- [2] H. J. Schäfer, M. Harenbrock, E. Klocke, M. Plate, A. Weiper-Idelmann, *Pure Appl. Chem.* **2007**, *79*, 2047–2057.
- [3] E. Steckhan, T. Arns, W. R. Heineman, G. Hilt, D. Hoormann, J. Jörissen, L. Kröner, B. Lewall, H. Pütter, *Chemosphere* **2001**, *43*, 63–73.
- [4] J. Simonet, J. F. Pilard, in *Organic Electrochemistry* (Eds.: H. Lund, O. Hammerich), M. Dekker, New York, **2001**, p. 1163.
- [5] J. H. Utley, M. Folmer Nielsen, P. B. Wyatt, in *Organic Electrochemistry* (Eds.: O. Hammerich, B. Speiser), CRC Press, Boca Raton, **2016**, p. 1625.
- [6] J. Yoshida, K. Kataoka, R. Horcajada, A. Nagaki, *Chem. Rev.* **2008**, *108*, 2265–2299.
- [7] J. B. Sperry, D. L. Wright, *Chem. Soc. Rev.* **2006**, *35*, 605–621.
- [8] K. D. Moeller, *Tetrahedron* **2000**, *56*, 9527–9554.
- [9] O. Hammerich, B. Speiser, *Organic Electrochemistry*, CRC Press, Boca Raton, **2016**.
- [10] A. J. Fry, *Synthetic Organic Electrochemistry*, Wiley, New York, **1989**.
- [11] H. Lund, *J. Electrochem. Soc.* **2002**, *149*, S21.
- [12] J. Utley, *Industrial Electrochemistry*, **1997**.
- [13] H. Pütter, in *Org. Electrochem.* (Eds.: H. Lund, O. Hammerich), M. Dekker, New York, **2001**, p. 1259.
- [14] E. Steckhan, in *Ullmann's Encyclopedia of Industrial Chemistry*, Wiley-VCH, Weinheim, **2012**, p. 315.
- [15] M. Yan, Y. Kawamata, P. S. Baran, *Angew. Chem. Int. Ed.* **2017**, DOI 10.1002/anie.201707584.
- [16] J. Yoshida, *Electrochem. Soc. Interface* **2009**, *18*, 40–45.
- [17] A. Ziogas, G. Kolb, M. O'Connell, A. Attour, F. Lapique, M. Matlosz, S. Rode, *J. Appl. Electrochem.* **2009**, *39*, 2297–2313.
- [18] D. Horii, M. Atobe, T. Fuchigami, F. Marken, *Electrochem. Commun.* **2005**, *7*, 35–39.
- [19] A. Attour, P. Dirrenberger, S. Rode, A. Ziogas, M. Matlosz, F. Lapique, *Chem. Eng. Sci.* **2011**, *66*, 480–489.
- [20] K. Watts, A. Baker, T. Wirth, *J. Flow Chem.* **2014**, *4*, 2–11.
- [21] D. Pletcher, R. A. Green, R. C. D. Brown, *Chem. Rev.* **2017**, DOI: 10.1021/acs.chemrev.7b00360.

- [22] A. A. Folgueiras-Amador, T. Wirth, *J. Flow Chem.* **2017**, *7*, 94–95.
- [23] A. Volta, *Phil. Trans. R. Soc. London* **1800**, *90*, 403–431.
- [24] W. Nicholson, *J. Nat. Philos. Chem. Arts* **1801**, *4*, 179–187.
- [25] M. Faraday, *Phil. Trans. R. Soc. London* **1834**, *124*, 77–122.
- [26] M. Faraday, *Experimental Researches in Electricity, Volume 1*, Dent, London, **1839**.
- [27] H. Kolbe, *Justus Liebigs Ann. Chem.* **1849**, *69*, 257–294.
- [28] J. Volke, F. Liska, *Electrochemistry in Organic Synthesis*, Springer-Verlag, Germany, **1994**.
- [29] M. M. Baizer, *Naturwissenschaften* **1969**, *56*, 405–409.
- [30] C. A. Paddon, M. Atobe, T. Fuchigami, P. He, P. Watts, S. J. Haswell, G. J. Pritchard, S. D. Bull, F. Marken, *J. Appl. Electrochem.* **2006**, *36*, 617–634.
- [31] D. E. Danly, *J. Electrochem. Soc.* **1984**, *131*, 435C–442C.
- [32] D. Pletcher, F. C. Walsh, *Industrial Electrochemistry*, Blackie Academic & Professional, Glasgow, **1990**.
- [33] T. Fuchigami, M. Atobe, S. Inagi, *Fundamentals and Applications of Organic Electrochemistry*, Wiley & Sons, Ltd, **2015**.
- [34] B. Speiser, *Encyclopedia of Electrochemistry Volume 8*, Wiley-VCH, **2004**.
- [35] R. A. Green, R. C. D. Brown, D. Pletcher, *J. Flow Chem.* **2015**, *5*, 31–36.
- [36] R. Francke, R. D. Little, *Chem. Soc. Rev.* **2014**, *43*, 2492–2521.
- [37] H. Tanaka, Y. Kawakami, K. Goto, M. Kuroboshi, *Tetrahedron Lett.* **2001**, *42*, 445–448.
- [38] H. Shiigi, H. Mori, T. Tanaka, Y. Demizu, O. Onomura, *Tetrahedron Lett.* **2008**, *49*, 5247–5251.
- [39] E. Steckhan, Ed. , *Topics in Current Chemistry, Electrochemistry I*, Springer-Verlag, New York, **1987**.
- [40] W. Schmidt, E. Steckhan, *Angew. Chem. Int. Ed.* **1978**, *17*, 673–674.
- [41] A. M. Couper, D. Pletcher, F. C. Walsh, *Chem. Rev.* **1990**, *90*, 837–865.
- [42] C. G. Zoski, Ed. , *Handbook of Electrochemistry*, Elsevier, **2007**.
- [43] J. D. Watkins, F. Marken, in *Org. Electrochem.* (Eds.: O. Hammerich, B. Speiser), CRC Press, Boca Raton, **2016**, pp. 331–335.
- [44] J. P. Hallett, T. Welton, *Chem. Rev.* **2011**, *111*, 3508–3576.
- [45] T. Wirth, Ed. , *Microreactors in Organic Synthesis and Catalysis*, Wiley-VCH, Weinheim, **2008**.
- [46] J. Yoshida, *Flash Chemistry: Fast Organic Synthesis in Microsystems*, Wiley-

- VCH, Weinheim, **2008**.
- [47] M. Küpper, V. Hessel, H. Löwe, W. Stark, J. Kinkel, M. Michel, H. Schmidt-Traub, *Electrochim. Acta* **2003**, *48*, 2889–2896.
- [48] J. Jörissen, B. Speiser, in *Org. Electrochem.* (Eds.: O. Hammerich, B. Speiser), CRC Press, Boca Raton, **2016**, p. 263.
- [49] H. Lund, in *Org. Electrochem.* (Eds.: H. Lund, O. Hammerich), M. Dekker, New York, **2001**, p. 223.
- [50] S. Suga, S. Suzuki, A. Yamamoto, J. Yoshida, *J. Am. Chem. Soc.* **2000**, *122*, 10244–10245.
- [51] J. Yoshida, S. Suga, S. Suzuki, N. Kinomura, A. Yamamoto, K. Fujiwara, *J. Am. Chem. Soc.* **1999**, *121*, 9546–9549.
- [52] S. Suga, M. Okajima, K. Fujiwara, J. Yoshida, *QSAR Comb. Sci.* **2005**, *24*, 728–741.
- [53] S. Suga, M. Okajima, K. Fujiwara, J. Yoshida, *J. Am. Chem. Soc.* **2001**, *123*, 7941–7942.
- [54] C. Gütz, M. Bänziger, C. Bucher, T. R. Galvão, S. R. Waldvogel, *Org. Process Res. Dev.* **2015**, *19*, 1428–1433.
- [55] C. Gütz, A. Stenglein, S. R. Waldvogel, *Org. Process Res. Dev.* **2017**, *21*, 771–778.
- [56] R. Horcajada, M. Okajima, S. Suga, J. Yoshida, *Chem. Commun.* **2005**, 1303–1305.
- [57] K. D. Moeller, *Top. Curr. Chem.* **1997**, *185*, 50–86.
- [58] H. J. Schäfer, in *Org. Electrochem.* (Eds.: H. Lund, O. Hammerich), M. Dekker, New York, **2001**, p. 883.
- [59] S. Torii, H. Tanaka, in *Org. Electrochem.* (Eds.: H. Lund, O. Hammerich), M. Dekker, New York, **2001**, p. 499.
- [60] K. Uneyama, *Tetrahedron* **1991**, *47*, 555–562.
- [61] K. Arai, K. Watts, T. Wirth, *Chemistry Open* **2014**, *3*, 23–28.
- [62] Y. Chen, S. Yekta, A. K. Yudin, *Chem. Rev.* **2003**, *103*, 3155–3211.
- [63] M. C. Kozlowski, B. J. Morgan, E. C. Linton, *Chem. Soc. Rev.* **2009**, *38*, 3193.
- [64] M. L. Mohler, G. S. Kang, S. S. Hong, R. Patil, O. V. Kirichenko, W. Li, I. M. Rakov, E. E. Geisert, D. D. Miller, *J. Med. Chem.* **2006**, *49*, 5845–5848.
- [65] J. Xie, J. G. Pierce, R. C. James, A. Okano, D. L. Boger, *J. Am. Chem. Soc.* **2011**, *133*, 13946–13949.
- [66] S. Inagi, S. Hayashi, K. Hosaka, T. Fuchigami, *Macromolecules* **2009**, *42*, 3881–3883.
- [67] M. Tange, T. Okazaki, S. Iijima, *ACS Appl. Mater. Interfaces* **2012**, *4*, 6458–6462.

- [68] L. Ebersson, M. P. Hartshorn, O. Persson, *J. Chem. Soc., Perkin Trans. 2* **1995**, 1735–1744.
- [69] L. Ebersson, M. P. Hartshorn, O. Persson, *Angew. Chem. Int. Ed.* **1995**, *34*, 2268–2269.
- [70] I. A. Shuklov, N. V. Dubrovina, A. Börner, *Synthesis* **2007**, 2925–2943.
- [71] A. Kirste, B. Elsler, G. Schnakenburg, S. R. Waldvogel, *J. Am. Chem. Soc.* **2012**, *134*, 3571–3576.
- [72] A. Kirste, G. Schnakenburg, F. Stecker, A. Fischer, S. R. Waldvogel, *Angew. Chem. Int. Ed.* **2010**, *49*, 971–975.
- [73] A. Kirste, G. Schnakenburg, S. R. Waldvogel, *Org. Lett.* **2011**, *13*, 3126–3129.
- [74] A. Kirste, S. Hayashi, G. Schnakenburg, I. M. Malkowsky, F. Stecker, A. Fischer, T. Fuchigami, S. R. Waldvogel, *Chem. Eur. J.* **2011**, *17*, 14164–14169.
- [75] B. Riehl, K. M. Dyballa, R. Franke, S. R. Waldvogel, *Synthesis* **2017**, *49*, 252–259.
- [76] S. Lips, A. Wiebe, B. Elsler, D. Schollmeyer, K. M. Dyballa, R. Franke, S. R. Waldvogel, *Angew. Chem. Int. Ed.* **2016**, *55*, 10872–10876.
- [77] A. Wiebe, D. Schollmeyer, K. M. Dyballa, R. Franke, S. R. Waldvogel, *Angew. Chem. Int. Ed.* **2016**, *55*, 11801–11805.
- [78] B. Elsler, A. Wiebe, D. Schollmeyer, K. M. Dyballa, R. Franke, S. R. Waldvogel, *Chem. Eur. J.* **2015**, *21*, 12321–12325.
- [79] L. Schulz, M. Enders, B. Elsler, D. Schollmeyer, K. M. Dyballa, R. Franke, S. R. Waldvogel, *Angew. Chem. Int. Ed.* **2017**, *56*, 4877–4881.
- [80] T. Kashiwagi, B. Elsler, S. R. Waldvogel, T. Fuchigami, M. Atobe, *J. Electrochem. Soc.* **2013**, *160*, G3058–G3061.
- [81] J. Yoshida, M. Sugawara, M. Tatsumi, N. Kise, *J. Org. Chem.* **1998**, *63*, 5950–5961.
- [82] D. Horii, T. Fuchigami, M. Atobe, *J. Am. Chem. Soc.* **2007**, *129*, 11692–11693.
- [83] G. P. Roth, R. Stalder, T. R. Long, D. R. Sauer, S. W. Djuric, *J. Flow Chem.* **2013**, *3*, 34–40.
- [84] F. H. Osman, F. A. El-Samahy, *Chem. Rev.* **2002**, *102*, 629–677.
- [85] D. Nematollahi, E. Tammari, *J. Org. Chem.* **2005**, *70*, 7769–7772.
- [86] M. E. Jung, F. Perez, *Org. Lett.* **2009**, *11*, 2165–2167.
- [87] A. R. Fakhari, D. Nematollahi, M. Shamsipur, S. Makarem, S. S. H. Davarani, A. Alizadeh, H. R. Khavasi, *Tetrahedron* **2007**, *63*, 3894–3898.
- [88] H. W. Wanzlick, M. Lehmann-Horchler, S. Mohrmann, R. Gritzky, H. Heidepriem, B. Pankow, *Angew. Chem. Int. Ed.* **1964**, *3*, 401–408.
- [89] T. Kashiwagi, F. Amemiya, T. Fuchigami, M. Atobe, *J. Flow Chem.* **2013**, *3*, 17–

- 22.
- [90] B. Meunier, S. P. Visser, S. Shaik, *Chem. Rev.* **2004**, *104*, 3947–3980.
- [91] D. J. Waldon, Y. Teffera, A. E. Colletti, J. Liu, D. Zurcher, K. W. Copeland, Z. Zhao, *Chem. Res. Toxicol.* **2010**, *23*, 1947–1953.
- [92] K. Speck, T. Magauer, *Beilstein J. Org. Chem.* **2013**, *9*, 2048–2078.
- [93] W. Tang, R. A. Stearns, S. M. Bandiera, Y. Zhang, C. Raab, M. P. Braun, D. C. Dean, J. Pang, K. H. Leung, G. A. Doss, et al., *Drug Metab. Dispos.* **1999**, *27*, 365–372.
- [94] R. Stalder, G. P. Roth, *ACS Med. Chem. Lett.* **2013**, *4*, 1119–1123.
- [95] H. A. El-Masri, C. J. Portier, *Drug Metab. Dispos.* **1998**, *26*, 585–594.
- [96] S. H. Curry, *Anal. Chem.* **1968**, *40*, 1251–1255.
- [97] H. P. Permentier, A. P. Bruins, R. Bischoff, *Mini. Rev. Med. Chem.* **2008**, *8*, 46–56.
- [98] U. Karst, *Angew. Chem. Int. Ed.* **2004**, *43*, 2476–2478.
- [99] A. M. Jones, C. E. Banks, *Beilstein J. Org. Chem.* **2014**, *10*, 3056–3072.
- [100] T. Shono, Y. Matsumura, K. Tsubata, *Org. Synth.* **1985**, *63*, 206.
- [101] E. Gravel, E. Poupon, *Nat. Prod. Rep.* **2010**, *27*, 32–56.
- [102] M. A. Kabeshov, B. Musio, P. R. D. Murray, D. L. Browne, S. V. Ley, *Org. Lett.* **2014**, *16*, 4618–4621.
- [103] R. A. Green, D. Pletcher, S. G. Leach, R. C. D. Brown, *Org. Lett.* **2015**, *17*, 3290–3293.
- [104] J. Mahatthananchai, J. W. Bode, *Acc. Chem. Res.* **2014**, *47*, 696–707.
- [105] A. Grossmann, D. Enders, *Angew. Chem. Int. Ed.* **2012**, *51*, 314–325.
- [106] A. T. Biju, N. Kuhl, F. Glorius, *Acc. Chem. Res.* **2011**, *44*, 1182–1195.
- [107] V. Nair, S. Vellalath, B. P. Babu, *Chem. Soc. Rev.* **2008**, *37*, 2691–2698.
- [108] R. A. Green, D. Pletcher, S. G. Leach, R. C. D. Brown, *Org. Lett.* **2016**, *18*, 1198–1201.
- [109] R. A. Green, K. E. Jolley, A. A. M. Al-Hadedi, D. Pletcher, D. C. Harrowven, O. De Frutos, C. Mateos, D. J. Klauber, J. A. Rincón, R. C. D. Brown, *Org. Lett.* **2017**, *19*, 2050–2053.
- [110] P. He, P. Watts, F. Marken, S. J. Haswell, *Angew. Chem. Int. Ed.* **2006**, *45*, 4146–4149.
- [111] P. He, P. Watts, F. Marken, S. J. Haswell, *Lab. Chip* **2007**, *7*, 141–143.
- [112] N. A. Porter, D. M. Scott, I. J. Rosenstein, B. Giese, A. Veit, H. G. Zeitz, *J. Am. Chem. Soc.* **1991**, *113*, 1791–1799.

- [113] J. P. Devlin, W. D. Ollis, J. E. Thorpe, R. J. Wood, B. J. Broughton, P. J. Warren, K. R. H. Wooldridge, D. E. Wright, *J. Chem. Soc., Perkin Trans. 1* **1975**, 830.
- [114] G. Sabitha, R. Srividya, J. S. Yadav, *Tetrahedron* **1999**, *55*, 4015–4018.
- [115] M. R. Chapman, Y. M. Shafi, N. Kapur, B. N. Nguyen, C. E. Willans, *Chem. Commun.* **2015**, *51*, 1282–4.
- [116] F. Amemiya, D. Horii, T. Fuchigami, M. Atobe, *J. Electrochem. Soc.* **2008**, *155*, E162-165.
- [117] J. T. Hill-Cousins, J. Kuleshova, R. A. Green, P. R. Birkin, D. Pletcher, T. J. Underwood, S. G. Leach, R. C. D. Brown, *ChemSusChem* **2012**, *5*, 326–331.
- [118] R. Ciriminna, M. Pagliaro, *Org. Process Res. Dev.* **2010**, *14*, 245–251.
- [119] L. Tebben, A. Studer, *Angew. Chem. Int. Ed.* **2011**, *50*, 5034–5068.
- [120] K. Alfonsi, J. Colberg, P. J. Dunn, T. Fevig, S. Jennings, T. A. Johnson, H. P. Kleine, C. Knight, M. A. Nagy, D. A. Perry, et al., *Green Chem.* **2008**, *10*, 31–36.
- [121] A. Bogdan, D. T. McQuade, *Beilstein J. Org. Chem.* **2009**, *5*, 34–36.
- [122] J. Chen, L. Zhou, C. K. Tan, Y. Y. Yeung, *J. Org. Chem.* **2012**, *77*, 999–1009.

CHAPTER 2: Flow electrochemical reactor design and manufacture

CHAPTER 2: Flow electrochemical reactor design and manufacture	51
2.1. Introduction	53
2.1.1. Flow electrochemical cells.....	53
2.1.2. Stereolithography (SLA) printers	63
2.2. Reactor design.....	64
2.2.1. Aluminium electrochemical reactor.....	68
2.2.2. 3D printed flow electrochemical reactor	69
2.3. Conclusions	71
2.4. References	72

2.1. Introduction

2.1.1. Flow electrochemical cells

In this section, the most relevant and sophisticated electrochemical flow cells currently designed will be described.

In 2015 Waldvogel *et al.* published a flow electrochemical reactor that was developed to perform dehalogenation.^[1] The flow electrochemical cell was designed to scale up the desired reaction, which has been already reported under batch conditions, and applied to a broad scope of substrates of dibromocyclopropane derivatives,^[2] but shows some limitations in the productivity rate.

The electrochemical reactor consists of a divided cell and the outer body comprises two blocks made of Teflon[®], which are connected by two stainless steel plates. Each Teflon[®] piece has a small space where the electrodes can be placed, creating the reaction chambers. Graphite felt is used as anode material, and leaded bronze (15% Pb) is used as cathode. A Nafion[®] membrane separates the anodic and cathodic chambers (Figure 2.1).

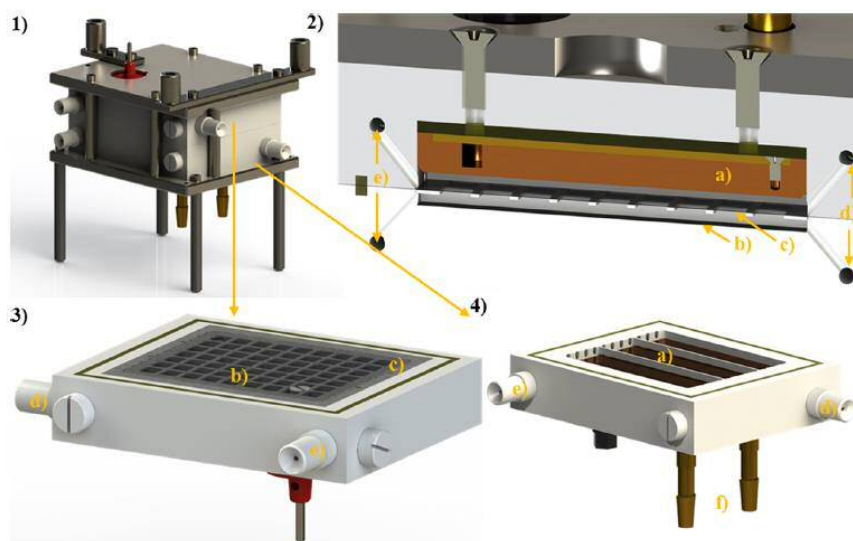
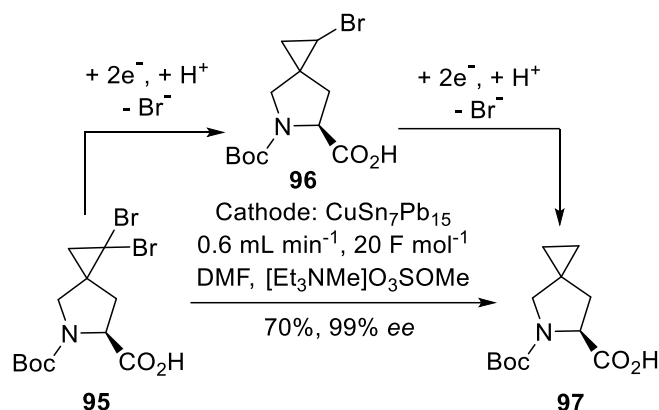


Figure 2.1: 1) Total view of the flow cell, 2) cross section of the whole cell, 3) anodic half-cell and Nafion[®] separator, 4) cathodic half-cell: a) cathode, CuSn₇Pb₁₅; b) anode, graphite; c) Nafion[®] membrane; d) inlets for electrolyte; e) outlets for electrolyte; f) contacts for cooling media.^[1] (Reproduced with permission from ref.^[1] Copyright (2015) American Chemical Society).

Compound **97** was synthesised from the dibrominated spirocyclopropane-proline derivative **95** in good yield without racemisation occurring (Scheme 2.1).



Scheme 2.1: Electrolytical dehalogenation.^[1]

Methanol is used as sacrificial compound to be oxidised at the anode and this anolyte solution is recycled continuously, while the catholyte is collected and the product is isolated after a single pass through the flow cell (Figure 2.2).

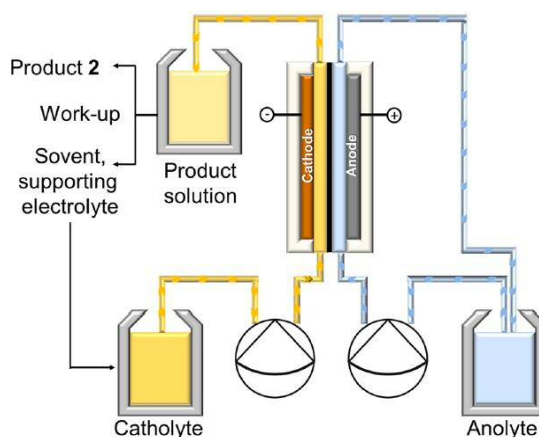


Figure 2.2: Schematic set-up of the flow electrochemical cell and the recycling streams.^[1] (Reproduced with permission from ref.^[1] Copyright (2015) American Chemical Society).

More recently in 2017, Waldvogel and coworkers reported a modular electrochemical flow cell.^[3] The cell consists of two Teflon[®] blocks (100 x 40 x 16 mm) with an opening (60 x 20 x 3 mm) where the electrode can be placed (Figure 2.3). The electrode is positioned onto the Teflon[®] piece by thermal treatment, causing it to expand upon heating to 200 °C. The electrode is placed in the cavity and when the Teflon[®] cools down, it contracts and holds the electrode, sealing the gap created. If the electrode is to be removed, it can be done by thermal treatment in a similar way as described above. A gasket/spacer with variable thickness (between 0.12 and 2.0 mm) is used to separate both electrodes and it will serve as reaction channel. This reactor can also be employed as a divided cell if a Nafion[®] membrane sandwiched between two spacers is used. The whole

device is tightened up by eight screws and two plates made of stainless steel. The electrode material can be selected according to the reaction of interest.

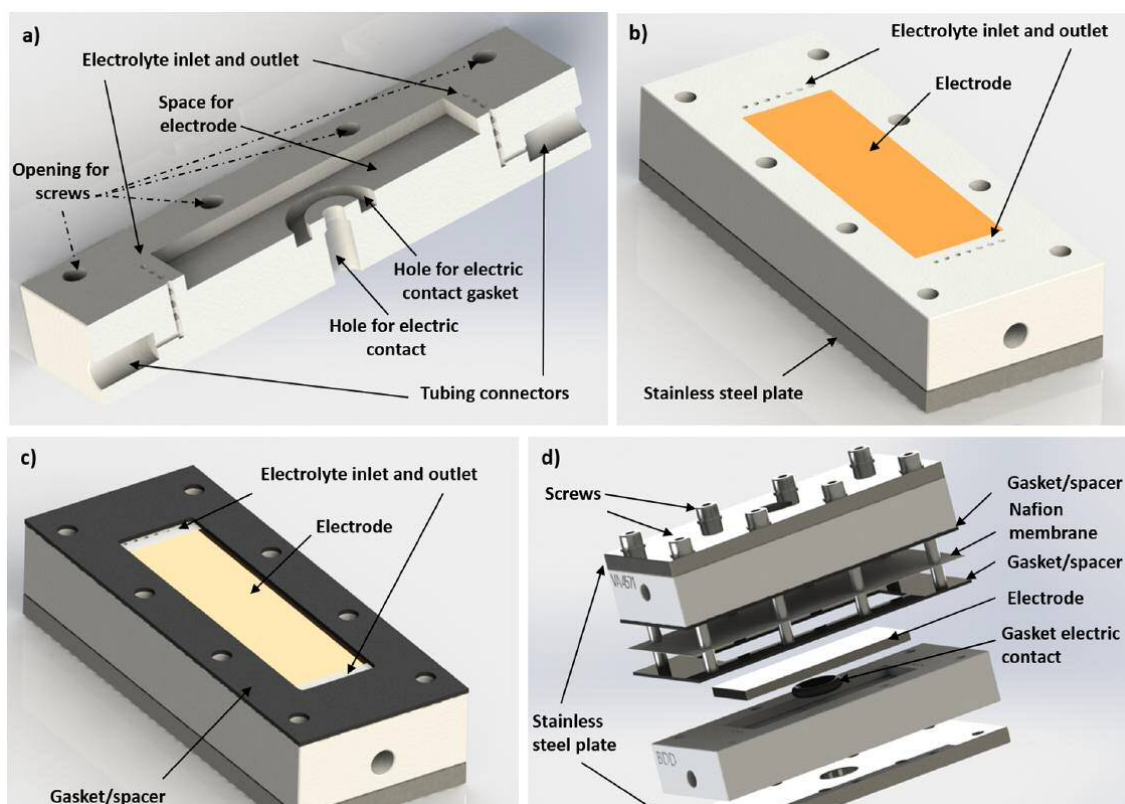
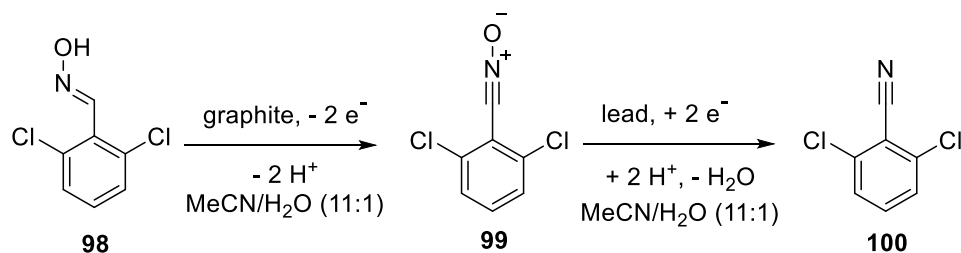


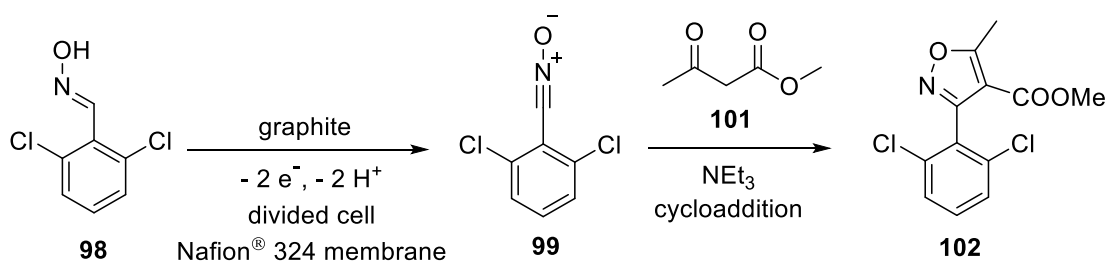
Figure 2.3: a) Cross-section of the Teflon[®] block; b) half-cell with the stainless steel plate, the Teflon[®] block and the electrode placed in the Teflon[®] block; c) half part of the cell with the gasket; d) Complete reactor as a divided cell. For an undivided cell, only one gasket is needed, the second one and the Nafion[®] membrane are excluded.^[3] (Reproduced with permission from ref.^[3] Copyright (2017) American Chemical Society).

The reactor was tested for two different kind of synthesis, using either an undivided cell arrangement or a divided cell. For the application of the undivided cell, oxime **98** was oxidised at the anode to form the nitrile-*N*-oxide **99**, which is subsequently reduced at the cathode to give the nitrile **100** (Scheme 2.2). The use of a thin spacer is crucial in this transformation (0.12 mm), since a good mass transfer between the anode and the cathode is required because product **99**, formed at the anode, has to diffuse to the cathode to undergo the second transformation to product **100**. This efficient mass transfer between both electrode surfaces is easily achieved using a flow-type reactor, demonstrating one of the clear advantages of such devices. The desired nitrile (**100**) was obtained in 63% yield, improving the 41% yield obtained in batch.



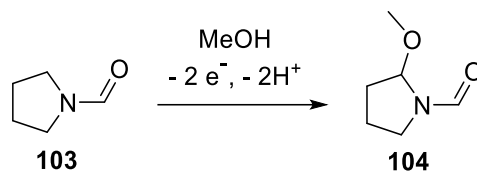
Scheme 2.2: Synthesis of nitriles and aldoximes from a domino-oxidation-reduction.^[3]

As for the divided mode of the flow cell, a similar transformation was studied, but in this case making use of the divided compartments. The nitrile-*N*-oxide **99** from the anolyte was not reduced as in the previous transformation, since the cathode and anode compartments were separated in this case. Instead, **99** reacted with methyl acetoacetate (**101**) to perform a 1,3-dipolar cycloaddition and afford the corresponding product **102** (Scheme 2.3).



Scheme 2.3: Electrochemical oxidation of 1 in a divided cell and subsequent 1,3-dipolar cycloaddition.^[3]

Brown, Pletcher and coworkers have contributed significantly to the emerging technology of flow electrosynthesis, developing several electrochemical flow cells in the last few years, improving the design of the reactors and aiming to achieve a multigram per hour rate of the electrochemical transformation. The electrochemical methoxylation of *N*-formylpyrrolidine (**103**) has been used as a test reaction for investigating the efficacy of different flow electrochemical reactors, in order to improve the productivity of this type of cells.



Scheme 2.4: Methoxylation of *N*-formylpyrrolidine.

Four different flow electrolytic cells have been tested and optimised to achieve a high conversion in a single pass, rapid electrolysis and operation with low or no loading of supporting electrolyte.^[4-7] In 2011, a star shaped microchannel electrolytical cell was developed with a 600 mm long x 1 mm wide channel and 500 μm interelectrode gap, and it was used to perform the methoxylation of *N*-formylpyrrolidine (Figure 2.4a).^[4] The same authors studied the same reaction using the commercially available flow electrochemical reactor supplied by Syrris Ltd (Figure 2.4b and Figure 2.4c), with a patterned recessed channel 700 mm long x 1.5 mm wide and 200 μm interelectrode gap, providing a bigger reaction volume. This reactor makes the production of the desired product possible in shorter time.^[5]

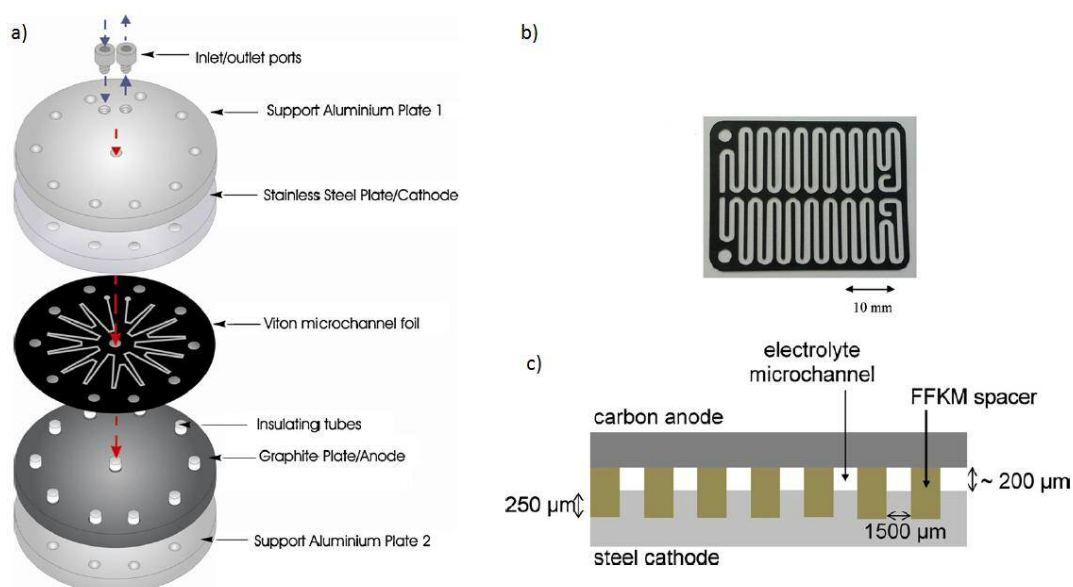


Figure 2.4: a) Microflow reactor with the main components of the cell, b) cell spacer for the Syrris Flux module, c) flow electrolytical cell diagram.^[4,5] (Reproduced from ref.^[4,5] with kind permission from Elsevier).

In 2015, a flow electrolysis cell (Ammonite 15 cell available from Cambridge Reactor Design Ltd, Cambridge, UK) with a 5 mL internal volume was developed, which enables laboratory synthesis on a multigram scale. This cell has a spiral reaction channel 2000 mm long and 5 mm wide (Figure 2.5), with an interelectrode gap of 500 μm .^[6] With the Ammonite 15 electrochemical reactor a production of 20 grams per hour was achieved. However, the performance of the cell is limited by the current density accessible from the anode material available for this reactor.

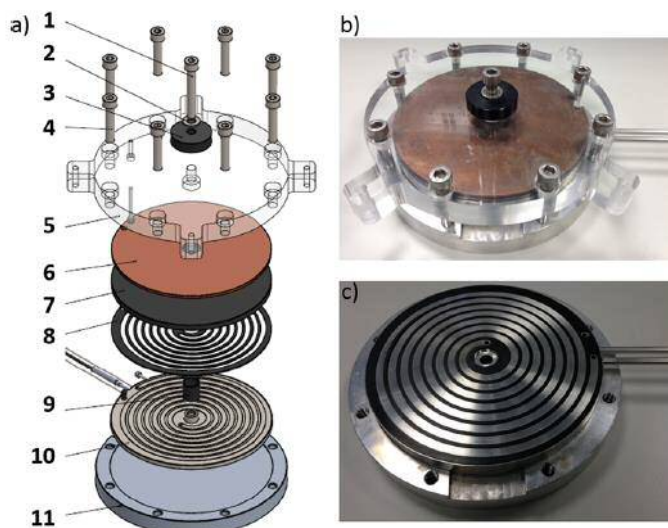


Figure 2.5: Ammonite 15 electrolysis cell: a) Components of the flow electrolysis cell; 1 Central bolt; 2. Washer; 3. Insulating tube; 4. Peripheral bolt; 5. Perspex top plate; 6. Cu baking plate; 7. Carbon/polymer anode plate; 8. Perfluoroelastomer gasket; 9. Insulating tube around central bolt; 10. Stainless steel cathode plate with spiral groove; 11. Aluminium base plate. b) Picture of the assembled reactor. c) Picture of the open reactor with gasket fitted into the cathode plate (spiral channel).^[6]

A smaller version of this cell was designed and published in 2016, also manufactured by Cambridge Reactor Design Ltd (commercial name: Ammonite 8 electrolysis cell). Intended for use in a synthetic organic laboratory, this latter version has a smaller volume (1 mL) and it has been optimised by extending the length of the flow channel, which is 1000 mm long and 2 mm wide with an interelectrode gap of 500 μm , giving a narrower flow path that can improve the electrochemical reaction (Figure 2.6).^[7]

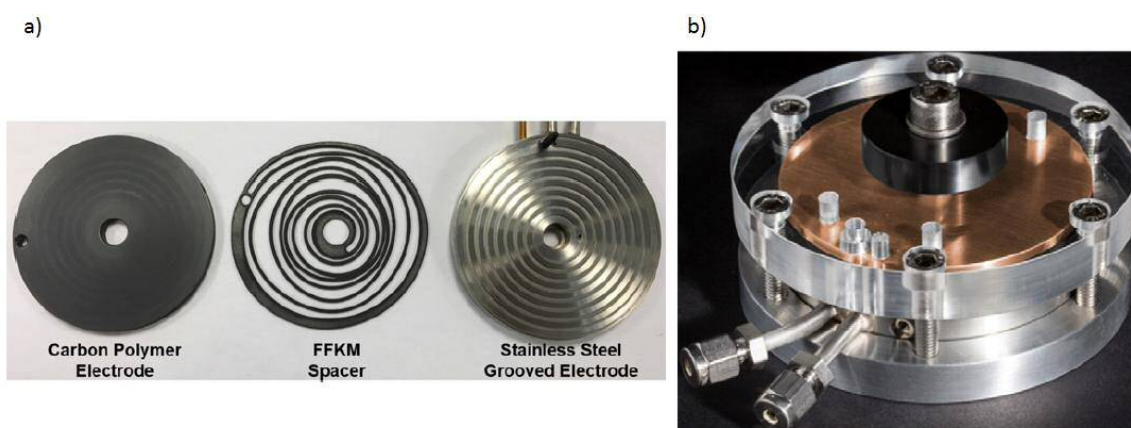


Figure 2.6: Ammonite 8 electrolysis cell: a) Components of the extended channel length flow electrolysis cell; b) the complete cell.^[7]

A comparison of the outcome of the four flow electrochemical reactors described above is summarised in Table 2.1.

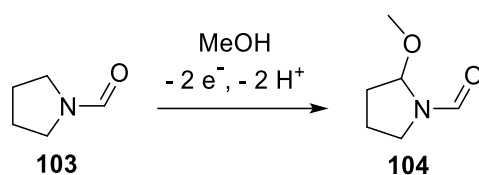


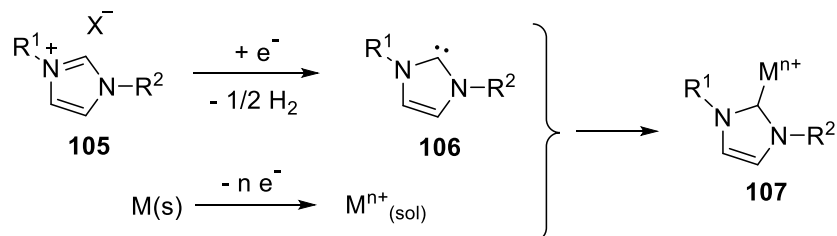
Table 2.1: Comparison of the outcome of the different flow electrochemical reactors.^[4-7]

Entry	Cell description	Flow rate (mL min ⁻¹)	Conversion (%)	Rate max ^a (g h ⁻¹)	Ref
1	Star shaped microchannel: 600 mm long x 1 mm wide (500 μm interelectrode gap)	0.1	96	0.078	[4]
		3.5	33	0.95	
2	Patterned recessed channel: 700 mm long x 1.5 mm wide (200 μm interelectrode gap)	3	>95	1.8	[5]
3	Spiral shaped microchannel: 2000 mm long x 5 mm wide (500 μm interelectrode gap)	16	88	20.7	[6]
4	Spiral shaped microchannel: 1000 mm long x 2 mm wide (500 μm interelectrode gap)	1	82	3.16	[7]

^a Maximum rate of product formation

In 2015 Willians *et al.* reported the development of a flow reactor for the synthesis of *N*-heterocyclic carbenes (NHCs, **106**), which are very important motifs for organometallic chemistry and catalysis such as hydrosilylation, olefin metathesis, hydrogenation and cross-coupling reactions.^[8,9] They also have recently become promising for the synthesis of antimicrobials and for chemotherapeutics.^[10,11] In the report by Willians, metal-NHCs are produced electrochemically *via* reduction of an imidazolium ion (**105**) at the cathode, releasing hydrogen, to form the free *N*-heterocyclic

carbene (**106**).^[12] At the same time, a copper anode is used as a sacrificial electrode to be oxidized and form copper (I) ions. The free carbene and the copper (I) ion combine to give the Cu-NHC complex (**107**, Scheme 2.5).



Scheme 2.5: Electrochemical synthesis of metal-NHC complexes.

The flow reactor designed for the synthesis of the desired Cu-NHC complex (Figure 2.7) consists of six square copper plates (50 x 50 x 1 mm), which are separated by five Teflon[®] spacers (1 mm thick). These spacers are cut with the shape of the channel used for the reaction (4 mm wide and 200 mm long). This design provides a total reactor volume of 4 mL and a surface area of 40 cm² (for each anode and cathode), which makes the reactor highly efficient, improving the output of the previously designed reactor where only two copper plates were used.

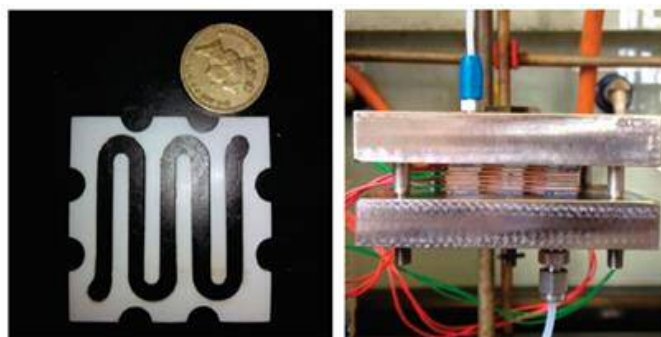
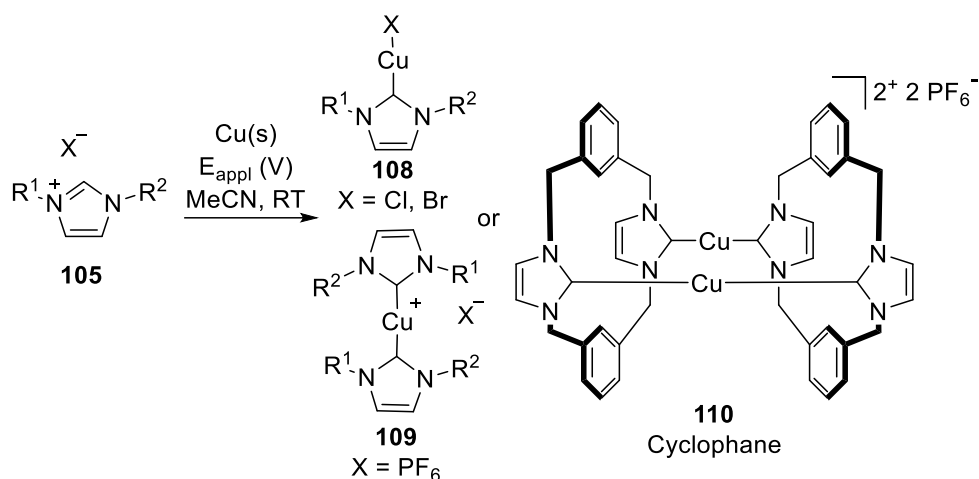


Figure 2.7: Picture of the Teflon[®] spacer with the reactor channel cut (left) and the electrochemical flow-reactor (right).^[12] (Reproduced from ref.^[12] with kind permission from the Royal Society of Chemistry).

A variety of Cu^I-mono- and bis-NHC complexes with different nitrogen-substituents have been synthesised in high yields under neutral and ambient conditions with yields up to 95% (Scheme 2.6).



Scheme 2.6: Cu-NHC complexes.

The continuous flow electrochemical module Asia Flux developed by Syrris Ltd (Figure 2.8 and Figure 2.4b) has been used by several research groups to study different reactions.^[5,13–18] The Asia Flux module and electrolytic cell can be used with a range of electrodes, which can be exchanged with no need for specific tools. The module can be used in galvanostatic (constant current) or potentiostatic (constant voltage) mode. This reactor can operate with pressures up to 5 bar and temperatures from 0 to 60 °C. It consists of two electrodes separated by a gasket with a snaking channel, which are the flow path (225 μ L).

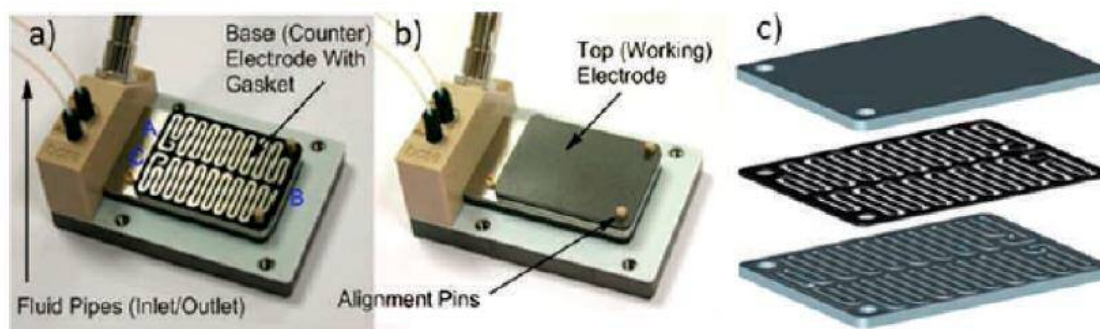


Figure 2.8: Asia Flux module for continuous flow electrochemistry, supplied by Syrris Ltd. a) Internal picture of the reactor showing the grooved electrode and elastomer gasket to form meandered channel; b) cell with the top electrode in place; c) schematic picture of the grooved electrode and top electrode, with the gasket in between them.^[19]

IKA[®] has also developed a flow electrochemical cell, the ElectraSyn flow. The reactor consists of two parts, the so-called “half cells”, and each of them holds an electrode. There are nine different half cells available with different electrode materials that can be

combined. It can be used as either undivided or divided cell, using a Nafion[®] membrane as separator (Figure 2.9).

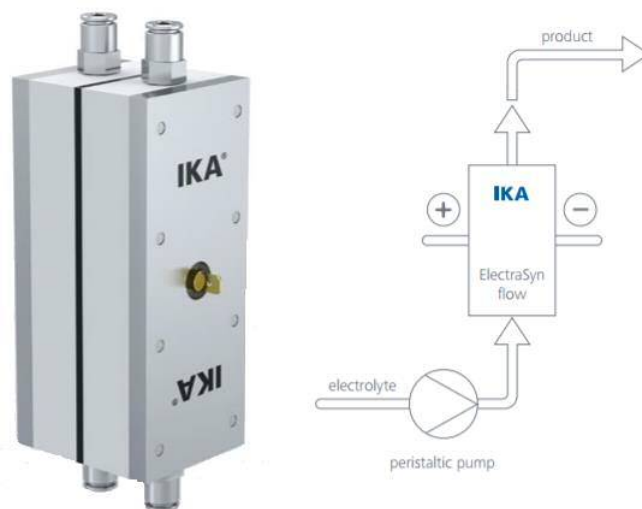


Figure 2.9: IKA[®] ElectraSyn flow cell. Image reproduced with kind permission from IKA[®] <http://www.ikaprocess.com/Products/Continuous-flow-cell-cph-45/>

In 2011 Wirth *et al.* designed a microflow electrochemical reactor that consists of two platinum electrodes that are separated by a fluorinated ethylene propylene (FEP) foil of different thicknesses, into which a reaction channel is cut (Figure 2.10).^[20] This reactor has been used for the synthesis of diaryliodonium salts (**117**), as they are attractive alternatives to heavy metal based catalysts, since they can be used in similar reactions.^[21,22] They are synthesised in one-step by electrochemical oxidation of an iodoarene (**114**) in the presence of another arene (**115**).^[20]

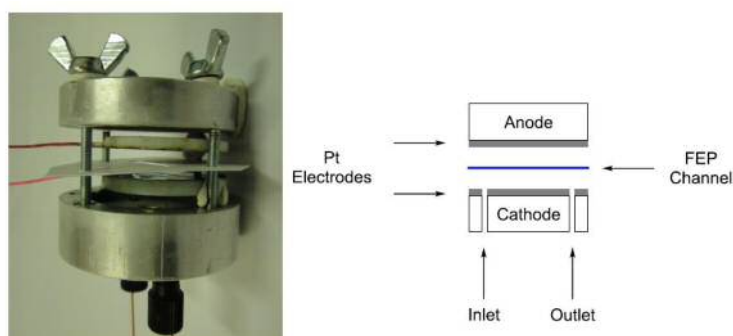
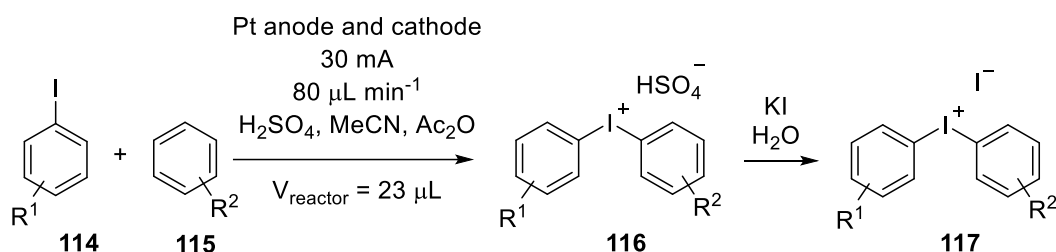


Figure 2.10: Electrochemical flow microreactor.^[20]

Wirth and coworkers examined the oxidation of compound **114** at the anode. The reaction produces a radical cation that undergoes a reaction with arene **115**, forming an intermediate that will lose a second electron (**116**).^[23] The reduction of sulfuric acid is

used as the counter reaction at the cathode (proton reduction to form hydrogen gas), and also as counter ion for the positively charged iodonium salt. After the reaction, the reaction mixture was treated with potassium iodide in water to give the more soluble diaryliodonium iodide salts (**117**) in up to 72% yield (Scheme 2.7).



Scheme 2.7: Electrochemical generated diaryliodonium salts.

2.1.2. Stereolithography (SLA) printers

The term “stereolithography” was introduced by Charles Hull in 1986, when he patented the first stereolithography printer.^[24] The word is a combination of the Greek words “stereos” (solid), “lithos” (stone or rock) and “graphia” (writing). The patent “Apparatus for Production of Three-Dimensional Objects by Stereolithography” described a device to make solid objects by successively creating layers of a polymerizable material. It consists of a liquid photosensitive resin that is able to polymerise and solidify when exposed to light.

As SLA is considered as an easy and rapid technique for additive manufacturing (3D printing), it has been used for a broad range of applications. The electronic, packaging and medical industries, among others, use this kind of printing, that has evolved significantly in the last few years.

A computer aided design or computer aided manufacturing (CAD/CAM) software is used to draw the desire design of the object to be 3D printed, which will then be transferred onto the 3D printer device.

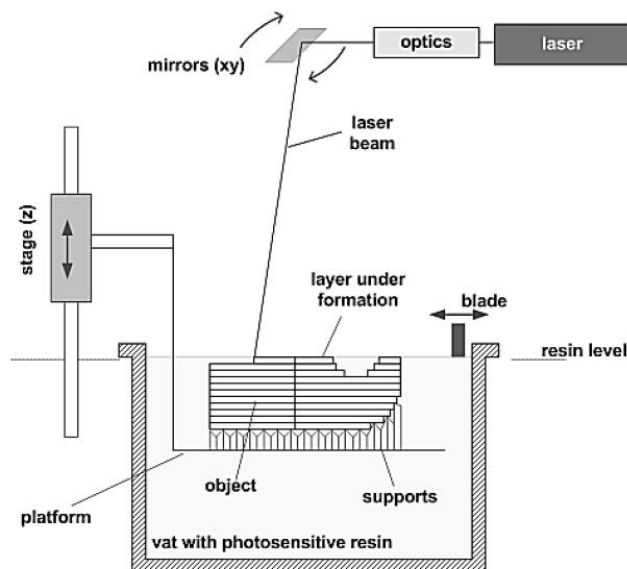


Figure 2.11: Sketch of the stereolithography printing process.^[25]

In these apparatuses, an elevator platform is used to support the base of the printed object. There is a vat where the liquid resin is contained, and this platform will move up or down the distance equivalent to the thickness of the layer that will be printed (typically from 0.025 to 0.15 mm). The subsequent layer will be formed in the same way, having some fresh material on the surface and curing it with the light beam to make it solid (Figure 2.11). This process is repeated for every layer until the 3D printing is complete.

For the manufacture of the reactor described in this thesis, a FormLabs Form 2 SLA printer was used. The resins used consist of methacrylic acid esters, photoinitiators, proprietary pigment, which will depend on the type of resin used, and other ingredients that are kept secret by the manufacturing company. More detailed information about the construction of the reactor will be given in Section 2.2.2.

2.2. Reactor design

A second-generation flow electrochemical reactor has been designed and manufactured, and its features will be described in this section.

Work begun by testing the “first-generation reactor” designed by Wirth *et al.* in 2011,^[20] which is described in the last part of Section 2.1.1. . As described in Chapter 1, the reactor has been of use for several interesting transformations, but there were some features that could be improved.

- Connectors:

Firstly, the fitting used in the tubing to introduce the electrolyte into the reactor were studied. In the first-generation reactor, the tube was connected by fitting and ferrule, but this led to some leaking after a few minutes of reaction. To avoid this problem, coned PEEK™ HPLC fittings (Figure 2.12) were used to achieve a better sealing at the inlet and outlet of the reactor.



Figure 2.12: coned PEEK™ HPLC fitting.

- Electrode surface:

In the second-generation reactor, the electrode surface has been increased to 25 cm² (5 x 5 cm), which is 3 times bigger than the surface available to use in the first-generation reactor (8.5 cm², diameter = 3.3 cm). This greater electrode surface brings the possibility to perform reactions with a higher production rate, which is very desirable for any synthetic application. As the idea is to work with commercially available electrode materials, which can be purchased from different suppliers, no customised material would be needed and there would be no restrictions when it comes to fit or adjust the electrode into the reactor. Since most of these commercially available electrode materials come as a square sheet or foil, the reactor has been designed with a square shape to avoid the waste of cut off pieces, whose cost is significant. This problem was faced with the first-generation reactor, that was round-shaped, and its design led to some valuable electrode material cut off pieces.

- Easily exchangeable electrode materials:

In the first-generation cell, only platinum electrodes were used for the work reported. The platinum was glued onto a PTFE sheet, and fitted tightly in the cavity that was on the aluminium housing part of the reactor. This made the ejection of the PTFE sheet very laborious when the electrode material had to be repaired or changed. The round shape

also inhibited the use of rigid films such as graphite, which could not be fabricated as a round piece in our local workshop.

Overcoming this has been solved by using a square shape electrode, which makes easier the electrode cutting to fit it in the cell, and it also simplifies the process of fitting and remove the electrode to be exchanged as needed. The system has been equipped in our laboratory with common electrode materials such as platinum, graphite, nickel, copper and boron doped diamond (BDD).

- Electrode-wire connection:

The electrode has to be connected to the power supply *via* metal contact. This was one of the most fragile parts of the first-generation reactor, where the platinum sheet was connected to a copper wire. This wire was fitted through a drilled hole in the PTFE body to be in contact with the electrode (Figure 2.13). This juncture was delicate and it had to be replaced after several uses. It also created some deformation on the platinum sheet, making it uneven in the part where the wire was located.



Figure 2.13: First-generation reactor electrode-wire connection.

To solve this electrode connection problem, a similar system was developed, but instead of having the hole drilled in the PTFE piece to hold the wire, the copper wire was connected to the central part of the electrode with tape (Figure 2.14). A hole in the middle part of the reactor housing was made for the wire to exit the reactor. This connection reduced the problem, however it still needed replacement occasionally. The PTFE sheet to which the platinum electrode was glued, after months of use under pressure also needed replacing, as the polymer was misshaped and did not remain flat. This also led to deformation of the platinum sheet.

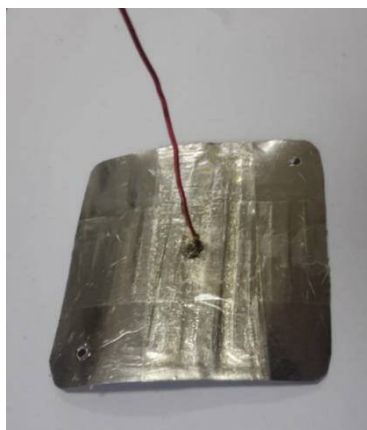


Figure 2.14: Pt electrode connected to wire.

The second attempt to improve the connection was to use auxiliary metal plates. For the electrodes that come as a thin and flexible sheet, such as platinum or nickel (0.05 – 0.1 mm thick), a 1.6 mm thick copper plate was used as a support for the electrode film. This copper plate is welded to a copper wire, which is then connected to the crocodile clips of the power supply. A picture of such plate and wire is shown in Figure 2.15a. This would solve two problems, the fragile electrode-wire connection to the power supply, and the deformation of the metal electrode used as a thin film, since the copper is hard enough to maintain it flat, and it will not get distorted as the PTFE does. A similar arrangement is used for thicker electrode materials, such as graphite (2.5 mm thick), but in this case there is no need for a rigid metal plate like copper, so an inexpensive stainless steel thin sheet was welded to a copper wire and used to connect the electrode to the power supply (Figure 2.15b).

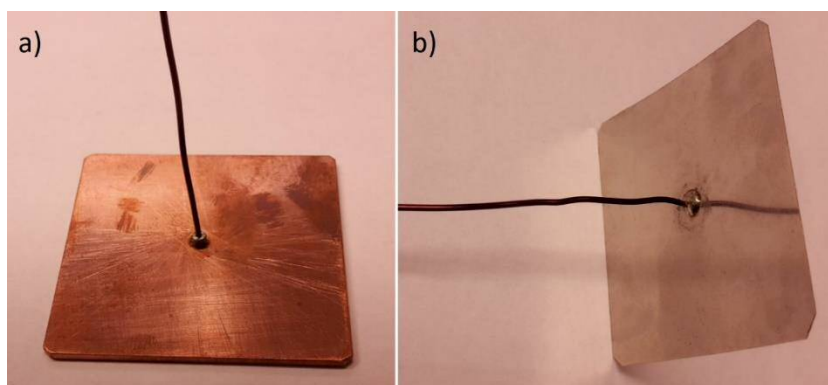


Figure 2.15: a) Copper plate welded to a copper wire, b) stainless steel plate welded to a copper wire.

With these new features, a second-generation flow electrochemical reactor was designed and manufactured, and will be described in the following sections.

2.2.1. Aluminium electrochemical reactor

The reactor was designed and built using two aluminium bodies as housing for the electrodes. This same material was also found optimum for the first-generation reactor, since it is a soft and ductile metal easy to work with.

The device comprises a flow electrochemical reactor made out of two aluminium bodies (75 x 75 x 25 mm, Figure 2.16a). The bodies have a square space in the centre (50 x 50 x 2.5 mm), where the electrodes are placed. Any electrode that comes as a sheet (such as nickel or platinum) can be easily used in the reactor. This will be connected by a copper plate attached to a wire, as described in the previous section, and connected to the power supply. The housing of the reactor has a hole in the middle that allows an easy connection of the electrodes to the power supply by the copper wire. The plate has another two holes, one for the inlet and one for the outlet of the reaction solution, and they are suitable to be connected by standard coned fittings, in order to avoid leakage in the system.

The two parts of the reactor are held apart by an FEP (fluorinated ethylene propylene) foil, into which a reaction channel is cut, giving different reaction volumes depending on the design of the flow path (an example is shown in Figure 2.16b). This foil can have different thicknesses (usually 50 μm to 500 μm). To avoid the use of a supporting electrolyte it is crucial to keep this small gap between the electrodes. The whole device is held together by steel screws, keeping an even pressure on the reactor.

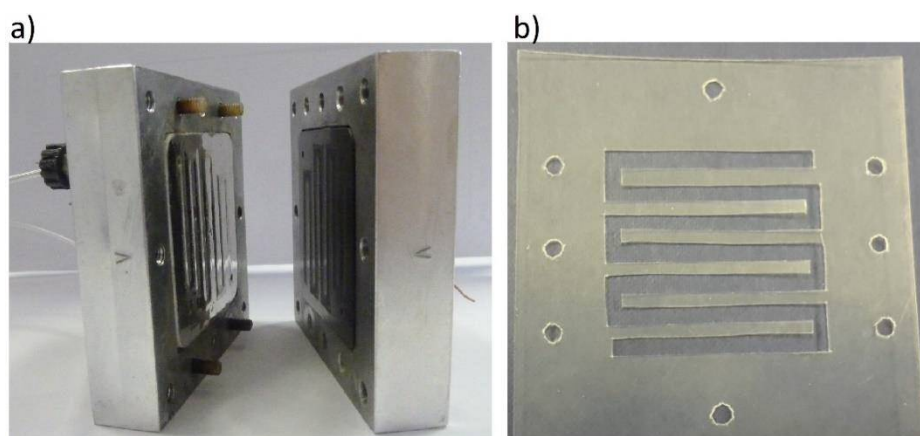


Figure 2.16: a) Electrochemical flow reactor with aluminium body; b) FEP spacer with flow channel.

2.2.2. 3D printed flow electrochemical reactor

Using a similar design to that made of aluminium, a third-generation reactor was built using a stereolithography 3D printer. The reactor design was transferred into a CAD file, in order to have all the information needed in a format that can be transferred to the printer. A 3D sketch of the design is shown in Figure 2.17.

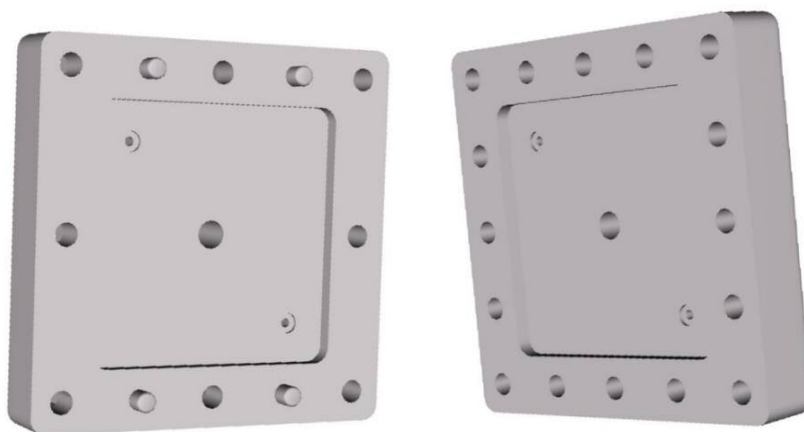


Figure 2.17: 3D image of the flow electrochemical reactor.

This method of manufacturing the reactor brings very clear advantages, such as:

- Significantly reduced human work, as the printing device will build the desired object in about 10 hours. Only the initial settings have to be adjusted, which will take about 10 minutes of the person in charge. There is a post-treatment of the 3D printed device, but this needs no expertise, special tools or third person (such as technician) to complete the work.
- Modifications to the design can be done very easily by remodelling the CAD file.
- The deepness of the space for the electrode in the 3D printed reactor can be modified as needed depending on the thickness of the electrode used.
- No need of additional insulation between the electrodes and the housing, since the polymer is not conductive.
- The 3D printed version avoids leaking in the edges by keeping the pressure on the reactor even. This is due to the material offering more flexibility, as it is not as hard as aluminium.

In this 3D printed version (Figure 2.18), the reactor is held together by screws and nuts, which are inserted and held in one of the blocks.

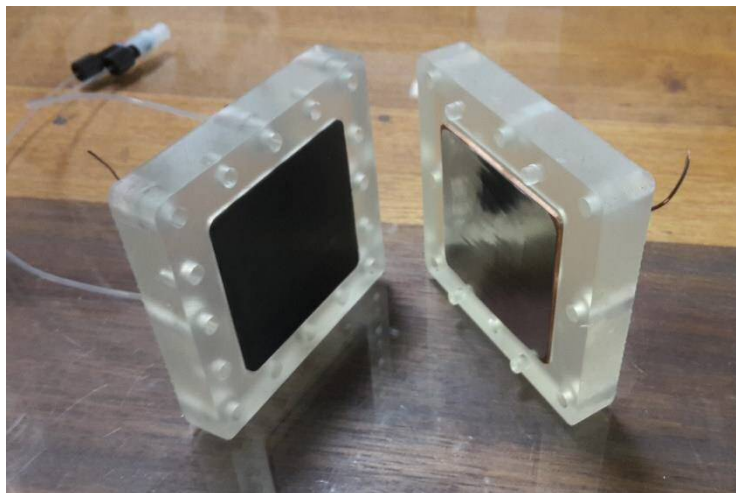


Figure 2.18: 3D printed reactor with electrodes: “Río”.

Figure 2.19 shows a picture of the device used for the 3D printing (Figure 2.19a), a closeup image of the status of the reactor after 8.5 hours of printing (Figure 2.19b), and in Figure 2.19c the final result can be observed. The reactor was called “Río”, and the name was written on the back of the 3D-printed version (see Experimental Part).

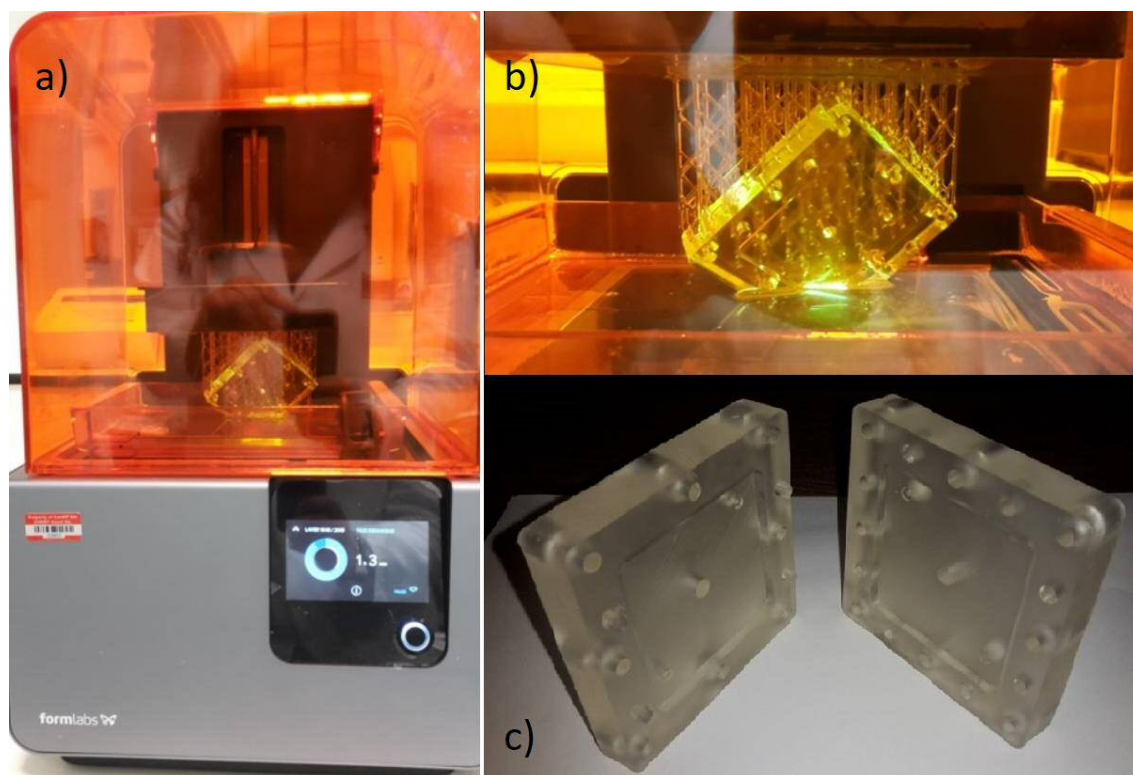


Figure 2.19: a) 3D printer; b) closeup to the 3D printer while printing the reactor; c) finished 3D printed reactor “Río”.

2.3. Conclusions and future work

In this chapter, the current literature of electrochemical reactors used for electrosynthesis in flow has been discussed. The design and construction of an improved electrochemical reactor to be used in this thesis has been explained and discussed. A second- and third-generation flow electrochemical reactor has been built, improving some features of the first-generation cell, such as: effective connectors, larger electrode surface, more robust electrode connection to the power supply and easily exchangeable electrode materials. Such reactor can be made of aluminium or a polymer, if 3D printed. The polymer reactor produced by additive manufacturing offers further advantages over the aluminium one, such as electrical insulation, easy manufacture, very even pressure on the reactor that avoids leaking, and easy modification of the design if needed.

A schematic representation with complete dimensions of both versions of the reactor can be found in the experimental part.

These reactors have already been published.^[26]

Future work:

The reactor design can be modified to control other parameters such as temperature, by adding a cooling/heating system in the body. The aluminium reactor would be more suitable for this purpose, as the thermal conductivity is greater than in the polymer. The housing could be drilled and connected to tubing where cold or hot fluid (as needed) would be pumped through the external part of the reactor at the required temperature.

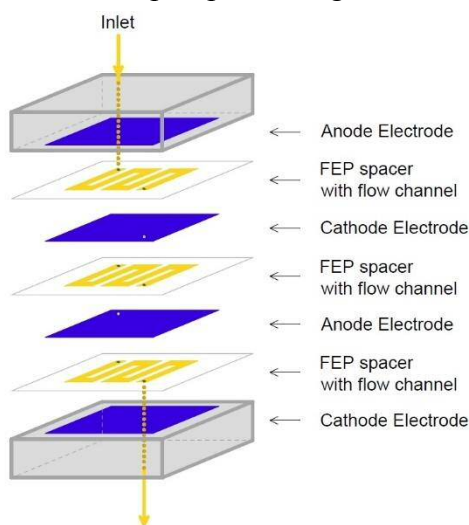


Figure 2.20: 4 layer-3 spacers electrochemical reactor.

A different version of the reactor similar to the one published by Willians^[12] could be made by using different layers of electrode material, as shown in Figure 2.20.

As the reactor can be modified easily by using additive manufacturing, different designs can be fabricated according to the needs of different applications.

2.4. References

- [1] C. Gütz, M. Bänziger, C. Bucher, T. R. Galvão, S. R. Waldvogel, *Org. Process Res. Dev.* **2015**, *19*, 1428–1433.
- [2] C. Gütz, M. Selt, M. Bänziger, C. Bucher, C. Römelt, N. Hecken, F. Gallou, T. R. Galvão, S. R. Waldvogel, *Chem. Eur. J.* **2015**, *21*, 13878–13882.
- [3] C. Gütz, A. Stenglein, S. R. Waldvogel, *Org. Process Res. Dev.* **2017**, *21*, 771–778.
- [4] J. Kuleshova, J. T. Hill-Cousins, P. R. Birkin, R. C. D. Brown, D. Pletcher, T. J. Underwood, *Electrochim. Acta* **2011**, *56*, 4322–4326.
- [5] J. Kuleshova, J. T. Hill-Cousins, P. R. Birkin, R. C. D. Brown, D. Pletcher, T. J. Underwood, *Electrochim. Acta* **2012**, *69*, 197–202.
- [6] R. A. Green, R. C. D. Brown, D. Pletcher, B. Harji, *Org. Process Res. Dev.* **2015**, *19*, 1424–1427.
- [7] R. A. Green, R. C. D. Brown, D. Pletcher, B. Harji, *Electrochem. Commun.* **2016**, *73*, 63–66.
- [8] E. A. B. Kantchev, C. J. O'Brien, M. G. Organ, *Angew. Chem. Int. Ed.* **2007**, *46*, 2768–2813.
- [9] M. N. Hopkinson, C. Richter, M. Schedler, F. Glorius, *Nature* **2014**, *510*, 485–496.
- [10] L. Mercks, M. Albrecht, *Chem. Soc. Rev.* **2010**, *39*, 1903–1912.
- [11] D. C. F. Monteiro, R. M. Phillips, B. D. Crossley, J. Fielden, C. E. Willans, *Dalt. Trans.* **2012**, *41*, 3720.
- [12] M. R. Chapman, Y. M. Shafi, N. Kapur, B. N. Nguyen, C. E. Willans, *Chem. Commun.* **2015**, *51*, 1282–4.
- [13] G. P. Roth, R. Stalder, T. R. Long, D. R. Sauer, S. W. Djuric, *J. Flow Chem.* **2013**, *3*, 34–40.
- [14] R. Stalder, G. P. Roth, *ACS Med. Chem. Lett.* **2013**, *4*, 1119–1123.
- [15] M. A. Kabeshov, B. Musio, P. R. D. Murray, D. L. Browne, S. V. Ley, *Org. Lett.* **2014**, *16*, 4618–4621.
- [16] R. A. Green, D. Pletcher, S. G. Leach, R. C. D. Brown, *Org. Lett.* **2015**, *17*, 3290–3293.
- [17] R. A. Green, D. Pletcher, S. G. Leach, R. C. D. Brown, *Org. Lett.* **2016**, *18*, 1198–1201.
- [18] J. T. Hill-Cousins, J. Kuleshova, R. A. Green, P. R. Birkin, D. Pletcher, T. J. Underwood, S. G. Leach, R. C. D. Brown, *ChemSusChem* **2012**, *5*, 326–331.
- [19] D. Pletcher, R. A. Green, R. C. D. Brown, *Chem. Rev.* **2017**, DOI: 10.1021/acs.chemrev.7b00360.
- [20] K. Watts, W. Gattrell, T. Wirth, *Beilstein J. Org. Chem.* **2011**, *7*, 1108–1114.

- [21] T. Wirth, *Angew. Chem. Int. Ed.* **2005**, *44*, 3656–3665.
- [22] T. Wirth, Ed. , *Hypervalent Iodine Chemistry*, Springer International Publishing, **2016**.
- [23] H. Hoffelner, H. W. Lorch, H. Wendt, *J. Electroanal. Chem.* **1975**, *66*, 183–194.
- [24] C. W. Hull, *US-4575330*, **1986**.
- [25] V. E. Beal, C. H. Ahrens, P. A. Wendhausen, *J. Brazilian Soc. Mech. Sci. Eng.* **2004**, *26*, 40–46.
- [26] A. A. Folgueiras-Amador, K. Philipps, S. Guilbaud, J. Poelakker, T. Wirth, *Angew. Chem. Int. Ed.* **2017**, *56*, 15446–15450.

CHAPTER 3: Electrosynthesis of nitrogen-containing heterocycles in flow

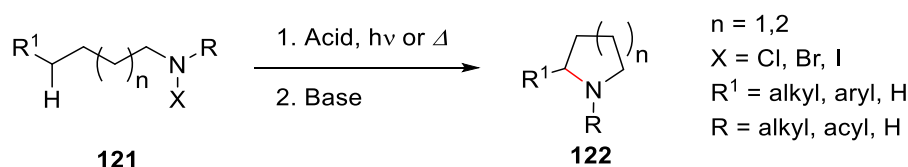
CHAPTER 3: Electrosynthesis of nitrogen-containing heterocycles in flow.....	74
3.1. Introduction.....	77
3.1.1. Nitrogen-centred radicals.....	77
3.1.2. Different methods for the synthesis of isoindolinones.....	79
3.2. Electrochemical addition of nitrogen-centred radicals to double bonds.....	81
3.2.1. Electrode screening.....	81
3.2.2. Solvent screening.....	85
3.2.3. Base screening.....	86
3.3. Isoindolinone derivatives synthesis.....	90
3.3.1. Synthesis of substrates.....	90
3.3.2. Inline Mass Spectrometry analysis for optimisation of reaction conditions	94
3.3.3. Base effect study for amides as substrates.....	97
3.3.4. Effect of different spacers.....	100
3.3.5. Scope of the reaction.....	101
3.3.6. Tandem cyclisation attempt.....	107
3.3.7. Proposed mechanism.....	109
3.4. Two-step flow approach: Electrochemical cyclisation and elimination of TEMPO to form alkenes.....	113
3.5. Two-step flow approach: Electrochemical cyclisation and N–O bond reductive cleavage to form alcohols.....	116
3.6. Two-step flow approach: Synthesis of carbamates in flow and subsequent electrochemical cyclisation.....	118
3.7. Conclusions.....	123

3.8. References	124
-----------------------	-----

3.1. Introduction

3.1.1. Nitrogen-centred radicals

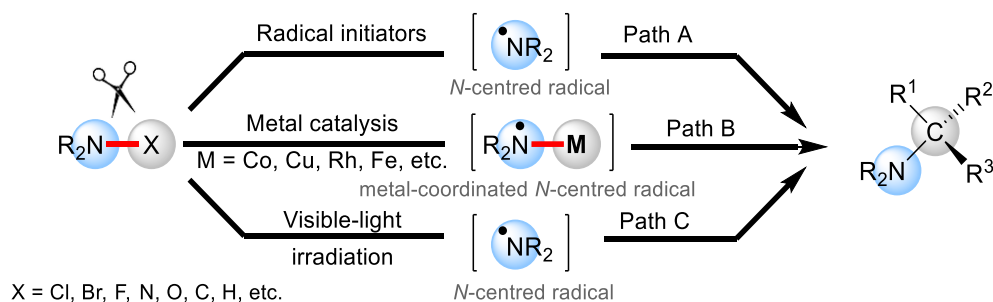
Nitrogen-containing heterocycles are very important components in drugs and bioactive natural products, and they have a broad application in the pharmaceutical and chemical industry.^[1,2] Their synthesis has been explored with different methodologies, many of them involving the use of precious metals or toxic reagents.^[3,4] Using nitrogen-centred radicals is an attractive pathway to obtain these *N*-containing compounds. The first example of a nitrogen-centred radical reaction dates from 1879,^[5] when Hofmann published the discovery of the well-known Hofmann-Löffler-Freytag reaction.^[6] This reaction afforded aminated five and six-membered ring motifs (**122**) from halogenated amines (**121**) via photochemical or thermal decomposition (Scheme 3.1).



Scheme 3.1: Hofmann-Löffler-Freytag reaction.

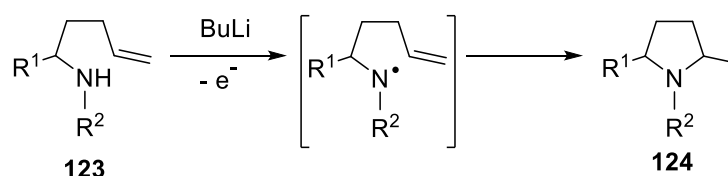
Nitrogen-centred radicals are very reactive species, and these intermediates usually have a short life-time. The radical formed can be stabilised *via* resonance when using neighbouring functional groups such as carbonyls or aromatics. Some nitrogen-centred radicals with considerable steric hinderance can even be isolated.

Generally, radical initiators are used to start the radical reaction by homo-cleavage of N-X bonds, where X can be oxygen, nitrogen, sulfur or a halogen (Cl, Br or I). Common radical initiators are (*n*Bu₃Sn)₂ and *hv*, di-*tert*-butylperoxide (DTBP), Et₃B and molecular oxygen, *tert*-butylhydroperoxide (TBHP) combined with iodine (I₂), or UV irradiation (Scheme 3.2, paths A and C).^[7,8] Recently, metal-coordinated nitrogen-centred radicals have played an important role in the synthesis of new C–N bonds, as they show more stability than free radicals. In 2005 Grützmacher reported the first aminyl transition metal complex stable to be isolated, and it was characterised by X-ray crystallography.^[9] Bruin *et al.* published a review about aminyl radical metal complexes and some applications for C–N bond formation (Scheme 3.2, path B).^[8,10]



Scheme 3.2: Nitrogen-centred radical pathways for C–N bond formation.^[8]

Electrochemistry has shown to be an efficient and mild methodology to create nitrogen-centred radicals. The addition of electrochemically generated nitrogen-radicals to double bonds has been known for the last century (Scheme 3.3),^[11] and this kind of transformation has been well studied in the last decade, especially by Moeller^[12–16] and Xu^[17–20].



Scheme 3.3: Electrochemical amination of olefins.

In this thesis, the synthesis of isoindolinone derivatives has been studied *via* anodic oxidation of amides and their subsequent addition to double bonds. Such isoindolinone motifs are found in many natural products, pharmaceutical and biologically active molecules (Figure 3.1).^[21]

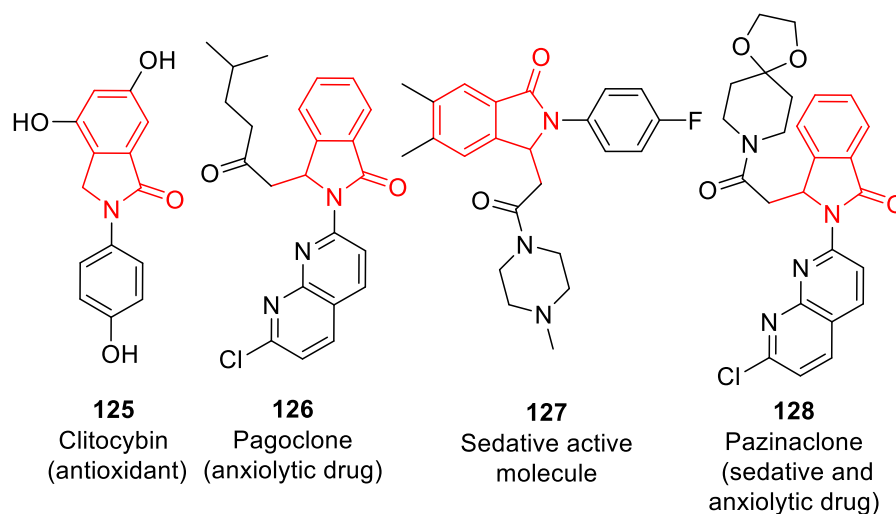
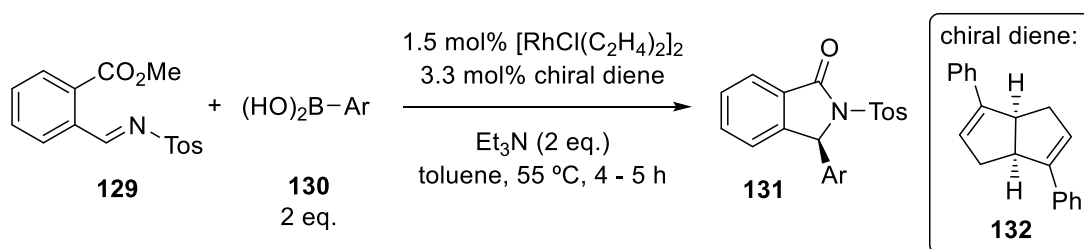


Figure 3.1: Biologically active isoindolinone derivatives.^[21]

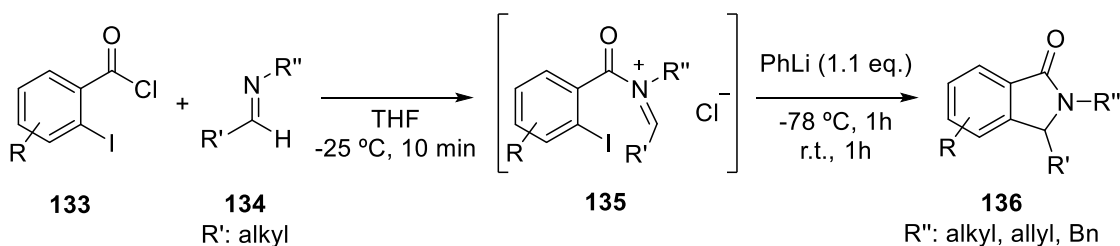
3.1.2. Different methods for the synthesis of isoindolinones

The isoindolinone core was discovered decades ago. Some of the recent literature is summarised in this section. In 2007, Xu, Lin and co-workers reported a new C_2 -symmetric chiral diene ligand for the synthesis of diarylmethylamines *via* asymmetric arylation of *N*-tosylarylimines (**129**) using a rhodium catalyst and arylboronic acids **130** (Scheme 3.4). The enantiomerically enriched isoindolinones **131** were obtained in 65 – 99% yield and with 98 – 99% *ee*.^[22]



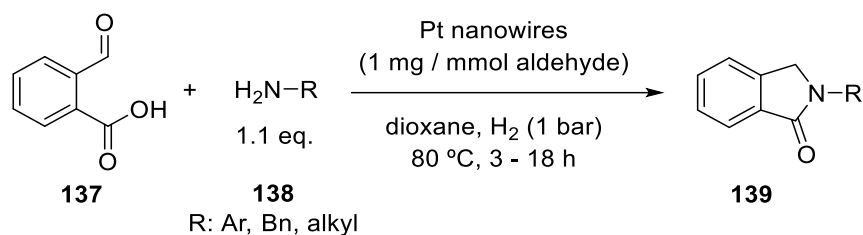
Scheme 3.4: Rh catalysed isoindolinone synthesis.

In 2010, Campbell *et al.* published the formation of *N*-acyliminium ions as adducts (**135**) from the addition of *o*-iodobenzoyl chlorides (**133**) to imines (**134**), and their subsequent reaction with phenyllithium. This reaction would be followed by an intramolecular Wurtz-Fittig coupling to give 2,3-dihydroisoindolinones (**136**) in yields up to 90% (Scheme 3.5). This method shows some inconveniences, such as the need for an inert atmosphere and low temperatures (-78 °C) for the addition of phenyllithium.^[23]



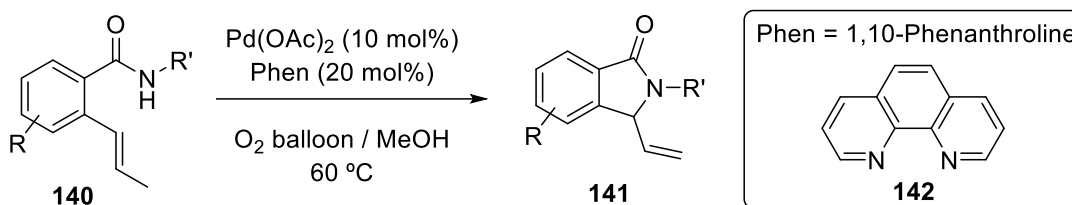
Scheme 3.5: Isoindolinone synthesis *via* lithium-iodide exchange intramolecular Wurtz-Fittig reaction from *o*-iodobenzoyl chloride and imine adducts.

In 2012, Cao and co-workers developed a method to produce *N*-substituted isoindolinones *via* reductive C–N coupling with hydrogen gas and intramolecular amidation of 2-carboxybenzaldehyde (**137**) with primary amines (**138**), catalysed by Pt nanowires (Scheme 3.6). The desired isoindolinone derivatives (**139**) are synthesised in good to excellent yields.^[24]



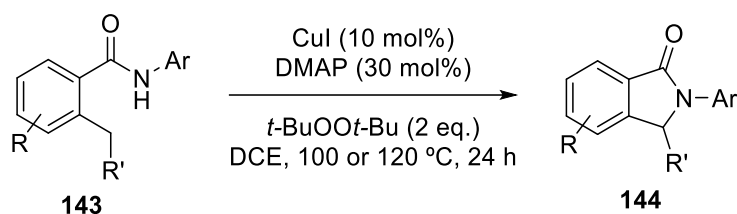
Scheme 3.6: *N*-substituted isoindolinone synthesis from 2-carboxybenzaldehyde and primary amines using Pt nanowires and H₂.

Later in 2012, Zhang *et al.* reported a Pd-catalysed regioselective intramolecular Wacker-type cyclisation for the formation of isoindolinones (**141**) under O₂ atmosphere (Scheme 3.7). In this paper the authors reported 16 examples with yields from 16% to 99%.^[25]



Scheme 3.7: Pd-catalysed formation of isoindolinones.

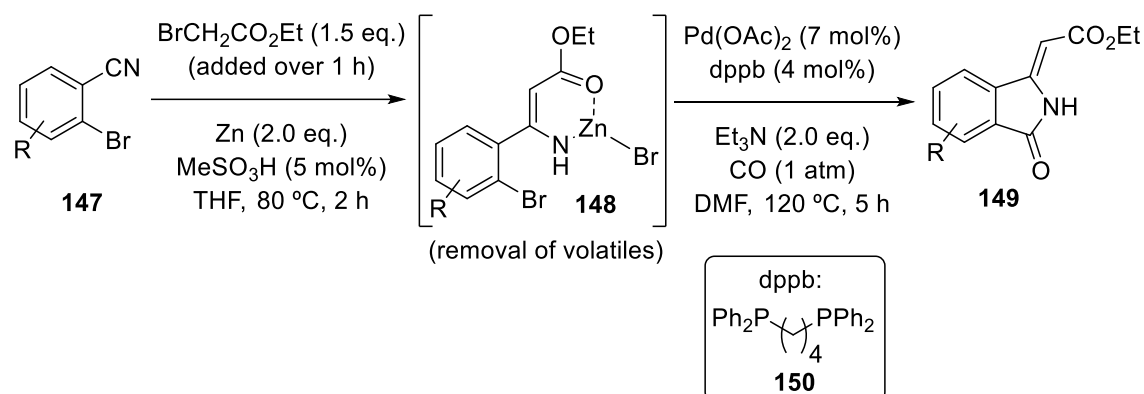
In 2015, Kondo and co-workers published the synthesis of isoindolinones *via* C–H functionalisation of 2-alkyl-*N*-substituted benzamides (**143**) using copper as catalyst and 2 equivalents of di-*tert*-butyl peroxide as oxidant (Scheme 3.8). The reaction only proceeds in the presence of a ligand and at elevated temperatures (100 or 120 °C).^[26]



Scheme 3.8: Intramolecular C–H amination of 2-Alkyl-*N*-arylbenzamides by the use of copper/oxidant combination.

A method reported by Lee *et al.* in 2016 shows a palladium catalysed two-step/one-pot synthesis of isoindolinone derivatives from 2-bromoarylnitriles (**147**). The transformation begins with the formation of the Blaise reaction intermediate **148**, and subsequent intramolecular aminocarbonylation using a Pd catalyst and an atmosphere of carbon

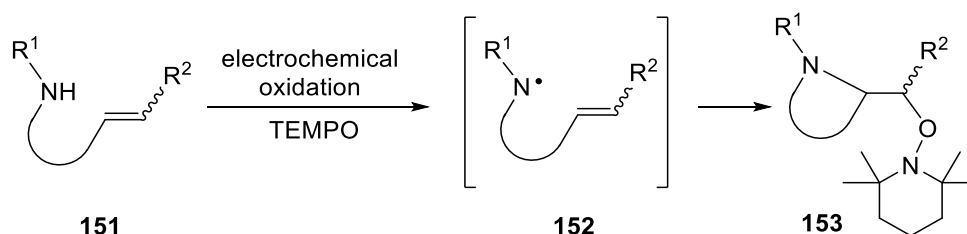
monoxide (1 atm). The use of a bisphosphine ligand (1,4-bis(diphenylphosphino)butane **150**, dppb) is essential for the desired tandem reaction (Scheme 3.9).^[27]



Scheme 3.9: Pd-catalysed aminocarbonylation of Blaise reaction intermediates for the synthesis of isoindolinones from nitriles.

3.2. Electrochemical addition of nitrogen-centred radicals to double bonds

The investigation of the electrochemical synthesis of nitrogen-containing heterocycles is described in this chapter. In order to find the optimum conditions to perform this reaction in the flow reactor, the most important parameters were screened separately. These are electrode, solvent and base.

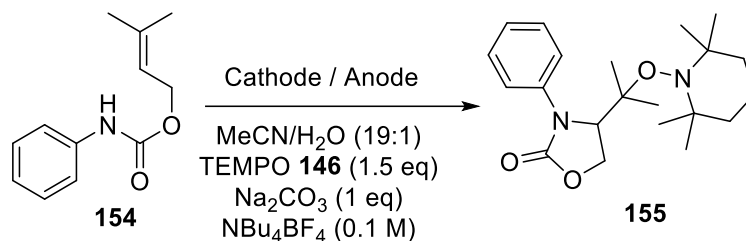


Scheme 3.10: Electrochemical synthesis of nitrogen-containing heterocycles.

3.2.1. Electrode screening

The electrode material used to perform an electrochemical transformation is crucial for the result of the reaction, as it was explained in Chapter 1 (general introduction). Therefore, different electrode materials as anode and cathode were tested in a batch reaction to transform the carbamate **154** to the cyclised product **155** (Figure 3.4). The reaction conditions were selected in accordance to the results presented in Xu's paper,^[17] where the cyclisation of carbamates was reported using reticulated vitreous carbon (RVC) anode and platinum cathode, and tetrabutylammonium tetrafluoroborate as supporting

electrolyte. A mixture of acetonitrile and water (19:1 v/v) was employed as solvent, sodium carbonate as a base (1.0 eq.) and 1.5 equivalents of TEMPO as a mediator and radical scavenger.



Scheme 3.11: Electrochemical nitrogen-centred radical generation and subsequent cyclisation.

The role of TEMPO in this reaction will be discussed in Section 3.3.7. In our case it was observed that 1.5 equivalents of TEMPO (**146**) were sufficient to give total consumption of the starting material to the desired product. Xu's manuscript states that the reaction must be done at 60 °C in order to achieve a high yield. However, in our case when the reaction was performed at room temperature the result was satisfactory, giving the compound of interest in 85% yield.

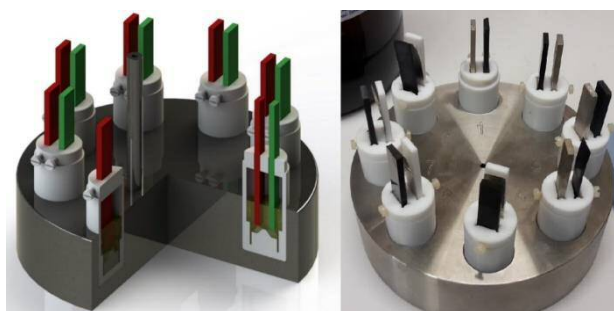


Figure 3.2: Set-up for multiple reaction screening in undivided cells.^[28] (Reproduced with permission from ref.^[28] Copyright (2016) American Chemical Society).

Different electrode material combinations were tested using a screening set-up developed by Waldvogel *et al.*,^[28] shown in Figure 3.2. The set-up consists of a stainless steel block with eight cavities where eight different cells can be inserted, making it possible to screen up to eight different reaction conditions at the same time. The cells have a volume of 5 mL and are made of Teflon[®]. Each of these cells have a magnetic stirrer bar and a cap that can hold two electrodes (70 x 10 x 3 mm), as can be observed in Figure 3.2. The stainless steel block is placed on a common magnetic stirring plate, and can be heated if

necessary. A programmable eight channel DC power supply is used to provide the electricity needed for the reactions (Figure 3.3).

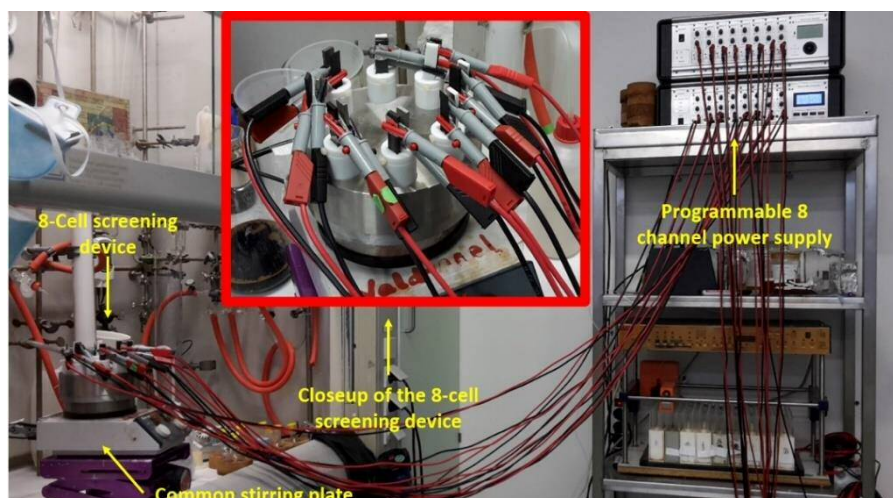


Figure 3.3: Whole set-up for multiple reaction screening, connected to the programmable 8 channel power supply.

This device was used to explore the effect of different electrodes in the reaction of interest. The reaction was monitored by gas chromatography after passing different amount of electricity through the electrochemical cell. The results are shown in Figure 3.4 (Graph a and Graph b).

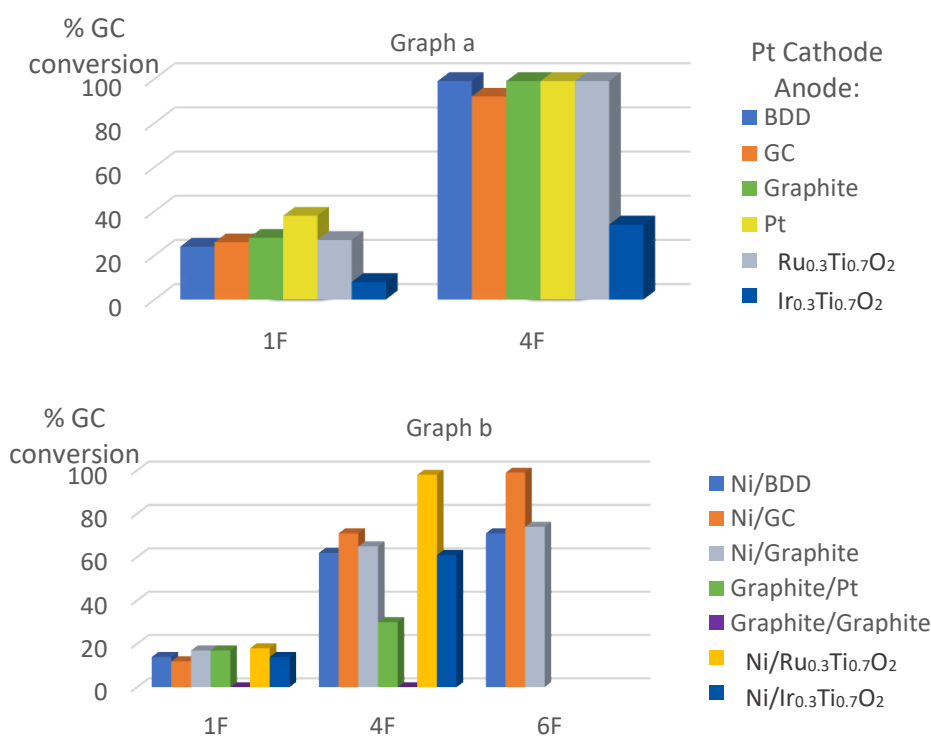


Figure 3.4: Electrode screening. BDD: Boron Doped Diamond; GC: Glassy Carbon.

When using platinum as the cathode (counter electrode), the reaction behaved very similar with any electrode material used as the anode (working electrode), except for $\text{Ir}_{0.3}\text{Ti}_{0.7}\text{O}_2$, which shows a significant decrease in conversion as can be observed in graph a (Figure 3.4). Nevertheless, graph b shows that the results are very different when the cathode material used is not platinum. The reaction did not go to completion in most cases after 4 F mol^{-1} , and in the case of using graphite as both anode and cathode, no conversion at all was observed. Having nickel as cathode and glassy carbon as anode gave full conversion, but only after 6 F mol^{-1} (Figure 3.4). These experiments were carried out in Waldvogel's laboratory in Mainz University, and the Ru and Ir based oxide electrodes ($\text{Ru}_{0.3}\text{Ti}_{0.7}\text{O}_2$ and $\text{Ir}_{0.3}\text{Ti}_{0.7}\text{O}_2$) were tested only to study the possible different reactivity that they could have. These electrode materials are not available from most common suppliers, therefore they will not be chosen as electrodes unless they show an optimum reactivity that cannot be achieved by any other common and easily accessible electrode material.

The results shown in Figure 3.4 lead to the conclusion that the counter electrode (cathode) has a bigger impact on the reaction than the working electrode (anode). This can be explained taking into account the mechanism proposed by Xu *et al.*^[17] (Figure 3.5).

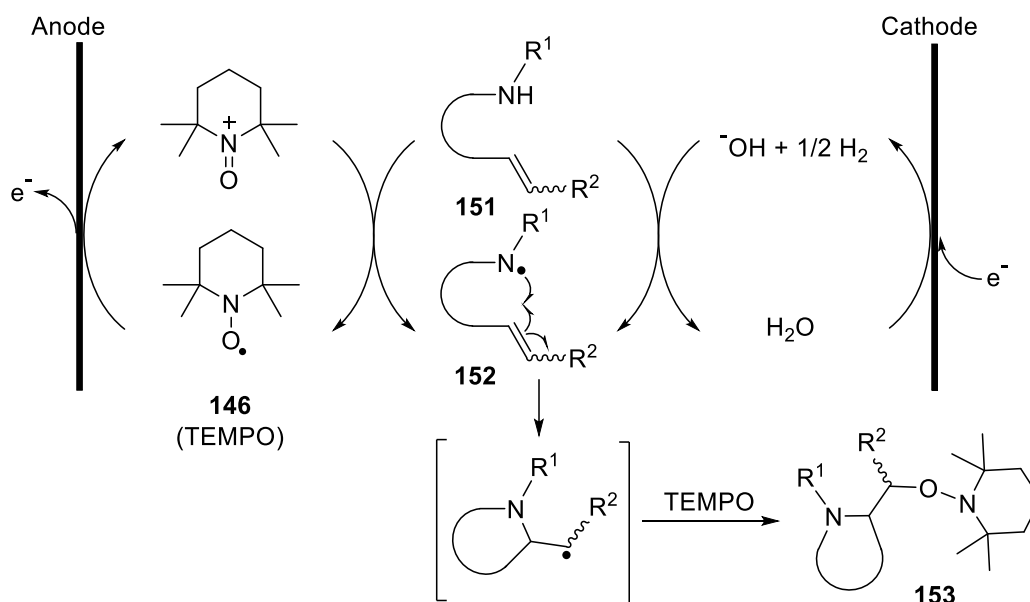


Figure 3.5: Proposed mechanism for TEMPO mediated aminooxygenation of alkenes.

The reaction that takes place at the cathode is proton reduction to form H_2 gas. In this case the protons come from the water present in the solvent mixture. This proposed

mechanism has been studied further and will be explained in Section 3.3.7. This proton reduction taking place at the cathode can explain why the nature of the electrode is very important in the reaction outcome, as different electrode materials will present different activation overpotential for hydrogen evolution.^[29] As one can observe in Table 3.1, the hydrogen activation overpotential is lower for platinum than for nickel, and much higher for graphite. This example shows the importance of taking into consideration the overall process in an electrochemical transformation, and not only the reaction of interest. In this case the desired reaction is the oxidation of the nitrogen-containing compound, but the set-up has to fulfil the requirements for the counter reaction to take place.

Table 3.1: H₂ activation overpotential of different electrode materials.^[29]

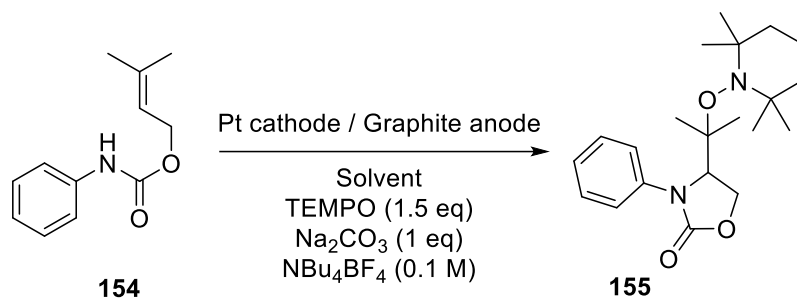
Electrode material (cathode)	H ₂ activation overpotential vs SHE	^a Electrochemical cyclisation conversion after 4 F mol ⁻¹
Platinum	-0.07 V	100%
Nickel	-0.28 V	71%
Graphite	-0.62 V	0%

^a carbon anode. SHE: standard hydrogen electrode

Since the result of the reaction was very similar when different anode materials were used, graphite has been chosen as an inexpensive and easily accessible electrode. Therefore, from these experiments it can be concluded that the optimum electrode materials for this type of reactions are platinum as the cathode and graphite as the anode.

3.2.2. Solvent screening

The effect of the solvent was also studied by performing the same reaction (Scheme 3.12) in different solvents or solvent mixtures, such as acetonitrile, methanol, 1,1,1,3,3,3-hexafluoro-*isopropyl* alcohol (HFIP) and water. Unfortunately, the cyclised product **155** was only observed when a mixture of acetonitrile and water was used. Further attempts with methanol as a protic solvent to replace water, or a mixture of acetonitrile and methanol as hydrogen source, did not give any desired product **155** (Scheme 3.12). HFIP was chosen as a solvent, since it is known to be a good cation and radical stabiliser.^[30,31] Unfortunately, when the reaction was performed in HFIP or a mixture of HFIP and water, it led to either recovery of the starting material (< 2 F mol⁻¹) or decomposition (> 3 F mol⁻¹).



Scheme 3.12: Solvent screening.

Solvent:

- ✗ MeOH
- ✗ MeCN
- ✓ **MeCN/H₂O (19:1) → >99% conversion**
- ✗ MeCN/MeOH (19:1)
- ✗ HFIP
- ✗ HFIP/H₂O (19:1)

In conclusion, the optimum solvent for the desired transformation is a mixture of acetonitrile and water (19:1 v/v).

3.2.3. Base screening

The use of a base can be favourable in anodic oxidations if the compound or its oxidised form can be deprotonated, as most anodic oxidations undergo loss of electrons and protons.^[13,17] For example, Xu *et al.*^[17] reported the cyclization of carbamates of type **154** in batch using lithium hydroxide or sodium carbonate as a heterogeneous base. The drawback of these bases is their low solubility in organic solvents which is clearly more problematic for flow than for batch processes. The proposed mechanism (Figure 3.5) shows that the cathode-generated hydroxide anion assists in the deprotonation of the carbamate before forming the nitrogen radical. With sodium carbonate as base the reaction proceeded to completion in the flow reactor after 3 F mol⁻¹. However, the amount of water had to be increased (50% in acetonitrile) in order to dissolve the inorganic base. This led to poor solubility of the product in the solvent mixture and to precipitation and blocking of the flow system after 10 minutes of operation (Figure 3.6), making this base/solvent system incompatible for continuous flow.



Figure 3.6: Product precipitate on anode surface.

To avoid this problem, different organic bases were investigated in the flow cyclisations. A summary of the results can be seen in Figure 3.7. All the reactions were carried out with the conditions previously studied; using platinum as cathode and graphite as anode, and a solvent mixture of acetonitrile/water (19:1 v/v). When no base is used (yellow bar in Figure 3.7) the reaction takes place but the cyclised product **155** is formed in only 32% conversion. Using sodium carbonate (purple bar) resulted in full conversion. However, as previously mentioned, the high percentage of water needed to dissolve the base makes the process inviable. 2,6-Lutidine (green bar) led to similar conversions (29%) as without base, showing no improvement. Using triethylamine inhibited the reaction (blue bar in Figure 3.7), and no product was observed at all, with only starting material being recovered.

Benzyltrimethylammonium hydroxide **156** was successfully used to accelerate the reaction (orange bar). The organic nature of the cation part of the base makes it highly soluble in organic solvents, overcoming the problem previously encountered when using sodium carbonate. Full conversion of **154** after 4 F mol^{-1} was achieved. Therefore, **156** was used as soluble base in further optimization studies.

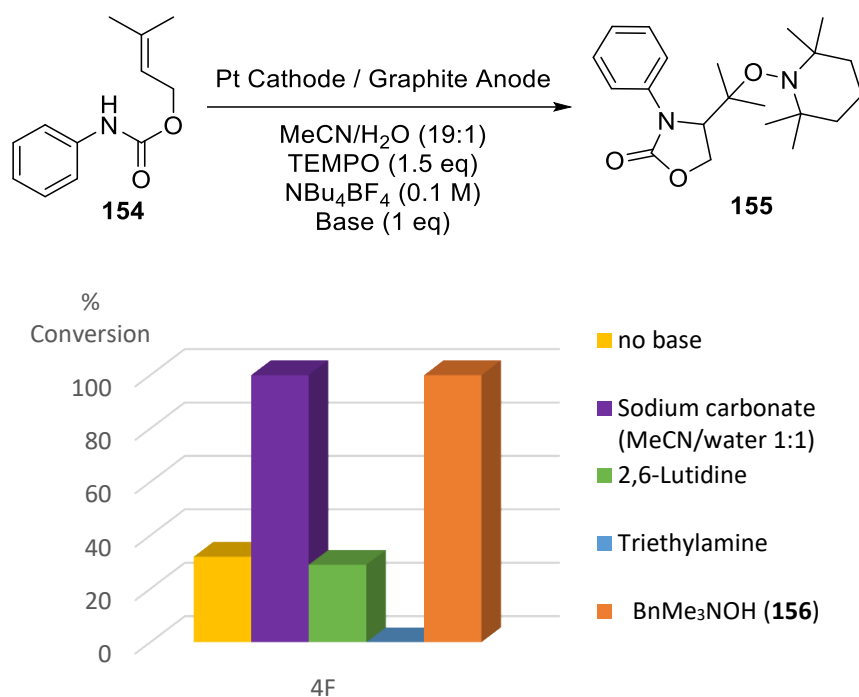


Figure 3.7: Base screening.

3.2.3.1. Cyclic voltammetry studies

These results could be explained by measuring the cyclic voltammogram of substrate **154** in the presence of the different bases. The oxidation potential of triethylamine (Figure 3.8d) is much lower than that of **154** (Figure 3.8a and c), so will be oxidised first, while the starting material remains unreacted. The oxidation potential of **154** after the addition of 2,6-lutidine remains practically unchanged (Figure 3.8b), which explains the similar result to that without base. Benzyltrimethylammonium hydroxide (**156**) lowers the oxidation potential of compound **154** from 1.74 V to 0.27 V (*vs* Ag/AgCl, Figure 3.8e). This supports the result obtained experimentally and makes this base the most efficient one tested to accelerate the desired cyclisation in flow.

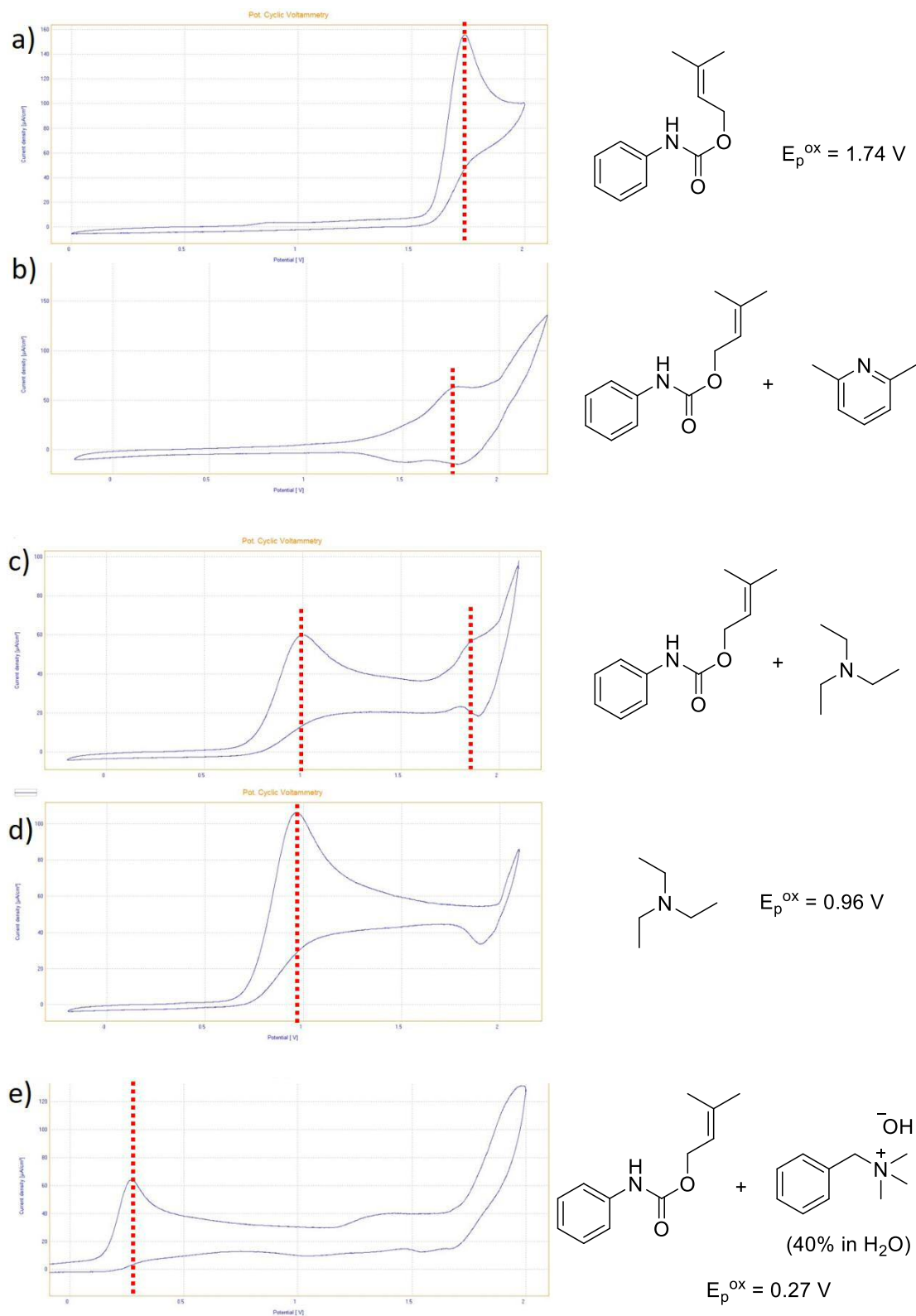


Figure 3.8: Cyclic voltammograms of compound 1 in the presence of different bases.

Oxidative cyclic voltammograms of the substrates (1 mM) recorded in 0.075 M Bu₄NBF₄/MeCN electrolyte at 100 mV/s scan rate. Working electrode: glassy carbon electrode tip (3 mm diameter); Counter electrode: platinum wire; Reference electrode: Ag/AgCl in 3 M NaCl.

3.3. Isoindolinone derivatives synthesis

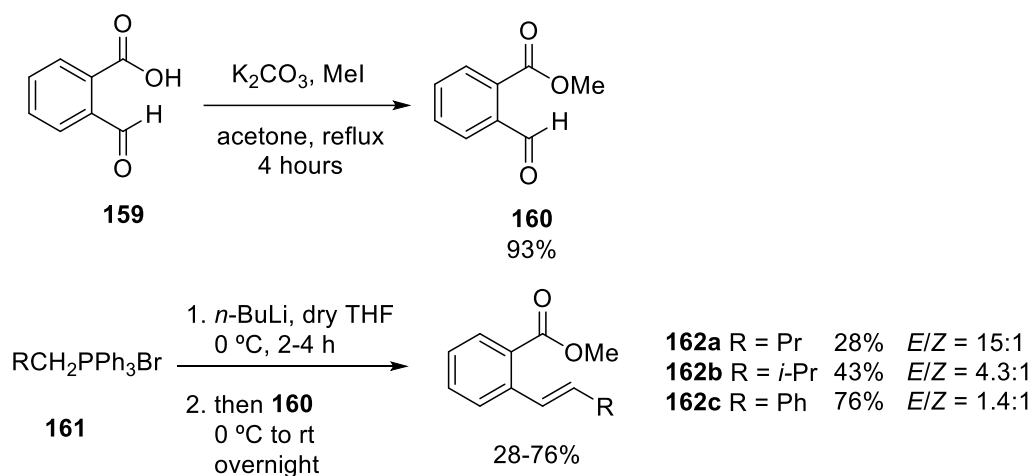
The optimised conditions were applied to the synthesis of isoindolinones in flow. Isoindolinone motifs are found in many natural products, pharmaceuticals and biologically active molecules (see Figure 3.1).^[21]

3.3.1. Synthesis of substrates

The isoindolinone derivatives were synthesised from functionalised amides. These amides were synthesised using the two different pathways described below (Path A and Path B).

3.3.1.1. Synthesis of amides: Path A

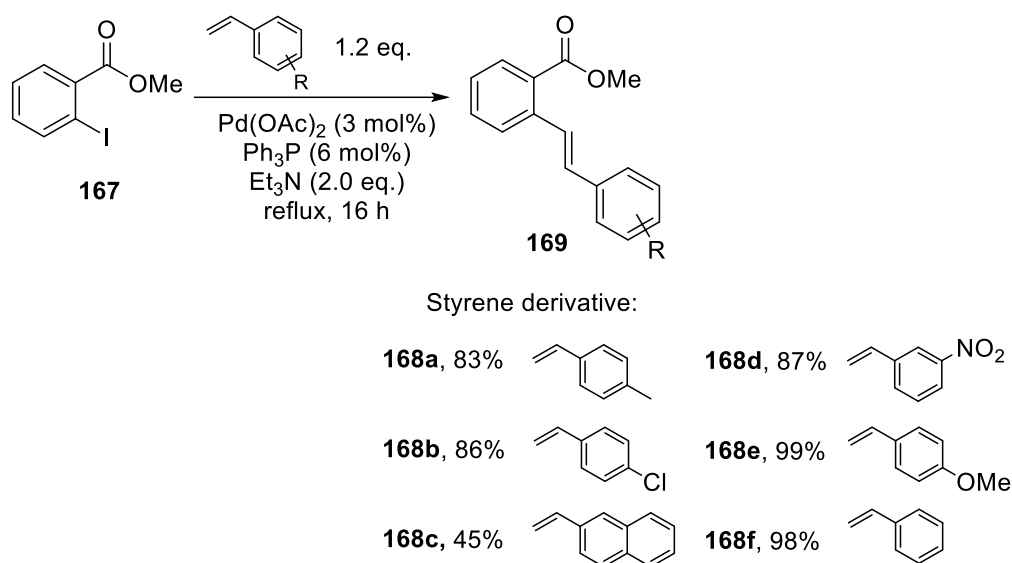
The first pathway towards the synthesis of the amide substrates started with the esterification of the commercially available 2-carboxybenzaldehyde **159** to form the methyl ester **160** in excellent yield (Scheme 3.13).



Scheme 3.13: Path A: Two first steps towards the synthesis of amides substrates.

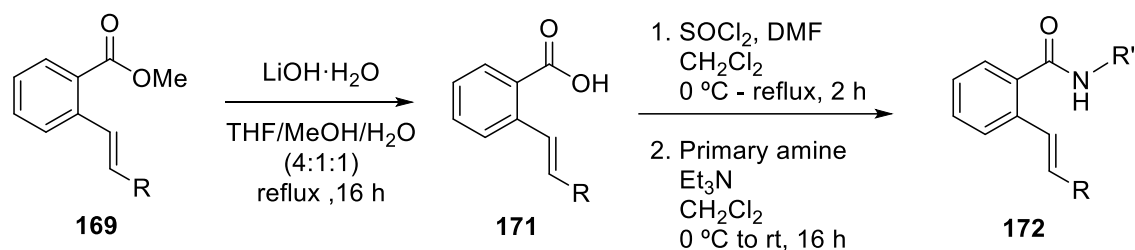
The second step was a Wittig transformation to attach the alkene functionality to the molecule. The Wittig reagent was either commercially available (R = Pr and Ph) or prepared from triphenylphosphine (**165**) and the appropriate alkyl halide (R = *i*-Pr, **166**, Scheme 3.14).

(Scheme 3.16), to give compounds **169** in high yield. This transformation gave the alkenes (**169**) with high selectivity towards the *E* isomer (> 20:1).



Scheme 3.16: Path B: Heck reaction with various styrenes.

The ester **169** was then hydrolysed to the corresponding carboxylic acid **171**, then converted to the acid chloride and reacted with different primary amines to give the desired amides (**172**) as shown before (Scheme 3.17).



Scheme 3.17: Path B for formation of amides.

A summary of the substrates synthesised *via* path B is shown in Figure 3.9.

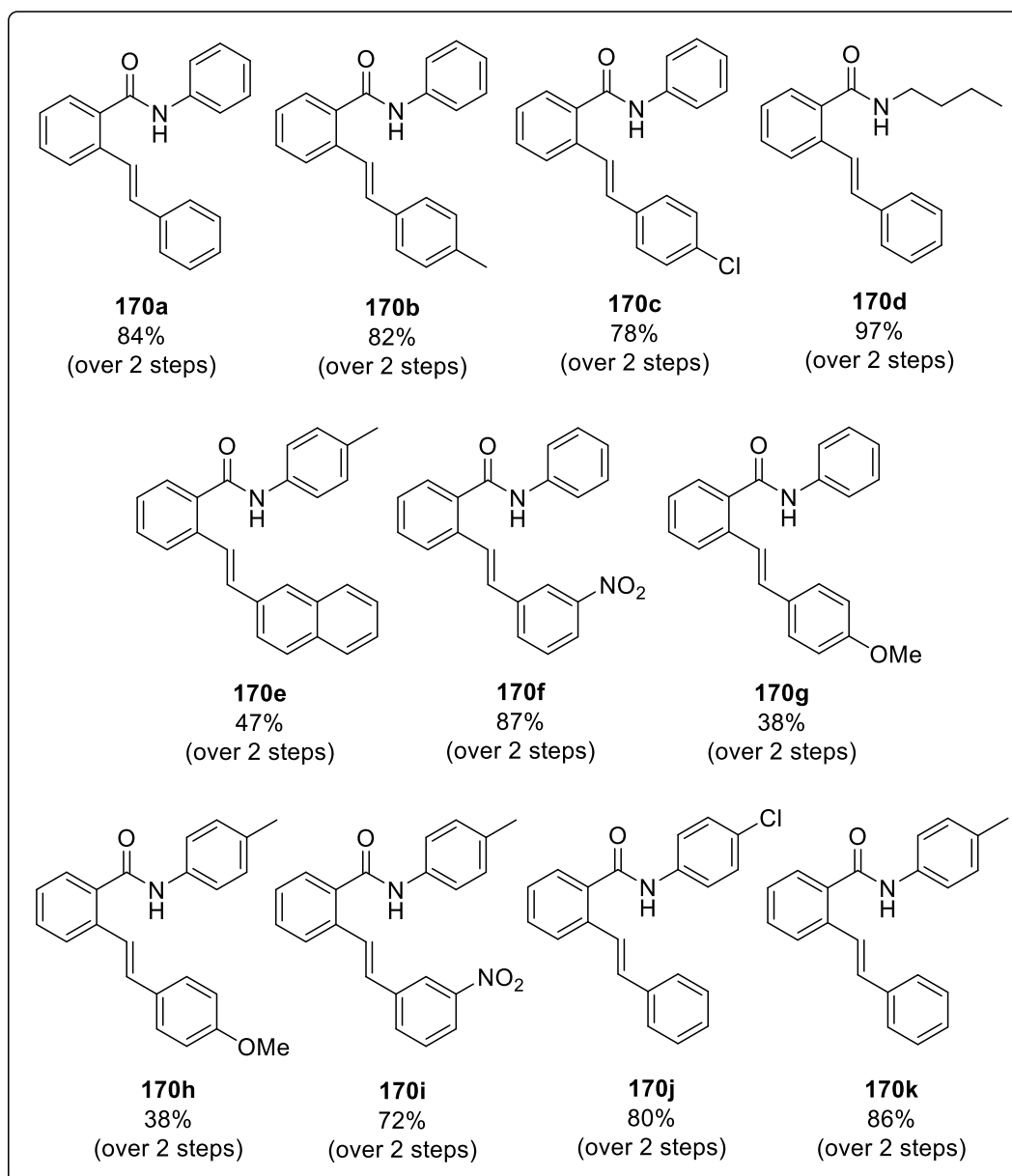
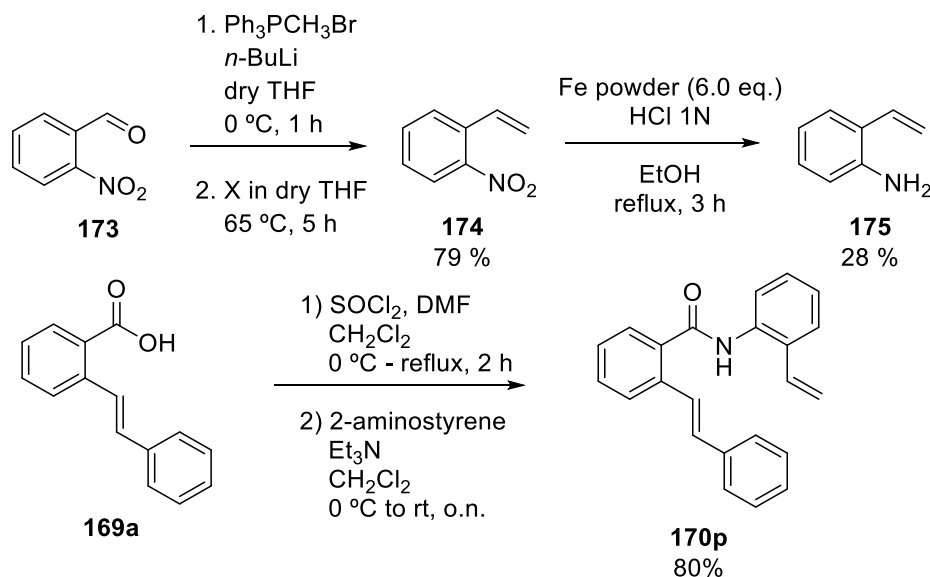
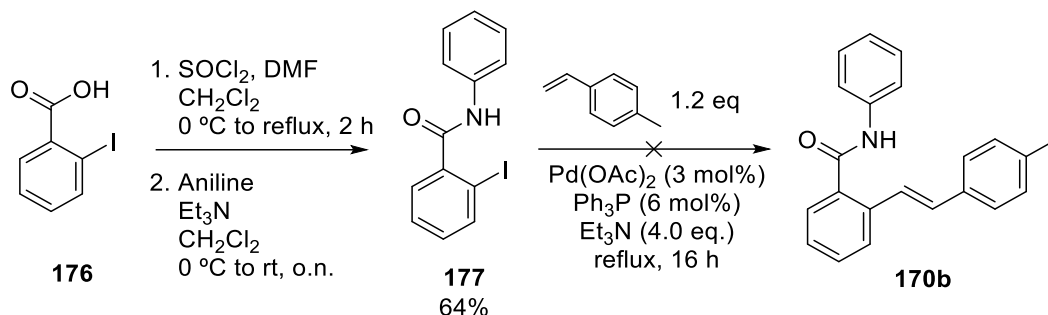


Figure 3.9: Summary of amide substrates.

A compound bearing two alkene functionalities was synthesised following the same protocol. 2-Aminostyrene was synthesised in two steps, starting with a Wittig reaction of 2-nitrobenzaldehyde (**173**) and methyltriphenylphosphonium bromide. Next, the reduction of the aromatic nitro group was performed using iron powder, hydrochloric acid and ethanol (Scheme 3.18). Compound **175** was only obtained in 28% yield, since it showed low stability and decomposed over time.

Scheme 3.18: Synthesis of compound **170p**.

An attempt to shorten the synthesis towards product **170b** is shown in Scheme 3.19. In this case, 2-iodobenzoic acid **176** was selected as the starting material to form directly 2-iodobenzamide **177**, and then couple it with the corresponding styrene to give the target molecule. Unfortunately, the Heck reaction did not lead to the formation of the desired product **170b**, and most of the starting material **177** was recovered after 16 hours under reflux.



Scheme 3.19: Attempt to the synthesis of benzamides in two steps.

In conclusion, path B gave higher overall yields and fewer steps were necessary to obtain the amides needed for the electrochemical cyclisations. Therefore, the majority of the substrates were synthesised using this method.

3.3.2. Inline Mass Spectrometry analysis for optimisation of reaction conditions

Having studied the general conditions in Section 3.2, the cyclisation of amides was investigated in more detail. Compound **170k** was chosen as a model substrate. The

electrochemical reactor was connected to an inline mass spectrometer, which allowed a rapid assessment of the required amount of electrons needed in the reaction.

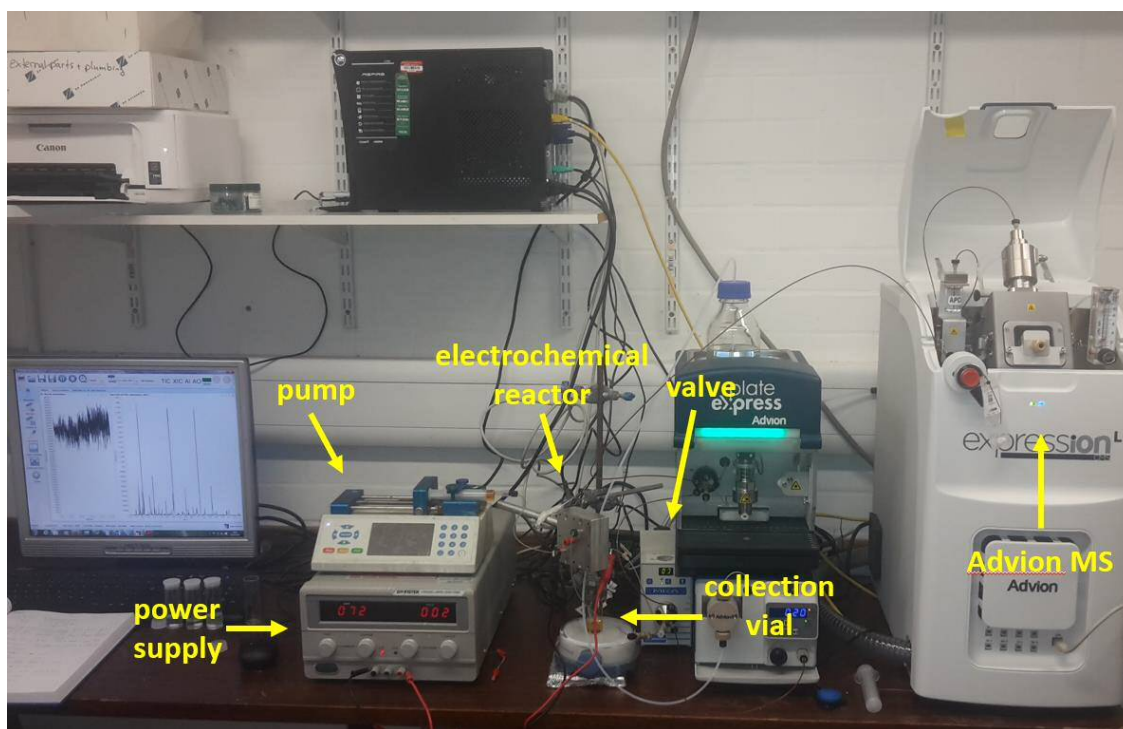
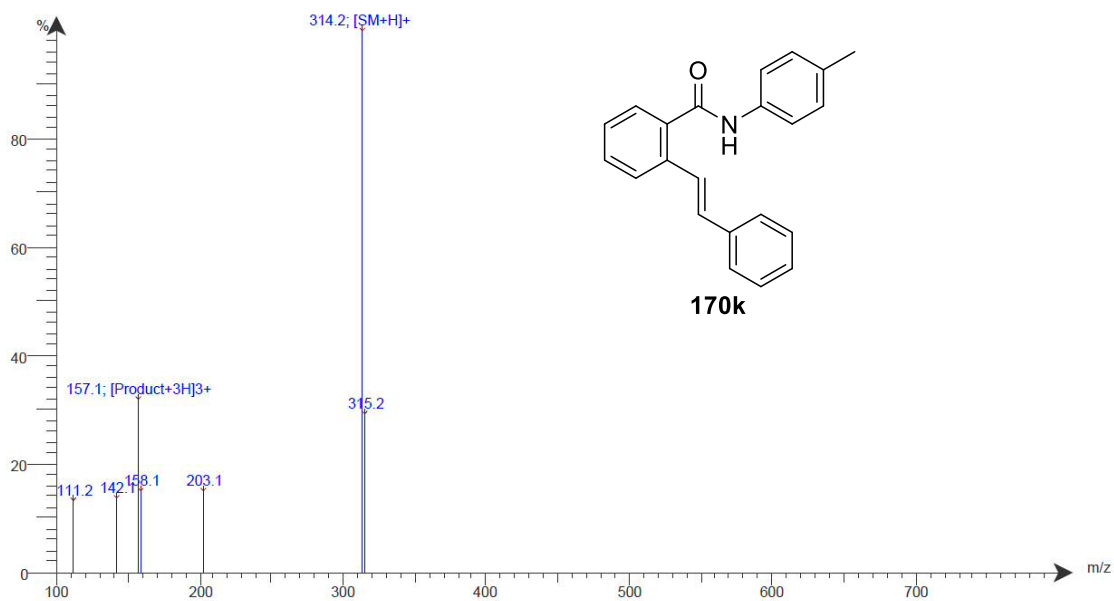
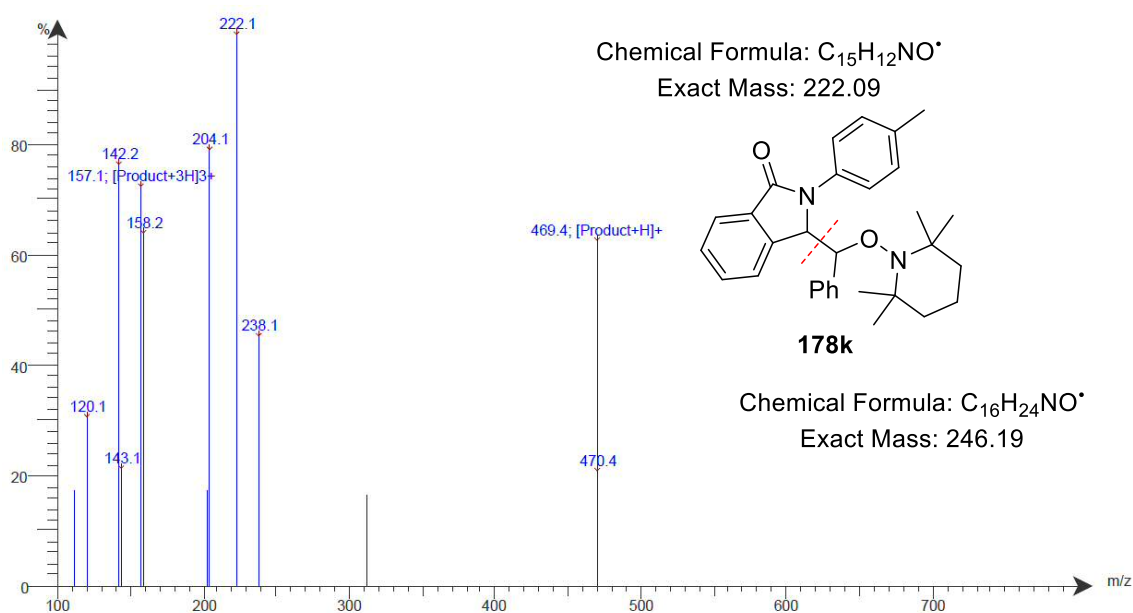


Figure 3.10: Set-up for inline mass spectrometry analysis.

Figure 3.10 shows the set-up used for the inline MS monitoring system. The outlet of the electrochemical reactor was connected to a valve that takes a small aliquot of the crude reaction mixture approximately every second. This valve is connected to the mass spectrometer by a capillary, so the crude sample can be analysed instantly. This system provides immediate information about the reaction, and the percentage of starting material and product can be observed in a chromatogram. By analysing the results obtained, parameters of the reaction can be tuned in order to achieve full conversion to the desired product.

Compound **178k** was produced by electrochemical cyclisation of compound **170k** (Figure 3.13). For compound **170k**, the base peak in the MS spectrum corresponds to the molecular ion (m/z : 314.2 $[M+H]^+$), therefore, it was chosen to follow the reaction, as it was the most intense peak (Figure 3.11). For the cyclised product **178k**, the molecular ion (m/z : 469.4) is not the most intense peak. Instead, a fragment of the molecule (see Figure 3.12) appears as the base peak in the spectrum, m/z : 222.1. This peak was chosen to follow the reaction in the inline MS analysis.

**Figure 3.11: MS of starting material 170k.****Figure 3.12: MS of product 178k, and fragmented molecule.**

After selecting the right peaks for starting material and product to follow the reaction *via* mass spectrometry, the electrochemical reaction was carried out. It was started just by pumping the mixture with the substrate and reagents, but without current flowing (0 F mol^{-1}). The current was increased gradually to the values that corresponded to 1, 2 and 3 F mol^{-1} , and it was observed that at least 3 F mol^{-1} was necessary in order to achieve full conversion, as shown in Figure 3.13 (result confirmed by $^1\text{H NMR}$). When a lower

amount of electricity was passed through the cell, the starting material was still observed in the chromatogram (red line, m/z : 314.5).

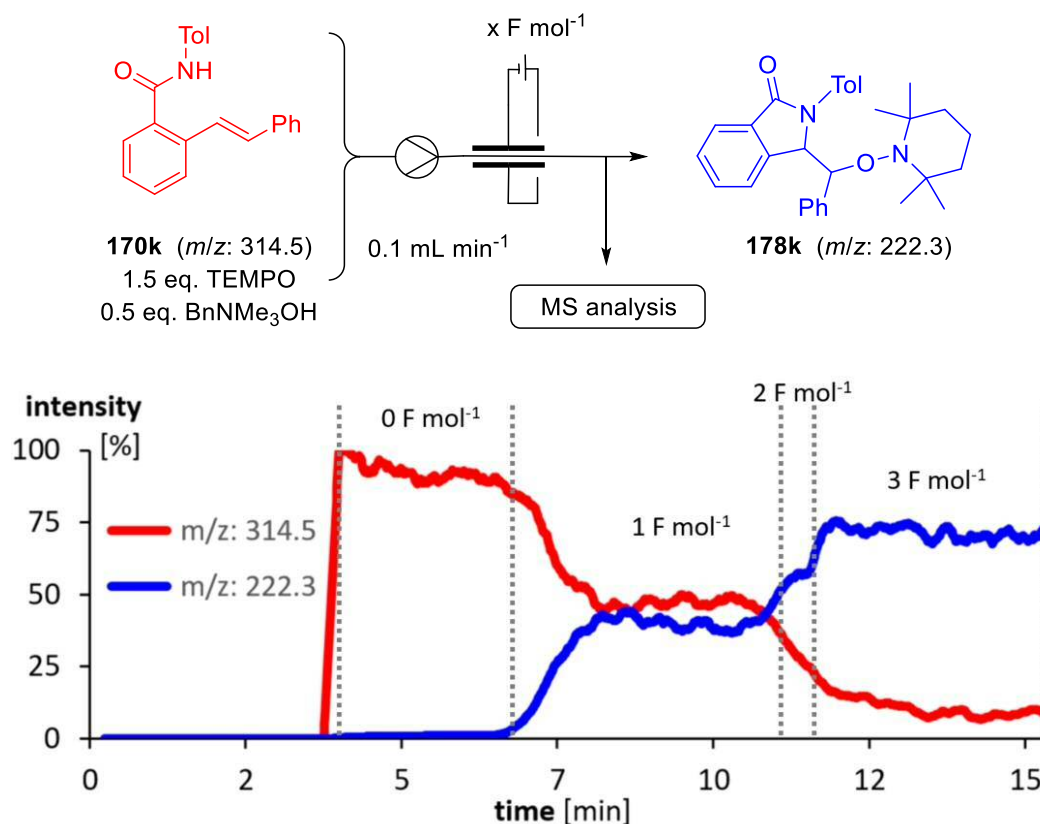


Figure 3.13: Inline mass spectrometry analysis of the electrochemical flow reaction.

The cyclisation reaction was carried out with 1 and 0.5 equivalent of base, and the same result was obtained in both cases. Further studies to try to avoid the use of a base were conducted, and are explained in the next section.

3.3.3. Base effect study for amides as substrates

The experiments carried out in the previous section show comparable results for the cyclisation when the base is used stoichiometrically and substoichiometrically (1 and 0.5 equivalents). The transformation of amide **164b** was explored with the base that was found the optimum (benzyltrimethylammonium hydroxide **156**), with the one that gave similar results to those in the absence of base (2,6-lutidine), and with no base. The results are summarised in Figure 3.14, and corroborate the results of the previous studies with the carbamate. The reaction proceeds to completion after 3 F mol⁻¹ when base **156** is used. When the reaction is carried out without the presence of base, a very high current is needed to produce the product, and even after 14 F mol⁻¹ the conversion obtained is not

higher than 87%. At this point some decomposition is already observed in the crude ^1H NMR due to the high current. These results highlight again that performing the reaction without a base is not efficient. That could be due not only to the ability of the base to deprotonate the amide, lowering its oxidation potential, but also to its effect as a supporting electrolyte, lowering the resistance in the solution.

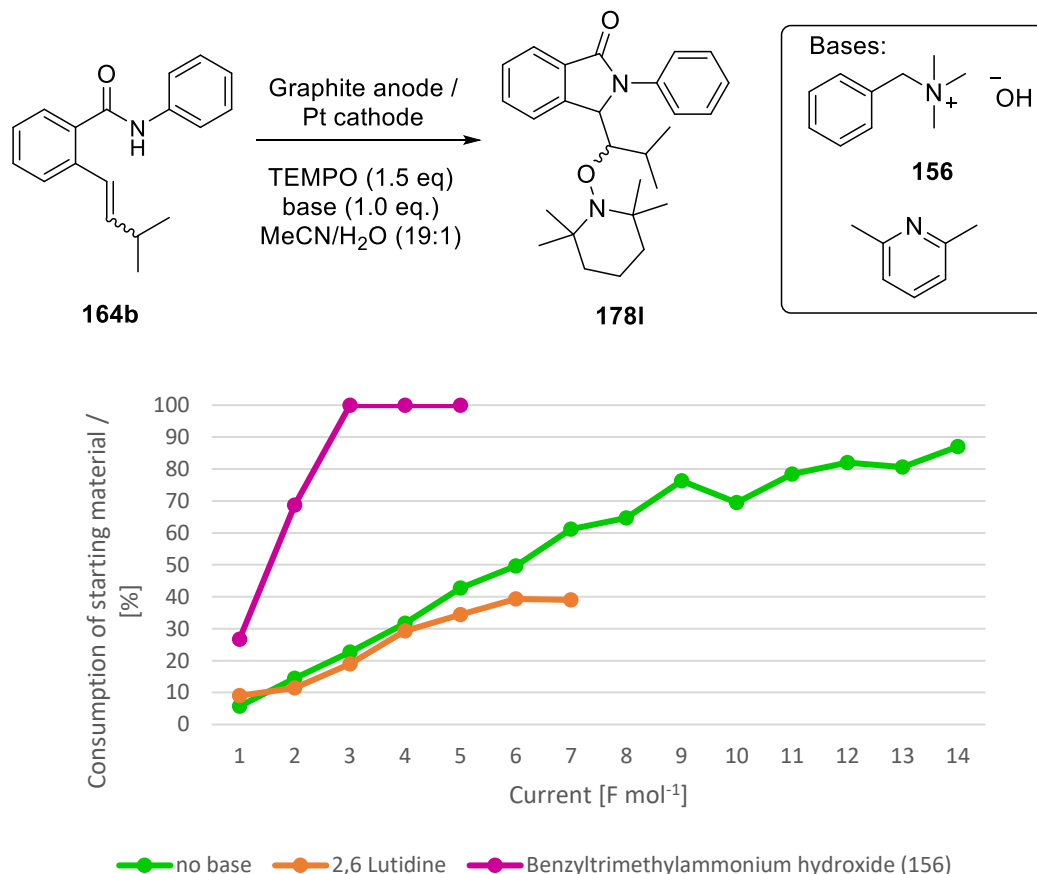


Figure 3.14: Base effect on the amide cyclisation. [Consumption of starting material measured by ^1H NMR]

Once the optimised conditions had been explored and established, a larger scale reaction was performed for 1.5 hours. Compound **178I** was obtained in 96% yield (180 mg). It is noteworthy that the same reaction performed in batch required the use of an external supporting electrolyte and led to product **178I** in only 51% yield (107 mg) after 6 hours. This also demonstrates the efficiency of the flow process, where an intentionally added supporting electrolyte is not necessary. This does not only reduce the amount of reagents used, but also the side products of the reaction.

The reaction gave product **178I** as a mixture of diastereoisomers. The major diastereomer ((*R,S*)/(*S,R*) isomer) is a colourless solid and the minor diastereomer ((*R,R*)/(*S,S*) isomer)

is a colourless oil. The structure of the major product (*(R,S)/(S,R)* isomer) was confirmed by X-ray crystallography, as shown in Figure 3.15.

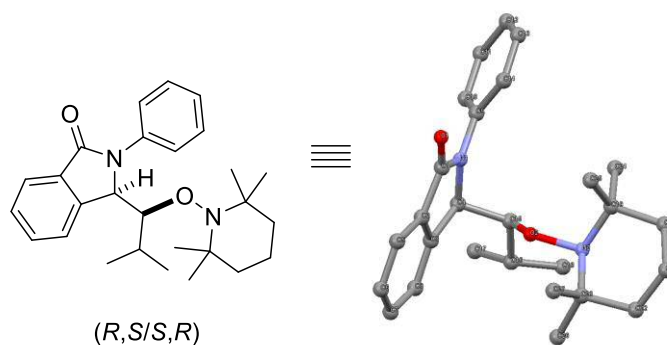


Figure 3.15: Crystal structure of compound X (*(R,S)/(S,R)* isomer).

Product **178I** was analysed by ^1H NMR (Figure 3.16), and proton H^{a} did not appear as clear doublet as it was expected. H^{a} appears as a broad singlet, and H^{b} appears as a doublet of doublet, as it is expected, but one of the coupling constants is very low. H^{a} should be a doublet coupling to H^{b} , but due to the small coupling constant ($J = 1.9$ Hz) the second peak from H^{a} cannot be observed in the spectrum, and it appears as a broad singlet.

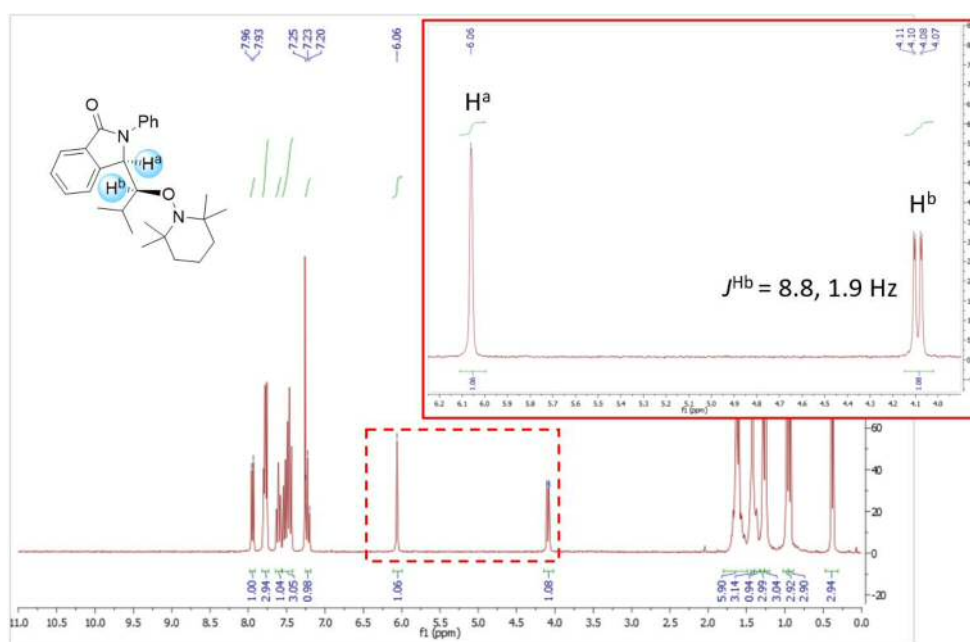


Figure 3.16: ^1H NMR of compound **178I**.

This coupling effect can be explained with the Karplus curve or Karplus equation. The Karplus curve exhibits the relation between the vicinal coupling constant and the dihedral angle of the two protons coupling.^[32,33] A simple illustration of the Karplus curve is shown in Figure 3.17. For dihedral angles of 0° or 180° , the coupling constant is large

($^3J_{HH'}$ = 7-15 Hz). As the dihedral angle increases from 0 ° to 90 °, the coupling constant decreases, until it reaches 90 °, when it will reach the lowest value ($^3J_{HH'}$ = 0-2 Hz). As the dihedral angle increases from 90 ° to 180 °, the coupling constant increases gradually with the angle, until it reaches the maximum at 180 °.

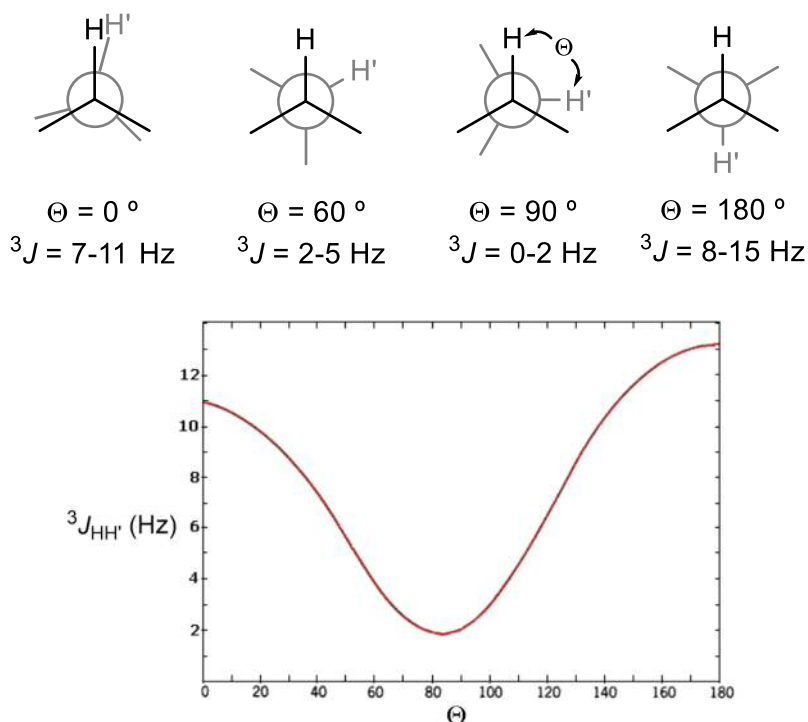


Figure 3.17: Karplus curve.

X-ray crystallography (Figure 3.15) helped to explain why the coupling constant observed is so low, making the proton H^a appear as a broad singlet and not as a doublet. Compound **178l** shows a dihedral angle between protons H^a and H^b of 94.3 °, therefore, according to the Karplus curve, the expected coupling constant would be between 0 and 2 Hz.

3.3.4. Effect of different spacers

The reaction of carbamate **154** to product **155** was investigated using different FEP spacers of varying thickness (250 and 500 μm) with the optimised reaction conditions. The reaction was performed on a 0.175 mmol scale, and the result analysed by ^1H NMR using 1,3,5-trimethoxybenzene as internal standard. When a 250 μm spacer is used, full conversion is achieved and compound **155** is obtained in 80% yield. When the 500 μm spacer is used, full conversion is achieved and compound **155** is obtained in 84% yield. With these results, it can be concluded that the thickness of the spacer used does not have

an effect on the reaction outcome. The choice of the thickness of the spacer will have to take into consideration the needs of the reaction and the resistance of the solution (for solutions with a higher resistance, a thinner spacer will be more appropriate).

3.3.5. Scope of the reaction

With the optimised conditions in hand, different substrates were examined varying the substituents on the amide and the moiety attached to the double bond (R'), shown in Table 3.2.

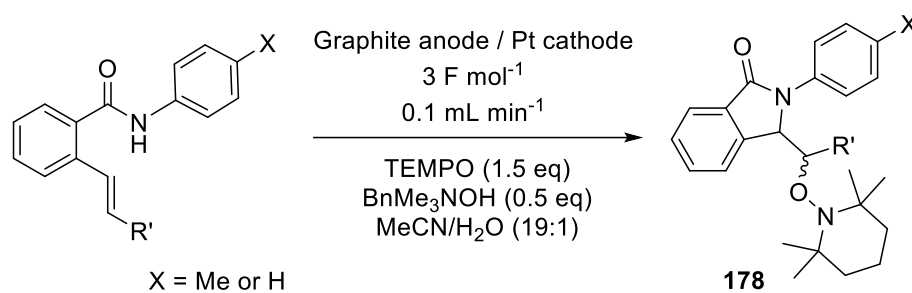
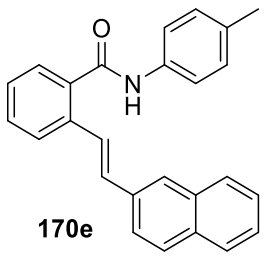
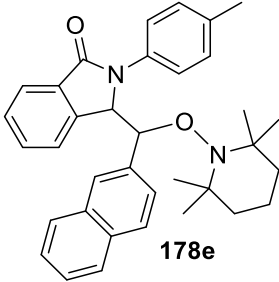
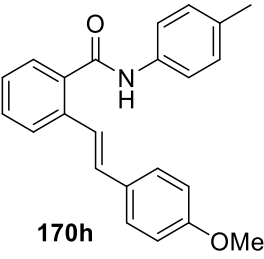
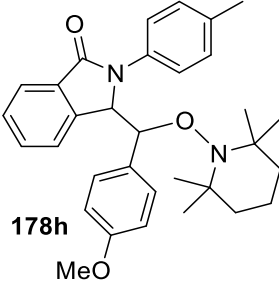
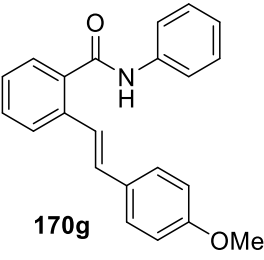
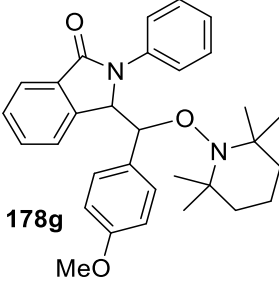


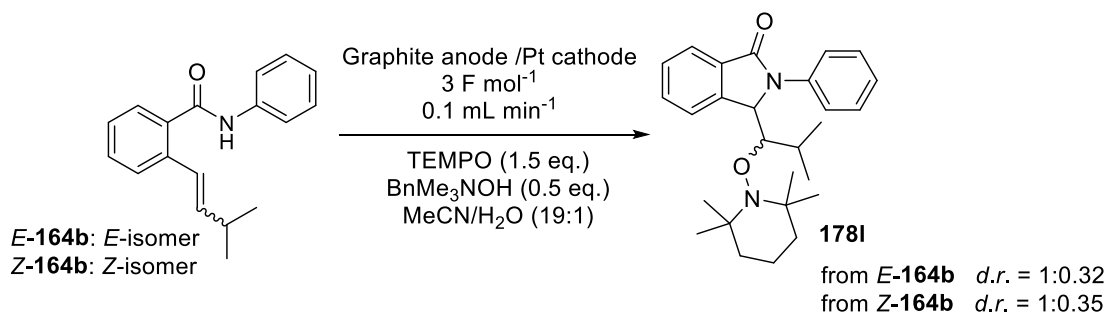
Table 3.2: Substrate scope with different alkenes

Entry	Substrate	Product	Yield [%]	<i>d.r.</i> ^a
1			75	1.65:1
2			96	3:1
3			62	1.15:1

4			79	1.57:1
5			21	1.27:1
6			18	1.21:1

^a The major diastereoisomer is the (*R,S/S,R*).

The reaction was performed with different substituents adjacent to the double bond, and the products were obtained in good yields with different aliphatic (**178m** and **178l**) and aromatic substituents (**178b**, **178e**, **178g** and **178h**). Only with strongly electron-donating substituent on the aromatic ring, such as the 4-OMe functionality, did the reaction result in a complex mixture of compounds. The desired product was obtained in 21 and 18% yield (Table 3.2, entries 5 and 6, respectively).



Scheme 3.20: Effect of the stereochemistry of the substrate in the product selectivity.

Due to the radical pathway of the cyclisation, the diastereoselectivities are low and were dictated only by steric effects. The stereochemistry of the substrate was also found not to

affect the selectivity, thus when pure *E*- or *Z*-isomers were used for the reaction, the same diastereomeric ratios were obtained for compound **178i**, as shown in Scheme 3.20.

The cyclisation was performed with electron-withdrawing substituents in the aromatic ring adjacent to the double bond, and the results are shown in Table 3.3.

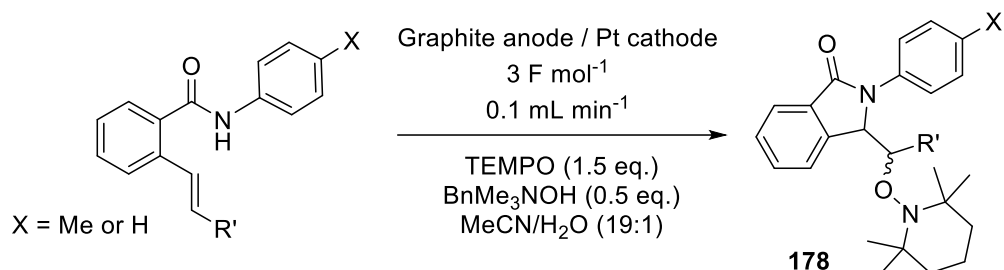


Table 3.3: Substrate scope with electron-poor aryl substituted alkenes

Entry	Substrate	Product	Yield [%]	<i>d.r.</i> ^a
1			56	1.29:1
			21 ^b	-
2			94	-
3			91	-

^aThe major diastereoisomer is the (*R,S/S,R*). ^bProduct obtained together with compound **178c**

When electron-withdrawing substituents such as chloride are attached to the aromatic ring adjacent to the double bond, the reduced product **178cb** was observed in addition to **178c**. With a 3-nitrophenyl substituent (**170i** and **170f**) the only compound obtained were the reduced products **180** and **181** (Table 3.3, entries 2 and 3), where no TEMPO addition was observed. In these reactions there was no gas evolution at the outlet of the reactor, as was observed in all other reactions, which implies that there is no gaseous H₂ formed from the H⁺ reduction. This suggests that there is another reduction reaction taking place, which is the reduction of the substrate **170i** and **170f**. This will not consume all the electrons, as we are using an excess (3 F mol⁻¹), but in this case TEMPO is not being consumed as it is not added to the final product. This means that the redox cycle can be completed by reducing the oxoammonium cation to the free radical, explaining the absence of gas evolution. It is known that alkenes bearing electron-withdrawing functionalities are favoured towards reduction,^[34] which endorses the results obtained with compounds **170i** and **170f**.

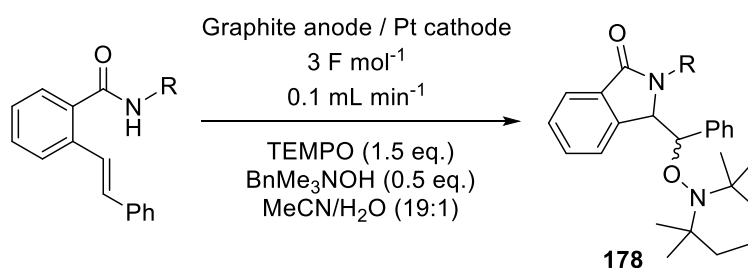
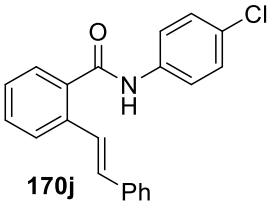
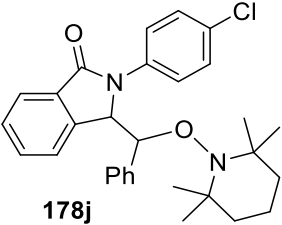
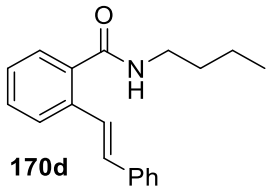
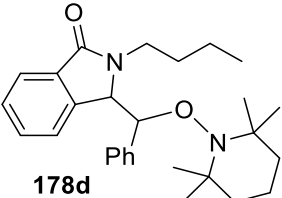


Table 3.4: Substrate scope with different amides

Entry	Substrate	Product	Yield [%]	<i>d.r.</i> ^a
1			72	1.14:1
2			78	1.24:1

3	 170j	 178j	56	1.04:1
4	 170d	 178d	0 (no reaction)	-

^a The major diastereoisomer is the (*R,S/S,R*).

The electrochemical cyclisation was performed using different substituents on the amide side, as shown in Table 3.4. When substituted aromatics were used, the reaction proceeded successfully to give the desired product, regardless of the nature of the substituent on the aromatic ring (Table 3.4, entries 1-3). However, when an aliphatic chain was attached to the nitrogen atom of the secondary amide, the cyclisation did not take place, and the starting material was recovered (Table 3.4, entry 4). These results could be due to the ability of the aromatic ring to stabilise the radical on the nitrogen, which would be less stable in the case of the aliphatic substituted amide.

Cyclic voltammetry studies show that compound **170d** (entry 4 in Table 3.4) can be oxidised at a potential of 1.50 V (*vs* Ag/AgCl), which seems feasible for an electrochemical oxidation (Figure 3.18). The CV measured in the presence of a base shows the disappearance of the oxidation peak, and no peak for oxidation or reduction is observed (Figure 3.19). This could explain why the reaction does not give any product and only starting material is recovered.

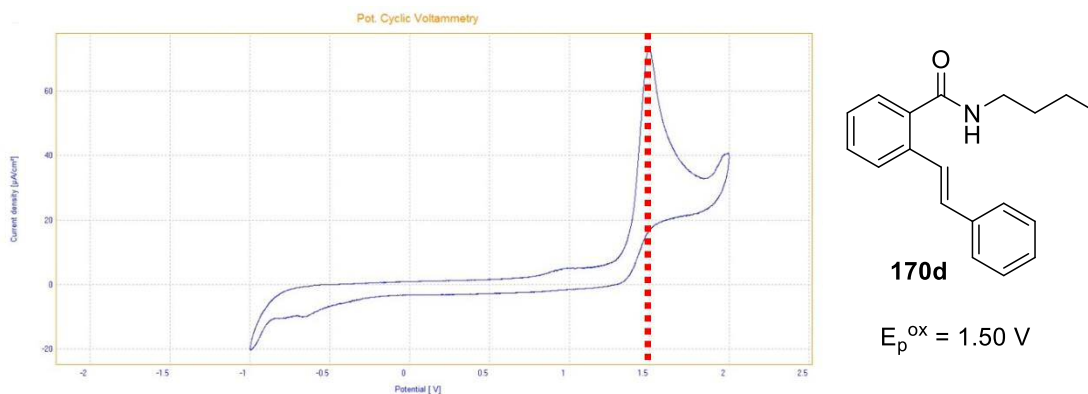


Figure 3.18: CV of substrate 170d.

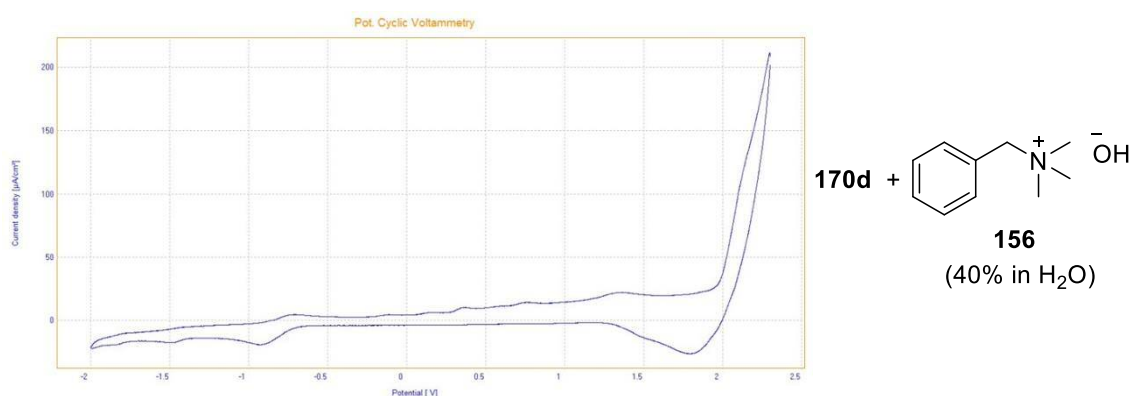
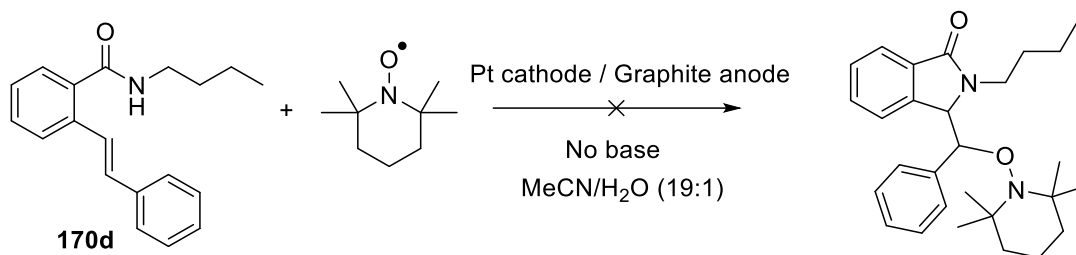


Figure 3.19: CV of substrate 170d in the presence of base 156.

Oxidative cyclic voltammograms of the substrates (1 mM) recorded in 0.075 M Bu₄NBF₄/MeCN electrolyte at 100 mV/s scan rate. Working electrode: glassy carbon electrode tip (3 mm diameter); Counter electrode: platinum wire; Reference electrode: Ag/AgCl in 3 M NaCl.

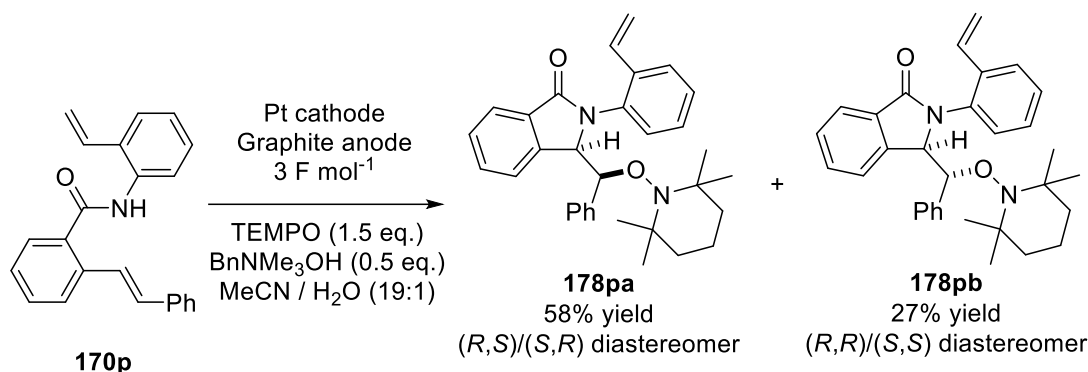
Our previous studies show that when the electrochemical transformation is performed in the absence of base, the reaction is slow but the product is obtained, even if full conversion cannot be achieved (Section 3.3.3). Thus, the electrochemical oxidation of substrate **170d** was carried out under the optimised conditions but without any base, as the CV studies exhibit a promising oxidation peak under neutral conditions (Figure 3.18). Unfortunately, even this attempt led only to recovery of starting material, and no cyclised product was detected (Scheme 3.21).



Scheme 3.21: Attempt of electrochemical cyclisation of compound **170d**.

3.3.6. Tandem cyclisation attempt

A tandem cyclisation reaction was attempted with a vinylphenyl substituent on the nitrogen (**170p**), but only monocyclised product **178p** was obtained (Scheme 3.22). This compound now bears a functionalised styrene moiety that can be used in subsequent reactions.



Scheme 3.22: Attempt to tandem cyclisation of **21**.

NMR characterisation of product **178p** was difficult due to the appearance of broad peaks, which could only slightly be improved at a high temperature NMR (Figures 3.20 and 3.21). Both compounds **178pa** and **178pb** were thick oils, therefore it was not possible to perform crystallographic studies to confirm the structure of the product obtained. As the ^1H NMR spectra suggested the presence of the TEMPO moiety in the aliphatic region, the product was further functionalised to the alcohol so the molecule could be analysed.

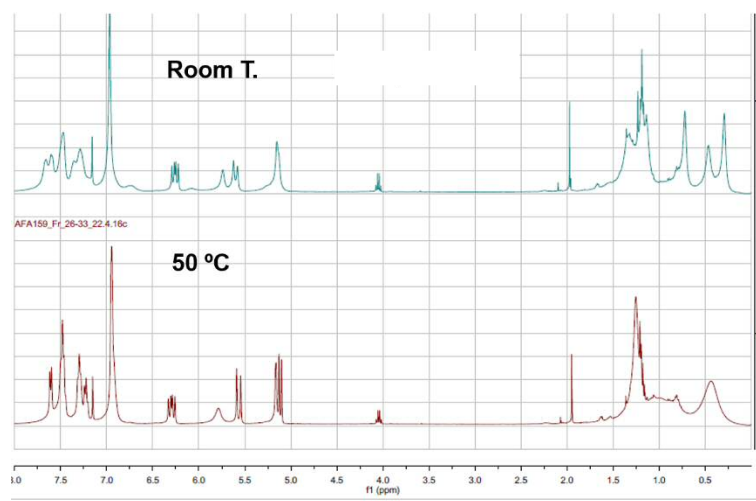


Figure 3.20: ^1H NMR of compound 178pa.

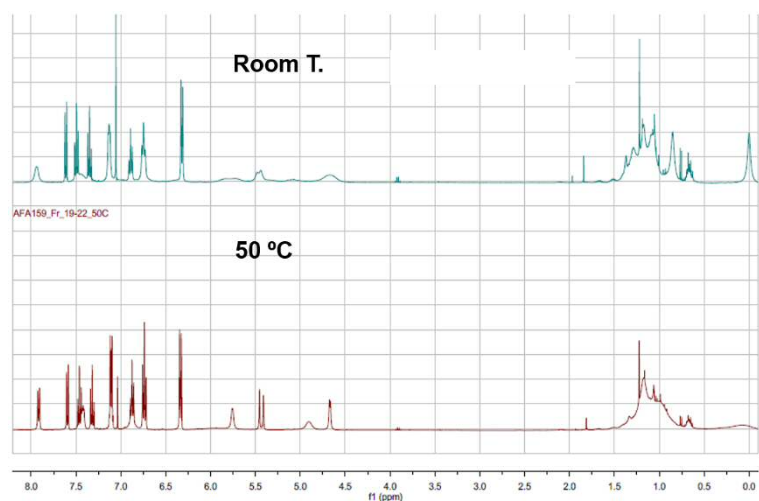
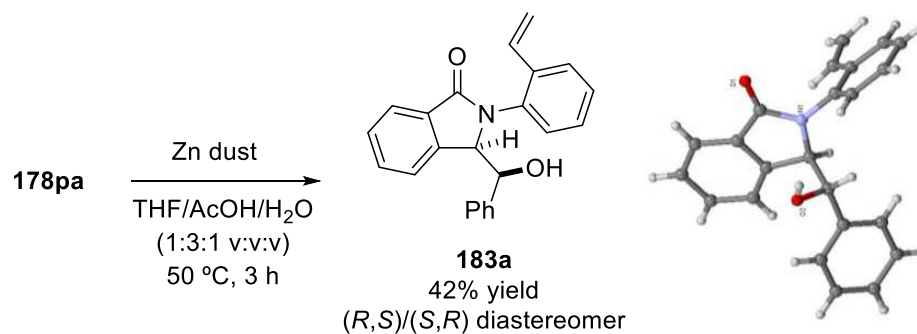
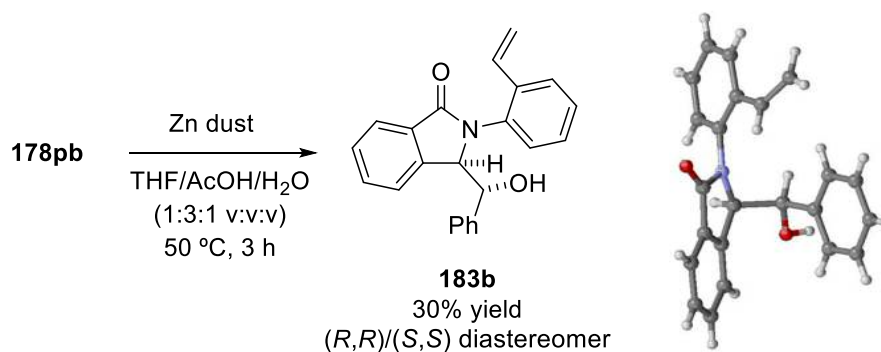


Figure 3.21: ^1H NMR of compound 178pb.

After separation of the diastereomers, the oxygen–nitrogen bond was cleaved with zinc and acetic acid. The alcohol products were colourless solids and the structures of the two diastereoisomers **183a** and **183b** were determined by X-ray crystallography analysis (Schemes 3.23 and 3.24).



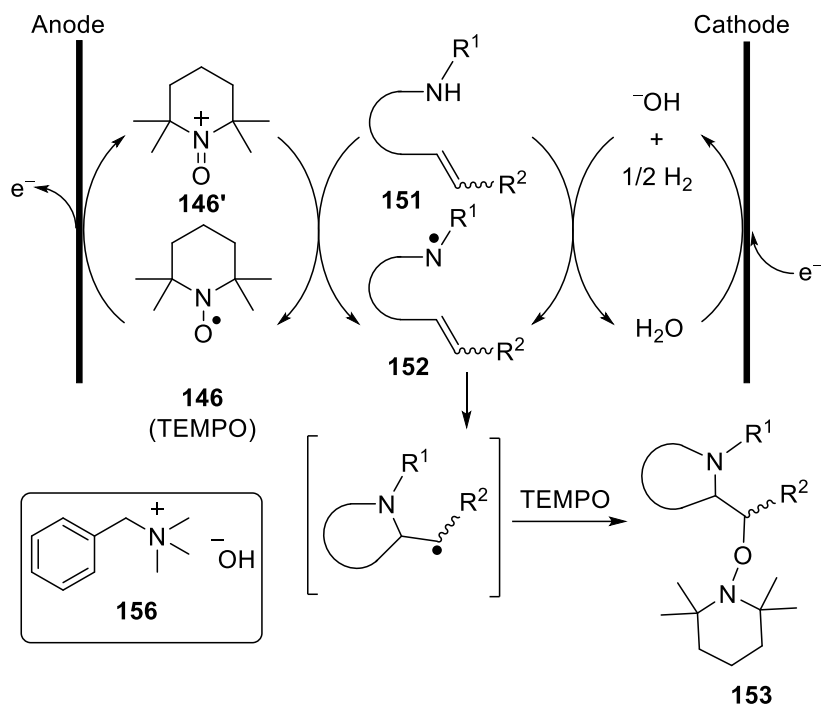
Scheme 3.23: N–O bond cleavage of 178pa, and X-ray analysis.



Scheme 3.24: N–O bond cleavage of 178pb, and X-ray analysis.

3.3.7. Proposed mechanism

The mechanism for such nitrogen-radical mediated cyclisations proposed by Xu *et al.*^[35] is shown in Scheme 3.25. They state that the hydroxide anion formed at the cathode helps to deprotonate the nitrogen-containing compound and then form the nitrogen-centred radical. Our results are in agreement with the proposed mechanism, and show that in our transformation the addition of a base will deprotonate the amide. This makes the oxidation potential of the anion formed much lower than that of the neutral species, favouring the oxidation (see Section 3.2.3 of this chapter).



Scheme 3.25: Proposed mechanism.

We have observed that the presence of TEMPO is necessary to obtain the desired product, and when less than 1.5 equivalents is used, the reaction does not go to completion. To confirm if TEMPO is acting as a mediator or only as a radical scavenger, some cyclic voltammetry studies have been conducted.

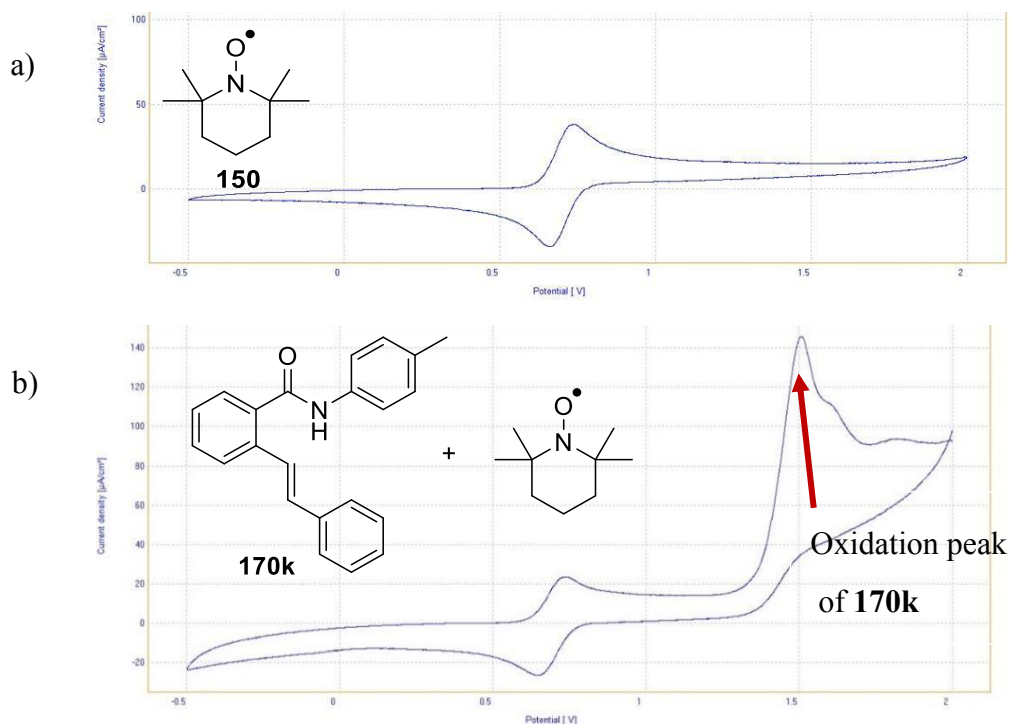


Figure 3.22: a) CV of TEMPO, b) CV of compound 170k and TEMPO.

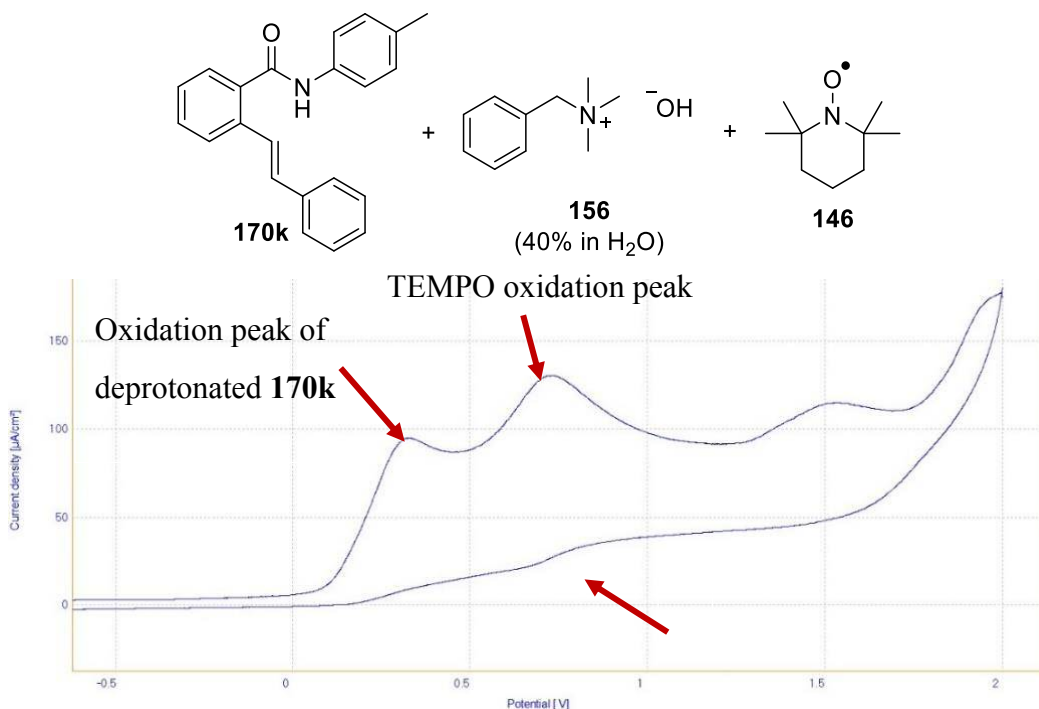


Figure 3.23: CV mechanistic studies.

Oxidative cyclic voltammograms of the substrates (1 mM) recorded in 0.075 M $\text{Bu}_4\text{NBF}_4/\text{MeCN}$ electrolyte at 100 mV/s scan rate. In Figure 3.23: substrate **170k** (5 mM) and TEMPO (1 mM). Working electrode: glassy carbon electrode tip (3 mm diameter); Counter electrode: platinum wire; Reference electrode: Ag/AgCl in 3 M NaCl.

The cyclic voltammogram of TEMPO was measured (Figure 3.22a), followed by that of the substrate **170k** in the presence of TEMPO (0.2 equivalents). The CV shows that the redox cycle of TEMPO remains intact (Figure 3.22b). A third measurement of a mixture of substrate **170k**, base and TEMPO was performed, and in this case the reduction peak of TEMPO disappeared (Figure 3.23), which indicates that the oxoammonium salt **146'** is not being reduced electrochemically, but chemically (*i.e.* oxidising substrate **170k**). This showcase that the electrochemical transformation does not occur directly on the surface of the electrode, but it is mediated by TEMPO.

It has been observed in previous studies that the oxoammonium salt **146'** can be unstable under basic conditions. To verify that the disappearance of the TEMPO reduction peak in Figure 3.23 is due to the chemical reaction and not to decomposition, some cyclic voltammetry studies were carried out in the presence of the base: benzyltrimethylammonium hydroxide. The amount of base was increased gradually from 0.25 to 1 equivalent (Figures 3.24, 3.25, 3.26 and 3.27).

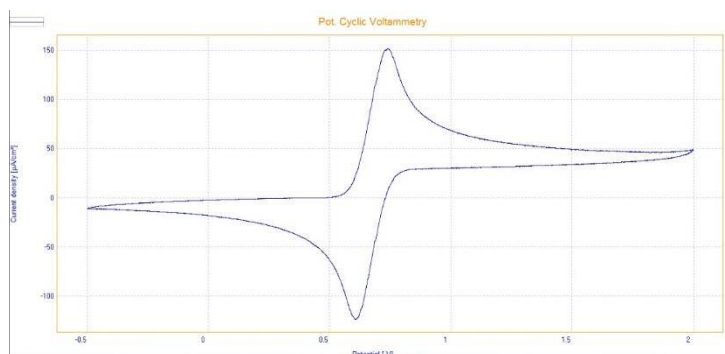


Figure 3.24: CV of TEMPO.

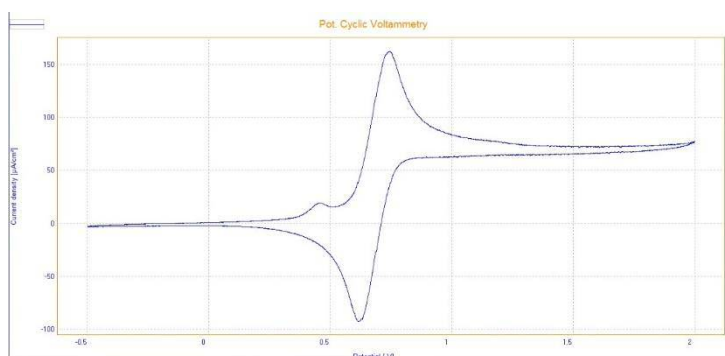


Figure 3.25: CV of TEMPO + 0.5 eq. base 156.

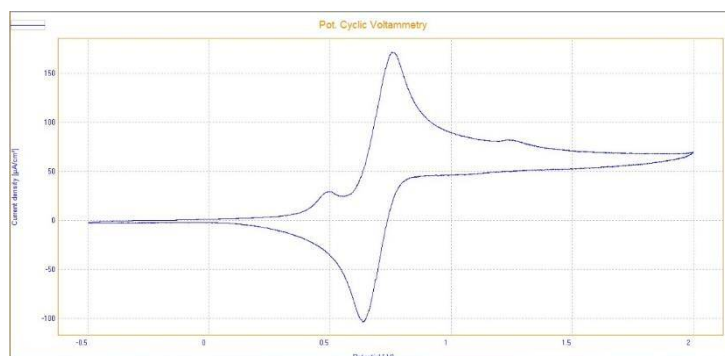


Figure 3.26: CV of TEMPO + 0.75 eq. base 156.

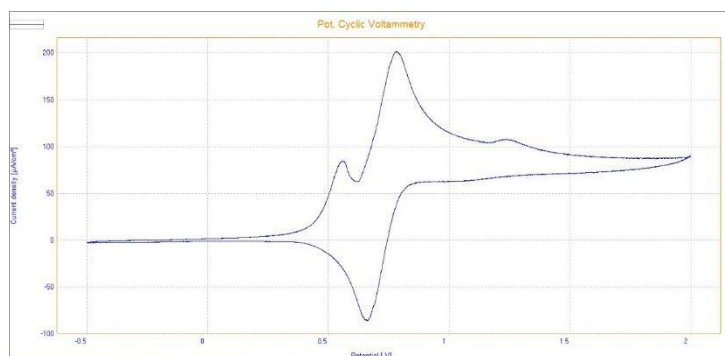


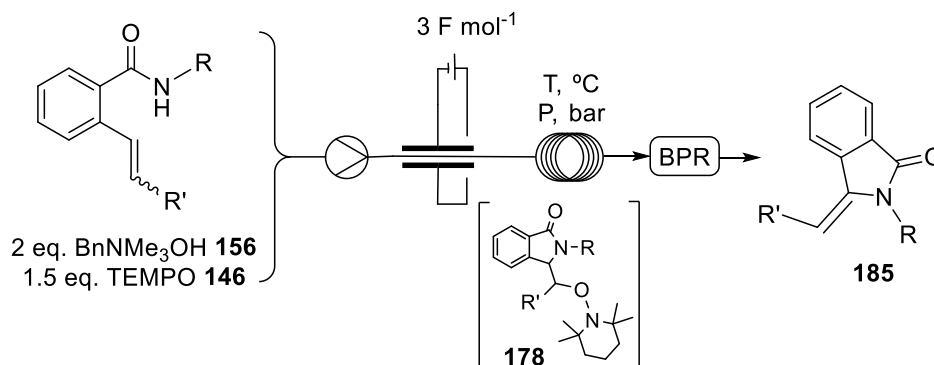
Figure 3.27: CV of TEMPO + 1 eq. base 156.

Some decomposition is observed after increasing the amount of base in the solution (Figures 3.25, 3.26 and 3.27), and the reduction peak intensity slightly decreases when more than 0.75 equivalents of base is added. Total decomposition is not observed, which indicates that the proposed mechanism of the oxidation mediated by TEMPO is possible. As in the reaction only 0.5 equivalents of the base are added, it is all used to deprotonate the substrate. In the CV carried out with the substrate **170k**, TEMPO and 0.5 equivalents of base, the reduction peak disappears completely (Figure 3.23), not only decreasing as observed in the one measured with TEMPO and 1 eq. of base (Figure 3.27). This indicates that the oxoammonium salt is consumed/used completely, showing that it cannot be due only to decomposition.

The product obtained in the electrochemical reaction can be further functionalised by eliminating the TEMPO moiety to obtain the alkene, or cleaving the N–O bond to give the alcohol. The next sections will explain the two-step flow approaches for such transformations.

3.4. Two-step flow approach: Electrochemical cyclisation and elimination of TEMPO to form alkenes

The TEMPO moiety present in the products obtained in the electrochemical cyclisation can be removed by elimination using a base and heat.^[36] This reaction can be coupled to the first electrochemical oxidation in a single flow system. The first product does not need to be isolated and can be used directly in the second flow reactor (Scheme 3.26). Elimination was performed with the same base as the one used in the cyclisation. The second flow reactor consists of a coil (PTFE tubing) of 0.5 mm internal diameter. Different coil lengths, and therefore different reaction times, were studied to obtain full conversion to the desired product. Compound **164b** was used as a model substrate. The reaction was first performed with a high flow rate (0.4 mL min⁻¹), a 1 mL coil (rt = 2.5 min) and heated up to 60 °C immersing the tubing in a water bath. The elimination product was obtained in 37% conversion (Table 3.5, entry 1).



Scheme 3.26: Two-step flow reaction: Cyclisation and elimination.
BPR: Back pressure regulator.

The flow rate was decreased to 0.1 mL min⁻¹ in order to increase the residence time, and the temperature was increased to 70 °C (entries 2 and 3). With these conditions the conversion improved but only to 67%. The reaction coil volume was doubled to 2 mL, so the reaction time could be increased to 20 minutes (entry 4). This longer residence time gave the desired elimination product in 91% conversion. Increasing the temperature to 85 °C only resulted in a slight improvement, and a longer reaction coil (2.5 mL, *rt* = 25 min) had to be used to achieve full conversion (entry 6).

Table 3.5: Two-step flow reaction optimisation for set-up in Scheme 3.26.

Entry	Flow rate, mL min ⁻¹	Res. time (step 2), min	Coil vol., mL	Coil T/P, °C/bar	¹ H NMR conv. (164b to 185), %
1	0.4	2.5	1	60/1	37
2	0.25	4	1	70/1	49
3	0.1	10	1	70/1	67
4	0.1	20	2	70/1	91
5	0.1	20	2	85/2.8	93
6*	0.1	25	2.5	85/2.8	>99

* 76% isolated yield (40 mg)

With these optimised conditions, a larger scale reaction was performed, and compound **185** was obtained in 76% isolated yield over two steps.

Compound **185** was obtained as a mixture of *E*- and *Z*-isomers, with an excess of the *E*-isomer (9:1). The configuration was determined by NOE NMR to study the interaction of two protons through space, and not through chemical bonds. The studies were focused on the aromatic region of the spectrum (Figure 3.28). The aromatic proton signals corresponding to H¹ and H² for each isomer could be identified, as H¹ corresponds to 1 proton, and H² to 2 protons.

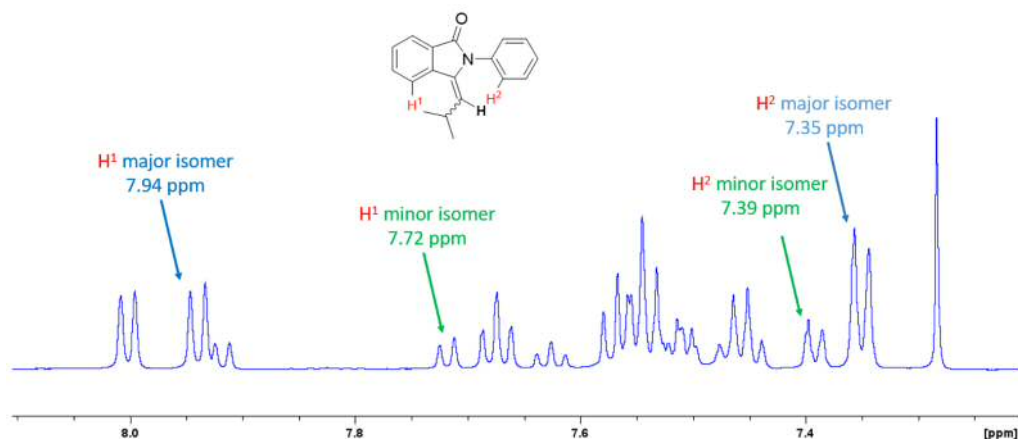


Figure 3.28: Aromatic region of the ¹H NMR of *E*- and *Z*-mixture of compound **185**.

The interaction between the two different alkene protons observed (for major and minor isomer) with H¹ and H² suggests that the minor product is the *Z*-isomer, and the major product is the *E*-isomer, as shown in Figure 3.29.

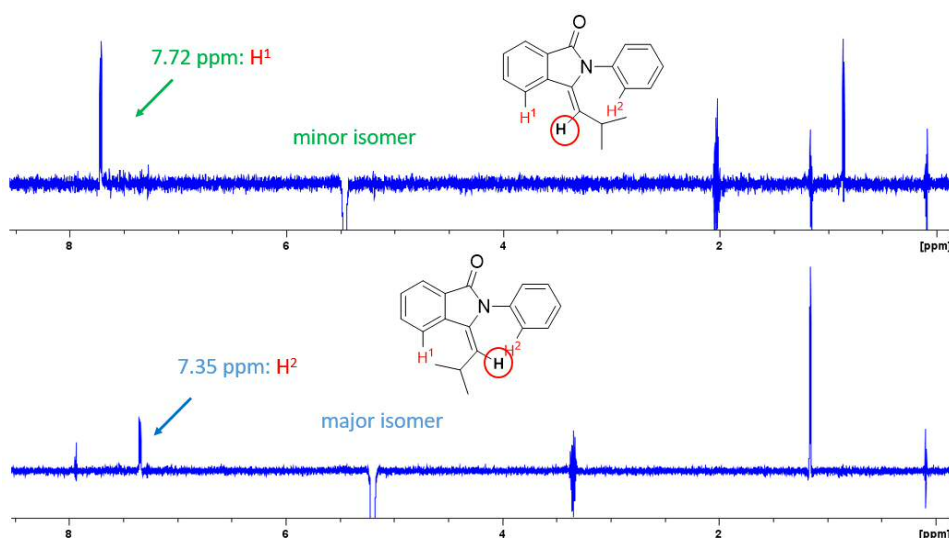


Figure 3.29: NOE NMR for compound **185**.

With the optimised conditions found in Table 3.5, a scope of substrates was studied (Figure 3.30). Different substituted aromatics were screened at the amide and the carbon

adjacent to the double bond. In all cases the reaction proceeded successfully with *E/Z* selectivities ranging from 5/1 (**188**), to 19/1 (**186** and **187**).

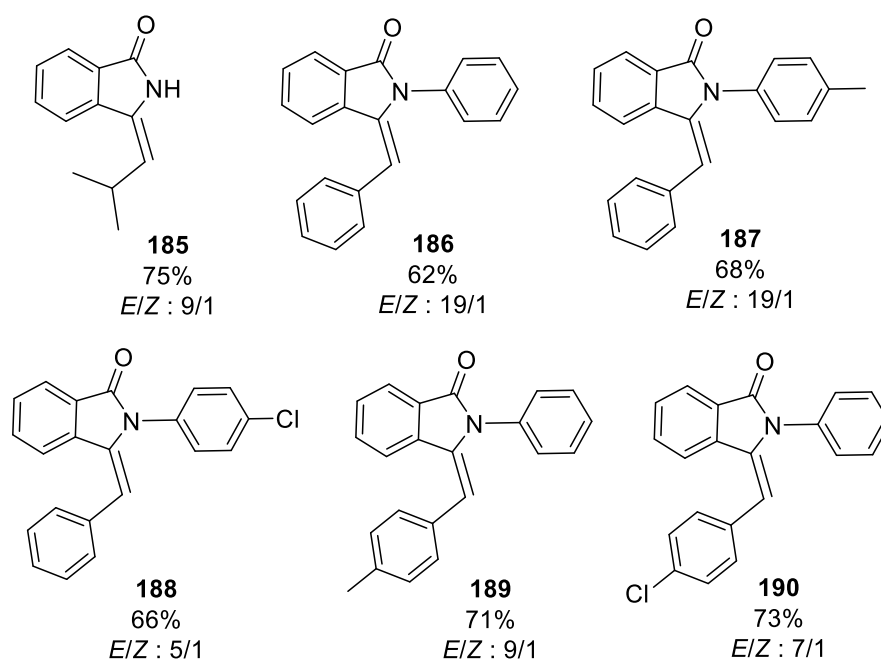
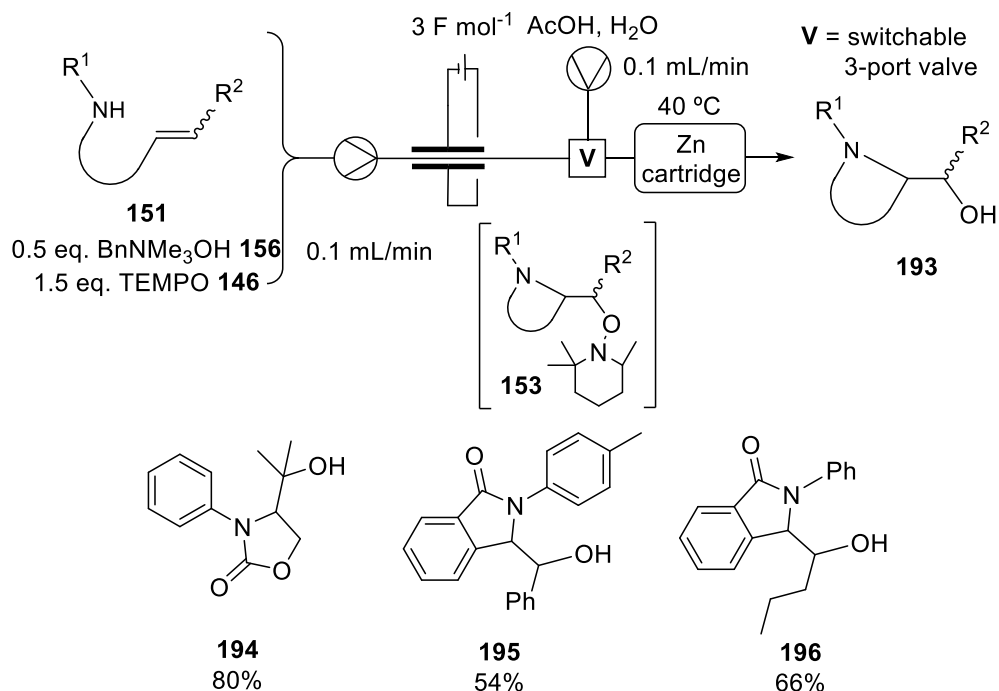


Figure 3.30: Substrate scope for elimination reaction.

3.5. Two-step flow approach: Electrochemical cyclisation and N–O bond reductive cleavage to form alcohols

The N–O bond from the TEMPO moiety present in the products obtained in the electrochemical cyclisation can be cleaved by using zinc and acetic acid.^[37,38] This transformation was done in batch with compounds **178pa** and **178pb**, as explained in Section 3.3.6. This second chemical transformation was performed in continuous flow by connecting the outlet of the electrochemical reactor to a cartridge containing Zn dust^[39] and a second stream pumping a mixture of acetic acid and water (Scheme 3.27). The three pieces of tubing were connected by a switchable 3-port valve (Figure 3.31).



Scheme 3.27: Two-step flow reaction: cyclisation and reduction.

The first attempt to pack the cartridge with Zn dust led to an overpressure in the system, due to the small size of the Zn dust particles (<10 μm). To overcome this problem, silica (60 – 100 mesh) was used as a support for the small Zn particles (50wt%). The cartridge was packed with the mixture of silica and zinc and the solvent passed through it smoothly. The carbamate precursor of compound **194** was used as a substrate to optimise the two-step chemical transformation.

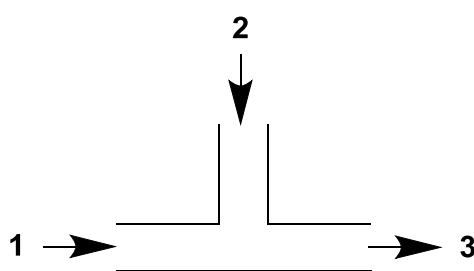


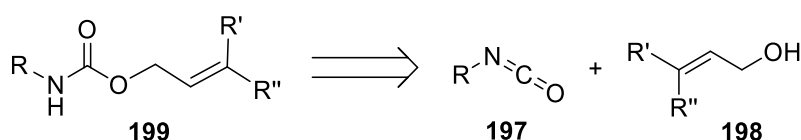
Figure 3.31: Switchable 3-port valve.

Firstly, the outlet of the electrochemical reactor was connected to the three-port valve with the three ports open. A mixture of acetic acid and water was mixed with the crude solution, prior to entering the Zn cartridge. Only traces of the desired alcohol product were observed. Flushing the cartridge with acid before the substrate was introduced could improve the reduction. The mixture of acetic acid and water was pumped through the Zn

cartridge with at least three cartridge volumes, using ports 2 and 3 of the valve, and keeping 1 closed. Then the electrochemical reaction was carried out, and the outlet mixed with the stream of acetic acid and water (ports 1, 2 and 3 open). In this case the desired alcohol product was obtained in 43% conversion, meaning that flushing the Zn cartridge with acid prior to the reaction improves the result of the transformation. To increase the reactivity, the Zn cartridge was heated up to 40 °C by immersing it in a water bath. This improved the result significantly, giving the alcohol product in more than 98% conversion. With these optimised conditions, three different substrates were tested in the two-step set up, leading to the corresponding alcohols in good yields over two steps (Scheme 3.27).

3.6. Two-step flow approach: Synthesis of carbamates in flow and subsequent electrochemical cyclisation

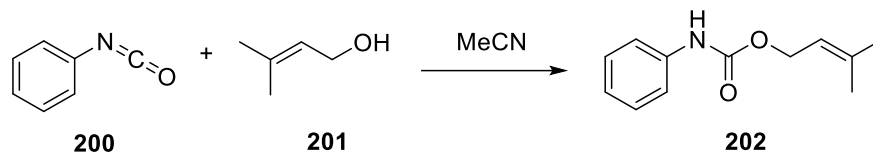
Carbamates **199** bearing an alkene moiety can be synthesised from the corresponding isocyanate **197** and allylic alcohol **198** (Scheme 3.28). Such compounds serve as substrates for the electrochemical cyclisation described herein. These compounds can be synthesised in one step from commercially available compounds. Therefore, their synthesis in continuous flow has been studied with the aim to feed the crude reaction mixture directly into the electrochemical reactor, making the whole process more efficient.



Scheme 3.28: Carbamate synthesis from isocyanates and allylic alcohols.

Work begun with adaptation of reaction conditions to the requirements of the electrochemical transformation. The standard procedure to synthesise the carbamates in batch uses triethylamine as a base and dichloromethane as solvent. From studies performed in Section 3.2.2, it was concluded that the electrochemical cyclisation must be done in acetonitrile as the main solvent, and that triethylamine suppressed the desired oxidation. Therefore, the coupling reaction between the isocyanate and allylic alcohol was performed in acetonitrile and in the absence of base (Scheme 3.29). The reaction was stirred at room temperature for 24 hours, but after that time there was still starting material

remaining. However, the reaction was heated up to 60 °C for one hour, and the starting material was fully consumed. This proved that the transformation could be performed under the desired conditions; in acetonitrile without a base.



Scheme 3.29: Carbamate synthesis in acetonitrile in batch conditions.

The same reaction was performed in continuous flow by mixing two streams, one containing the isocyanate **200** in acetonitrile, and the other with the alcohol **201**. They were pumped with a total flow rate of 0.1 mL min⁻¹ into a 2 mL coil that was heated up to 60 °C in a water bath. The reaction was analysed by gas chromatography, injecting the crude sample directly after 30 seconds collection. The chromatogram showed the formation of the carbamate (**202**), but with large amount of starting material remaining unreacted (Table 3.6, entry 1).

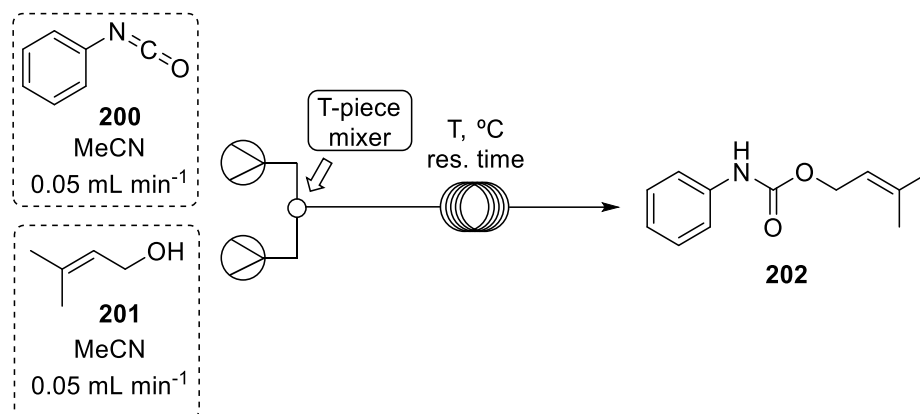
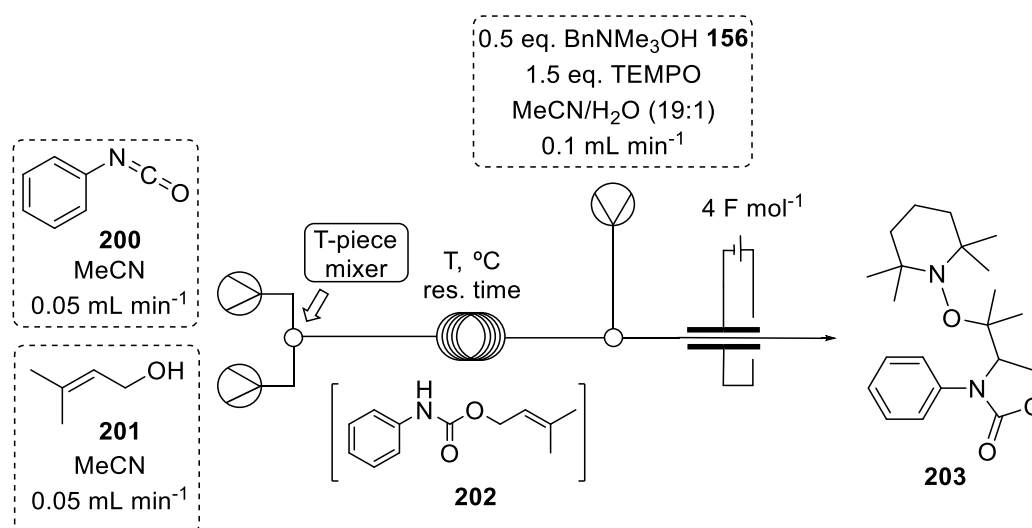


Table 3.6: Optimisation of carbamate synthesis in flow.

Entry	Temperature [°C]	Reactor size [mL]	Reaction time [min]	GC peaks ratio 200:201:202
1	60	2	20	1.21 : 1.26 : 1
2	80	2	20	0.42 : 0.45 : 1
3	80	4	40	0 : 0 : 1

The same reaction was performed at 80 °C, with improved conversion towards the desired carbamate, but there was still a significant amount of starting material remaining (entry 2). The reactor size was doubled (4 mL), and the reaction was carried out under the same conditions (0.1 mL min⁻¹, 80 °C). The isocyanate and alcohol were completely consumed, and the carbamate (**202**) was the only product observed in the gas chromatogram (entry 3). With the optimum conditions for the first reaction in hand, the outlet of the coil was mixed with a solution of benzyltrimethylammonium hydroxide **156** and TEMPO in a mixture of MeCN/H₂O (19:1), and pumped into the electrochemical reactor (Scheme 3.30). Unfortunately, only the carbamate **202** was observed, and no trace of the cyclised product **203** was detected.



Scheme 3.30: Two-step set-up: Carbamate synthesis and subsequent electrochemical cyclisation.

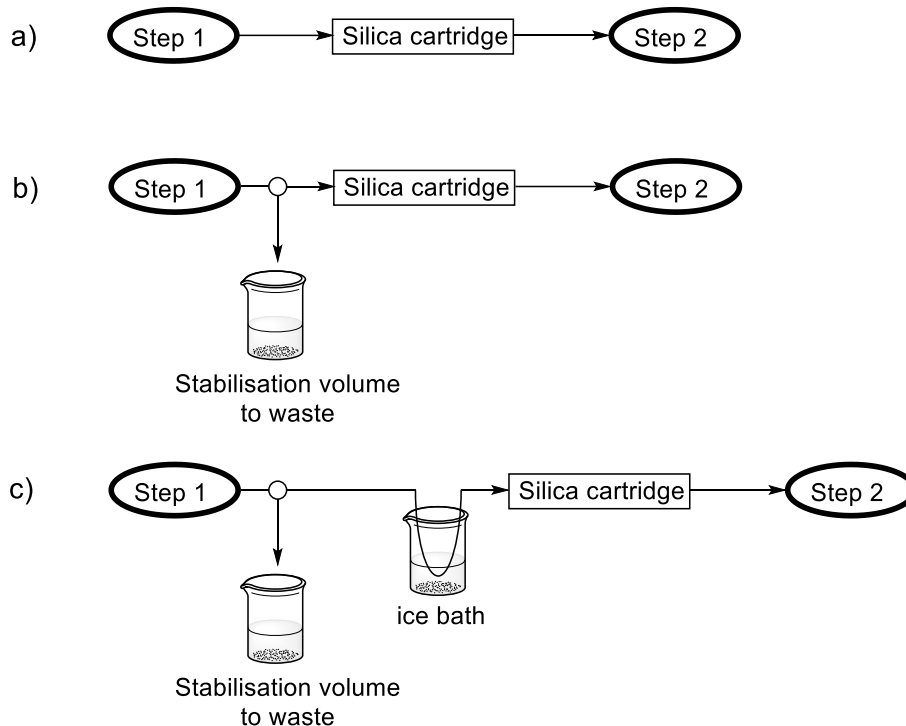
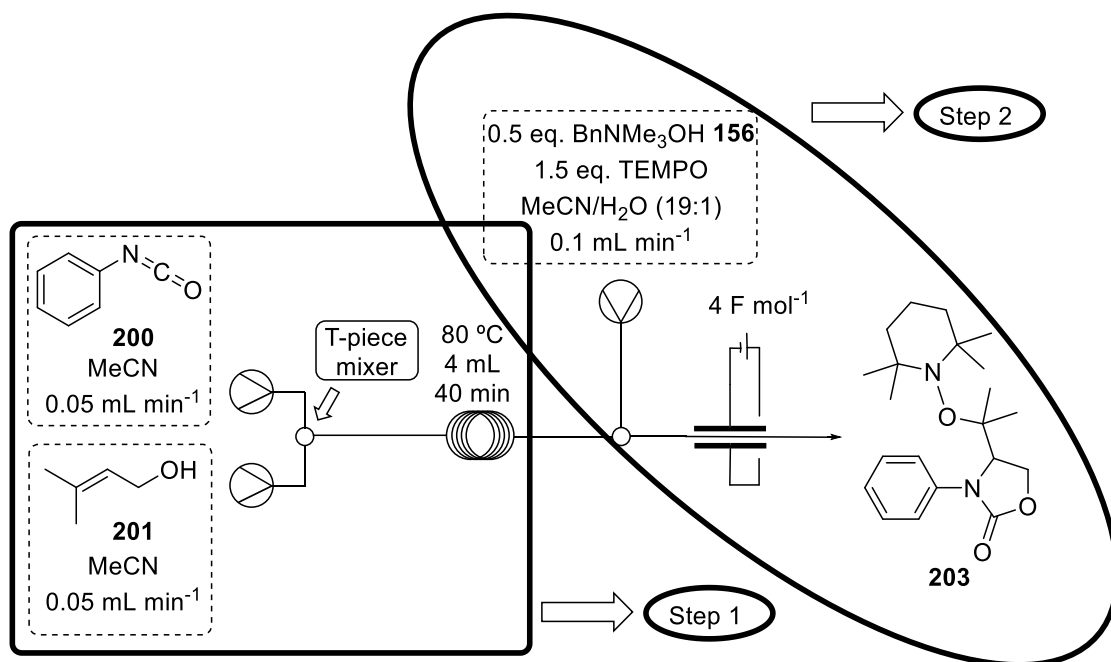
To study the sensitivity of the electrochemical reaction towards traces of impurities, the carbamate synthesised in batch was reacted under the flow electrochemical reaction conditions in 5 different forms:

- i) Crude mixture from the carbamate synthesis reaction: Electrochemical reaction hindered, only starting material recovered.
- ii) Carbamate after column chromatography: Cyclised product **203** obtained in full conversion and with no side-products.
- iii) Carbamate after quick silica plug: Cyclised product **203** obtained in full conversion and with no side-products.

- iv) Pure carbamate **202** + alcohol **201** (2-3 mol%): Cyclised product **203** obtained in 41% conversion.
- v) Pure carbamate **202** + isocyanate **200** (2-3 mol%): Electrochemical reaction hindered, only starting material recovered.

These results suggest that the electrochemical reaction can be easily impeded if traces of impurities or the isocyanate **200** are present, and slowed down if there is small amount of the alcohol **201** in the medium.

To overcome this problem in the flow synthesis approach, a silica plug was made for the flow system, packing a cartridge with silica and connecting it to the outlet of the first coil, before the second T-piece. The product from the first reaction coil was passed through the silica cartridge, and then mixed with the second stream, as shown in Scheme 3.31a. This reaction did not show any trace of the desired cyclised product **203**, and only the carbamate **202** and small amount of unidentified impurities were obtained. To avoid accumulation of impurities in the silica cartridge during the stabilisation time of the reaction (60 min), a switchable 3-port valve like that presented in Figure 3.31 was connected to the tubing before the silica plug, and the solution was pumped to a waste container. When the steady state of the reaction was reached, the valve was switched to pump the solution through the silica plug, before the mixing with the second stream and introduction of the combined flows into the electrochemical reactor (Scheme 3.31b). With this set-up a similar result was obtained, with no formation of compound **203**. The crude ¹H NMR showed mainly unreacted carbamate **202**, and a small amount of unidentified impurities. Finally, the tubing coming from the first reaction after the silica plug was introduced in an ice bath to cool it down before mixing this solution with the second stream, as the tubing of the reaction for the synthesis of the carbamate **202** was at 80 °C (Scheme 3.31c). The electrochemical reaction proceeds smoothly after a quick silica plug in batch, and the temperature was the only difference between both processes. Unfortunately this attempt in flow also failed to give the desired cyclised product **203**, and unreacted carbamate was recovered after passing the solution through the electrochemical reactor.



Scheme 3.31: Two-step flow approach, with silica plug purification between them.

A final attempt was performed with the same exact conditions as described in Scheme 3.31c, but with an excess of alcohol **201** (1.1 equiv.). This excess was to ensure the carbamate was fully consumed, as 2-3 mol% resulted in inhibition of the reaction. Similar results as described above were obtained when using an excess of alcohol, and product **203** was not formed.

In conclusion, the attempted two-step set-up to synthesise *in situ* the carbamate necessary to perform the electrochemical cyclisation did not lead to the desired results. Presumably the electrochemical transformation of such compounds is very sensitive to the presence of minor impurities, sometimes undetectable, and the reaction is impeded.

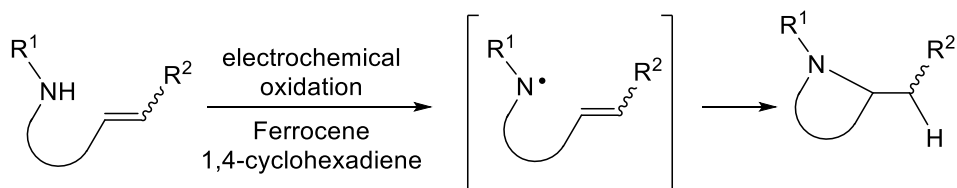
3.7. Conclusions and future work

In conclusion, a library of nitrogen heterocycles has been synthesised using the second-generation electrochemical flow reactor. This reaction was carried out smoothly without any intentionally added supporting electrolyte. In addition, two different set-ups have been developed to perform a combination of an electrochemical reaction with a second one in a single flow system, being one of the first examples reported in literature.^[40,41]

Parts of this work have been already published.^[42]

Future work:

The cyclisation reaction could be studied with other mediators different than TEMPO, and not necessarily one that acts as radical scavenger as TEMPO does. This would give a broader scope of products, not limiting it to the TEMPO addition to the molecule (Scheme 3.32). It has been previously reported the use of catalytic amount of ferrocene as mediator with 1,4-cyclohexadiene as hydrogen source for H-atom abstraction,^[18] but it has never been implemented in flow.



Scheme 3.32: Ferrocene mediated electrochemical cyclisation

The results presented in section 3.6 did not lead to a successful result. Thus, this could be further explored, studying the reasons why the electrochemical reaction is hindered after the carbamate production, and probably using some scavengers replacing the silica plug that was described in this work.

3.8. References

- [1] M. Asif, *Int. J. Bioorganic Chem.* **2017**, *2*, 146–152.
- [2] J. A. Joule, K. Mills, Eds., *Heterocyclic Chemistry*, Wiley-Blackwell, **2010**.
- [3] T. J. Donohoe, C. K. A. Callens, A. Flores, A. R. Lacy, *Chem. Eur. J.* **2011**, *17*, 58–76.
- [4] P. H. Fuller, J. Kim, S. R. Chemler, *J. Am. Chem. Soc.* **2008**, *130*, 17638–17639.
- [5] A. W. Hofmann, *Berichte der Dtsch. Chem. Gesellschaftllschaft* **1879**, *12*, 984–990.
- [6] M. E. Wolff, *Chem. Rev.* **1963**, *63*, 55–64.
- [7] S. Z. Zard, *Chem. Soc. Rev.* **2008**, *37*, 1603–1618.
- [8] T. Xiong, Q. Zhang, *Chem. Soc. Rev.* **2016**, *45*, 3069–3087.
- [9] T. Buttner, J. Geier, G. Frison, J. Harmer, C. Calle, A. Schweiger, H. Schönberg, H. Grützmacher, *Science* **2005**, *307*, 235–238.
- [10] A. I. O. Suarez, V. Lyaskovskyy, J. N. H. Reek, J. I. Van Der Vlugt, B. De Bruin, *Angew. Chem. Int. Ed.* **2013**, *52*, 12510–12529.
- [11] M. Tokuda, T. Miyamoto, H. Fujita, H. Sugimoto, *Tetrahedron* **1991**, *47*, 747–756.
- [12] H. C. Xu, K. D. Moeller, *J. Am. Chem. Soc.* **2008**, *130*, 13542–13543.
- [13] H. C. Xu, K. D. Moeller, *J. Am. Chem. Soc.* **2010**, *132*, 2839–2844.
- [14] H. C. Xu, K. D. Moeller, *Angew. Chem. Int. Ed.* **2010**, *49*, 8004–8007.
- [15] J. M. Campbell, H. C. Xu, K. D. Moeller, *J. Am. Chem. Soc.* **2012**, *134*, 18338–18344.
- [16] H. C. Xu, J. M. Campbell, K. D. Moeller, *J. Org. Chem.* **2014**, *79*, 379–391.
- [17] F. Xu, L. Zhu, S. Zhu, X. Yan, H. C. Xu, *Chem. Eur. J.* **2014**, *20*, 12740–12744.
- [18] L. Zhu, P. Xiong, Z. Y. Mao, Y. H. Wang, X. Yan, X. Lu, H. C. Xu, *Angew. Chem. Int. Ed.* **2016**, *55*, 2226–2229.
- [19] Z. W. Hou, Z. Y. Mao, H. B. Zhao, Y. Y. Melcamu, X. Lu, J. Song, H. C. Xu, *Angew. Chem. Int. Ed.* **2016**, *55*, 9168–9172.
- [20] P. Xiong, H. H. Xu, H. C. Xu, *J. Am. Chem. Soc.* **2017**, *139*, 2956–2959.
- [21] R. Manoharan, M. Jeganmohan, *Chem. Commun.* **2015**, *51*, 2929–2932.
- [22] Z. Q. Wang, C. G. Feng, M. H. Xu, G. Q. Lin, *J. Am. Chem. Soc.* **2007**, *129*, 5336–5337.
- [23] J. B. Campbell, R. F. Dedinas, S. Trumbower-Walsh, *Synlett* **2010**, 3008–3010.
- [24] L. Shi, L. Hu, J. Wang, X. Cao, H. Gu, *Org. Lett.* **2012**, *14*, 1876–1879.

- [25] G. Yang, W. Zhang, *Org. Lett.* **2012**, *14*, 268–271.
- [26] K. Nozawa-Kumada, J. Kadokawa, T. Kameyama, Y. Kondo, *Org. Lett.* **2015**, *17*, 4479–4481.
- [27] Z. Xuan, D. J. Jung, H. J. Jeon, S. G. Lee, *J. Org. Chem.* **2016**, *81*, 10094–10098.
- [28] C. Gütz, B. Klöckner, S. R. Waldvogel, *Org. Process Res. Dev.* **2016**, *20*, 26–32.
- [29] E. W. Washburn, *International Critical Tables of Numerical Data, Physics, Chemistry and Technology*. National Academy of Sciences, McGraw Hill, New York, **1926**.
- [30] L. Ebersson, M. P. Hartshorn, O. Persson, *Angew. Chem. Int. Ed.* **1995**, *34*, 2268–2269.
- [31] L. Ebersson, M. P. Hartshorn, O. Persson, *J. Chem. Soc., Perkin Trans. 2* **1995**, 1735–1744.
- [32] M. Karplus, *J. Am. Chem. Soc.* **1963**, *85*, 2870–2871.
- [33] L. M. Jackman, S. Sternhell, in *Application of NMR Spectroscopy in Organic Chemistry*, Pergamon, **1969**, pp. 281–283.
- [34] M. F. Nielsen, J. H. P. Utley, in *Organic Electrochemistry* (Eds.: H. Lund, O. Hammerich), M. Dekker, New York, **2001**, pp. 795–882.
- [35] F. Xu, L. Zhu, S. Zhu, X. Yan, H. C. Xu, *Chem. Eur. J.* **2014**, *20*, 12740–12744.
- [36] J. Gui, H. Tian, W. Tian, *Org. Lett.* **2013**, *15*, 4802–4805.
- [37] P. G. M. Wuts, Y. W. Jung, *J. Org. Chem.* **1988**, *53*, 1957–1965.
- [38] D. A. Dias, M. A. Kerr, *Org. Lett.* **2009**, *11*, 3694–3697.
- [39] L. Huck, M. Berton, A. de la Hoz, A. Díaz-Ortiz, J. Alcázar, *Green Chem.* **2017**, *19*, 1420–1424.
- [40] R. A. Green, D. Pletcher, S. G. Leach, R. C. D. Brown, *Org. Lett.* **2016**, *18*, 1198–1201.
- [41] R. Stalder, G. P. Roth, *ACS Med. Chem. Lett.* **2013**, *4*, 1119–1123.
- [42] A. A. Folgueiras-Amador, K. Philipps, S. Guilbaud, J. Poelakker, T. Wirth, *Angew. Chem. Int. Ed.* **2017**, *56*, 15446–15450.

CHAPTER 4: Electrosynthesis of benzothiazoles from *N*-arylthioamides

CHAPTER 4: Electrosynthesis of benzothiazoles from <i>N</i> -arylthioamides	126
4.1. Introduction	128
4.1.1. C–H and X–H cross-coupling reactions	128
4.1.2. Different methods for the synthesis of benzothiazoles from <i>N</i> -arylthioamides.....	128
4.2. Synthesis of substrates	132
4.3. Flow electrochemical synthesis of benzothiazoles	136
4.3.1. Optimisation of the reaction conditions.....	136
4.3.2. Scope of substrates.....	138
4.3.3. Gram-scale reaction	141
4.3.4. Proposed mechanism	141
4.4. Conclusions	143
4.5. References	144

4.1. Introduction

4.1.1. C–H and X–H cross-coupling reactions

The formation of carbon–carbon and carbon–heteroatom bonds is one of the most important transformations in organic chemistry. Direct cross-coupling reactions of C–H and X–H (X = C, N, O, S) have been widely studied due to the simplicity of the method.^[1–5] There is no need to prefunctionalise the substrate, as the introduction of activating or leaving groups typically leads to longer synthetic routes. Precious transition metals or stoichiometric amounts of organic oxidants are used in traditional cross-couplings methods, and this results in additional downstream processes when operating on large scale.^[6,7] Furthermore, even if the transition metals are used in catalytic amounts, there is still a drawback of these processes when considering pharmaceutical applications, as residual metal impurities must be avoided. This can lead to additional costs in order to reduce the residual metals below the permitted limit.^[8]

The benzothiazole scaffold is part of a large number of heterocyclic compounds that show biological activities, such as antiviral, antitumor, antiseptic compounds, tracers for β -amyloid plaques in Alzheimer disease, etc., as shown in Figure 4.1.^[9]

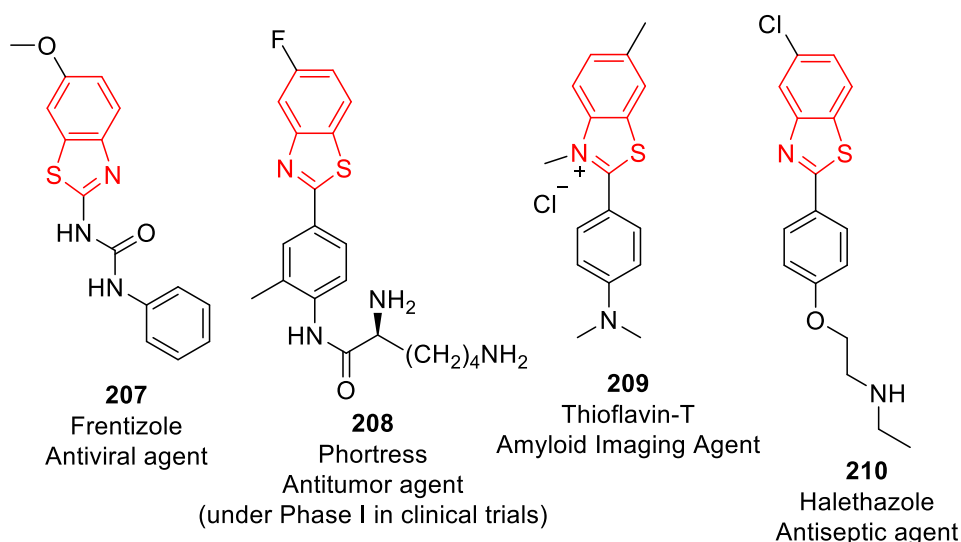


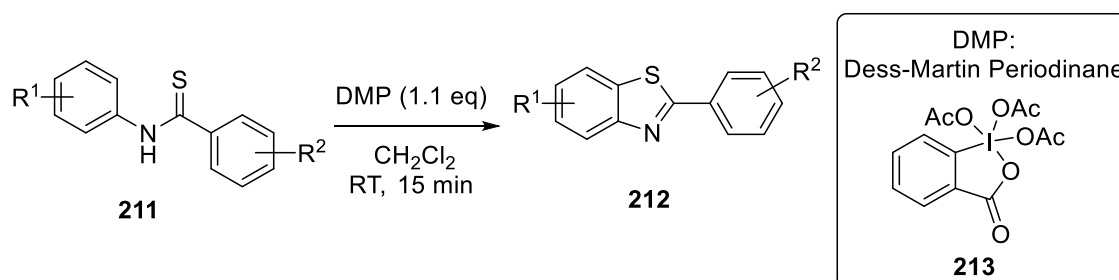
Figure 4.1: Benzothiazole based clinically available drugs.

4.1.2. Different methods for the synthesis of benzothiazoles from *N*-arylthioamides

Benzothiazoles can be synthesised by oxidative cyclisation of *N*-arylthioamides. In this chapter such transformation is achieved under mild conditions with high efficiency

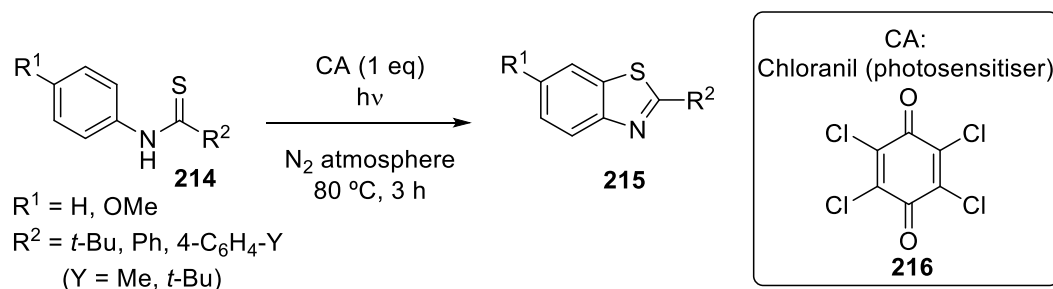
employing the flow electrochemical reactor designed. Some of the recent literature for the formation of benzothiazoles from *N*-arylthioamides is summarised in this section.

In 2006 Bose *et al.* reported such transformation employing Dess-Martin Periodinane (DMP **213**) as oxidant (Scheme 4.1). The benzothiazoles (**212**) were obtained in 85 – 95% yield, and eight different examples were reported.^[10]



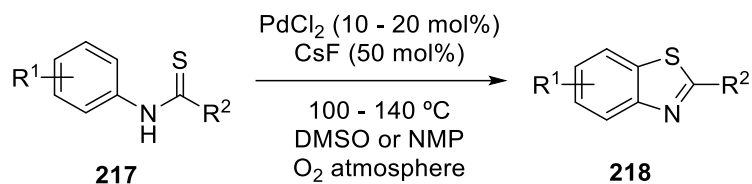
Scheme 4.1: Synthesis of benzothiazoles using hypervalent iodine (DMP).

In 2009 Peñeñory and coworkers published the formation of benzothiazoles from *N*-arylthioamides (**214**) using chloranil (CA **316**) as photosensitiser irradiated at $\lambda_{\text{max}} = 365$ nm at room temperature for 3 hours, under N₂ atmosphere at 80 °C (Scheme 4.2). The corresponding benzothiazoles were obtained in yields up to 80%. Desulfurisation of the thioamide was observed with some of the substrates, obtaining the corresponding amide as the major product.^[11]



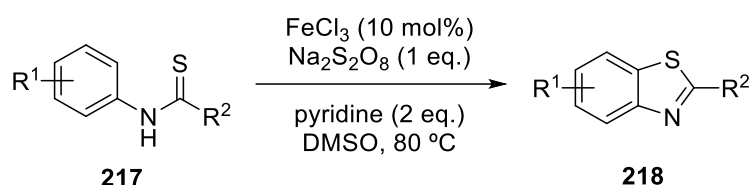
Scheme 4.2: Synthesis of benzothiazoles by chloranil and hv.

In 2010 Inamoto, Doi *et al.* developed a palladium-catalysed method to synthesise benzothiazoles and 2-aminobenzothiazoles from thioamides and thioureas respectively, employing O₂ as oxidant (Scheme 4.3). The reaction was carried out at elevated temperature (100 – 140 °C), and the use of cesium fluoride substoichiometrically is crucial to achieve high conversion. The cyclised products were obtained in 46 – 79% yield, but in all cases the corresponding desulfurised amide is recovered in 10 to 34% yield, depending on the substrate.^[12]



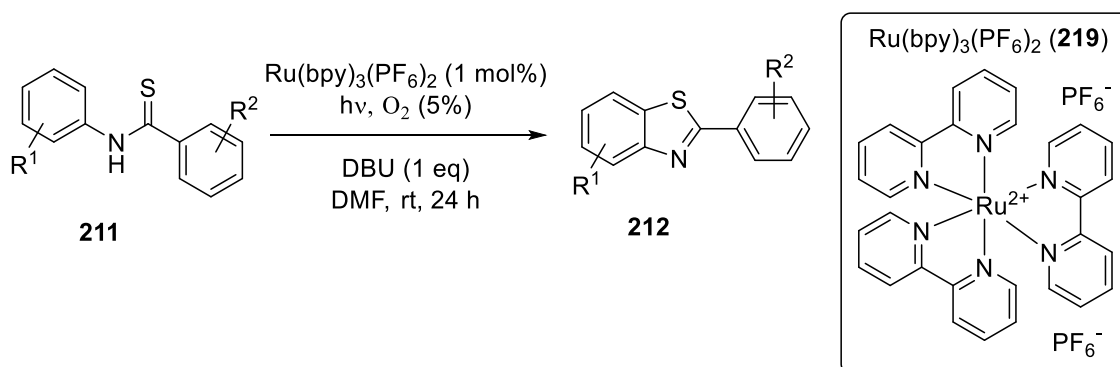
Scheme 4.3: Pd-catalysed benzothiazoles formation under O_2 atmosphere.

In 2012 Lei and coworkers reported a method for C–H thiolation of *N*-arylthioamides employing Fe catalyst and sodium persulfate as an oxidant. Pyridine (2 equivalents) is needed in the reaction to obtain high yield and selectivity towards the benzothiazole product, and reduce the desulfurisation of the thioamide to the corresponding amide.^[13]



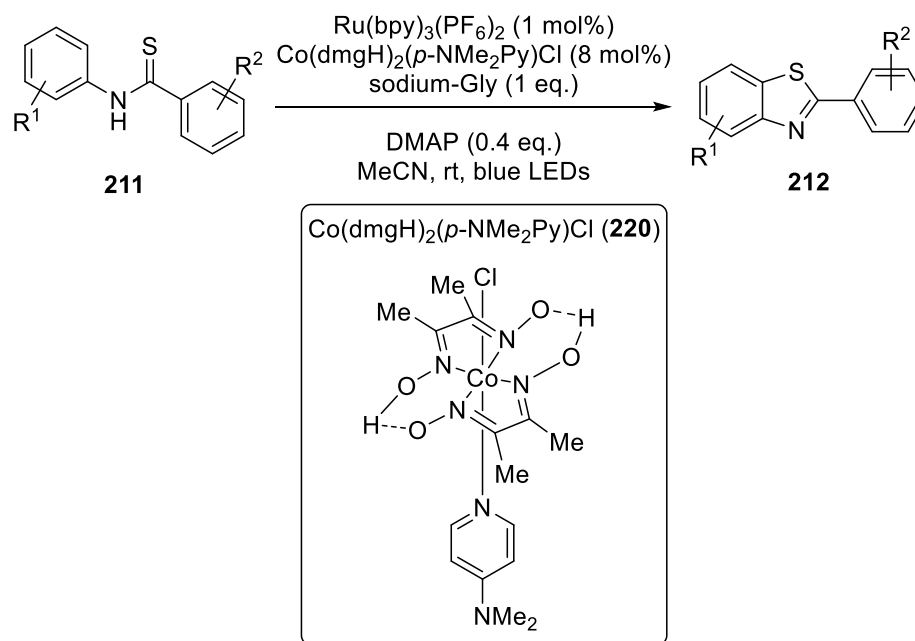
Scheme 4.4: Fe-catalysed C–H thiolation of *N*-arylthioamides using $\text{Na}_2\text{S}_2\text{O}_8$ as oxidant.

In 2012 Li *et al.* published the formation of benzothiazoles under 14 W CFL (compact fluorescent lamp) light to irradiate a ruthenium photocatalyst, molecular oxygen and DBU (1,8-diazabicyclo[5.4.0]undec-7-ene) as a base (Scheme 4.5). A variety of ruthenium catalysts were screened, since the nature of the catalyst has a high impact in the outcome of the reaction, leading either to the desired product or to the formation of the corresponding amide by desulfurisation of the thioamide. With the optimum catalyst (**219**), a scope of substrates was successfully cyclised to the benzothiazoles (**302**) in yields up to 91%.^[14]



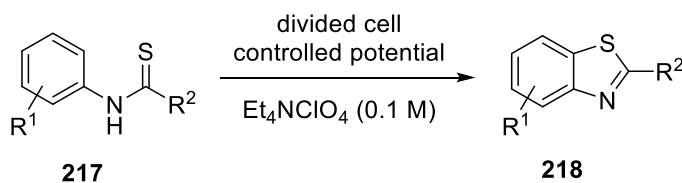
Scheme 4.5: Synthesis of benzothiazoles employing Ru-catalyst under visible light.

Later in 2015 Wu, Lei and coworkers developed a photoredox process for the synthesis of benzothiazoles (**212**) from *N*-arylthioamides (**211**) employing ruthenium and cobalt (**219**) as co-catalyst, and stoichiometric amount of base (Scheme 4.6). This methodology avoids the use of oxidants, and hydrogen gas is the only byproduct in the reaction. 28 examples of benzothiazoles were synthesised in good to excellent yields.^[15]



Scheme 4.6: Photoredox Ru- and Co-catalysed dehydrogenative C–S bond formation from *N*-arylthioamides.

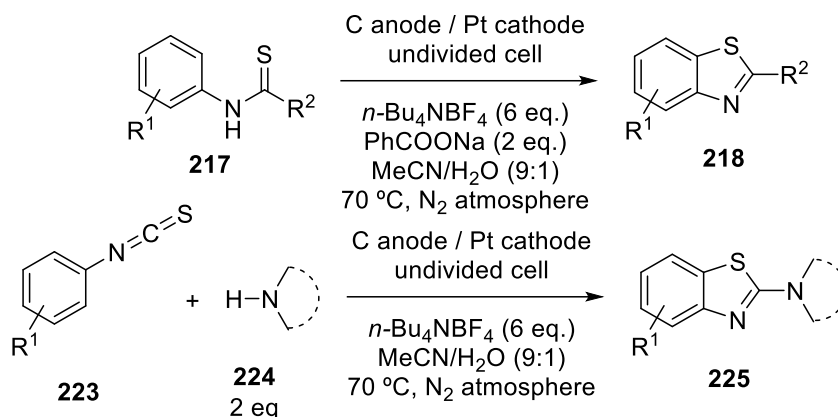
The first electrochemical example for the synthesis of benzothiazoles from *N*-arylthioamides was reported in 1979 by Tabaković. The benzothiazoles were synthesised in a divided cell under controlled potential (Scheme 4.7), and 9 examples were reported in moderate to good yields.^[16]



Scheme 4.7: First electrochemical synthesis of benzothiazoles from *N*-arylthioamides.

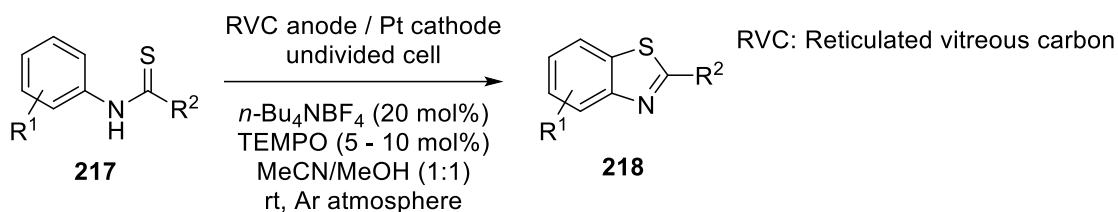
Later in 2017, Lei et al. published the formation of benzothiazoles and 2-aminobenzothiazoles (**225**) electrochemically from thioamides and thioureas respectively. The thioureas were synthesised *in situ* from isothiocyanates (**223**) and the corresponding secondary amine (**224**). This transformation was performed under inert

atmosphere at high temperature (70 °C), and 2 equivalents of base were needed for the formation of benzothiazoles from thioamides (Scheme 4.8). The dehydrogenative C–S bond formation products were obtained in good to excellent yields.^[17]



Scheme 4.8: Electrochemical dehydrogenative C–S bond formation of thioamides and thioureas.

Lastly, in 2017 Xu and coworkers reported a TEMPO-catalysed synthesis of benzothiazoles **218**. The reaction was run under argon atmosphere to keep the reaction yield high (Scheme 4.9). A broad variety of substrates was reported in yields up to 97%.^[18]



Scheme 4.9: TEMPO-catalysed electrochemical synthesis of benzothiazoles.

The aim of the project described and discussed in this chapter is to improve the outcome of the TEMPO-mediated dehydrogenative C–S bond formation performed electrochemically and developed by Xu *et al.* in batch conditions (Scheme 4.9) by using the flow electrochemical reactor. The objectives and results will be explained in more detail in Section 4.3 of this chapter.

4.2. Synthesis of substrates

The *N*-aryltioamides necessary to perform the electrochemical cyclisation to produce benzothiazoles were synthesised from the corresponding aryl-isothiocyanate and

Grignard reagent. The reaction was carried out in anhydrous THF. The addition of the Grignard reagent was performed at 0 °C, and the resulting mixture was allowed to warm up to room temperature. After 2 hours the reaction was complete, except when benzylmagnesium chloride was employed to introduce the benzyl substituent in the thioamide, which needed to be stirred at room temperature for 24 hours to achieve full conversion of the starting materials. 3-Pyridyl isothiocyanate (**227**) was also converted to the corresponding thioamides in good yields, as precursor to obtain thiazolopyridines (Table 4.1).

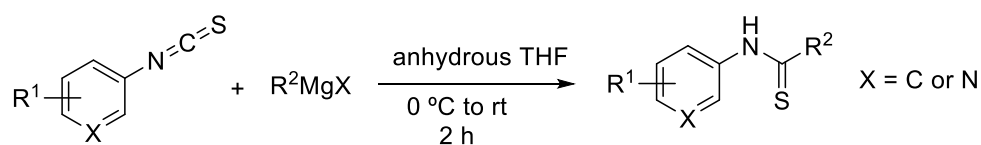


Table 4.1: Scope of thioamides.

Entry	Isothiocyanate	Grignard reagent	Product	Yield [%]
1				90
2				98
3				73 ^a
4				91
5				99

^a24 hour reaction

The substituents in the aromatic ring adjacent to the nitrogen were also explored, with molecules bearing both electron-donating and electron-withdrawing groups. The results

are summarised in Table 4.2. Most reactions proceeded smoothly to the desired thioamides. However, 4-methoxy- and 2,4-dimethyl-phenylisothiocyanate led to the corresponding thioamide with moderate yield of 65 and 67% respectively (entries 3 and 7, Table 4.2).

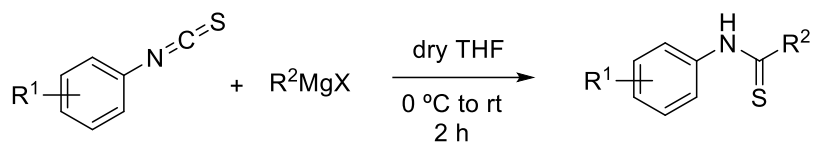
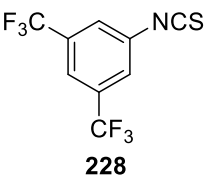
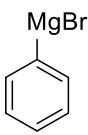
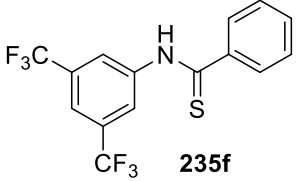
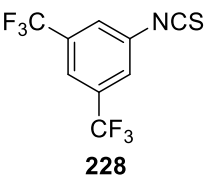
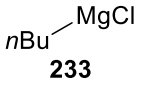
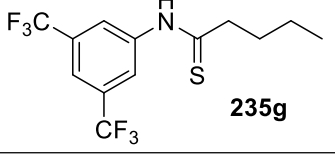
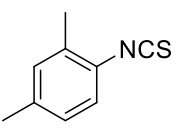
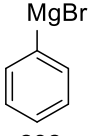
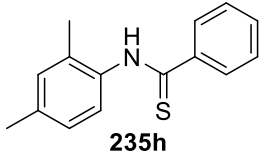
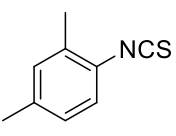
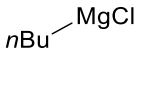
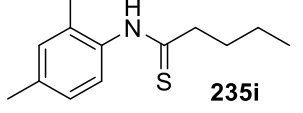
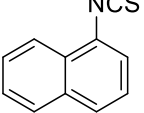
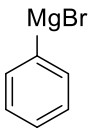
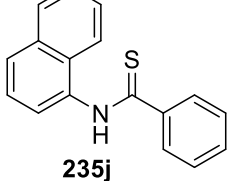
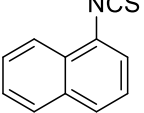
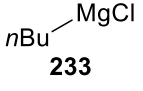
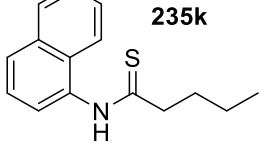
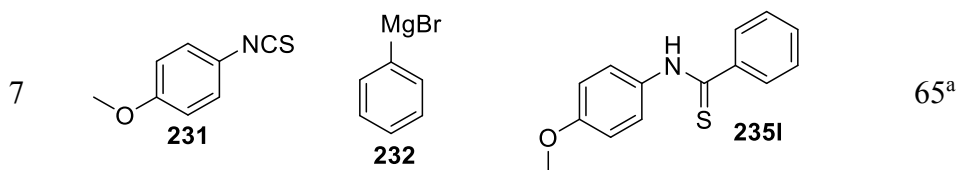


Table 4.2: N-Aryl-substituted thioamides.

Entry	Isothiocyanate	Grignard reagent	Product	Yield [%]
1				98
2				97
3				67
4				80
5				85
6				89



^a32 hours reaction

Most thioamides appear in the NMR spectrum as a mixture of rotamers. The ¹H NMR spectrum of compound **235b** is shown as an example (Figure 4.2). The title compound was a mixture of rotamers in a ratio of 3:1, and the peaks corresponding to each rotamer can be clearly identified here.

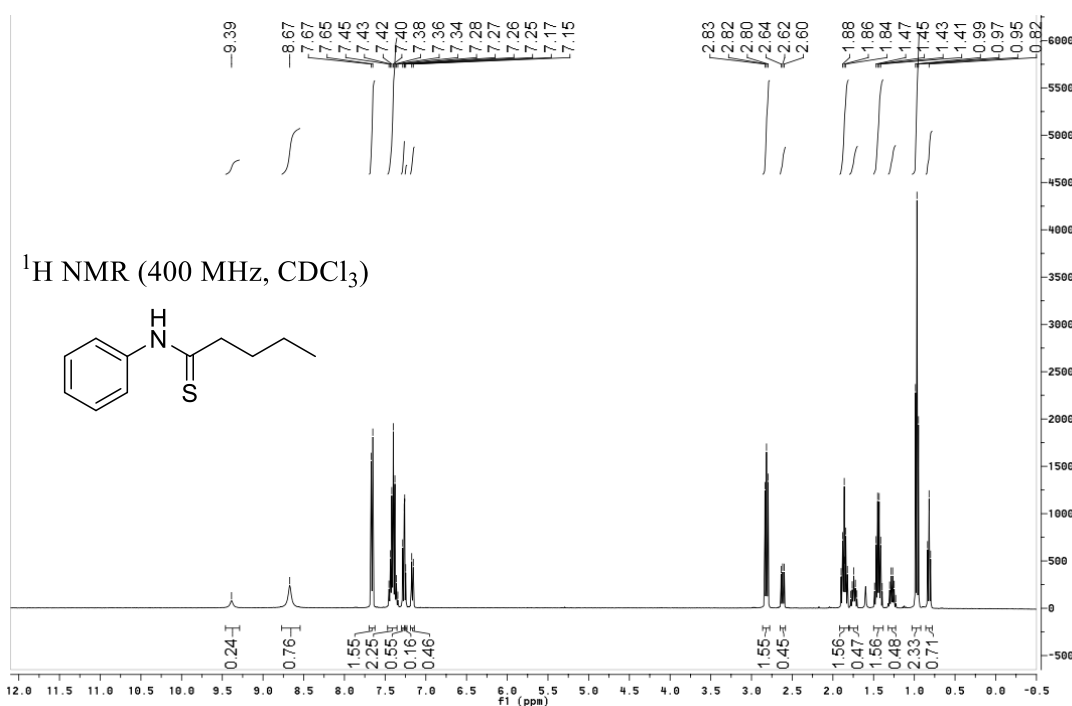
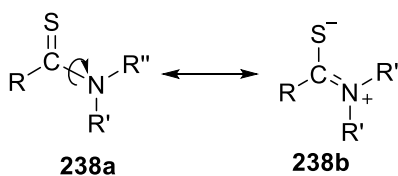


Figure 4.2: ¹H NMR of compound **235b**.

In compounds of the type (**238**), the central C–N bond can occur to show partial double-bond character.^[19,20] The electrons can be delocalised in the thioamide, as shown in Scheme 4.10, and this can lead to higher rotation barriers. Neuman and Young have reported higher barriers to rotation in thioamides than in the corresponding amides.^[21,22]

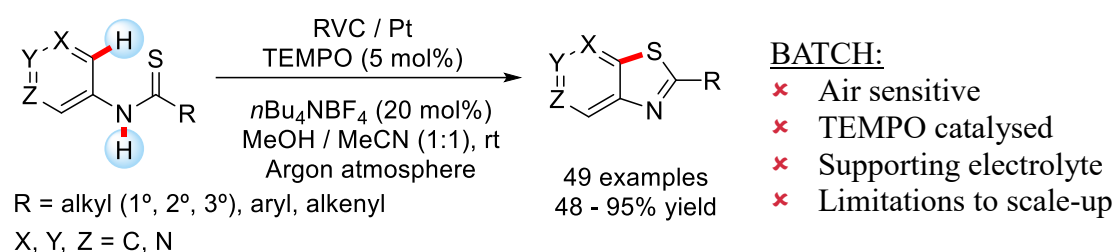


Scheme 4.10: Hindered rotation in partial double bonds.

Thus, some of these compounds can appear as rotational isomers, since thioamides are stable in the solid state, but in solution they form conformational isomers.^[23] This suggests that the carbon–nitrogen bond is expected to be shorter in thioamides than in the corresponding amides.^[21]

4.3. Flow electrochemical synthesis of benzothiazoles

This project has been executed in collaboration with Prof. Xu and Xiang-Yang Qian from Xiamen University (China). In this chapter, only the results obtained by myself will be discussed, and the substrates performed by the PhD student Xiang-Yang Qian are included in the supporting information and/or in the published manuscript.^[24] The aim of the project is to improve the outcome of the TEMPO-mediated dehydrogenative C–S bond formation performed electrochemically and developed by Xu *et al.* in batch conditions.^[18] They reported a broad scope of substrates in good to excellent yields, but the reaction had some drawbacks, such as: i) the need of argon atmosphere, ii) TEMPO is necessary as catalyst, iii) supporting electrolyte needed in the batch-type reactor, iv) inconvenient set-up and limitation to scale-up (Scheme 4.11).



Scheme 4.11: Batch TEMPO-mediated electrosynthesis of benzothiazoles.^[18]

4.3.1. Optimisation of the reaction conditions

The cyclisation of *N*-(quinoline-3-yl)butanethioamide **239** to product **240** was initially studied using similar batch mode conditions previously reported. Product **240** was studied as it is an intermediate in the synthesis of CL075 (a toll-like receptor 8 {TLR8} agonist).^[25] As the current density in batch conditions appeared to have a high impact in the outcome of the reaction, it was initially kept low (0.5 mA cm⁻²) (Figure 4.3).

<p>BATCH CONDITIONS:</p> <p>Q = 3.3 F mol⁻¹</p> <p>Current density: 0.1 mA/cm²</p> <p>0.2 eq. <i>n</i>-Bu₄NBF₄</p> <p>0.05 eq. TEMPO</p>	<p>INITIAL FLOW CONDITIONS:</p> <p>Q = 2 F mol⁻¹</p> <p>Current density: 0.5 mA/cm²</p> <p>Q_v = 50 μL/min</p> <p>0.05 eq. TEMPO</p>
---	---

Figure 4.3: Choice of initial flow conditions according to the established batch conditions.

Using the second-generation reactor (see Chapter 2 for details), platinum was used as the cathode and graphite as the anode (reported data by Xu *et al.*: Pt cathode and RVC anode),^[18] a solvent mixture of acetonitrile and methanol and catalytic amount of TEMPO (5 mol%). Table 4.3 shows the results from the optimisation of the reaction conditions.

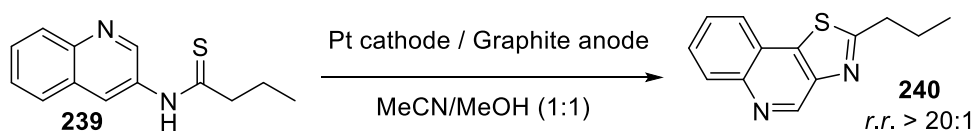


Table 4.3: Optimisation of the reaction conditions.

Entry	Concentration [mol L ⁻¹]	Flow rate [mL min ⁻¹]	Current density [mA cm ⁻²]	Current [F mol ⁻¹]	¹ H NMR conversion
1 ^a			0.49	2.0	33%
2 ^a	0.025	0.05	0.98	4.0	50%
3 ^a			1.46	6.0	98%
4		0.05	1.46		>99%
5	0.025	0.1	2.93	6.0	>99%
6		0.2	5.85		>99%
7			11.71	6.0	>99%
8			9.76	5.0	>99%
9			7.80	4.0	>99%
10	0.05	0.2	5.85	3.0	>99%
11 ^b			4.88	2.5	>99%
12			3.90	2.0	90%

^a 5 mol% of TEMPO ^b 97% isolated yield

Initial reactions used low current density (Table 4.3, entry 1), and product **240** was obtained in 33% conversion using 2 F mol^{-1} , which is the minimum theoretical current needed, as it is a two-electron oxidation transformation. With a low concentration and flow rate, 6 F mol^{-1} was needed in order to achieve full conversion (Table 4.3, entry 3). The same reaction was explored omitting the use of TEMPO as catalyst (Table 4.3, entry 4), and, to our delight, compound **240** was obtained with total consumption of the thioamide **239**.

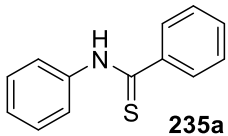
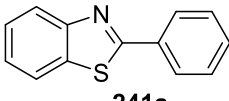
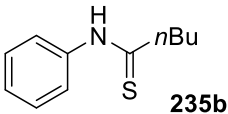
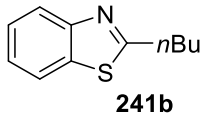
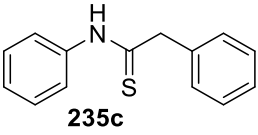
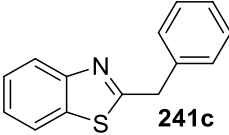
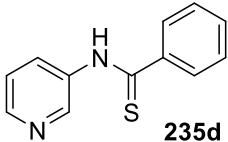
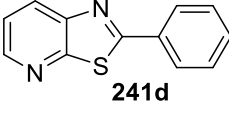
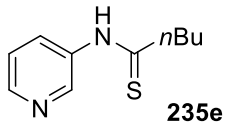
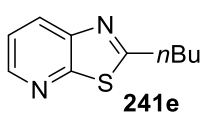
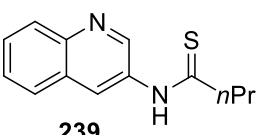
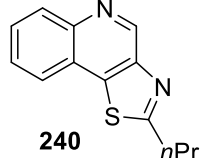
In order to increase the production rate, higher flow rates (entries 5 and 6) and also higher concentrations of the substrate (entry 7) were investigated. This led to similar results demonstrating that higher current densities can be tolerated in the flow reactor. Then, the amount of electricity used in the reaction was decreased, giving full conversion to the desired product with 5.0, 4.0, 3.0 and even 2.5 F mol^{-1} (entries 8 to 11). This result proves the importance of having a good mixing effect in the system, and that can be achieved with flow reactors: comparison of results shown in entry 1 (2 F mol^{-1} , 0.05 mL min^{-1}) and entry 12 (2 F mol^{-1} , 0.2 mL min^{-1}) shows that with the same amount of charge, in the case of using a low flow rate the conversion achieved is 33%, while using a higher flow rate the conversion increases up to 90%. This improvement can also be due to the higher amount of hydrogen evolved at the cathode, since the current density is higher. This gas evolution can affect positively in the mixing effect of the solution, which is also more efficient in flow than in a batch system.

A larger scale reaction (0.55 mmol) was performed using the optimum conditions (entry 11) and product **240** was isolated in 97% yield (121 mg).

4.3.2. Scope of substrates

With the optimised conditions in hand (Table 4.3, entry 11), the substrate scope was explored. Alkyl and aryl thioamides cyclisations proceeded smoothly with good yields (Table 4.4). In the case of compound **235a** (entry 1), the yield of the cyclised product increased when 3% of water was added to the solvent mixture. The reason is still unclear, but similar results have been reported previously.^[18] Amino-pyridine-derived thioamides underwent cyclisation successfully with the same methodology (entries 4.6).

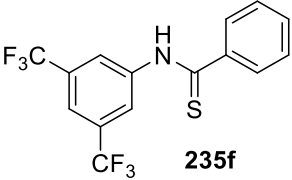
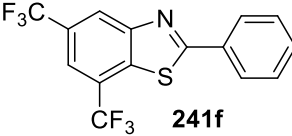
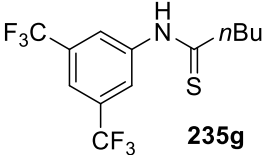
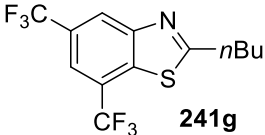
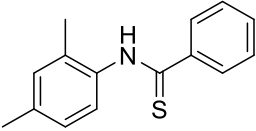
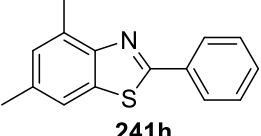
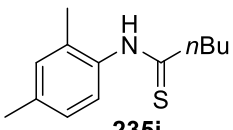

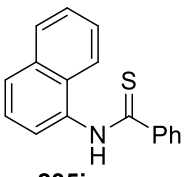
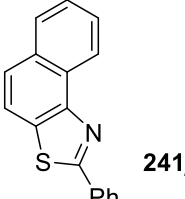
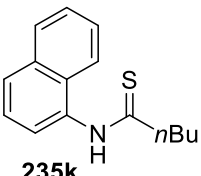
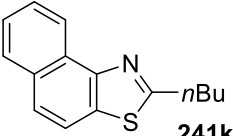
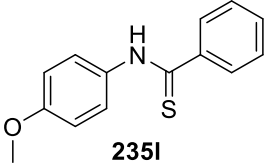
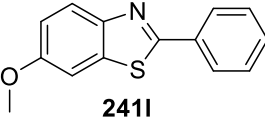
Table 4.4: Scope of substrates.

Entry	Thioamide	Product	Current [F mol ⁻¹]	Yield [%]
1	 235a	 241a	2.6	96 ^a
2	 235b	 241b	2.5	81
3	 235c	 241c	4.0	64
4	 235d	 241d	3.0	81 (<i>r.r.</i> = 19:1)
5	 235e	 241e	3.5	87 (<i>r.r.</i> = 19:1)
6	 239	 240	2.5	95 (<i>r.r.</i> > 20:1)

^a 3% H₂O was used in the solvent mixture

The cyclisation *via* dehydrogenative C–S bond formation was also performed with a variety of *N*-arylthioamides (Table 4.5). In all cases the product was obtained in good to excellent yields. Electron-donating groups (entries 3, 4 and 7), electron-withdrawing groups (entries 1 and 2) underwent cyclisation smoothly. Only in the case of 4-MeO substituted *N*-arylthioamide addition of water (3%) increased the yield of the desired cyclised product.

Table 4.5: Scope of substrates with *N*-aryl-substituted thioamides.

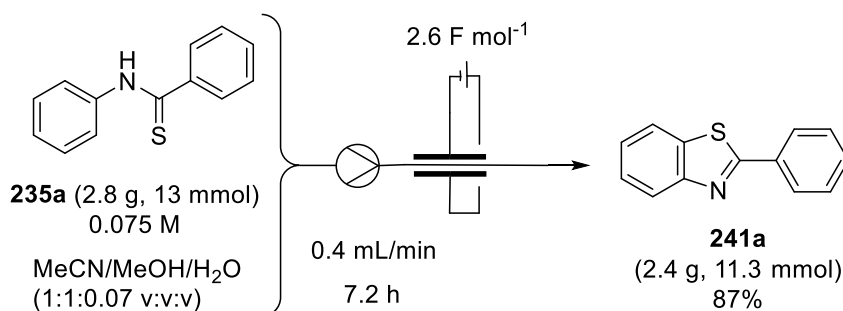
Entry	Thioamide	Product	Current [F mol ⁻¹]	Yield [%]
1	 235f	 241f	3.0	76
2	 235g	 241g	4.0	73
3	 235h	 241h	4.0	67
4	 235i	 241i	2.5	80
5	 235j	 241j	2.5	97
6	 235k	 241k	3.0	93
7	 235l	 241l	4.0	92 ^a

^a 3% H₂O was used in the solvent mixture

It is noteworthy that in none of the reactions the corresponding amide was observed as a desulfurisation product, which is a common problem with other methodologies of oxidative dehydrogenative C–S bond formation from *N*-aryltioamides, as described in the introduction of this chapter.

4.3.3. Gram-scale reaction

To show the potential of the developed method, a larger reaction using 13 mmol of substrate **235a** was performed using the same electrochemical reactor (Scheme 4.12). Compound **241a** was obtained in 87% yield (2.4 g). A higher flow rate and higher concentration than the one described in the general procedure was used, which allowed the reaction time to be shortened. This led to a slightly lower yield (87% instead of 96%), however, this compromise obtains large amount of product in a short time. This demonstrates one of the advantages of flow chemistry, which is an easier scale-up. Here the substrate was pumped through the same reactor for a longer time.

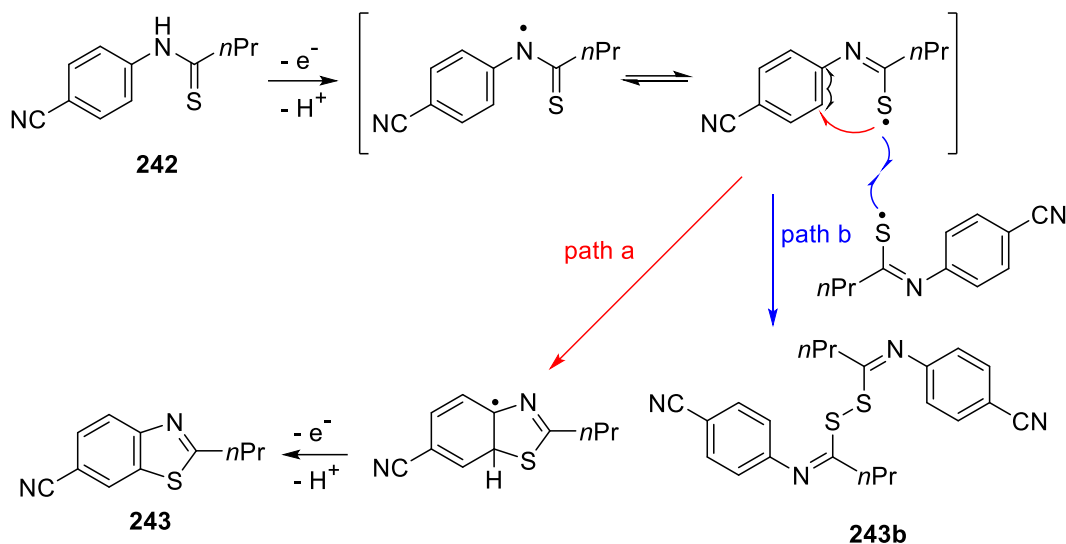


Scheme 4.12: Gram-scale reaction.

4.3.4. Proposed mechanism

When a 4-cyano substituent was attached to the *N*-aryl moiety (**242**), the dimer **243b** was obtained in 13% yield in addition to compound **243** (58% yield). A similar product has been previously reported in the oxidation of *N*-aryltioamides with 2,3-dichloro-5,6-dicyano-1,4-benzoquinone (DDQ) as an oxidant.^[26] In that report it was observed that with electron-withdrawing groups in the *N*-aryl ring, the radical formed dimerised to give similar compounds to **243b**, making this reaction predominant rather than the desired cyclisation. It was stated that the cyclised product can be obtained with electron-donating groups in the aromatic system due to the ability of such compounds to stabilise the radical intermediate formed, which is not favoured in the case of electron-withdrawing

functionalities. We only observed the dimerisation product with compound **242** and in low percentage (13%). It could be possible that the dimer was formed also with other electron-withdrawing substrates in such low yields that was undetectable after purification of the crude mixtures. In the manuscript reporting this transformation in batch by Xu *et al.* some mechanistic investigations are discussed, and it was proved that the thioamidyl radical was involved.^[18]



Scheme 4.13: Proposed mechanism.

Once the radical is formed (Scheme 4.13), it can follow two different paths, either cyclise onto the aryl group and undergo a second oxidation (path a), or react with a second radical molecule to form the dimer (path b).

Recently, Waldvogel *et al.* reported mechanistic studies of N–N bond formation from dianilides and benzoxazoles formation from amides by dehydrogenative coupling.^[27] Two different mechanisms are proposed. The first one proceeds through a cationic intermediate which can then undergo an oxa-Nazarov-type reaction, and substrates bearing electron-donating groups are more likely to proceed this way, as the oxidation potential is lower. The second proposed mechanism suggests a radical pathway for substrates with electron-withdrawing groups, as the oxidation potential is higher and once the radical is formed, it will be more difficult to undergo a second oxidation to form the cation. We performed cyclovoltammetric studies of some of our substrates with electron-rich arenes, and they show two oxidation peaks (see Supporting Information). This result could suggest that the electrochemical dehydrogenative C–S bond formation of electron-

rich *N*-arylthioamides could involve a cationic intermediate, as it was previously reported by Waldvogel, followed by an oxa-Nazarov-type reaction.^[28]

4.4. Conclusions and future work

In conclusion, a novel flow electrochemical method has been developed for the formation of benzothiazoles from *N*-arylthioamides. In this method there is no need for catalyst, mediator or supporting electrolyte to be used, only solvent and electricity is needed for the desired transformation. Laboratory grade solvents can be used without degassing or need for inert atmosphere. This shows the advantages of flow electrochemistry and largely improves the reported methods for the formation of benzothiazoles. A large scale reaction showed the potential to scale-up flow electrochemical processes.

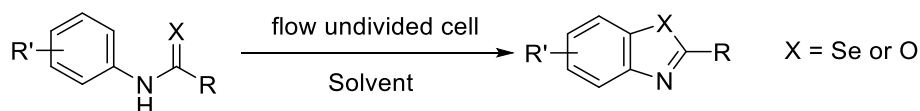
This work highlights three advantages of electrochemistry in flow, which are:

- A supporting electrolyte-free reaction.
- An easy scale-up of the reaction without the need for a larger reactor.
- The important and effective impact of having a good mixing of the reaction mixture, which can be achieved effectively with the use of flow systems.

This work has already been published.^[24]

Future work:

This type of cyclisations can be further extended to the synthesis of heterocycles bearing other heteroatoms. Selenoamides and amides could be interesting substrates to obtain benzoselenazoles and benzoxazoles respectively (Scheme 4.14). Electrochemical cyclisation of amides to synthesise benzoxazoles has been recently published in batch conditions, but the work presents a limited scope and restriction in the solvent used.^[29] This synthesis can be explored using the flow electrochemical reactor to overcome the limitations presented.



Scheme 4.14: Electrochemical cyclisation of amides and selenoamides.

4.5. References

- [1] S. A. Girard, T. Knauber, C. J. Li, *Angew. Chem. Int. Ed.* **2014**, *53*, 74–100.
- [2] C. Liu, D. Liu, A. Lei, *Acc. Chem. Res.* **2014**, *47*, 3459–3470.
- [3] C. S. Yeung, V. M. Dong, *Chem. Rev.* **2011**, *111*, 1215–1292.
- [4] C. Zhang, C. Tang, N. Jiao, *Chem. Soc. Rev.* **2012**, *41*, 3464–3484.
- [5] Q. Liu, R. Jackstell, M. Beller, *Angew. Chem. Int. Ed.* **2013**, *52*, 13871–13873.
- [6] C. Liu, H. Zhang, W. Shi, A. Lei, *Chem. Rev.* **2011**, *111*, 1780–1824.
- [7] S. Caron, R. W. Dugger, S. G. Ruggeri, J. A. Ragan, D. H. Brown-Ripin, *Chem. Rev.* **2006**, *106*, 2943–2989.
- [8] C. E. Garrett, K. Prasad, *Adv. Synth. Catal.* **2004**, *346*, 889–900.
- [9] P. C. Sharma, A. Sinhmar, A. Sharma, H. Rajak, D. P. Pathak, *J. Enzyme Inhib. Med. Chem.* **2013**, *28*, 240–266.
- [10] D. S. Bose, M. Idrees, *J. Org. Chem.* **2006**, *71*, 8261–8263.
- [11] V. Rey, S. M. Soria-Castro, J. E. Argüello, A. B. Peñeñory, *Tetrahedron Lett.* **2009**, *50*, 4720–4723.
- [12] K. Inamoto, C. Hasegawa, J. Kawasaki, K. Hiroya, T. Doi, *Adv. Synth. Catal.* **2010**, *352*, 2643–2655.
- [13] H. Wang, L. Wang, J. Shang, X. Li, H. Wang, J. Gui, A. Lei, *Chem. Commun.* **2012**, *48*, 76–78.
- [14] Y. Cheng, J. Yang, Y. Qu, P. Li, *Org. Lett.* **2012**, *14*, 98–101.
- [15] G. Zhang, C. Liu, H. Yi, Q. Meng, C. Bian, H. Chen, J. X. Jian, L. Z. Wu, A. Lei, *J. Am. Chem. Soc.* **2015**, *137*, 9273–9280.
- [16] I. Tabaković, M. Trkovnik, M. Batušić, K. Tabaković, *Synthesis* **1979**, 590–592.
- [17] P. Wang, S. Tang, A. Lei, *Green Chem.* **2017**, *19*, 2092–2095.
- [18] X.-Y. Qian, S.-Q. Li, J. Song, H.-C. Xu, *ACS Catal.* **2017**, *7*, 2730–2734.
- [19] L. W. Reeves, R. C. Shaddick, K. N. Shaw, *J. Phys. Chem.* **1971**, *75*, 3372–3374.
- [20] R. C. Neuman, L. B. Young, *J. Phys. Chem.* **1965**, *69*, 2570–2576.
- [21] R. C. Neuman, L. B. Young, *J. Phys. Chem.* **1965**, *69*, 1777–1780.
- [22] H. Kessler, *Angew. Chem. Int. Ed.* **1970**, *9*, 219–235.
- [23] H.-K. Lee, G. Querijero, *J. Pharm. Sci.* **1985**, *74*, 273–276.
- [24] A. A. Folgueiras-Amador, X.-Y. Qian, H.-C. Xu, T. Wirth, *Chem. Eur. J.* **2017**, *24*, 487–491.
- [25] H. P. Kokatla, E. Yoo, D. B. Salunke, D. Sil, C. F. Ng, R. Balakrishna, S. S. Malladi, L. M. Fox, S. A. David, *Org. Biomol. Chem.* **2013**, *11*, 1179–1198.

- [26] W. S. Lo, W. P. Hu, H. P. Lo, C. Y. Chen, C. L. Kao, J. K. Vandavasi, J. J. Wang, *Org. Lett.* **2010**, *12*, 5570–5572.
- [27] T. Gieshoff, A. Kehl, D. Schollmeyer, K. D. Moeller, S. R. Waldvogel, *J. Am. Chem. Soc.* **2017**, *139*, 12317–12324.
- [28] M. J. Di Grandi, *Org. Biomol. Chem.* **2014**, *12*, 5331–5345.
- [29] T. Gieshoff, A. Kehl, D. Schollmeyer, K. D. Moeller, S. R. Waldvogel, *Chem. Commun.* **2017**, *53*, 2974–2977.

CHAPTER 5: Electrochemical synthesis of benzoxazoles

CHAPTER 5: Electrochemical synthesis of benzoxazoles.....	146
5.1. Introduction.....	148
5.1.1. Typical methods for the synthesis of benzoxazoles.....	148
5.1.2. Electrochemical methods for the synthesis of benzoxazoles.....	151
5.2. Trifluoromethylation of resorcinol.....	153
5.3. Electrochemical synthesis of benzoxazoles from phenol derivatives and nitriles 155	
5.3.1. Acid screening.....	156
5.3.2. Electrode screening.....	156
5.3.3. Other conditions screening.....	157
5.3.4. Scope of substrates.....	159
5.3.5. Proposed mechanism.....	161
5.4. Conclusions and outlook.....	162
5.5. References.....	163

5.1. Introduction

Benzoxazoles, also known as 1,3-benzoxazoles, are important heterocyclic compounds. The benzoxazole scaffold is present in a number of natural products and has diverse pharmaceutical applications. Therefore, it is one of the skeletons used for drug and agrochemical discovery programs.^[1-3] Some examples of natural products containing the benzoxazole structure include the antimycobacterial Ileabethoxazole^[4] and Salvianen,^[5] among others. Commercially available drugs used in medicine also contain the benzoxazole scaffold, such as the non-steroidal anti-inflammatory drug Flunoxaprofen.^[6] The applications of benzoxazole derivatives are broader, and they are used for instance in laundry detergents as optical brightener. Benzoxazoles and oxazoles bearing an aryl substituent at C2 are fluorescent, this is the reason why some washing agents incorporate additives such as 4,4'-bis(benzoxazole-2-yl)stilbene (Figure 5.1). The clothes fibres absorb such fluorescent compound and the clothes become whiter.^[7]

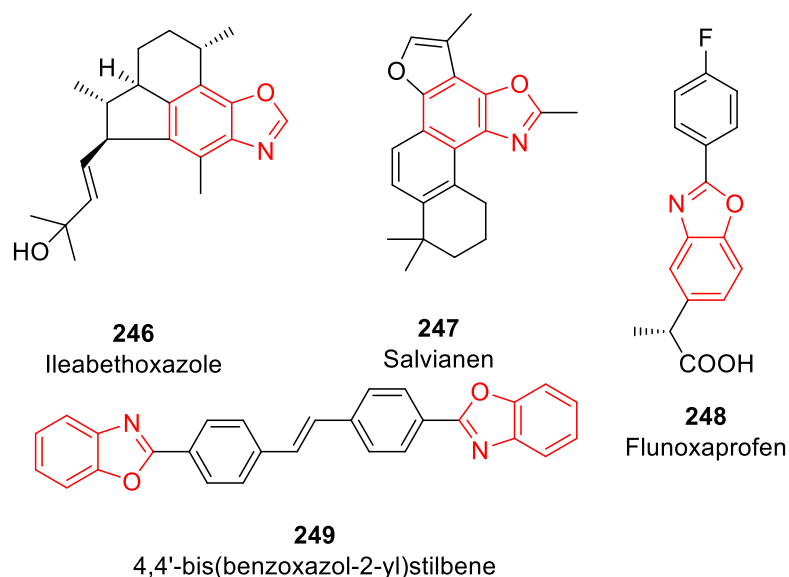


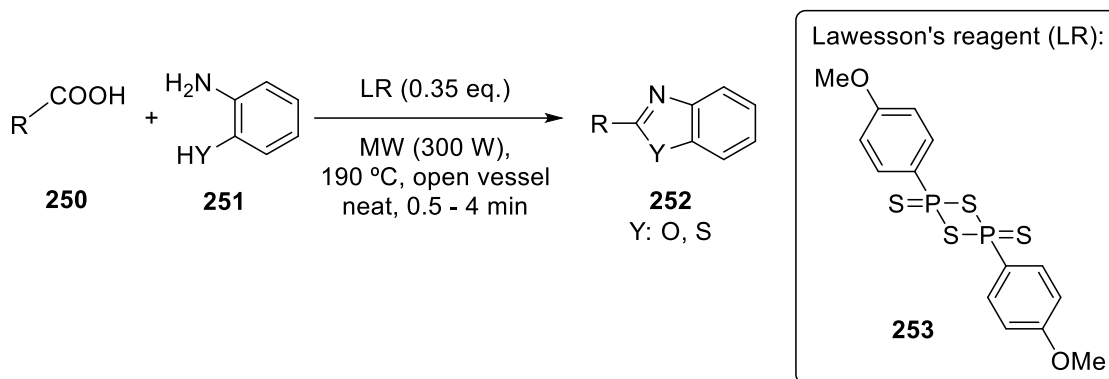
Figure 5.1: Benzoxazole derivatives in natural products and chemical industry.

5.1.1. Typical methods for the synthesis of benzoxazoles

Multiple approaches have been used to synthesise benzoxazoles. Only some examples in the recent literature will be covered in this chapter. Overviews with the various strategies for the synthesis of benzoxazoles are available.^[2,8]

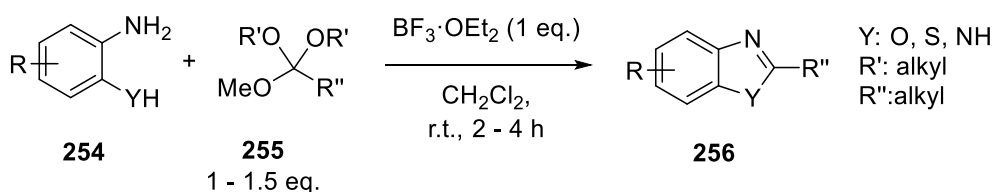
A frequent approach to produce benzoxazoles is the coupling of 2-aminophenol with carboxylic acid derivatives. Seijas, Vázquez-Tato and coworkers published in 2007 a

solvent-free microwave assisted synthesis of 2-substituted benzoxazoles from 2-aminophenol and carboxylic acids, promoted by Lawesson's reagent **253** (Scheme 5.1). This synthetic method is also applicable to the synthesis of benzothiazoles. Various aromatic, heteroaromatic and aliphatic carboxylic acids have been used in good yields.^[9]



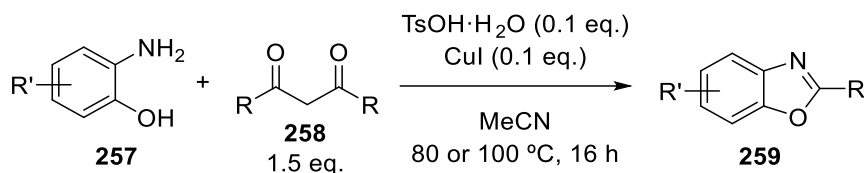
Scheme 5.1: Lawesson's reagent promoted microwave assisted synthesis of benzoxazoles.^[9]

The reaction of functionalised orthoesters with 2-substituted anilines **254** was reported in 2012 by Markó *et al.* to synthesise benzoxazoles, benzothiazoles and benzimidazoles (Scheme 5.2). The transformation was carried out in the presence of $\text{BF}_3 \cdot \text{OEt}_2$ at room temperature to give the corresponding compound in good yields.^[10]



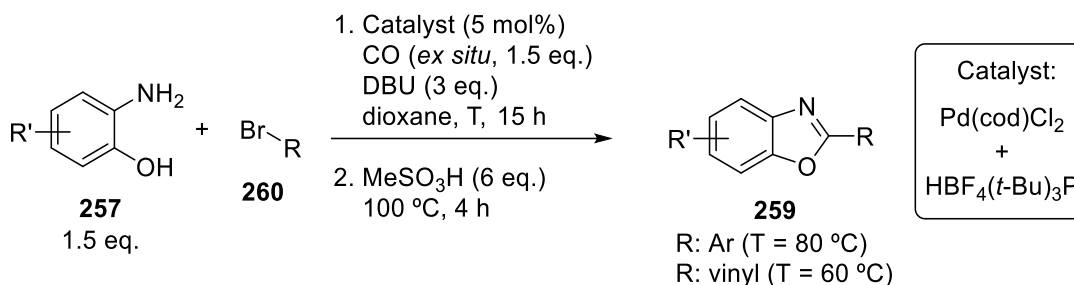
Scheme 5.2: Benzoxazoles synthesis from functionalised orthoesters and *ortho*-substituted anilines.^[10]

2-Aminophenols (**257**) react also with β -diketones (**258**) to give the corresponding benzoxazoles (**259**). Yu, Bao and coworkers developed a method in 2014 for the formation of 2-substituted benzoxazoles where a combination of Brønsted acid and copper iodide catalyses the reaction, which is performed at high temperature (80 or 100 °C, Scheme 5.3).^[11]



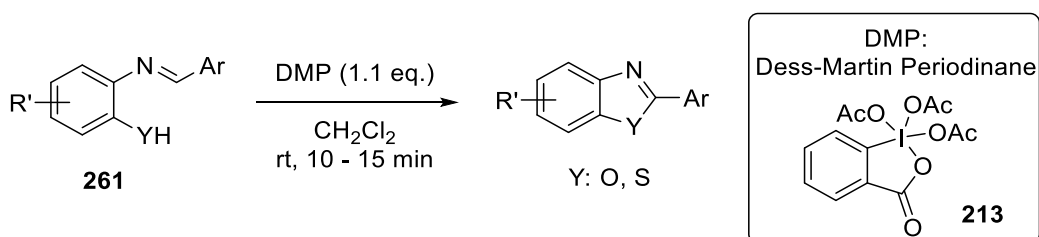
Scheme 5.3: Synthesis of benzoxazoles from 2-aminophenols and β -diketones.^[11]

In 2015, Lindhardt, Skrydstrup *et al.* reported the formation of benzoxazoles (**259**) from 2-aminophenols (**257**), aryl and vinyl bromides (**260**) and carbon monoxide. The reaction consists of two steps, where the first one is a Pd-catalysed aminocarbonylation of 2-aminophenols as nucleophiles, followed by a ring closure mediated by methanesulfonic acid. The reaction is carried out sequentially in one pot at high temperature, as shown in Scheme 5.4, to give 2-(hetero)aryl and 2-styryl benzoxazoles in moderate to excellent yields.^[12]



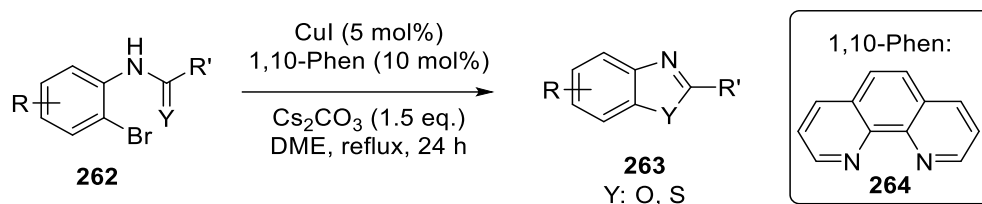
Scheme 5.4: Benzoxazoles synthesis from 2-aminophenols, aryl or vinyl bromides and carbon monoxide.^[12]

Benzoxazoles can also be produced from the condensation of 2-aminophenols (**257**) and aldehydes, and subsequent oxidation to perform the ring-closure using an oxidant, typically in excess. An example of such transformation was published by Bose *et al.* in 2010, using Dess-Martin periodinane (**213**, DMP) as oxidant to perform the intramolecular cyclisation of phenolic Schiff bases **261** (Scheme 5.5). Benzoxazoles and benzothiazoles were synthesised within 10 – 15 minutes in good yields.^[13]



Scheme 5.5: DMP mediated intramolecular cyclisation to form benzoxazoles.^[13]

A different approach towards the synthesis of benzoxazoles is *via* the copper-catalysed cyclisation of *ortho*-haloanilides (**262**). In 2006, Batey *et al.* reported an example of such transformation using 5 mol% of copper iodide, 10 mol% of ligand **264** and 1.5 eq. of caesium carbonate as base (Scheme 5.6). The reaction proceeds through an intramolecular C–O cross-coupling of the *ortho*-haloanilides, and it is also applicable to the synthesis of benzothiazoles **263** starting from the corresponding thioamide **262**.^[3]

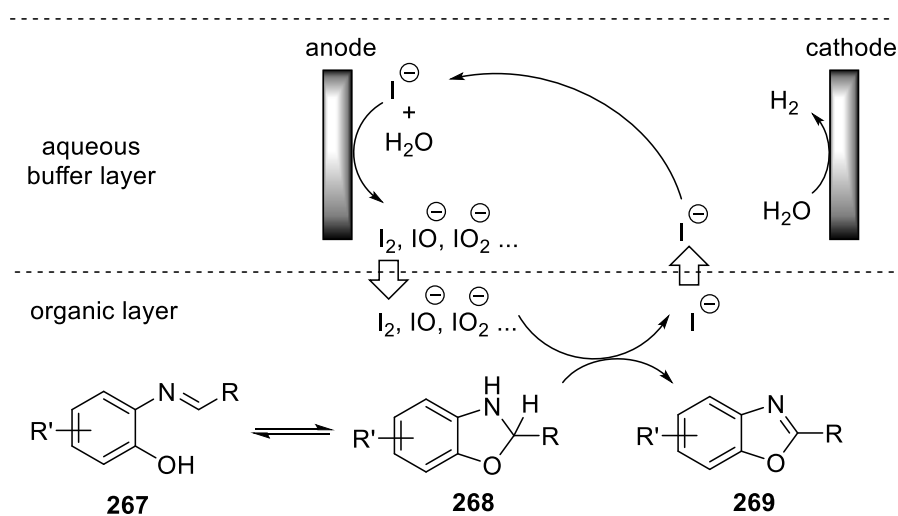


Scheme 5.6: Copper-catalysed synthesis of benzoxazoles from *ortho*-haloanilides.^[3]

5.1.2. Electrochemical methods for the synthesis of benzoxazoles

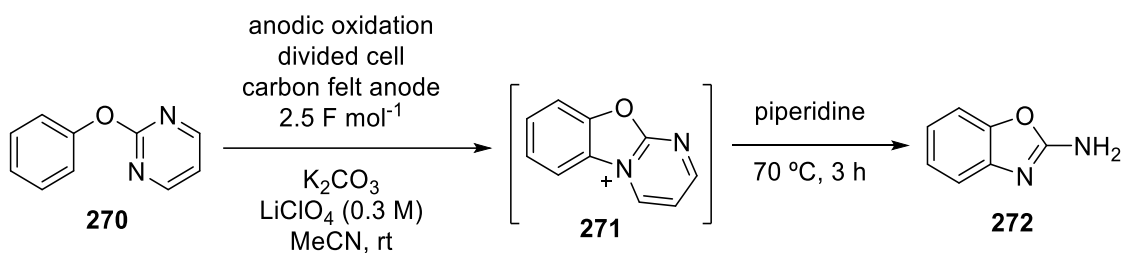
The electrochemical synthesis of benzoxazoles has also been reported in the literature, and relevant examples will be described in this section.

In 2013 Zeng, Little *et al.* developed an indirect electrochemical method for the formation of 2-substituted benzoxazoles (**269**) *via* anodic oxidation of a Schiff base of 2-aminophenol (**267**) using a catalytic amount of sodium iodide as a redox catalyst. A two-phase buffer system was used as solvent, and no supporting electrolyte was needed, as the iodide salt serves as an electrolyte (Scheme 5.7).^[14]



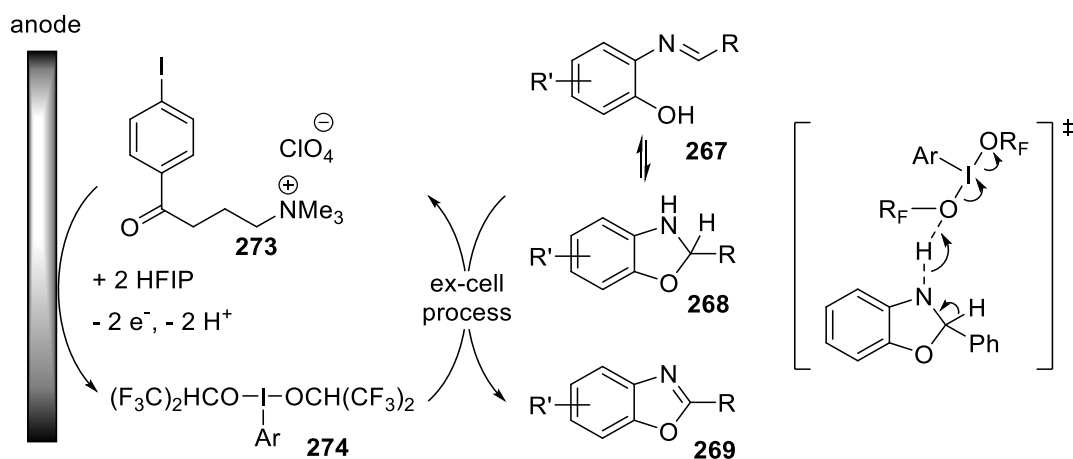
Scheme 5.7: Iodide-mediated electrochemical synthesis of benzoxazoles.^[14]

Later in 2015, Yoshida and coworkers published a method for the electrochemical oxidation of 2-pyrimidylbenzenes (**270**) to give the corresponding pyrimidinium ions (**271**), which can be transformed into 2-amino-benzoxazoles (**272**) upon reaction with piperidine (Scheme 5.8). The electrochemical reaction was performed in a divided cell using potassium carbonate as a base, and the cyclised pyrimidinium ion **271** was then treated with piperidine at 70 °C to give the desired benzoxazole.^[15]



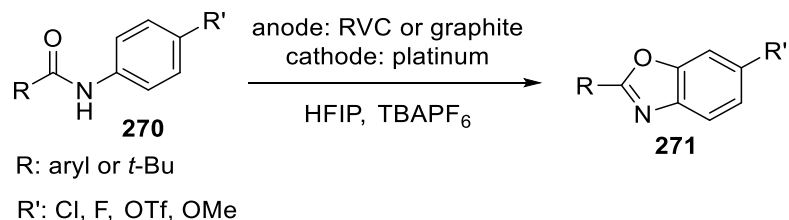
Scheme 5.8: Synthesis of 2-aminobenzoxazoles by electrochemical intramolecular C–H amination.^[15]

In 2017, Roemelt, Suna, Francke *et al.* reported a method for the synthesis of benzoxazoles from *ortho*-iminophenols using electrochemically generated iodine (III) (**274**) compounds from iodoarenes (**273**) in HFIP. The formation of benzoxazoles is performed “ex-cell”, i.e. a solution of the electrochemically generated hypervalent iodine compound is added to another solution containing the *ortho*-iminophenols (**267**, Scheme 5.9). This “ex-cell” approach makes possible the use of substrates bearing functional groups that are sensitive towards electrochemical transformations, such as alkene, carboxylic acid and bromine. The redox mediator iodoarene (**273**) was tethered to contain a tetraalkylammonium moiety, making this compound more conductive and avoiding the use of an external supporting electrolyte. The iodoarene species can be recovered (92 – 94%) by precipitation after completion of the reaction.^[16]



Scheme 5.9: Electrochemically generated I(III) for the synthesis of benzoxazoles.^[16]

A recent method developed by Waldvogel and coworkers in 2017 shows the direct formation of benzoxazoles (**271**) from amides (**270**) using carbon anode (RVC or graphite) and platinum cathode. The reaction was carried out in HFIP, since other solvents led to degradation of the starting materials, which suggests that the transformation is slow, and the radical intermediates formed need to be stabilised by the solvent (Scheme 5.10).^[17]

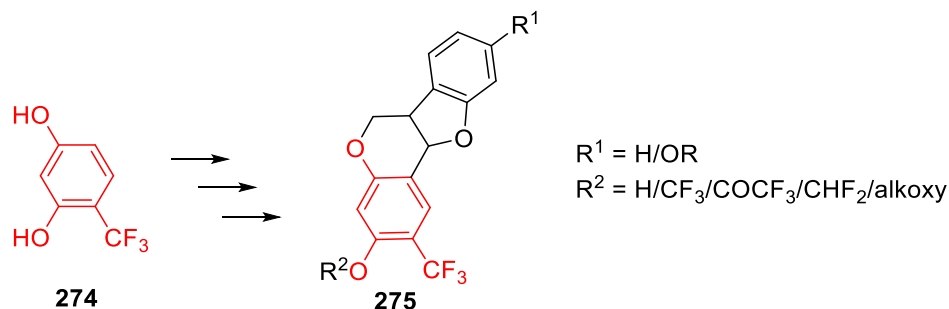


Scheme 5.10: Electrosynthesis of benzoxazoles from amides.^[17]

5.2. Trifluoromethylation of resorcinol

It is well known that the incorporation of CF₃ groups in biologically active compounds increases the therapeutic efficacy by substitution of hydrogen and hydroxyl groups for fluorine.^[18] Fluorine's electronegativity, size, lipophilicity and electrostatic interactions can dramatically influence the chemical stability and molecular target specificity.

Scheme 5.11 shows trifluororesorcinol (**274**) as a precursor for a trifluoromethylated pterocarpan derivative (**275**). Compounds containing the pterocarpan skeleton are bone anabolic agents with low oral bioavailability.^[19] The incorporation of a CF₃ group could potentially improve the pharmacokinetic profile and efficacy of this compound.



Scheme 5.11: Synthetic application of 4-trifluororesorcinol.

The first step would then be the trifluoromethylation of resorcinol to achieve **274**. To the best of our knowledge, its synthesis has been reported only by Yang *et al.* in 1998 from 4-iodoresorcinol in 15% yield.^[20] The compound is commercially available from HE (China) and it has a price of \$4000 per gram. Therefore, its synthesis *via* electrochemical trifluoromethylation of inexpensive resorcinol would be desirable. CF_3 radicals can be generated electrochemically from trifluoroacetic acid (TFA)^[21] *via* Kolbe electrolysis, and then react with phenol derivatives to give the trifluoromethylated aromatic ring.^[22]

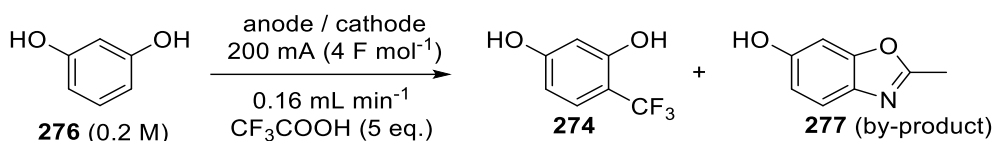


Table 5.1: Synthesis of 4-trifluororesorcinol.

Entry	Solvent	Anode	Cathode	Result (yield) ^a
1	MeCN/H ₂ O (7:1)	Pt	Graphite	277 (12%) / 276 (21 %)
2	THF	Pt	Graphite	276 recovered ^b
3	TFA	Pt	Graphite	276 recovered ^c
4	H ₂ O	Pt	Graphite	276 recovered
5	MeCN	Graphite	Pt	277 (2%) / 276 (26%) ^d
6	MeCN	BDD	Pt	277 (18%) ^d
7 ^f	HFIP/H ₂ O (9:1)	Pt	Graphite	276 recovered ^e

^aYield calculated by GC using 1,3,5-trimethoxybenzene as internal standard; ^bpoor conductivity of the solvent; ^cTFA too corrosive; ^d**274** possibly formed, analysed by GC-MS; ^e18 recovered when $I < 50$ mA, decomposition observed when $I > 80$ mA. ^f0.08 mL min⁻¹.

Resorcinol was treated under different electrochemical conditions with 5 eq. of TFA, 4 F mol⁻¹, and the results are shown in Table 5.1. The reaction was analysed by GC using 1,3,5-trimethoxybenzene as an internal standard. A brown thick oil was encountered in the crude mixture of all the reactions, which is thought to be formed due to decomposition of the starting material. This oil is insoluble in most organic solvents, and does not show any clear compound by ¹H NMR. Therefore, the crude mixture of the reaction was passed through a silica plug before being injected in the gas chromatograph, to avoid contamination of the column. Unfortunately, the desired product **274** was not obtained after varying different reaction parameters such as solvent, anode and cathode material. Only when platinum was used as the cathode and graphite or boron-doped diamond (BDD) as the anode, there was a new peak observed by GC (entries 5 and 6), although its intensity was low. This crude sample was analysed by GC-MS, and the chromatogram suggested that this new peak might correspond to the target molecule of trifluororesorcinol (**274**). Since the amount generated was very small, the compound could not be isolated. It could not be found on TLC or recognised in the crude ¹H NMR, therefore, its full characterisation could not be achieved. Further investigation is necessary in order to confirm the structure of the potentially trifluororesorcinol obtained and to optimise the reaction conditions that could lead to its synthesis in an efficient way.

When the reaction described in Table 5.1 was first performed, the main product observed was not the expected trifluororesorcinol **274**, but the benzoxazole **277**. Acetonitrile was reacting with resorcinol to give **277** in 12% yield. Despite the fact that this was not the planned reaction, the synthesis of benzoxazoles from accessible and inexpensive starting materials, such as resorcinol and acetonitrile, seemed to be very promising. Therefore, the reactivity of this reaction was explored, and it is explained in the next sections.

5.3. Electrochemical synthesis of benzoxazoles from phenol derivatives and nitriles

As mentioned in the previous section, the benzoxazole **277** was obtained when resorcinol was treated with trifluoroacetic acid (TFA, 5 equiv.) in acetonitrile in the flow electrochemical reactor. In order to understand this reaction, and therefore optimise the benzoxazole synthesis, several parameters were investigated, such as the use of acid and electrode materials.

5.3.1. Acid screening

In the first instance, the reaction took place in the presence of trifluoroacetic acid (TFA). When the same reaction was carried out in the exact same conditions but without the acid, no product was observed, only starting material. To investigate the role of TFA, different acids were screened to determine whether the reaction could be performed in presence of other acids as well:

- i) Acetic acid: No conversion to the desired product. Mainly resorcinol recovered.
- ii) *p*-Toluenesulfonic acid monohydrate: < 1% GC conversion.
- iii) Sulfuric acid: No product observed, only decomposition, the crude was a complex mixture.
- iv) Triflic acid: complex crude mixture obtained.
- v) Trifluoroacetic acid (1 eq.): 20% GC yield (2% of resorcinol recovered).
- vi) No acid: No conversion to the desired product, resorcinol was recovered. Since the conductivity was very poor, 0.2 equiv. of Et₄NBF₄ was added as supporting electrolyte.

Since all the attempts to perform the reaction with different acids were unsuccessful, we proposed the theory that TFA could be acting as a radical stabiliser,^[23] helping in the course of the reaction. So as to explore this hypothesis, trifluoroacetic acid was replaced by hexafluoroisopropanol (HFIP), which is known to be a better radical stabiliser than TFA.^[24] Unfortunately, the reaction carried out in HFIP led to the recovery of the starting material when the current used was low (< 2 F mol⁻¹), or decomposition when the current used was high (> 3 F mol⁻¹).

The reasons why TFA permits the electrochemical production of benzoxazole are not very clear, but it can be concluded that the use of TFA is necessary and it cannot be replaced by other acids or the radical stabiliser tested. Further investigation is needed in order to explain its role in the mechanism.

5.3.2. Electrode screening

Different electrode materials were investigated in the electrochemical formation of benzoxazoles, and the results are shown in Table 5.2. The starting conditions were the

same as shown in Table 5.1, entry 1, but excluding the use of water. This led to a higher yield of compound **277** (Table 5.2, entry 1).

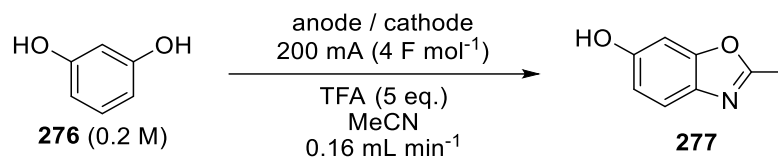


Table 5.2: Electrode screening for the synthesis of benzoxazoles.

Entry	Anode	Cathode	GC yield of 277 [%] ^a	GC recovery of 276 [%] ^a
1	Pt	Graphite	25	5
2	Graphite	Pt	2	15
3	BDD	Pt	18	3
4 ^b	Pt	BDD	14	1

^aYield calculated by GC using 1,3,5-trimethoxybenzene as internal standard

^b0.05 M, 60 mA (4.6 F mol⁻¹)

These results show that swapping platinum and graphite for cathode and anode (entry 2) did not improve the result, but led to poor yield and decomposition of the starting material. Using boron-doped diamond (BDD) as the anode and platinum as the cathode gave similar results (entry 3) as the electrode combination used for previous experiments. A large scale reaction (2 mmol) was performed with the conditions from entry 1, and benzoxazole **277** was obtained in 23% isolated yield, corroborating the result analysed by GC.

It is worth noting that in all cases resorcinol was not recovered back, or only recovered in a very small amount. It is known that phenols can be easily decomposed electrochemically,^[25] therefore making this process more challenging to optimise. As explained in Section 5.2, there was always a brown thick oil obtained that suggests decomposition of substrates and/or product intermediates.

5.3.3. Other conditions screening

The same reaction was performed under the same conditions as shown in Table 5.2, entry 1, but adding 5 equiv. of HFIP as radical stabiliser. When the current was high (200 mA, 4 F mol⁻¹), no benzoxazole **277** was observed by ¹H NMR, only traces of resorcinol and a complex mixture in the aliphatic region of the spectrum. When a lower

current was applied (100 mA or 50 mA, 2 and 1 F mol⁻¹ respectively), resorcinol was the main compound observed in the crude ¹H NMR.

Since decomposition seemed to be the main problem in this reaction, as the starting material was consumed in most cases, the current density was decreased in order to avoid such degradation. The first parameter changed was the flow rate, that was decreased to half (0.08 mL min⁻¹). Therefore, according to the equation to calculate the current needed in a flow electrochemical reaction (Chapter 1), the current used was 100 mA (still corresponding to 4 F mol⁻¹). Under these conditions, the benzoxazole was obtained in 24% yield, and resorcinol was recovered in 1% yield. Thus, it was concluded that lowering the current density did not lead to a better outcome of the reaction, and resorcinol was still being fully consumed.

The next attempt to decrease the current density was by decreasing the concentration from 0.2 M to 0.05 M, so the current needed is lower than that used with high concentrations. Table 5.3 shows the results when 3.0, 3.8 and 4.6 F mol⁻¹ were used. In all cases there was some resorcinol recovered, but the amount was not significant to conclude that there was less degradation occurring. However, the yield of the desired benzoxazole **277** did not improve.

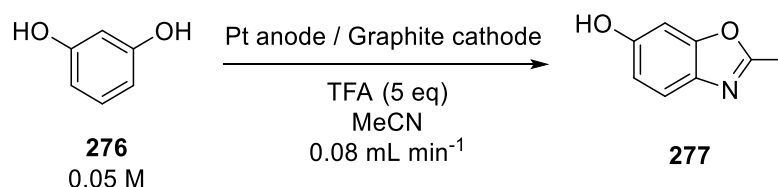


Table 5.3: Experiments with lower concentration of starting material.

Entry	Current [mA]	F mol ⁻¹	GC yield of 277 [%]	GC recovery of 276 [%]
1	20	3.0	17	8
2	25	3.8	20	2
3	30	4.6	25	3

The use of a lower current density does not affect significantly the result of the transformation, and the degradation of the starting material and/or intermediates cannot be avoided this way.

Addition of water to the solvent mixture (0.2 M of **276**) slowed down the reaction and led to a lower yield of **277**. With a flow rate of 0.08 mL min⁻¹ and current of 100 mA (4 F mol⁻¹), the benzoxazole **277** and resorcinol **276** were obtained in 8 and 19% yield respectively. Increasing the flow rate to 0.16 mL min⁻¹, and therefore the current to 200 mA (4 F mol⁻¹) led to a similar result, where **277** was formed in 12% yield and **276** recovered in 21% yield.

5.3.4. Scope of substrates

Since the benzoxazole starting from resorcinol could not be synthesised with a higher yield than 25%, different phenol derivatives and nitriles were explored to investigate if the stability of the intermediates could be improved.

A variety of phenol derivatives were used in the reaction, and it is shown in Table 5.4. None of the substrates proved to be more stable than resorcinol, since for most of them decomposition was observed by ¹H NMR and no starting material was recovered after the reaction.

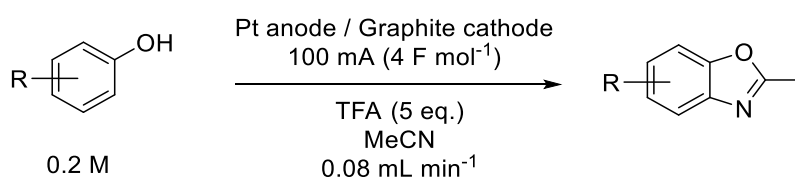
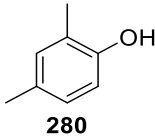
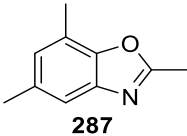
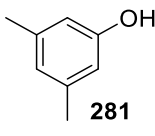
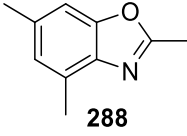
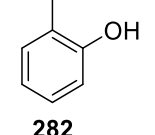
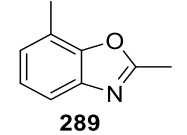


Table 5.4: Phenol derivatives for the synthesis of benzoxazoles.

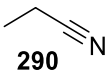
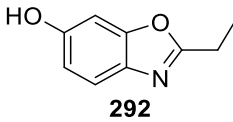
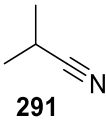
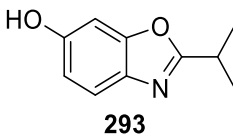
Entry	Phenol derivative	Benzoxazole derivative	Result ^a
1 ^c			23% isolated yield
2 ^c			Complex mixture. Traces of product
3			7% yield ^b

4			Complex mixture
5			Complex mixture
6			Complex mixture

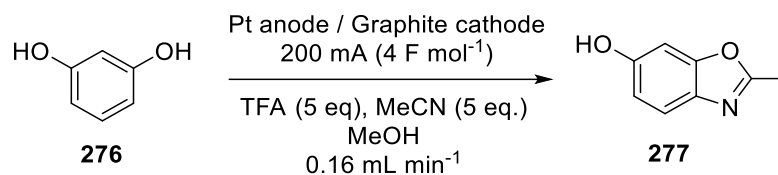
^aanalysed by ¹H NMR; ^bmeasured by ¹H NMR with benzyl mandelate as internal standard; ^c0.16 mL min⁻¹, 200 mA (4 F mol⁻¹)

When the reaction was carried out with different nitriles and resorcinol, the results were more successful (Table 5.5). When propionitrile (**290**) was used, the expected compound **292** was obtained in 34% yield. The same result was obtained with isobutyronitrile (**291**), but in this case a ratio of 7:3 (product : starting material) was observed in the crude ¹H NMR. In both cases the nitrile was used in a large excess, since it was used as solvent.

Table 5.5: Different nitriles for the synthesis of benzoxazoles.

Entry	Current [F mol ⁻¹]	Nitrile	Benzoxazole derivative	Yield [%]
1	4.8			34
2	4			34

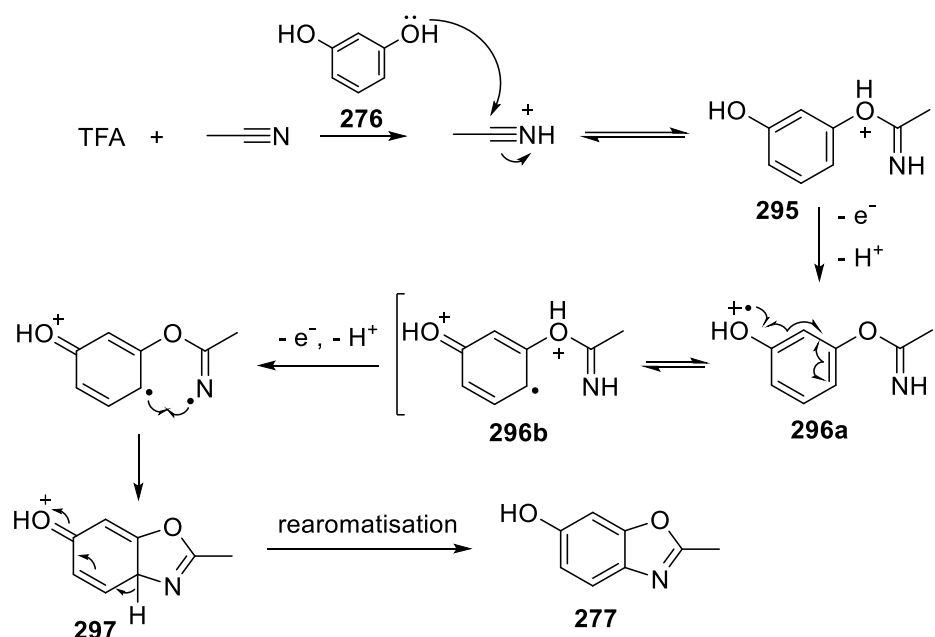
Finally, to investigate if the reaction could be performed in lower excess of the corresponding nitrile, an experiment was carried out in methanol with 5 equiv. of acetonitrile (Scheme 5.12). Product **277** was obtained in less than 3% yield, and resorcinol recovered as the main compound.



Scheme 5.12: Electrochemical formation of 276 in methanol with 5 equivalents of acetonitrile.

5.3.5. Proposed mechanism

The mechanism of the reaction is unclear, but it has been proved that the presence of trifluoroacetic acid is necessary for the reaction to take place. A proposed mechanism is shown in Scheme 5.13, where firstly the nitrile moiety can act as a Lewis base and be protonated in the presence of TFA. Then, one of the hydroxy groups attacks the electrophilic carbon of the nitrile, and form compound **295**. This can then be electrochemically oxidised to form **296**,^[22] which will undergo a second oxidation, and then perform an intramolecular cyclisation. Rearomatisation of the species **297** will give the more stable benzoxazole product **277**. This mechanism could also explain why the reaction is more efficient when two alcohol moieties are present in the aromatic ring, since one is used as a nucleophile to react with the nitrile, and the other one is necessary to induce the oxidation of the aromatic ring. Further investigation would be necessary to explain why the reaction does not take place in the presence of other acids.



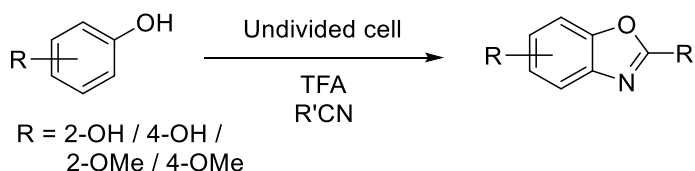
Scheme 5.13: Proposed mechanism.

5.4. Conclusions and future work

In conclusion, a new synthetic method for the electrochemical formation of benzoxazoles from easily accessible and inexpensive resorcinol and nitriles has been discovered. Unfortunately, the yields achieved are low (25 to 34%), and different attempts to improve these results were unsuccessful.

Further investigation in the mechanism to avoid the degradation of intermediates formed is necessary to understand the reaction and improve the outcome of such transformation. Cyclic voltammetry studies of resorcinol and phenol would be desirable to compare the reactivity of both substrates and understand better the oxidation pathway.

The reaction studied only gave some product when resorcinol or 3-methoxyphenol was used as starting material. Therefore, other substrates bearing at least two hydroxy groups (such as catechol) or one hydroxy and one methoxy group in the ortho or para position could be studied, as the proposed mechanism shows that both oxygens are needed, one to act as a nucleophile and the other one to induce the oxidation of the aromatic ring (Scheme 5.14).



Scheme 5.14: Substrates to be studied.

Attempts to use the nitrile source in stoichiometric amount led to unsuccessful results (Scheme 5.12). This should be further investigated once the reaction mechanism is better understood, and the use of other solvents should be explored to replace acetonitrile. This will allow the substrate scope to be broader, as other non-volatile nitriles could be used as reactants.

5.5. References

- [1] P. Lokwani, B. P. Nagori, N. Batra, A. Goyal, S. Gupta, N. Singh, *J. Chem. Pharm. Res.* **2011**, *3*, 302–311.
- [2] R. D. Viirre, G. Evindar, R. A. Batey, *J. Org. Chem.* **2008**, *73*, 3452–3459.
- [3] G. Evindar, R. A. Batey, *J. Org. Chem.* **2006**, *71*, 1802–1808, and references cited herein.
- [4] I. I. Rodríguez, A. D. Rodríguez, Y. Wang, S. G. Franzblau, *Tetrahedron Lett.* **2006**, *47*, 3229–3232.
- [5] M. Don, C. Shen, Y. Lin, W. Syu, Y. Ding, C. Sun, *J. Nat. Prod.* **2005**, *68*, 1066–1070.
- [6] C. Sacchi, F. Magni, A. Toia, F. Cazzaniga, G. Galli, F. Berti, *Pharmacol. Res.* **1989**, *21*, 177–182.
- [7] J. J. Li, Ed., *Heterocyclic Chemistry in Drug Discovery*, Wiley, **2013**.
- [8] M. Schnurch, J. Hammerle, P. Stanetty, in *Sci. Synth. Knowl. Updat.*, Thieme, Stuttgart, **2010**, pp. 153–206.
- [9] J. A. Seijas, M. P. Vázquez-Tato, M. R. Carballido-Reboredo, J. Crecente-Campo, L. Romar-López, *Synlett* **2007**, 313–317.
- [10] G. Bastug, C. Eviolitte, I. E. Markó, *Org. Lett.* **2012**, *14*, 3502–3505.
- [11] M. S. Mayo, X. Yu, X. Zhou, X. Feng, Y. Yamamoto, M. Bao, *J. Org. Chem.* **2014**, *79*, 6310–6314.
- [12] K. T. Neumann, A. T. Lindhardt, B. Bang-Andersen, T. Skrydstrup, *Org. Lett.* **2015**, *17*, 2094–2097.
- [13] D. S. Bose, M. Idrees, *Synthesis* **2010**, 398–402.
- [14] W. C. Li, C. C. Zeng, L. M. Hu, H. Y. Tian, R. D. Little, *Adv. Synth. Catal.* **2013**, *355*, 2884–2890.
- [15] T. Morofuji, A. Shimizu, J. I. Yoshida, *Chem. Eur. J.* **2015**, *21*, 3211–3214.
- [16] O. Koleda, T. Broese, J. Noetzel, M. Roemelt, E. Suna, R. Francke, *J. Org. Chem.* **2017**, *82*, 11669–11681.
- [17] T. Gieshoff, A. Kehl, D. Schollmeyer, K. D. Moeller, S. R. Waldvogel, *Chem. Commun.* **2017**, *53*, 2974–2977.
- [18] J. Wang, M. Sánchez-Roselló, J. L. Aceña, C. Del Pozo, A. E. Sorochinsky, S. Fustero, V. A. Soloshonok, H. Liu, *Chem. Rev.* **2014**, *114*, 2432–2506.
- [19] N. D. Kiss, T. Kurta, *Chirality* **2003**, *15*, 558–563.
- [20] J. Yang, D. Su, A. Vij, T. L. Hubler, L. Kirchmeier, J. M. Shreeve, *Heteroatom Chem.* **1998**, *9*, 229–239.
- [21] K. Arai, K. Watts, T. Wirth, *Chemistry Open* **2014**, *3*, 23–28.

- [22] A. Kirste, G. Schnakenburg, F. Stecker, A. Fischer, S. R. Waldvogel, *Angew. Chem. Int. Ed.* **2010**, *49*, 971–975.
- [23] L. Ebersson, M. P. Hartshorn, O. Persson, *J. Chem. Soc., Perkin Trans. 2* **1995**, 1735–1744.
- [24] L. Ebersson, M. P. Hartshorn, O. Persson, *Angew. Chem. Int. Ed.* **1995**, *34*, 2268–2269.
- [25] A. Kirste, B. Elsler, G. Schnakenburg, S. R. Waldvogel, *J. Am. Chem. Soc.* **2012**, *134*, 3571–3576.

CHAPTER 6: Experimental Part

CHAPTER 6: Experimental Part	165
6.1. General methods.....	167
6.2. Experimental data for Chapter 2: Flow electrochemical reactor design	169
6.2.1. Reactor design.....	169
6.2.2. Schematic representation of the aluminium reactor	171
6.2.3. Schematic representation of the 3D-printed Río reactor	173
6.3. Experimental data for Chapter 3: Electrosynthesis of isoindolinones and its functionalisation in flow	175
6.3.1. Cyclic voltammetry.....	175
6.3.2. Synthesis of substrates	177
6.3.3. Electrochemical synthesis of isoindolinones	196
6.3.4. Elimination products.....	210
6.3.5. Reduction products	214
6.4. Experimental data for Chapter 4: Electrosynthesis of benzothiazoles from <i>N</i> -arylthioamides in flow	218
6.4.1. Cyclovoltammetric measurements.....	218
6.4.2. Synthesis of substrates	219
6.4.3. Electrochemical synthesis of benzothiazoles.....	224
6.5. Experimental data for Chapter 5: Electrochemical synthesis of benzoxazoles in flow from resorcinol and nitriles	231
6.6. References	233

6.1. General methods

The reactions were performed using standard laboratory equipment. In all the reactions, standard reagent grade solvents and chemicals from Sigma Aldrich, Alfa Aesar, Acros Organic and FluoroChem were used without further purification, unless otherwise specified. All air sensitive reactions were carried out under argon or nitrogen atmosphere using oven dried glassware. All reactions were stirred using a stirrer plate and a magnetic stirrer bar and heating if necessary over a hotplate with a temperature probe control and adapted heating block. Lower temperatures were achieved using ice/water bath (0 °C) or dry ice/acetone bath (-78 °C). Dry ether and THF were collected from a solvent purification system (SPS) from the company MBRAUN (MB SPS-800). Dry CH₂Cl₂ was distilled over calcium hydride under nitrogen atmosphere. Büchi rotavapors were used for solvent evaporations (reduced pressure up to 8 mbar) and a high vacuum apparatus was used to further dry the products.

Thin-layer chromatography (TLC) was performed on pre-coated aluminium sheets of Merck silica gel 60 F254 (0.20 mm) and visualised by UV radiation (254 nm). Automated column chromatography was performed on a Biotage[®] Isolera Four using Biotage[®] cartridges SNAP Ultra 10 g, SNAP Ultra 25 g, SNAP Ultra 50 g, SNAP Ultra 100 g, Telos[®] 12 g and Telos[®] 20 g. The solvents used for the purification are indicated in the text and were purchased from Fischer Scientific as laboratory grade.

¹H NMR and ¹³C NMR spectra were measured on Bruker DPX 300, 400 or 500 apparatus and were referenced to the residual proton solvent peak (¹H: CDCl₃, δ 7.26 ppm; DMSO-*d*₆, δ 2.54 ppm) and solvent ¹³C signal (CDCl₃, δ 77.2 ppm, DMSO-*d*₆, δ 39.5 ppm). Chemical shifts δ were reported in ppm downfield of tetramethylsilane (δ = 0 ppm), multiplicity of the signals was declared as followed: s = singlet, d = doublet, t = triplet, q = quartet, quin = quintet, sex = sextet, hep = septet, dd = doublet of doublets, m = multiplet, b = broad; and coupling constants (*J*) in Hertz.

Mass spectrometric measurements were performed by the EPSRC Mass Spectrometry Facility in Swansea University on a Waters Xevo G2-S and on a Thermo Scientific LTQ Orbitrap XL machine for high-resolution mass spectroscopy (HRMS) or by R. Jenkins, R. Hick, T. Williams and S. Waller at Cardiff University on a Water LCR Premier XE-tof. Ions were generated by the Atmospheric Pressure Ionisation Techniques (APCI),

Electrospray (ESI), Electron Ionisation (EI) or Nanospray Ionisation (NSI). The molecular ion peaks values quoted for either molecular ion $[M]^+$, molecular ion plus hydrogen $[M+H]^+$, molecular ion plus sodium $[M+Na]^+$ or molecular ion plus potassium $[M+K]^+$.

IR spectra were recorded on a Shimadzu FTIR Affinity-1S apparatus. Wavenumbers are quoted in cm^{-1} . All compounds were measured neat directly on the crystal of the IR machine. Melting points were measured using a Gallenkamp variable heater with samples in open capillary tubes.

X-Ray crystallographic studies were carried out at the X-Ray Crystallography Service at Cardiff University. The data were collected on an Agilent SuperNova Dual Atlas diffractometer with a mirror monochromator, equipped with an Oxford cryosystems cooling apparatus. Crystal structures were solved and refined using SHELX. Non-hydrogen atoms were refined with anisotropic displacement parameters. Hydrogen atoms were inserted in idealised positions. The structure was solved by a direct method and refined by a full matrix least-squares procedure on F2 for all reflections (SHELXL-97).

In the flow set-ups, the syringe pumps that were used were KR Analytical Ltd Fusion 100 Touch syringe pumps. The electrochemical reactions were carried out in a galvanostatic mode using a GWINSTEK GPR-30H10D. The cyclic voltammogram studies were performed in a Orygalys OGF500 Potentiostat / Galvanostat with OGFPWR power supply. The in-line MS analysis was carried out using Advion Expression[®] CMS (Atmospheric Pressure Ionisation Techniques (APCI)) and an MRA[®] valve.

The 3D-printed reactor was printed with a Formlabs[®] Form 2 SLA 3D printer using clear resin.

6.2. Experimental data for Chapter 2: Flow electrochemical reactor design

6.2.1. Reactor design

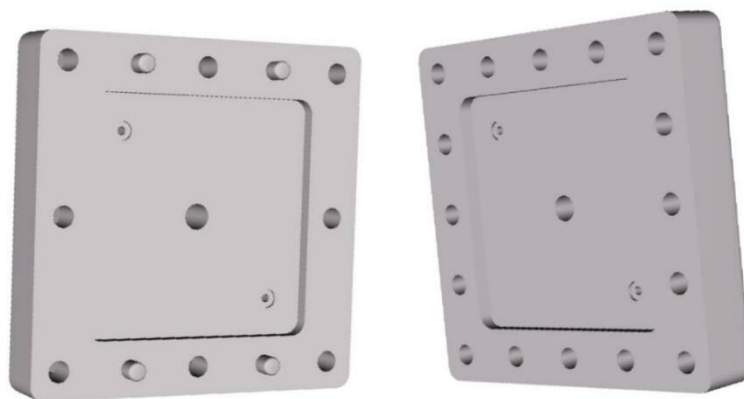


Figure 6.1: Design of the Ríó reactor.

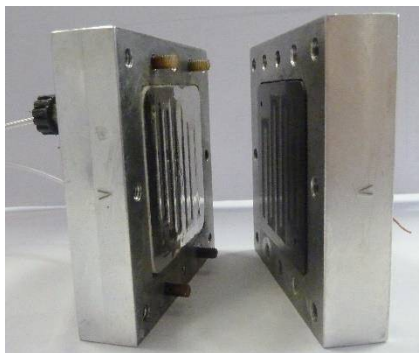


Figure 6.2: Aluminium reactor.

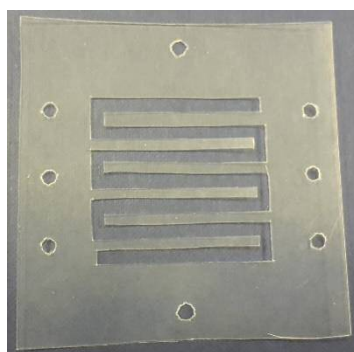


Figure 6.3: FEP flow channel.

Meandering spacer, with channel 3 mm width.
thickness: 250 μm
volume: 205 μL
exposed electrode surface: 8.2 cm^2

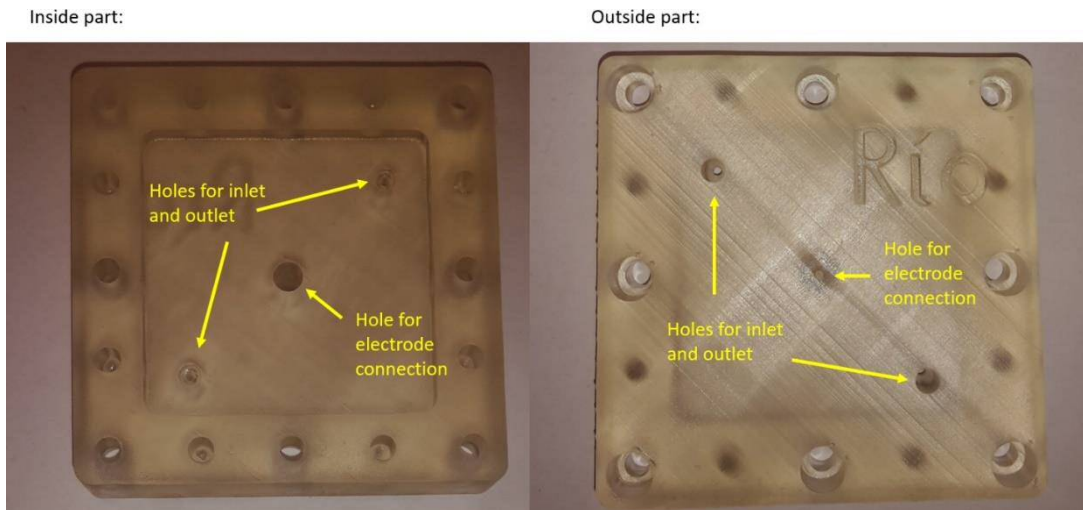


Figure 6.4: 3D printed Río reactor.

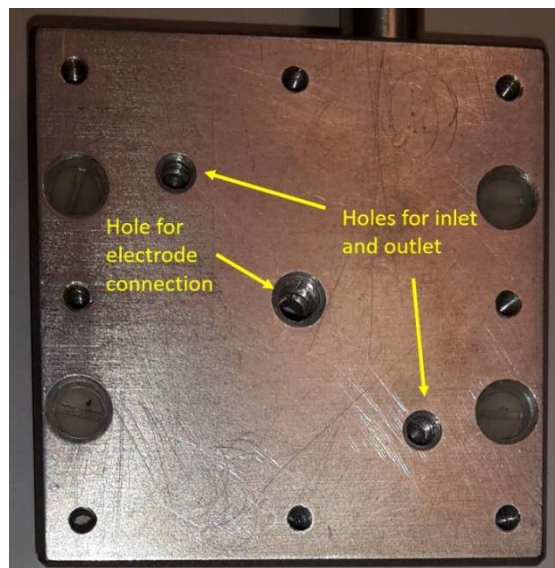
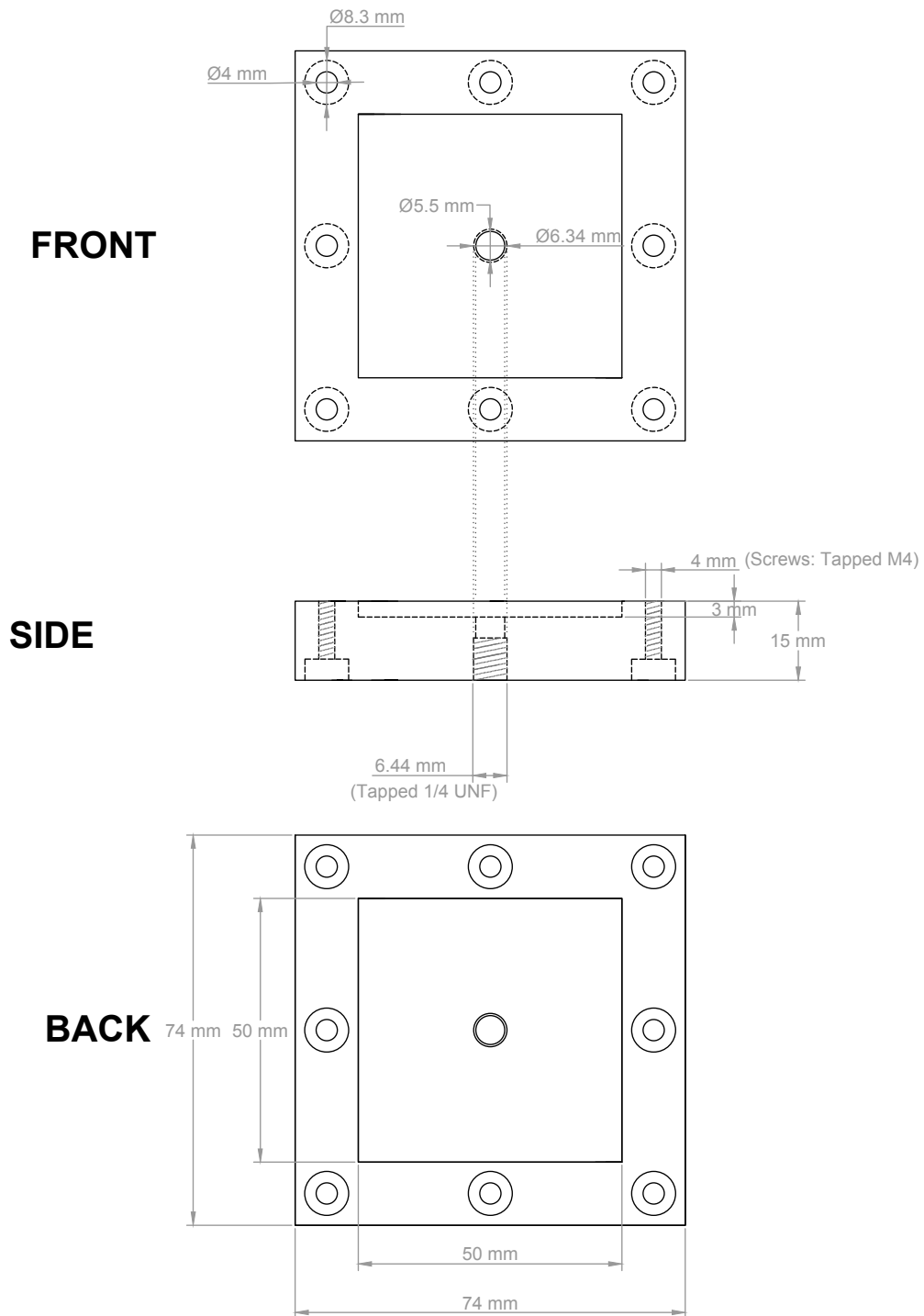
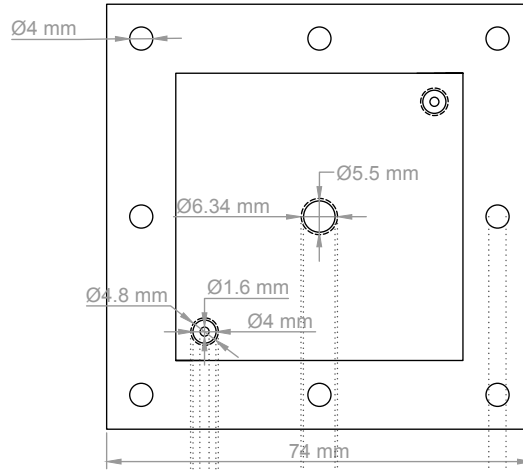


Figure 6.5: Aluminium reactor.

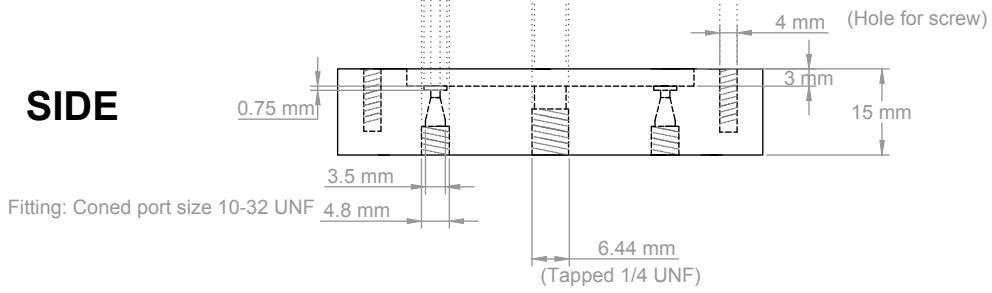
6.2.2. Schematic representation of the aluminium reactor**Aluminium Body for Electrochemical micro-reactor. PART A**

Aluminium Body for Electrochemical micro-reactor. PART B

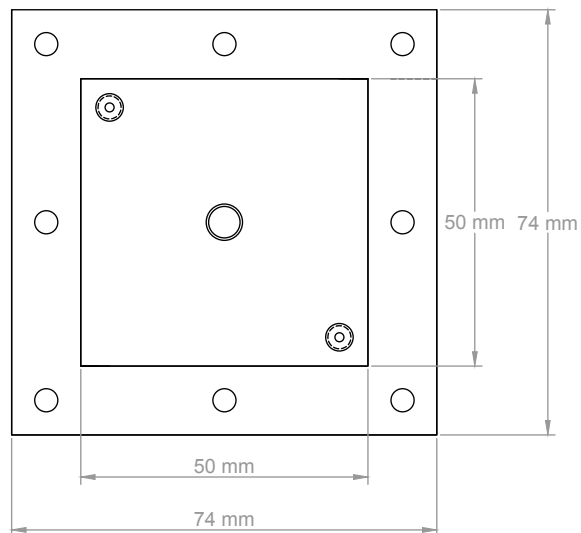
FRONT



SIDE

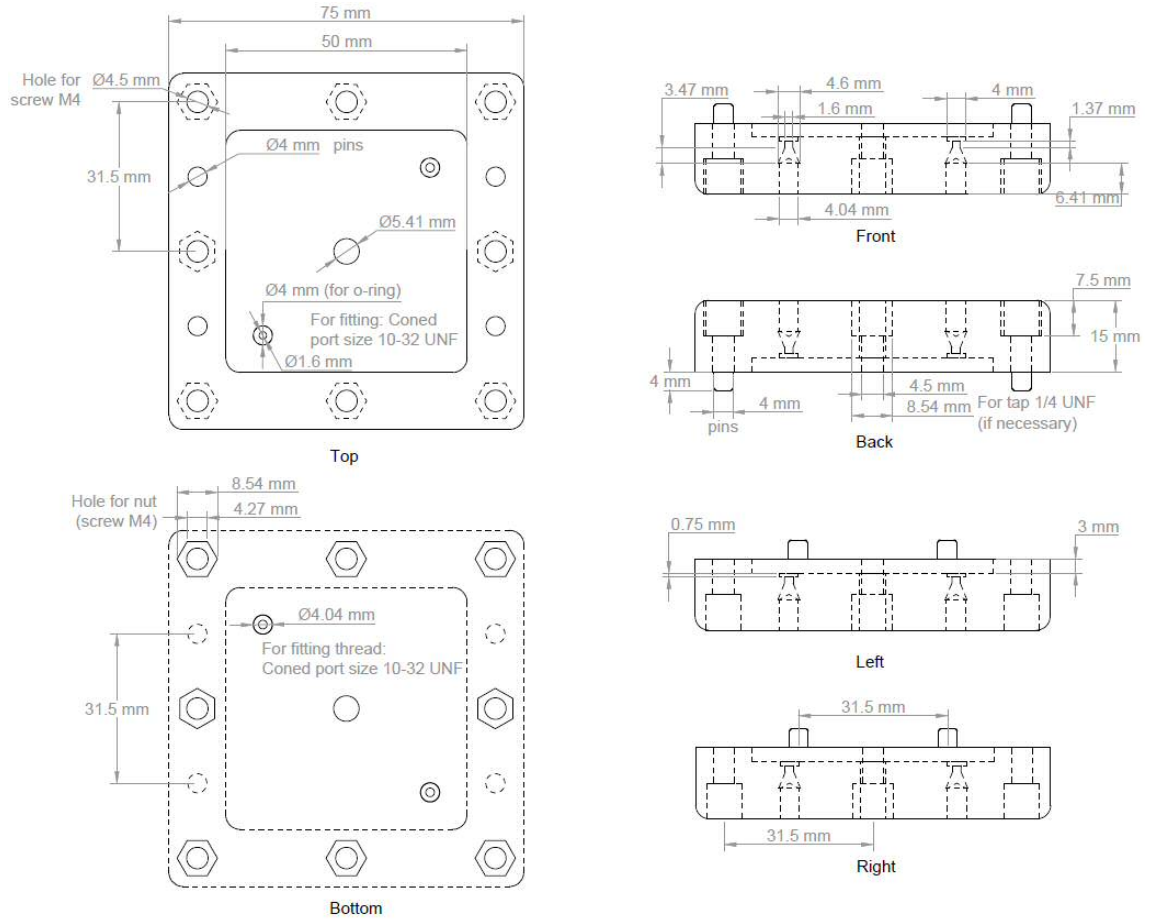


BACK

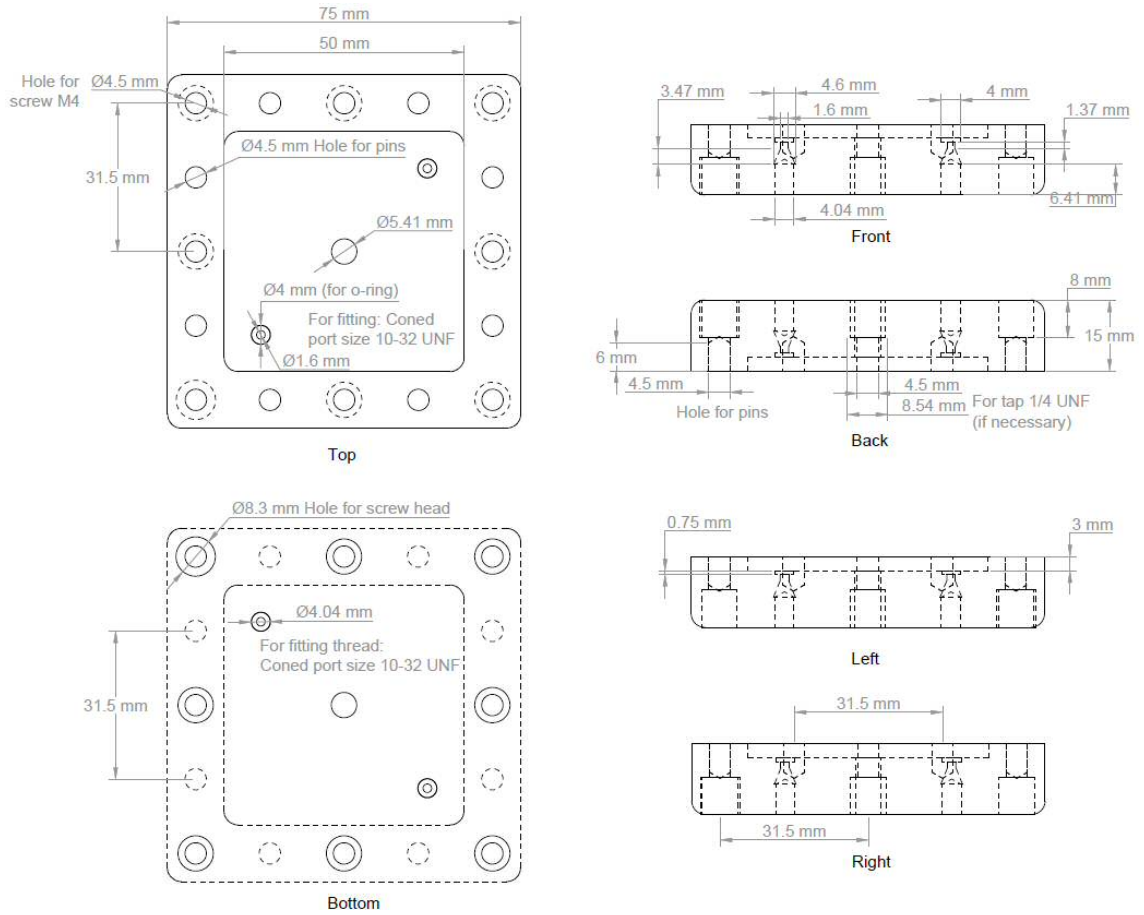


6.2.3. Schematic representation of the 3D-printed Río reactor

3D-Printed Río reactor, Part A:

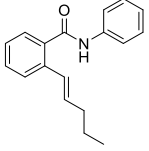
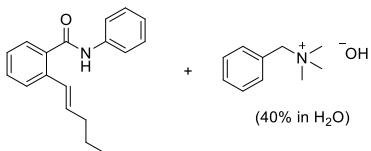
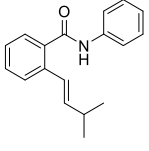
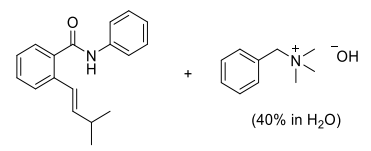
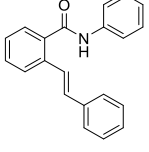
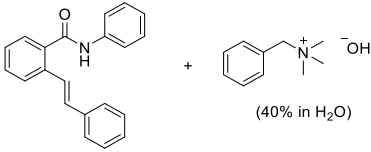
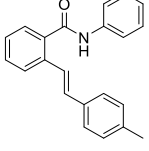
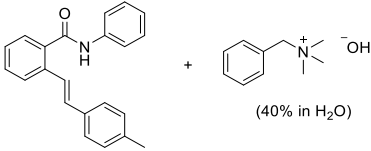
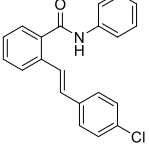
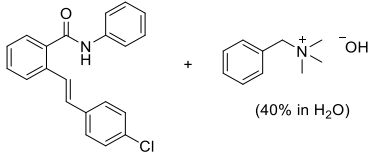
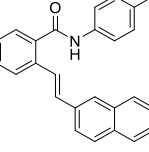
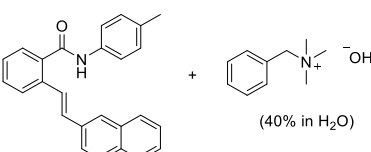


3D-Printed Río reactor, Part B:



6.3. Experimental data for Chapter 3: Electrochemical synthesis of isoindolinones and its functionalisation in flow

6.3.1. Cyclic voltammetry

Entry	Compound	E_p^{ox}	Compound + base	E_p^{ox}
1	 164a	1.67 V		0.33 V
2	 164b	1.67 V		0.31 V
3	 170a	1.42 V		0.27 V
4	 170b	1.37 V		0.22 V
5	 170c	1.50 V		0.25 V
6	 170e	1.41 V		0.18 V

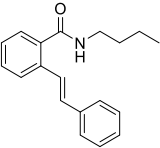
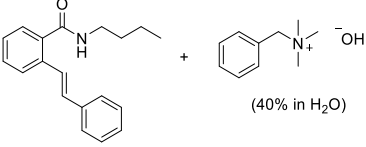
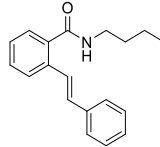
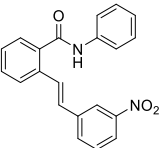
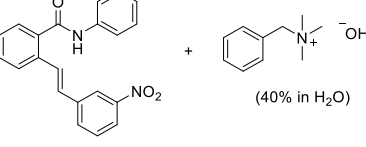
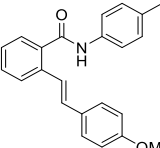
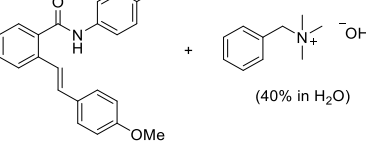
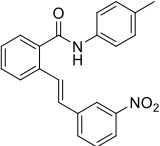
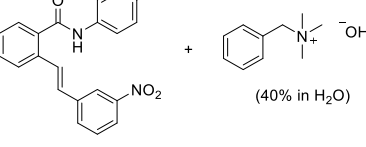
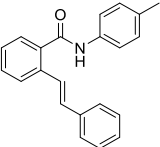
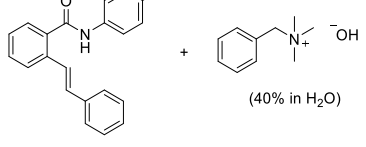
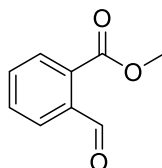
7	 170d	 $>2.2\text{V}$
		 1.50 V
8	 170f	 0.13 V
9	 170h	 0.13 V
10	 170i	 0.12 V
11	 170k	 0.16 V

Table 6.1: Oxidative cyclic voltammograms of the substrates (1 mM) recorded in 0.075 M Bu₄NBF₄/MeCN electrolyte at 100 mV/s scan rate (Entry 2: 300 mV/s). Working electrode: glassy carbon electrode tip (3 mm diameter); Counter electrode: platinum wire; Reference electrode: Ag/AgCl in 3 M NaCl.

6.3.2. Synthesis of substrates

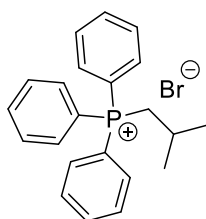
Methyl 2-formylbenzoate 160:



Procedure:^[1] Potassium carbonate (6.92 g, 50 mmol) and 2-carboxybenzaldehyde (3.00 g, 20 mmol) were dissolved in acetone (50 mL). Iodomethane (1.38 mL, 3.12 g, 22 mmol) was added dropwise in 5 min at room temperature, and the solution was refluxed under N₂ for 4 h. After cooling to room temperature, the solution was filtered and the solvent was evaporated under reduced pressure. The product was extracted with diethyl ether (3 x 30 mL), washed with brine, and the combined organic layers were dried over anhydrous magnesium sulfate. The solvent was evaporated under reduced pressure, and the product was purified by flash column chromatography (*n*-hexane:ethyl acetate; 9:1) to give compound **S1** (2.95 g, 90% yield) as a colourless oil.

¹H NMR (300 MHz, CDCl₃): δ = 10.61 (s, 1H, CHO), 7.98 – 7.93 (m, 2H, ArH), 7.69 – 7.62 (m, 2H, ArH), 3.97 (s, 3H, OCH₃) ppm. Spectrum in accordance with literature.^[2]

Isobutyltriphenylphosphonium bromide 161b:

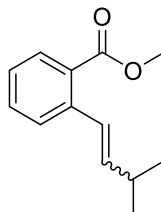


Procedure:^[3] 1-Bromo-2-methylpropane (8.70 mL, 80 mmol) and triphenylphosphine (20.98 g, 80 mmol) were dissolved in toluene (60 mL) and the solution was heated under reflux. The solid that precipitated was filtered off after 24 h and washed with diethyl ether. The filtrate was refluxed again for seven days in total and the solid was filtered off and washed with diethyl ether every two days. The solid obtained was dried using high vacuum to give compound **S2** (11.78 g, 37% yield) as a colourless solid.

¹H NMR (300 MHz, CDCl₃): δ = 7.92 – 7.85 (m, 6H, ArH), 7.81 – 7.75 (m, 3H, ArH), 7.72-7.66 (m, 6H, ArH), 3.78 (dd, *J* = 12.9, 6.3 Hz, 2H, PCH₂CH), 2.14-1.97 (m, 1H,

$\text{CH}_2\text{CH}(\text{CH}_3)_2$, 1.07 (d, $J = 6.6$ Hz, 6H, $\text{CH}(\text{CH}_3)_2$) ppm. Spectrum in accordance with literature.^[4] m.p. = 198 – 202 °C (Lit.: 200 – 202 °C).^[4]

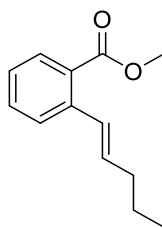
Methyl (*E/Z*)-2-(3-methylbut-1-en-1-yl)benzoate **162b:**



General procedure A: Isobutyltriphenylphosphonium bromide **161b** (3.67 g, 9.20 mmol) was transferred into a round bottom flask and was further dried using high vacuum. The flask was flushed with argon and dry tetrahydrofuran (50 mL) was added. The solution was cooled down to 0 °C, *n*-butyllithium (4.01 mL, 10.03 mmol, 2.5 M solution in hexanes) was added dropwise and the solution was stirred for 40 min at 0 °C. After that time, methyl-2-formylbenzoate **160** (1.37 g, 8.36 mmol) was added dropwise and the solution was allowed to warm up to room temperature and stirred overnight. The reaction mixture was quenched with water, THF was evaporated under reduced pressure, and the aqueous phase was extracted with ethyl acetate (3 x 40 mL). The combined organic phases were washed with brine and dried over anhydrous magnesium sulfate. The solution was concentrated *in vacuo*, and the product was purified using a silica plug (*n*-hexane:ethyl acetate; 19:1) to yield compound **162b** (0.795 g, 47% yield) as a yellow oil. The *E*-isomer was the main isomer formed (d.r. *E*:*Z* = 4.3:1).

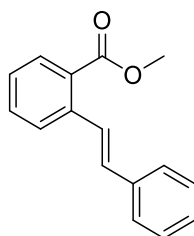
E-isomer: ¹H NMR (400 MHz, CDCl₃): $\delta = 7.84$ (dd, $J = 7.9, 1.2$ Hz, 1H, ArH), 7.56 – 7.53 (m, 1H, ArH), 7.46 – 7.40 (m, 1H, ArH), 7.25 (td, $J = 7.6, 1.3$ Hz, 1H, ArH), 7.10 (d, $J = 15.8$ Hz, 1H, ArCH=CH), 6.10 (dd, $J = 15.8, 6.8$ Hz, 1H, ArCH=CHCH), 3.90 (s, 3H, OCH₃), 2.51 (dhep, $J = 6.8, 5.4$ Hz, 1H, CHCH(CH₃)₂), 1.11 (d, $J = 6.8$ Hz, 6H, CH(CH₃)₂) ppm.

Z-isomer: ¹H NMR (400 MHz, CDCl₃): $\delta = 7.92$ (dd, $J = 7.8, 1.2$ Hz, 1H, ArH), 7.46 (td, $J = 7.8, 1.2$ Hz, 1H, ArH), 7.33 – 7.28 (m, 2H, ArH), 6.72 (d, $J = 11.5$ Hz, 1H, ArCH=CH), 5.51 (dd, $J = 11.5, 10.4$ Hz, 1H, ArCH=CHCH), 3.87 (s, 3H, OCH₃), 2.61 – 2.55 (m, 1H, CHCH(CH₃)₂), 0.97 (d, $J = 6.6$ Hz, 6H, CH(CH₃)₂) ppm. Spectra in accordance with literature.^[5]

Methyl (*E*)-2-(pent-1-en-1-yl)benzoate **162a:**

Synthesized according to the general procedure A on a 2.50 mmol scale, using butyltriphenylphosphonium bromide (1.10 g, 2.75 mmol). The addition of methyl-2-formylbenzoate **160** was done at $-78\text{ }^{\circ}\text{C}$; **162a** (0.1421 g, 28% yield) was obtained as a colourless oil (d.r. *E/Z* = 15: 1).

^1H NMR (400 MHz, CDCl_3): δ = 7.84 (dd, J = 7.8, 1.0 Hz, 1H, ArH), 7.54 (d, J = 7.9 Hz, 1H, ArH), 7.44 (td, J = 7.7, 0.9 Hz, 1H, ArH), 7.28 – 7.22 (m, 1H, ArH), 7.13 (d, J = 15.7 Hz, 1H, ArCH=CH), 6.14 (dt, J = 15.6, 6.9 Hz, 1H, ArCH=CHCH₂), 3.90 (s, 3H, OCH₃), 2.23 (q, J = 7.5 Hz, 2H, =CHCH₂CH₂), 1.51 (hep, J = 7.3 Hz, 2H, CH₂CH₂CH₃), 0.97 (t, J = 7.4 Hz, 3H, CH₂CH₃) ppm. ^{13}C NMR (126 MHz, CDCl_3): δ = 168.2, 139.8, 134.0, 132.0, 130.4, 128.7, 128.2, 127.3, 126.6, 77.2, 68.1, 52.1, 35.4, 25.7, 22.6, 13.9 ppm. The spectra are in accordance to the literature.^[6]

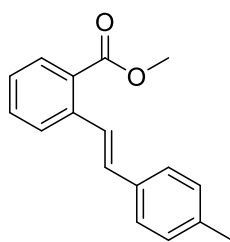
Methyl (*E*)-2-styrylbenzoate **169f:**

General procedure B:^[1] Pd(OAc)₂ (68 mg, 0.3 mmol) and triphenylphosphine (158 mg, 0.6 mmol) were added to an oven-dried flask, which was evacuated and filled with argon. Triethylamine (2.8 mL, 20 mmol) was added at room temperature, followed by the addition of methyl-2-iodobenzoate (1.81 mL, 10 mmol) and styrene (1.38 mL, 12 mmol). The mixture was heated up under reflux overnight. The solid products were diluted with 1 M HCl and extracted with dichloromethane (3 x 30 mL). The combined organic layers were washed with brine and dried over anhydrous magnesium sulfate. The solution was concentrated *in vacuo*, and the product was purified by flash column chromatography (*n*-

hexane:ethyl acetate; 9:1) to yield compound **169f** (2.38 g, 98% yield) as a yellow oil (*E*-isomer).

$^1\text{H NMR}$ (400 MHz, CDCl_3): $\delta = 8.00$ (d, $J = 16.2$ Hz, 1H, ArCH=CH), 7.94 (dd, $J = 7.9$, 1.4 Hz, 1H, ArH), 7.73 (d, $J = 7.9$ Hz, 1H, ArH), 7.59 – 7.55 (m, 2H, ArH), 7.54 – 7.49 (m, 1H, ArH), 7.40 – 7.31 (m, 3H, ArH), 7.31 – 7.26 (m, 1H, ArH), 7.02 (d, $J = 16.2$ Hz, 1H, ArCH=CH), 3.94 (s, 3H, OCH_3) ppm. The spectrum is in accordance to literature.^[1]

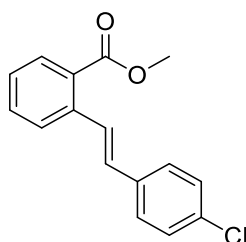
Methyl (*E*)-2-(4-methylstyryl)benzoate **169a:**



Synthesized according to the general procedure B on a 2.4 mmol scale, using 4-methylstyrene (0.283 g, 2.4 mmol); **169a** (0.50 g, 83% yield) was obtained as a colourless solid (*E*-isomer).

$^1\text{H NMR}$ (400 MHz, CDCl_3): $\delta = 7.94$ (d, $J = 16.4$ Hz, 1H, ArCH=CH), 7.92 (d, $J = 7.8$ Hz, 1H, ArH), 7.72 (d, $J = 7.9$ Hz, 1H, ArH), 7.54 – 7.42 (m, 3H, ArH), 7.31 (t, $J = 7.6$ Hz, 1H, ArH), 7.17 (d, $J = 7.7$ Hz, 2H, ArH), 7.00 (d, $J = 16.3$ Hz, 1H, ArCH=CH), 3.93 (s, 3H, OCH_3), 2.36 (s, 3H, ArCH₃) ppm. The spectrum is in accordance to literature.^[1]

Methyl (*E*)-2-(4-chlorostyryl)benzoate **169b:**

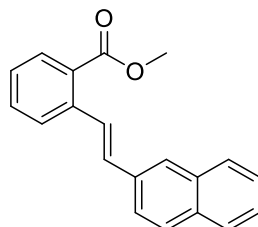


Synthesized according to the general procedure B on a 2.4 mmol scale, using 4-chlorostyrene (0.333 g, 2.4 mmol); **169b** (0.564 g, 86% yield) was obtained as a colourless solid (*E*-isomer).

$^1\text{H NMR}$ (300 MHz, CDCl_3): $\delta = 7.98$ (d, $J = 15.8$ Hz, 1H, ArCH=CH), 7.97 – 7.91 (m, 1H, ArH), 7.71 (d, $J = 7.9$ Hz, 1H, ArH), 7.58 – 7.44 (m, 3H, ArH), 7.39 – 7.29 (m, 3H,

ArH), 6.95 (d, $J = 16.5$ Hz, 1H, ArCH=CH), 3.93 (s, 3H, OCH₃) ppm. The spectrum is in accordance to literature.^[7]

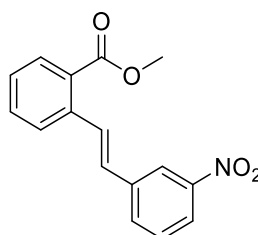
Methyl (*E*)-2-(2-(naphthalen-2-yl)vinyl)benzoate **169c:**



Synthesized according to the general procedure B on a 2.5 mmol scale, using 2-vinyl naphthalene (0.463 g, 3 mmol); **169c** (0.324 g, 45% yield) was obtained as a yellow solid (*E*-isomer).

¹H NMR (400 MHz, CDCl₃): $\delta = 8.15$ (d, $J = 16.2$ Hz, 1H, ArCH=CH-naph), 7.97 (dd, $J = 7.9, 1.4$ Hz, 1H, ArH), 7.89 (s, 1H, ArH), 7.87 – 7.78 (m, 5H, ArH), 7.54 (dt, $J = 7.4, 4.2$ Hz, 1H, ArH), 7.51 – 7.44 (m, 2H, ArH), 7.35 (td, $J = 7.7, 1.2$ Hz, 1H, ArH), 7.19 (d, $J = 16.2$ Hz, 1H, ArCH=CH-naph), 3.96 (s, 3H, CH₃) ppm. ¹³C NMR (101 MHz, CDCl₃): $\delta = 168.0, 139.4, 135.1, 133.8, 133.3, 132.3, 131.7, 130.9, 128.7, 128.5, 128.2, 127.9, 127.8, 127.3, 127.2, 127.1, 126.4, 126.1, 124.0, 52.3$ ppm. Spectra in accordance to literature.^[7]

Methyl (*E*)-2-(3-nitrostyryl)benzoate **169d:**

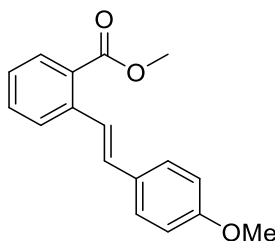


Synthesized according to the general procedure B on a 2.5 mmol scale, using 3-nitrostyrene (0.42 mL, 3 mmol); **169d** (0.613 g, 87% yield) was obtained as a yellow solid (*E*-isomer).

¹H NMR (400 MHz, CDCl₃): $\delta = 8.34$ (t, $J = 2.0$ Hz, 1H, ArH), 8.11 (d, $J = 16.1$ Hz, 1H, ArCH=CH-Ar), 8.12 – 8.07 (m, 1H, ArH), 7.98 (dd, $J = 7.9, 1.4$ Hz, 1H, ArH), 7.88 – 7.82 (m, 1H, ArH), 7.70 (d, $J = 7.9$ Hz, 1H, ArH), 7.58 – 7.48 (m, 2H, ArH), 7.38 (td, $J = 7.7, 1.2$ Hz, 1H, ArH), 7.00 (d, $J = 16.2$ Hz, 1H, ArCH=CH-Ar), 3.94 (s, 3H, CH₃) ppm. ¹³C NMR (101 MHz, CDCl₃): $\delta = 167.7, 148.8, 139.4, 138.6, 132.5, 132.4, 131.0, 129.7,$

128.9, 128.8, 128.1, 127.4, 122.4, 121.7, 52.4 ppm. HRMS (APCI) $[M - CH_3OH + H]^+$ calc. 252.0655, found 252.0655 $[C_{15}H_{10}NO_3]^+$. IR (neat): 1713, 1524, 1348, 1246, 1076, 962, 752, 706, 673 cm^{-1} . m.p. = 81 – 83 °C.

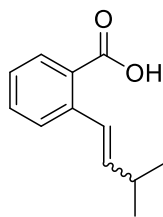
Methyl (*E*)-2-(4-methoxystyryl)benzoate **169e:**



Synthesized according to the general procedure B on a 2.5 mmol scale, using 4-methoxystyrene (0.4 mL, 3 mmol); **169e** (0.726 g, 99% yield) was obtained as a pale yellow solid (*E*-isomer).

1H NMR (500 MHz, $CDCl_3$): δ = 7.92 (d, J = 7.8 Hz, 1H, ArH), 7.88 (d, J = 16.2 Hz, 1H, ArCH=CH-Ar), 7.71 (d, J = 7.8 Hz, 1H, ArH), 7.53 – 7.45 (m, J = 6.6 Hz, 3H, ArH), 7.29 (t, J = 7.5 Hz, 1H, ArH), 6.99 (d, J = 16.2 Hz, 1H, ArCH=CH-Ar), 6.91 (d, J = 7.7 Hz, 2H, ArH), 3.93 (s, 3H, $COOCH_3$), 3.83 (s, 3H, OCH_3) ppm. ^{13}C NMR (126 MHz, $CDCl_3$): δ = 168.1, 159.6, 139.6, 132.2, 131.1, 130.8, 130.4, 128.4, 128.2, 126.9, 126.8, 125.3, 114.2, 55.4, 52.2 ppm. Spectra in accordance to literature.^[7]

(*E/Z*)-2-(3-Methylbut-1-en-1-yl) benzoic acid **163b:**

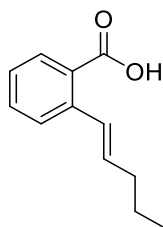


General procedure III:^[7] Methyl (*E/Z*)-2-(3-methylbut-1-en-1-yl) benzoate **162b** (0.394 g, 1.93 mmol) was dissolved in THF: methanol: water (4:1:1) (20 mL). Lithium hydroxide (0.139 g, 5.78 mmol) was added at room temperature and the solution was refluxed overnight. The reaction was quenched with 1 M hydrochloric acid until the solution had pH = 6. The solution was extracted with ethyl acetate (3 x 20 mL), the combined organic phases were washed with brine and dried over anhydrous magnesium sulfate. The solvent was evaporated under reduced pressure to give the acid **163b** (0.360 g, 98% yield) as a yellow solid.

E-isomer: ^1H NMR (300 MHz, CDCl_3): $\delta = 7.99$ (dd, $J = 7.9, 1.2$ Hz, 1H, ArH), 7.60 – 7.45 (m, 2H, ArH), 7.30 (dd, $J = 7.9, 1.2$ Hz, 1H, ArH), 7.22 (d, $J = 16.0$ Hz, 1H, ArCH=CH), 6.12 (dd, $J = 15.8, 6.8$ Hz, 1H, CH=CHCH), 2.63-2.45 (dhep, $J = 6.8, 5.5$ Hz, 1H, CHCH(CH₃)₂), 1.12 (d, $J = 6.8$ Hz, 6H, CH(CH₃)₂) ppm. Spectrum in accordance with literature.^[8]

Z-isomer: ^1H NMR (300 MHz, CDCl_3): $\delta = 8.07$ (dd, $J = 7.8, 1.2$ Hz, 1H, ArH), 7.60 – 7.45 (m, 2H, ArH), 7.36 (dd, $J = 7.8, 1.2$ Hz, 1H, ArH), 6.80 (d, $J = 11.3$ Hz, 1H, ArCH=CH), 5.54 (dd, $J = 11.5, 10.5$ Hz, 1H, CH=CHCH), 2.63 – 2.45 (m, 1H, CHCH(CH₃)₂), 0.99 (d, $J = 6.6$ Hz, 6H, CH(CH₃)₂) ppm. m.p. = 59 – 60 °C (*E/Z* – mixture) (Lit (*E*-isomer): 62 – 63 °C).^[8]

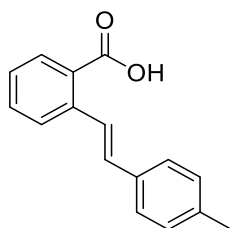
(*E*)-2-(Pent-1-en-1-yl)benzoic acid S163a:



Synthesized according to the general procedure III on a 0.69 mmol scale; **163a** (0.114 g, 87% yield) was obtained as a pale yellow solid.

^1H NMR (300 MHz, CDCl_3): $\delta = 8.01$ (dd, $J = 7.9, 1.3$ Hz, 1H, ArH), 7.57 (d, $J = 7.7$ Hz, 1H, ArH), 7.51 – 7.46 (m, 1H, ArH), 7.33 – 7.27 (m, 1H, ArH), 7.25 (d, $J = 15.6$ Hz, 1H, ArCH=CHCH₂), 6.17 (dt, $J = 15.7, 6.9$ Hz, 1H, ArCH=CHCH₂), 2.25 (q, $J = 6.9$ Hz, 2H, =CHCH₂CH₂), 1.61 – 1.46 (hep, $J = 7.3$ Hz, 2H, CH₂CH₂CH₃), 0.98 (t, $J = 7.4$ Hz, 3H, CH₂CH₃) ppm. ^{13}C NMR (126 MHz, CDCl_3): $\delta = 173.3, 140.8, 134.3, 132.9, 131.4, 128.9, 127.6, 127.2, 126.7, 35.4, 22.6, 13.8$ ppm. The spectra are in accordance to the literature.^[9]

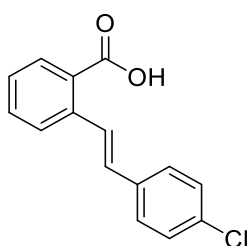
(*E*)-2-(4-Methylstyryl)benzoic acid 170a:



Synthesized according to the general procedure on a 1.93 mmol scale; **170a** (0.463 g, 99% yield) was obtained as a colourless solid.

^1H NMR (400 MHz, CDCl_3): δ = 10.38 (bs, 1H, COOH), 8.06 (d, J = 7.9 Hz, 1H, ArH), 8.01 (d, J = 16.2 Hz, 1H, ArCH=CH), 7.75 (d, J = 8.0 Hz, 1H, ArH), 7.56 (t, J = 7.3 Hz, 1H, ArH), 7.46 (d, J = 7.9 Hz, 2H, ArH), 7.35 (t, J = 7.6 Hz, 1H, ArH), 7.18 (d, J = 7.7 Hz, 2H, ArH), 7.02 (d, J = 16.1 Hz, 1H, ArCH=CH), 2.37 (s, 3H, CH_3) ppm. Spectrum in accordance to literature.^[1]

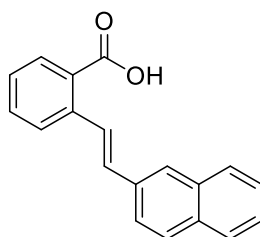
2-(4-Chlorostyryl)benzoic acid **170b**:



Synthesized according to the general procedure III on a 2.06 mmol scale; **170b** (0.513 g, 97% yield) was obtained as a colourless solid.

^1H NMR (400 MHz, CDCl_3): δ = 8.10 (d, J = 7.8 Hz, 1H, ArH), 8.04 (d, J = 16.3 Hz, 1H, ArCH=CH), 7.73 (d, J = 7.8 Hz, 1H, ArH), 7.59 (t, J = 7.6 Hz, 1H, ArH), 7.48 (d, J = 8.1 Hz, 2H, ArH), 7.39 (t, J = 7.5 Hz, 1H, ArH), 7.34 (d, J = 8.0 Hz, 2H, ArH), 6.97 (d, J = 16.2 Hz, 1H, ArCH=CH) ppm. Spectrum in accordance to literature.^[7]

(*E*)-2-(2-(Naphthalen-2-yl)vinyl)benzoic acid **170c**:

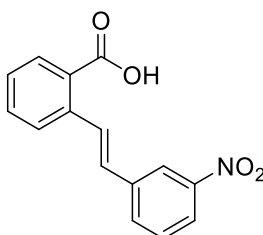


Synthesized according to the general procedure III on a 1.08 mmol scale; **170c** (0.165 g, 56% yield) was obtained as a colourless solid.

^1H NMR (500 MHz, DMSO-d_6): δ = 8.07 (d, J = 16.3 Hz, 1H, ArCH=CH), 8.00 (s, 1H, ArH), 7.96 – 7.86 (m, 5H, ArH), 7.78 (dd, J = 8.6, 1.5 Hz, 1H, ArH), 7.60 (td, J = 10.5, 5.3 Hz, 1H, ArH), 7.55 – 7.47 (m, 2H, ArH), 7.44 – 7.38 (m, 1H, ArH), 7.34 (d, J = 16.3 Hz, 1H, ArCH=CH), 3.67 (bs, 1H, OH) ppm. ^{13}C NMR (126 MHz, DMSO-d_6): δ = 168.7,

137.9, 134.8, 133.3, 132.7, 132.0, 130.7, 130.4, 129.8, 128.4, 128.0, 127.7, 127.6, 127.5, 126.7, 126.7, 126.6, 126.2, 123.6 ppm. HRMS (ASAP) $[M+H]^+$ calc. 275.1072, found 275.1073 $[C_{19}H_{15}O_2]^+$. IR (neat): 3402, 3051, 2808, 1672, 1300, 1285, 1273, 1248, 962, 822, 741, 662, 478, 472, 415 cm^{-1} . M.p. = 170 – 172 °C.^[7]

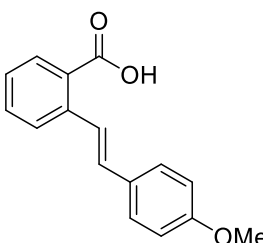
(E)-2-(3-Nitrostyryl)benzoic acid 170d:



Synthesized according to the general procedure III on a 2.61 mmol scale; **170d** (0.542 g, 95% yield) was obtained as a yellow solid.

1H NMR (500 MHz, DMSO- d_6): δ = 13.12 (bs, 1H, COOH), 8.37 (t, J = 1.7 Hz, 1H, ArH), 8.14 (dd, J = 7.9, 1.9 Hz, 1H, ArH), 8.08 (d, J = 16.4 Hz, 1H, ArCH=CH), 8.02 (d, J = 7.8 Hz, 1H, ArH), 7.92 – 7.83 (m, 2H, ArH), 7.69 (t, J = 8.0 Hz, 1H, ArH), 7.64 – 7.58 (m, 1H, ArH), 7.46 – 7.41 (m, 1H, ArH), 7.32 (d, J = 16.4 Hz, 1H, ArCH=CH) ppm. ^{13}C NMR (126 MHz, DMSO- d_6): δ = 168.5, 148.3, 139.1, 137.3, 132.6, 132.0, 130.4, 130.3, 130.2, 130.1, 128.3, 128.1, 127.0, 122.3, 120.9 ppm. IR (neat): 3063, 2872, 2920, 1684, 1522, 1304, 1269, 1248, 959, 756, 733, 663 cm^{-1} . HRMS (NSI) $[M-H]^-$ calc. 268.0615, found 268.0616 $[C_{15}H_{10}NO_4]^-$. m.p. = 204 – 206 °C.

(E)-2-(4-Methoxystyryl)benzoic acid 170e:

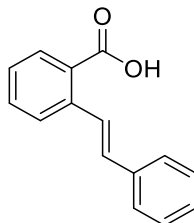


Synthesized according to the general procedure III on a 2.61 mmol scale; **170e** (0.623 g, 94% yield) was obtained as a colourless solid.

1H NMR (400 MHz, DMSO): δ = 13.03 (bs, 1H, COOH), 7.87 – 7.81 (m, 2H, ArH), 7.78 (d, J = 15.7 Hz, 1H, ArCH=CH), 7.55 (td, J = 7.8, 1.4 Hz, 1H, ArH), 7.52 – 7.47 (m, 2H,

ArH), 7.35 (td, $J = 7.6, 1.1$ Hz, 1H, ArH), 7.13 (d, $J = 16.3$ Hz, 1H, ArCH=CH), 7.04 – 6.93 (m, 2H, ArH), 3.78 (s, 3H, OCH₃) ppm. Spectrum in accordance to literature.^[7]

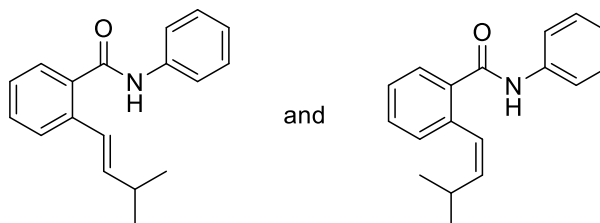
(E)-2-Styrylbenzoic acid 170f:



Synthesized according to the general procedure III on a 1.58 mmol scale; **170f** (0.335 g, 94% yield) was obtained as a pale yellow solid.

¹H NMR (400 MHz, CDCl₃): $\delta = 8.09$ (dd, $J = 7.7, 1.4$ Hz, 1H, ArH), 8.06 (d, $J = 16.1$ Hz, 1H, ArCH=CH), 7.75 (d, $J = 7.9$ Hz, 1H, ArH), 7.58 – 7.53 (m, 3H, ArH), 7.40 – 7.33 (m, 3H, ArH), 7.32 – 7.26 (m, 1H, ArH), 7.03 (d, $J = 16.2$ Hz, 1H, ArCH=CH) ppm. m.p. = 148 - 149 °C (Lit. = 150 - 152 °C). Data in accordance with literature.^[1]

2-(3-Methylbut-1-en-1-yl)-N-phenylbenzamide 164b:



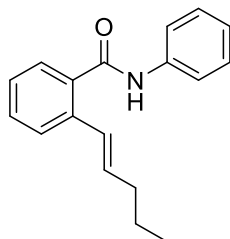
General procedure IV:^[10] (*E/Z*)-2-(3-Methylbut-1-en-1-yl) benzoic acid **163b** (0.317 g, 1.67 mmol) was dissolved in dry dichloromethane (8.5 mL) under argon atmosphere, and dimethylformamide (5 μ L, 0.0167 mmol) was added. The solution was cooled down to 0 °C and thionyl chloride (0.6 mL, 8.36 mmol) was added dropwise. The solution was heated under reflux for 3 h, then solvent and unreacted thionyl chloride were evaporated under reduced pressure. The yellow oil formed was dissolved in dry dichloromethane (8.5 mL), the solution was cooled down to 0 °C, and aniline **168f** (0.19 mL, 2.01 mmol) was added dropwise. After 5 min, trimethylamine (0.695 mL, 5.01 mmol) was added dropwise and the solution was allowed to warm up to room temperature and stirred overnight. The solution quenched with 1 M HCl, the product was extracted with dichloromethane (3 x 20 mL), washed with brine and dried over anhydrous magnesium sulfate. The solvent was evaporated *in vacuo* and the product was purified by column chromatography

(*n*-hexane:ethyl acetate, 9:1), giving the amide **164b** (0.383 g, 86% yield) as a colourless solid.

E-isomer: ^1H NMR (400 MHz, CDCl_3): $\delta = 7.61$ (d, $J = 7.8$ Hz, 3H, ArH), 7.52 (d, $J = 7.8$ Hz, 1H, ArH), 7.49 (s, 1H, NH), 7.45 – 7.34 (m, 3H, ArH), 7.31 (t, $J = 7.4$ Hz, 1H, ArH), 7.16 (t, $J = 7.4$ Hz, 1H, ArH), 6.72 (d, $J = 15.8$ Hz, 1H, ArCH=CH), 6.20 (dd, $J = 15.8, 7.0$ Hz, 1H, CH=CHCH), 2.55 – 2.43 (dhep, $J = 6.8, 6.7$ Hz, 1H, CHCH(CH₃)₂), 1.08 (d, $J = 6.7$ Hz, 6H, CHCH(CH₃)₂) ppm. ^{13}C NMR (126 MHz, CDCl_3): $\delta = 167.6, 142.3, 138.1, 136.2, 134.9, 130.8, 129.3, 128.1, 127.3, 127.1, 124.7, 124.5, 119.7, 31.9, 22.6$ ppm. M.p. = 132 – 133 °C. Spectrum in accordance with literature.^[10]

Z-isomer: ^1H NMR (400 MHz, CDCl_3): $\delta = 7.97$ (bs, 1H, NH), 7.88 (d, $J = 7.7$ Hz, 1H, ArH), 7.60 (d, $J = 7.9$ Hz, 2H, ArH), 7.46 (t, $J = 7.4$ Hz, 1H, ArH), 7.42 – 7.33 (m, 3H, ArH), 7.27 (d, $J = 8.9$ Hz, 1H, ArH), 7.14 (t, $J = 7.4$ Hz, 1H, ArH), 6.60 (d, $J = 11.4$ Hz, 1H, ArCH=CH), 5.74 (dd, $J = 11.2, 10.6$ Hz, 1H, CH=CHCH), 2.73 (dsept, $J = 10.5, 6.6$ Hz, 1H, CHCH(CH₃)₂), 1.05 (d, $J = 6.6$ Hz, 6H, CHCH(CH₃)₂) ppm. ^{13}C NMR (126 MHz, CDCl_3): $\delta = 167.6, 142.3, 138.1, 136.3, 134.9, 130.7, 129.3, 128.1, 127.3, 127.1, 124.7, 124.6, 119.8, 31.9, 22.6$ ppm. HRMS (NSI) $[\text{M}+\text{H}]^+$ calc. 266.1539, found 266.1541 $[\text{C}_{18}\text{H}_{20}\text{NO}]^+$. IR (neat): 3238, 2957, 2864, 1649, 1597, 1535, 1489, 1439, 1325, 1264, 961, 756, 746 cm^{-1} .

(*E*)-2-(Pent-1-en-1-yl)-*N*-phenylbenzamide **164a**:

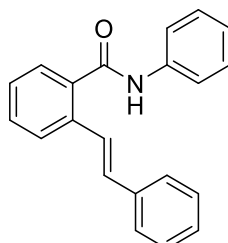


Synthesized according to the general procedure IV on a 0.85 mmol scale; **164a** (0.112 g, 50% yield) was obtained as a colourless solid.

^1H NMR (300 MHz, CDCl_3): $\delta = 7.70 - 7.28$ (m, 9H, NH, ArH), 7.16 (t, $J = 7.3$ Hz, 1H, ArH), 6.76 (d, $J = 15.5$ Hz, 1H, CH=CHCH₂), 6.25 (dt, $J = 15.1, 6.9$ Hz, 1H, CH=CHCH₂), 2.21 (dd, $J = 7.4, 7.0$ Hz, 2H, CH=CHCH₂), 1.54 – 1.40 (m, 2H, CH₂CH₂CH₃), 0.94 (t, $J = 7.3$ Hz, 3H, CH₂CH₃) ppm. ^{13}C NMR (126 MHz, CDCl_3): $\delta = 167.7, 138.1, 136.3, 135.3, 134.9, 130.7, 129.3, 128.0, 127.4, 127.2, 127.0, 124.7, 119.8,$

35.4, 22.6, 13.9 ppm. m.p. = 101 – 101 °C. HRMS (NSI) $[M+H]^+$ calc. 266.1539, found 266.1541 $[C_{18}H_{20}NO]^+$. IR (neat): 3235, 2957, 2924, 1647, 1597, 1535, 1491, 1439, 1325, 961, 692, 679, 588 cm^{-1} .

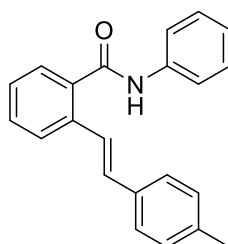
(E)-N-Phenyl-2-styrylbenzamide 170a:



Synthesized according to the general procedure IV on a 1.00 mmol scale; **170a** (0.267 g, 89% yield) was obtained as a colourless solid.

1H NMR (400 MHz, $CDCl_3$): 1H NMR (400 MHz, $CDCl_3$): δ = 7.74 (d, J = 7.8 Hz, 1H, ArH), 7.68 – 7.58 (m, 3H), 7.53 – 7.47 (m, 4H), 7.41 – 7.30 (m, 5H), 7.30 – 7.24 (m, 2H), 7.19 – 7.15 (m, 1H), 7.12 (d, J = 16.3 Hz, 1H, C(O)ArCH=CHAr) ppm. ^{13}C NMR (126 MHz, $CDCl_3$): δ = 167.6, 138.0, 136.9, 135.9, 135.5, 132.1, 130.8, 129.3, 128.9, 128.2, 128.0, 127.8, 127.0, 126.7, 125.7, 124.8, 120.1 ppm. m.p. = 167 – 170 °C (Lit. = 171 - 172 °C)^[11]. HRMS (NSI) $[M+H]^+$ calc. 300.1383, found 300.1385 $[C_{21}H_{18}NO]^+$. IR (neat): 3319, 3053, 3021, 1647, 1593, 1516, 1495, 1433, 1317, 1251, 953, 750, 687, 500 cm^{-1} .

(E)-2-(4-Methylstyryl)-N-phenylbenzamide 170b:

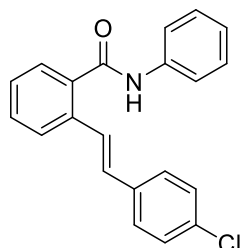


Synthesized according to the general procedure IV on a 1.93 mmol scale; **170b** (0.502 g, 83% yield) was obtained as a colourless solid.

1H NMR (400 MHz, $CDCl_3$): δ = 7.73 (d, J = 7.8 Hz, 1H, ArH), 7.65 – 7.57 (m, 3H, ArH), 7.53 (s, 1H, NH), 7.51 – 7.45 (m, 2H, ArH), 7.42 – 7.32 (m, 5H, ArH), 7.19 – 7.13 (m, 3H, ArH), 7.09 (d, J = 16.3 Hz, 1H, ArCH=CHArMe), 2.35 (s, 3H, CH_3) ppm. ^{13}C NMR (126 MHz, $CDCl_3$): δ = 167.6, 138.3, 138.0, 136.0, 135.4, 134.2, 132.2, 130.8, 129.6,

129.3, 128.0, 127.6, 126.9, 126.6, 124.8, 124.6, 120.1, 21.4 ppm. HRMS (NSI) $[M+H]^+$ calc. 314.1539, found 314.1542 $[C_{22}H_{20}NO]^+$. IR (neat): 3310, 3059, 3038, 3015, 1651, 1597, 1520, 1514, 1437, 1319, 953, 802, 750, 743, 691, 532 cm^{-1} . m.p. = 168 – 171 °C.

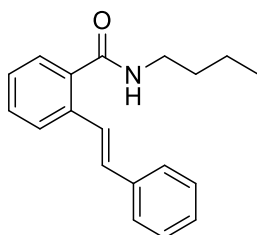
(E)-2-(4-Chlorostyryl)-N-phenylbenzamide 170c:



Synthesized according to the general procedure IV on a 2.06 mmol scale; **170c** (0.547 g, 80% yield) was obtained as a colourless solid.

1H NMR (400 MHz, $CDCl_3$): δ = 7.74 (d, J = 7.9 Hz, 1H, ArH), 7.65 – 7.58 (m, 3H, ArH), 7.57 – 7.47 (m, 3H, ArH), 7.44 – 7.34 (m, 5H, ArH), 7.30 (d, J = 7.7 Hz, 2H, ArH), 7.17 (t, J = 7.5 Hz, 1H, ArH), 7.06 (d, J = 16.2 Hz, 1H, ArCH=CHArCl) ppm. ^{13}C NMR (126 MHz, $CDCl_3$): δ = 167.4, 137.8, 135.6, 135.4, 135.4, 133.7, 130.8, 130.5, 129.2, 128.9, 128.0, 127.8, 127.7, 126.5, 126.2, 124.8, 119.9 ppm. HRMS (NSI) $[M+H]^+$ calc. 334.0993, found 334.0995 $[C_{21}H_{17}ClNO]^+$. IR (neat): 3308, 3055, 3042, 3019, 1651, 1597, 1520, 1491, 1437, 1319, 1252, 953, 810, 752, 743, 691, 528 cm^{-1} . m.p. = 170 – 172 °C.

(E)-N-Butyl-2-styrylbenzamide 170d:

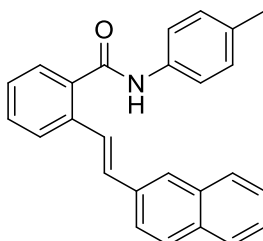


Synthesized according to the general procedure IV on a 2.00 mmol scale; **170d** (0.554 g, 99% yield) was obtained as a colourless solid.

1H NMR (400 MHz, $CDCl_3$): δ = 7.69 (d, J = 7.9 Hz, 1H, ArH), 7.53 – 7.39 (m, 5H, ArH), 7.39 – 7.33 (m, 2H, ArH), 7.32 – 7.27 (m, 2H, ArH), 7.06 (d, J = 16.3 Hz, 1H, C(O)ArCH=CH), 5.79 (s, J = 10.7 Hz, 1H, NH), 3.47 (dt, J = 7.1, 5.9 Hz, 2H, HNCH₂CH₂), 1.63 – 1.52 (m, 2H, HNCH₂CH₂), 1.44 – 1.33 (m, 2H, CH₂CH₃), 0.91 (t, J

= 7.3 Hz, 3H, CH₂CH₃) ppm. ¹³C NMR (126 MHz, CDCl₃): δ = 169.6, 137.1, 136.1, 135.4, 131.4, 130.2, 128.8, 128.1, 127.8, 127.6, 126.9, 126.3, 126.1, 39.9, 31.9, 20.3, 13.9 ppm. HRMS (NSI) [M+H]⁺ calc. 280.1696, found 280.1694 [C₁₉H₂₂NO]⁺. IR (neat): 3265, 2953, 2926, 2864, 1626, 1547, 1493, 1447, 1429, 1310, 966, 762, 689, 528 cm⁻¹. m.p. = 160 – 162 °C.

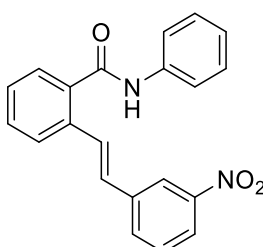
(*E*)-2-(2-(Naphthalen-2-yl)vinyl)-*N*-(*p*-tolyl)benzamide 170e:



Synthesized according to the general procedure IV on a 0.5 mmol scale; **170e** (0.149 g, 83% yield) was obtained as a colourless solid.

¹H NMR (500 MHz, CDCl₃): δ = 7.85 (s, 1H), 7.83 – 7.76 (m, 4H), 7.72 – 7.62 (m, 3H), 7.55 – 7.48 (m, 4H), 7.48 – 7.42 (m, 2H), 7.37 (t, *J* = 7.4 Hz, 1H), 7.27 (d, *J* = 16.0 Hz, 1H, ArCH=CH), 7.17 (d, *J* = 8.2 Hz, 2H), 2.34 (s, 3H, ArCH₃) ppm. ¹³C NMR (126 MHz, CDCl₃): δ = 167.5, 136.0, 135.7, 135.5, 134.6, 133.7, 133.4, 132.2, 130.8, 129.8, 128.6, 128.3, 128.1, 127.9, 127.8, 127.3, 126.7, 126.5, 126.3, 126.1, 123.8, 120.2, 21.1 ppm. HRMS (ASAP) [M+H]⁺ calc. 364.1701, found 364.1695 [C₂₆H₂₂NO]⁺. IR (neat): 3285, 3030, 2970, 2945, 1738, 1638, 1605, 1539, 1510, 1325, 1217, 814, 746, 731, 509, 477 cm⁻¹. m.p. = 160 – 162 °C.

(*E*)-2-(3-Nitrostyryl)-*N*-phenylbenzamide 170f:

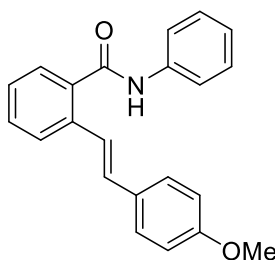


Synthesized according to the general procedure IV on a 1.0 mmol scale; **170f** (0.314 g, 92% yield) was obtained as a yellow solid.

¹H NMR (500 MHz, CDCl₃): δ = 8.28 (s, 1H, ArH), 8.10 (d, *J* = 8.2 Hz, 1H, ArH), 7.83 (d, *J* = 7.8 Hz, 1H, ArH), 7.76 (d, *J* = 7.9 Hz, 1H, ArH), 7.69 (d, *J* = 16.2 Hz, 1H,

ArCH=CH), 7.65 – 7.45 (m, 6H, ArH), 7.45 – 7.34 (m, 3H, ArH), 7.18 (t, $J = 7.4$ Hz, 1H, ArH), 7.12 (d, $J = 16.2$ Hz, 1H, ArCH=CH) ppm. ^{13}C NMR (126 MHz, CDCl_3): $\delta = 167.3, 148.8, 138.9, 137.9, 135.9, 135.4, 132.2, 131.0, 129.7, 129.4, 129.1, 128.6, 127.7, 127.0, 125.0, 122.6, 122.0, 120.1$ ppm. HRMS (NSI) $[\text{M}+\text{H}]^+$ calc. 345.1234, found 345.1237 $[\text{C}_{21}\text{H}_{17}\text{N}_2\text{O}_3]^+$. IR (neat): 3306, 2980, 2884, 1645, 1597, 1518, 1437, 1358, 1321, 1254, 957, 748, 687, 669, 507 cm^{-1} . m.p. = 180 – 182 $^\circ\text{C}$.

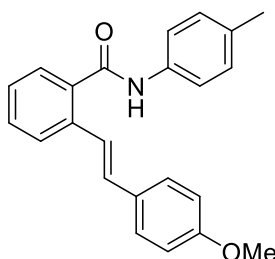
(E)-2-(4-Methoxystyryl)-N-phenylbenzamide 170g:



Synthesized according to the general procedure IV on a 1.2 mmol scale; **170g** (0.160 g, 40% yield) was obtained as a colourless solid.

^1H NMR (500 MHz, CDCl_3): $\delta = 7.71$ (d, $J = 7.9$ Hz, 1H, ArH), 7.61 (t, $J = 7.0$ Hz, 3H, ArH), 7.56 (s, 1H, NH), 7.50 – 7.42 (m, 3H, ArH), 7.39 (d, $J = 15.9$ Hz, 1H, ArCH=CH), 7.37 – 7.31 (m, 3H, ArH), 7.16 (t, $J = 7.4$ Hz, 1H, ArH), 7.06 (d, $J = 16.2$ Hz, 1H, ArCH=CH), 6.89 – 6.85 (m, 2H, ArH), 3.82 (s, 2H, OCH₃) ppm. ^{13}C NMR (126 MHz, CDCl_3): $\delta = 167.7, 159.8, 138.1, 136.2, 135.3, 131.9, 130.8, 129.8, 129.3, 128.3, 128.1, 127.4, 126.5, 124.8, 123.5, 120.1, 114.3, 55.5$ ppm. HRMS (NSI) $[\text{M}+\text{H}]^+$ calc. 330.1489, found 330.1491 $[\text{C}_{22}\text{H}_{20}\text{NO}_2]^+$. IR (neat): 3291, 2961, 2911, 2835, 1647, 1595, 1508, 1312, 1244, 1173, 1034, 812, 662, 540 cm^{-1} . m.p. = 139 – 141 $^\circ\text{C}$.

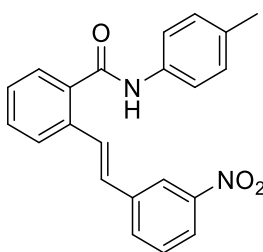
(E)-2-(4-Methoxystyryl)-N-(p-tolyl)benzamide S170h:



Synthesized according to the general procedure IV on a 1.2 mmol scale; **170h** (0.165 g, 40% yield) was obtained as a colourless solid.

^1H NMR (500 MHz, CDCl_3): $\delta = 7.70$ (d, $J = 7.9$ Hz, 1H, ArH), 7.60 (d, $J = 7.5$ Hz, 1H, ArH), 7.54 (s, 1H, NH), 7.51 – 7.41 (m, 5H, ArH), 7.38 (d, $J = 16.2$ Hz, 1H, ArCH=CH), 7.32 (t, $J = 7.4$ Hz, 1H, ArH), 7.16 (d, $J = 8.2$ Hz, 2H, ArH), 7.05 (d, $J = 16.2$ Hz, 1H, ArCH=CH), 6.89 – 6.84 (m, 2H, ArH), 3.82 (s, 3H, OCH_3), 2.34 (s, 3H, ArCH_3) ppm. ^{13}C NMR (126 MHz, CDCl_3): $\delta = 167.6, 159.8, 136.1, 135.5, 135.5, 134.4, 131.7, 130.7, 129.8, 129.7, 128.2, 128.0, 127.4, 126.4, 123.6, 120.1, 114.3, 55.5, 21.1$ ppm. HRMS (NSI) $[\text{M}+\text{H}]^+$ calc. 344.1645, found 344.1648 $[\text{C}_{23}\text{H}_{22}\text{NO}_2]^+$. IR (neat): 3298, 2980, 2884, 1647, 1508, 1437, 1250, 1173, 961, 812, 752, 689 cm^{-1} . m.p. = 146 – 148 $^\circ\text{C}$.

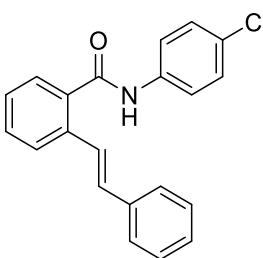
(E)-2-(3-Nitrostyryl)-N-(p-tolyl)benzamide 170i:



Synthesized according to the general procedure IV on a 1.0 mmol scale; **170i** (0.273 g, 76% yield) was obtained as a yellow solid.

^1H NMR (500 MHz, CDCl_3): $\delta = 8.27$ (s, 1H, ArH), 8.09 (dd, $J = 8.2, 1.1$ Hz, 1H, ArH), 7.82 (d, $J = 7.8$ Hz, 1H, ArH), 7.74 (d, $J = 7.8$ Hz, 1H, ArH), 7.68 (d, $J = 16.2$ Hz, 1H, ArCH=CH), 7.61 (d, $J = 7.5$ Hz, 1H, ArH), 7.57 – 7.46 (m, 5H, ArH), 7.40 (t, $J = 7.5$ Hz, 1H, ArH), 7.18 (d, $J = 8.1$ Hz, 2H, ArH), 7.11 (d, $J = 16.2$ Hz, 1H, ArCH=CH), 2.34 (s, 1H, ArCH_3) ppm. ^{13}C NMR (126 MHz, CDCl_3): $\delta = 167.2, 148.8, 139.0, 136.0, 135.3, 134.8, 132.2, 130.9, 129.8, 129.7, 129.2, 129.2, 128.5, 127.7, 126.9, 122.6, 122.0, 120.2, 21.1$ ppm. HRMS (NSI) $[\text{M}+\text{H}]^+$ calc. 359.1390, found 359.1393 $[\text{C}_{22}\text{H}_{19}\text{N}_2\text{O}_3]^+$. IR (neat): 3294, 2980, 2884, 1643, 1516, 1362, 1315, 1252, 957, 810, 752, 692, 671, 509 cm^{-1} . m.p. = 182 – 183 $^\circ\text{C}$.

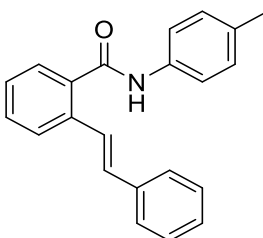
(E)-N-(4-Chlorophenyl)-2-styrylbenzamide 170j:



Synthesized according to the general procedure IV on a 2.00 mmol scale using 4-chloro aniline; **170j** (0.567 g, 85% yield) was obtained as a colourless solid.

^1H NMR (400 MHz, CDCl_3) δ = 7.74 (d, J = 7.7 Hz, 1H, ArH), 7.63 (d, J = 7.7 Hz, 1H, ArH), 7.56 (d, J = 8.8 Hz, 2H, ArH), 7.54 – 7.45 (m, 5H), 7.40 – 7.26 (m, 6H), 7.11 (d, J = 16.2 Hz, 1H, C(O)ArCH=CH) ppm. ^{13}C NMR (126 MHz, CDCl_3): δ = 167.5, 136.9, 136.5, 136.0, 135.1, 132.4, 131.1, 129.3, 129.0, 128.9, 128.4, 128.0, 127.8, 126.9, 126.8, 125.6, 121.3 ppm. HRMS (NSI) $[\text{M}+\text{H}]^+$ calc. 334.0990, found 334.0993 $[\text{C}_{21}\text{H}_{17}\text{ClNO}]^+$. IR (neat): 3262, 3186, 3119, 3059, 3021, 1645, 1541, 1491, 1398, 1323, 953, 826, 756, 689, 515 cm^{-1} . m.p. = 130 – 132 $^\circ\text{C}$.

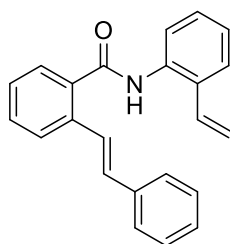
(E)-2-Styryl-N-(p-tolyl)benzamide 170k:



Synthesized according to the general procedure IV on a 2.00 mmol scale using p-toluidine; **170k** (0.540 g, 86% yield) was obtained as a colourless solid.

^1H NMR (400 MHz, CDCl_3): δ = 7.74 (d, J = 7.8 Hz, 1H, ArH), 7.63 (dd, J = 7.7, 1.0 Hz, 1H, ArH), 7.54 (d, J = 16.3 Hz, 1H, C(O)ArCH=CH), 7.51 – 7.43 (m, 6H, ArH), 7.39 – 7.30 (m, 3H, ArH), 7.29 – 7.23 (m, 1H, ArH), 7.17 (d, J = 8.3 Hz, 2H ArH), 7.11 (d, J = 16.3 Hz, 1H, C(O)ArCH=CH), 2.34 (s, 3H, CH_3) ppm. ^{13}C NMR (126 MHz, CDCl_3): δ = 167.5, 137.0, 135.9, 135.7, 135.4, 134.5, 132.1, 130.8, 129.8, 128.9, 128.2, 128.0, 127.8, 127.0, 126.6, 125.8, 120.1, 21.1 ppm. HRMS (NSI) $[\text{M}+\text{H}]^+$ calc. 314.1540, found 314.1539 $[\text{C}_{22}\text{H}_{20}\text{NO}]^+$. IR (neat): 3269, 3217, 3061, 3021, 2916, 1643, 1605, 1541, 1512, 1331, 953, 754, 735, 517 cm^{-1} . m.p. = 148 – 150 $^\circ\text{C}$.

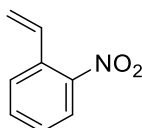
(E)-2-Styryl-N-(2-vinylphenyl)benzamide 170p:



Synthesized according to the general procedure IV on a 0.65 mmol scale using 2-amino styrene **175**; **170p** (0.169 g, 80% yield) was obtained as a colourless solid.

^1H NMR (400 MHz, CDCl_3): δ = 8.13 (d, J = 8.0 Hz, 1H, ArH), 7.77 (d, J = 7.7 Hz, 1H, ArH), 7.60 (d, J = 16.2 Hz, 1H, C(O)ArHCH=CH), 7.56 (s, 1H, NH), 7.56 – 7.48 (m, 3H, ArH), 7.48 – 7.34 (m, 5H, ArH), 7.33 – 7.29 (m, 1H, ArH), 7.15 (d, J = 16.2 Hz, 1H, C(O)ArHCH=CH), 6.75 (dd, J = 17.3, 10.9 Hz, 1H, ArCH=CH₂), 5.59 (dd, J_{trans} = 17.3, 1.2 Hz, 1H, ArCH=CHH), 5.17 (dd, J_{cis} = 11.0, 0.6 Hz, 1H, ArCH=CHH) ppm. ^{13}C NMR (101 MHz, CDCl_3): δ = 167.7, 136.9, 136.0, 135.5, 134.5, 132.5, 132.0, 130.9, 130.5, 128.9, 128.7, 128.3, 128.1, 127.9, 127.1, 127.1, 126.9, 126.0, 125.6, 123.3, 118.6 ppm. HRMS (NSI) $[\text{M}+\text{H}]^+$ calc. 325.4138, found 325.4140 $[\text{C}_{23}\text{H}_{20}\text{NO}]^+$. IR (neat): 3318, 3068, 3059, 3045, 3018, 1648, 1519, 1491, 1435, 1318, 953, 752, 688, 533 cm^{-1} . M.p. = 184 – 186 °C.

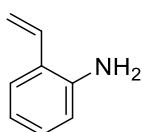
2-Nitrostyrene **174**:



Procedure:^[12] To a solution of methyltriphenylphosphonium bromide (3.3 mmol, 1.179 g) in dry THF (12 mL) was added *n*-BuLi (3.6 mmol, 1.44 mL, 2.5 M in hexanes) dropwise at 0 °C under argon. The reaction mixture was stirred at room temperature for 1 h. Then, 2-nitrobenzaldehyde (454 mg, 3 mmol) was added as a solution in dry THF (2 mL) and the mixture was heated to 65 °C for 5 h. The reaction was cooled down to room temperature, quenched with water (20 mL), extracted with ethyl acetate (3 x 30 mL) and dried over magnesium sulfate. The crude mixture was filtered through a plug of silica to afford the desired product **174** as a yellow oil in 79% yield.

^1H NMR (300 MHz, CDCl_3): δ = 7.94 (d, J = 8.2 Hz, 1H), 7.67 – 7.54 (m, 2H), 7.47 – 7.38 (m, 1H), 7.24 – 7.10 (m, 1H), 5.75 (d, J = 17.3 Hz, 1H), 5.49 (d, J = 10.9 Hz, 1H) ppm. The spectroscopy data are in agreement with literature.^[13]

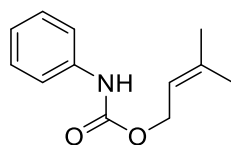
2-Aminostyrene **175**:



Procedure:^[14] To a solution of 2-nitrostyrene **174** (2.37 mmol, 353 mg) in ethanol (8 mL) were added iron powder (14.7 mmol, 821 mg) and 1 M HCl (2.84 mL), and the reaction was heated up under reflux for 3 h. The mixture was cooled down to room temperature and Na₂CO₃ was added until gas evolution ceased. The crude mixture was filtered over celite, and the filtrate was extracted with Et₂O (3 x 20 mL). The combined organic layers were washed with water and brine, dried over MgSO₄ and concentrated *in vacuo*. The product was purified by flash column chromatography (*n*-hexane: ethyl acetate; 7:3) to give compound **175** (0.191 g, 28% yield) as a pale yellow oil.

¹H NMR (400 MHz, CDCl₃): δ = 7.29 (dd, *J* = 7.7, 1.5 Hz, 1H), 7.09 (td, *J* = 7.7, 1.5 Hz, 1H), 6.83 – 6.73 (m, 2H), 6.69 (dd, *J* = 8.0, 1.1 Hz, 1H), 5.63 (dd, *J* = 17.4, 1.5 Hz, 1H), 5.32 (dd, *J* = 11.0, 1.5 Hz, 1H), 3.75 (s, 2H) ppm. The spectroscopy data are in agreement with literature.^[15]

3-Methylbut-2-en-1-yl phenylcarbamate **154**:

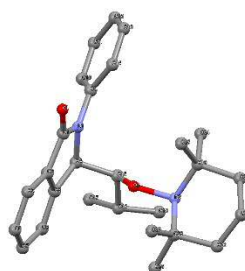
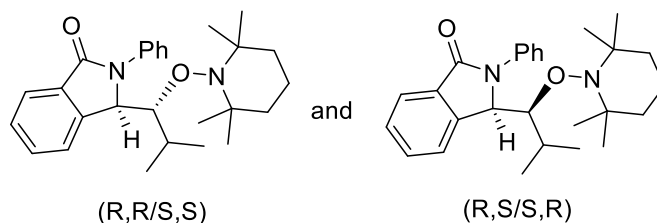


Procedure:^[16] 3-Methyl-2-buten-1-ol (1.02 mL, 10 mmol) was dissolved in dichloromethane (20 mL) and phenylisocyanate (1.09 mL, 10 mmol) was added at room temperature. Triethylamine (2.79 mL, 20 mmol) was added and the solution was stirred at room temperature overnight. The solvent was evaporated and the product was purified by column chromatography (*n*-hexane : ethyl acetate, 9:1), giving 1.815 g of pure product **154** as a colourless solid in 88% yield.

¹H NMR (300 MHz, CDCl₃): δ = 7.48 – 7.22 (m, 4H, *ArH*), 7.13 – 6.96 (m, 1H, *ArH*), 6.60 (brs, 1H, *NH*), 5.44 – 5.35 (m, 1H, OCH₂CH=CH), 4.66 (d, *J* = 7.3 Hz, 2H, OCH₂CH=), 1.78 (s, 3H, CHCH₃), 1.75 (s, 3H, CHCH₃) ppm. m.p. = 63 – 65 °C. The spectroscopy data are in agreement with literature.^[16]

6.3.3. Electrochemical synthesis of isoindolinones

3-(2-Methyl-1-((2,2,6,6-tetramethylpiperidin-1-yl)oxy)propyl)-2-phenylisoindolin-1-one **178l**:



CCDC 1569516

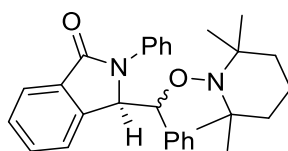
General procedure V: (*E/Z*)-2-(3-Methylbut-1-en-1-yl)-*N*-phenylbenzamide **164b** (0.133 g, 0.5 mmol) was dissolved in a mixture of acetonitrile/water (19:1, 10 mL). TEMPO (0.117 g, 0.75 mmol) and benzyltrimethylammonium hydroxide solution (40% w, 0.105 g, 0.25 mmol) were added to the solution, and the solution pumped through in the electrochemical reactor (0.205 mL inner volume; 24 mA; 3 F/mol, 1–3 V) using a syringe pump (0.1 mL/min). After reaching the steady state, the solution was collected for 90 min. The outlet was quenched with saturated ammonium chloride aqueous solution, extracted with diethyl ether (3 x 10 mL) and washed with brine. The combined organic layers were dried over anhydrous magnesium sulfate, the solvent was evaporated under reduced pressure and the product was purified by column chromatography (hexane/ethyl acetate, 8:2), giving 0.180 g of **178l** as a diastereomeric mixture (3.3:1 d.r.) in 95% yield. The major diastereomer ((*R,S*)/(*S,R*) isomer) is a colourless solid and the minor diastereomer ((*R,R*)/(*S,S*) isomer) is a colourless oil.

Major product: (*R,S*)/(*S,R*)-isomer: ^1H NMR (300 MHz, CDCl_3): δ = 7.95 (d, J = 7.4 Hz, 1H, ArH), 7.82 – 7.73 (m, 3H, ArH), 7.61 (td, J = 7.5, 1.2 Hz, 1H, ArH), 7.56 – 7.41 (m, 3H, ArH), 7.23 (t, J = 7.4 Hz, 1H, ArH), 6.06 (s, 1H, NCHCH-O), 4.09 (dd, J = 8.8, 1.9 Hz, 1H, NCHCH-O), 1.72 – 1.51 (m, 6H, NCCH₂CH₂CH₂CN) 1.42 (s, 3H, N-CCH₃),

1.39 – 1.33 (m, 1H, CHCH(CH₃)₂), 1.28 (s, 3H, N-CCH₃), 1.25 (s, 3H, N-CCH₃), 0.97 (s, 3H, N-CCH₃), 0.93 (d, *J* = 6.9 Hz, 3H, CHCH(CH₃)₂), 0.38 (d, *J* = 6.7 Hz, 3H, CHCH(CH₃)₂) ppm. ¹³C NMR (126 MHz, CDCl₃): δ = 167.3, 143.0, 137.2, 133.5, 131.4, 129.0, 128.3, 125.4, 124.7, 124.4, 124.1, 83.2, 76.9, 62.1, 60.6, 60.1, 41.7, 35.6, 30.2, 21.3, 21.0, 20.9, 19.3, 17.1 ppm. m.p. = 157 – 158 °C. HRMS (NSI) [M+H]⁺ calc. 421.2850, found 421.2850 [C₂₇H₃₇N₂O₂]⁺. IR (neat): 2959, 2932, 2874, 1701, 1597, 1501, 1385, 756, 702 cm⁻¹.

Minor product: (*R,R*)/(*S,S*)-isomer: ¹H NMR (400 MHz, CDCl₃) δ = 7.94 (d, *J* = 7.5 Hz, 1H, ArH), 7.67 (d, *J* = 7.7 Hz, 2H, ArH), 7.60 – 7.53 (m, 2H, ArH), 7.49 – 7.39 (m, 3H, ArH), 7.20 (t, *J* = 7.4 Hz, 1H, ArH), 5.55 (s, 1H, NCHCH-O), 4.11 (d, *J* = 7.2 Hz, 1H, NCHCH-O), 2.55 – 2.42 (m, 1H, CHCH(CH₃)₂), 1.32 – 1.11 (m, 12H, CH(CH₃)₂, NCCH₂CH₂CH₂CN), 0.81 (s, 6H, N-CCH₃), 0.68 (s, *J* = 6.9 Hz, 3H, N-CCH₃), 0.40 (s, *J* = 6.0 Hz, 3H, N-CCH₃) ppm. HRMS (NSI) [M+H]⁺ calc. 421.2850, found 421.2840 [C₂₇H₃₇N₂O₂]⁺. IR (neat): 3009, 2967, 2926, 2870, 1736, 1695, 1682, 1373, 1634, 1217, 752, 700 cm⁻¹. m.p. = 131 – 133 °C.

2-Phenyl-3-(phenyl((2,2,6,6-tetramethylpiperidin-1-yl)oxy)methyl)isoindolin-1-one
178a:



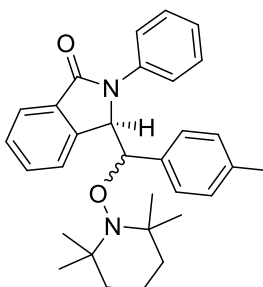
Synthesized according to the general procedure V on a 0.50 mmol scale; **178a** (0.163 g, 72% yield, d.r.: 1.47:1) was obtained as a colourless solid.

Minor product: (*R,R*)/(*S,S*)-isomer: colourless solid. ¹H NMR (400 MHz, CDCl₃): δ = 7.70 (d, *J* = 7.7 Hz, 2H, ArH), 7.67 – 7.56 (m, 3H, ArH), 7.50 – 7.37 (m, 3H, ArH), 7.25 – 7.22 (m, 1H, ArH), 7.08 – 7.02 (m, 1H, ArH), 6.98 (t, *J* = 7.1 Hz, 2H, ArH), 6.70 – 6.62 (m, 2H, ArH), 6.16 (s, 1H, NCHCH-O), 5.36 (s, 1H, ArCH-O), 1.69 – 1.59 (m, 2H, NCCH₂CH₂CH₂N), 1.52 (s, 3H, NCCH₃), 1.27 (m, 4H, NCCH₂CH₂CH₂N), 1.16 (s, 3H, NCCH₃), 0.73 (s, 3H, NCCH₃), 0.31 (s, 3H, NCCH₃) ppm. ¹³C NMR (126 MHz, CDCl₃): δ = 167.9, 142.5, 138.6, 136.6, 132.5, 131.9, 128.7, 128.4, 128.4, 127.6, 127.1, 125.4, 124.6, 124.2, 122.9, 92.8, 65.6, 40.8, 35.2, 34.5, 20.8, 20.3, 17.1, 14.4, 13.9 ppm. m.p. =

164 – 167 °C. HRMS (ASAP) $[M+H]^+$ calc. 455.2699, found 455.2708 $[C_{30}H_{35}N_2O_2]^+$. IR (neat): 2947, 2922, 1682, 1499, 1383, 1298, 754, 714, 692, 633 cm^{-1} .

Major product: (*R,S*)/(*S,R*)-isomer: colourless solid. 1H NMR (400 MHz, $CDCl_3$): δ = 8.07 (d, J = 7.4 Hz, 1H, ArH), 7.69 – 7.56 (m, 4H, ArH), 7.54 – 7.42 (m, 3H, ArH), 7.29 – 7.23 (m, 1H, ArH), 7.02 (t, J = 7.2 Hz, 1H, ArH), 6.90 (t, J = 7.4 Hz, 2H), 6.46 (d, J = 7.4 Hz, 2H, ArH), 6.09 (d, J = 3.9 Hz, 1H, NCHCH-O), 5.19 (d, J = 3.5 Hz, 1H, ArCH-O), 1.64 (s, 3H, $NCCH_3$), 1.45 (s, 3H, $NCCH_3$), 1.41 – 1.28 (m, 4H, $NCCH_2CH_2CH_2N$), 1.07 (s, 3H, $NCCH_3$), 0.96 – 0.76 (m, 2H, $NCCH_2CH_2CH_2N$), 0.42 (s, 3H, $NCCH_3$) ppm. ^{13}C NMR (126 MHz, $CDCl_3$) δ = 167.2, 142.2, 137.4, 136.6, 133.5, 131.6, 129.2, 128.6, 127.9, 127.7, 127.0, 125.3, 124.7, 123.9, 123.0, 86.6, 61.9, 60.3, 60.3, 40.7, 35.1, 34.2, 21.0, 20.6, 17.2, ppm. m.p. = 160 – 163 °C. HRMS (ASAP) $[M+H]^+$ calc. 455.2699, found 455.2704 $[C_{30}H_{35}N_2O_2]^+$. IR (neat): 2961, 2943, 2928, 2870, 1686, 1456, 1381, 1042, 752, 712, 692, 584 cm^{-1} .

2-Phenyl-3-(((2,2,6,6-tetramethylpiperidin-1-yl)oxy)(*p*-tolyl)methyl)isoindolin-1-one **178b:**



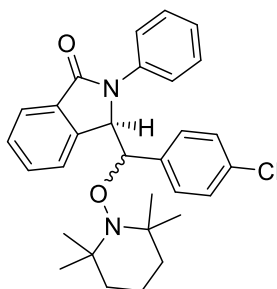
Synthesized according to the general procedure V on a 0.47 mmol scale; **178b** (0.136 g, 62% yield, d.r. 1.15:1).

Minor product: (*R,R*)/(*S,S*)-isomer: pale yellow solid, 23% yield. 1H NMR (400 MHz, $CDCl_3$): δ = 8.07 (d, J = 7.8 Hz, 1H, ArH), 7.68 (d, J = 7.4 Hz, 1H, ArH), 7.63 (t, J = 7.4 Hz, 1H, ArH), 7.57 (d, J = 7.9 Hz, 2H, ArH), 7.52 – 7.42 (m, 3H, ArH), 7.25 (m, 1H, ArH), 6.69 (d, J = 7.7 Hz, 2H, ArH), 6.31 (d, J = 7.9 Hz, 2H, ArH), 6.06 (d, J = 4.4 Hz, 1H, NCHCH-O), 5.13 (d, J = 4.2 Hz, 1H, NCHCH-O), 2.14 (s, 3H, ArCH₃), 1.76 – 1.56 (m, 6H, $NCCH_2CH_2CH_2CN$), 1.44 (s, 3H, $NCCH_3$), 1.36 (s, 3H, $NCCH_3$), 1.06 (s, 3H, $NCCH_3$), 0.43 (s, 3H, $NCCH_3$) ppm. ^{13}C NMR (126 MHz, $CDCl_3$): δ = 167.2, 142.3, 137.4, 137.2, 133.6, 133.5, 131.6, 129.2, 128.6, 127.8, 127.8, 125.2, 124.7, 123.9, 123.1, 86.6, 62.0, 60.2, 60.2, 40.7, 35.1, 34.3, 21.2, 21.0, 20.6, 17.2 ppm. HRMS (NSI) $[M+H]^+$

calc. 469.2850, found 469.2844 [C₃₁H₃₇N₂O₂]⁺. IR (neat): 3005, 2968, 2959, 2930, 1693, 1379, 1362, 1217, 1042, 820, 746, 696, 536 cm⁻¹. m.p. = 154 – 156 °C.

Major product: (*R,S*)/(*S,R*)-isomer: colourless solid, 39% yield. ¹H NMR (400 MHz, CDCl₃): δ = 7.70 (d, *J* = 8.6, Hz, 2H, Ar*H*), 7.66 – 7.58 (m, 3H, Ar*H*), 7.47 – 7.38 (m, 3H, Ar*H*), 7.26 – 7.22 (m, 1H, Ar*H*), 6.77 (d, *J* = 8.0 Hz, 2H, Ar*H*), 6.53 (d, *J* = 7.2 Hz, 2H, Ar*H*), 6.14 (d, *J* = 1.2 Hz, 1H, NCHCH-O), 5.32 (d, *J* = 1.6 Hz, 1H, NCHCH-O), 2.17 (s, 3H, ArCH₃), 1.65 – 1.43 (m, *J* = 30.4 Hz, 6H, NCCH₂CH₂CH₂CN), 1.28 (s, 3H, NCCH₃), 1.15 (s, 3H, NCCH₃), 0.73 (s, 3H, NCCH₃), 0.33 (s, 3H, NCCH₃) ppm. ¹³C NMR (126 MHz, CDCl₃): δ = 167.9, 142.6, 138.6, 137.0, 133.5, 132.4, 131.8, 128.5, 128.3, 128.2, 127.7, 125.2, 124.6, 124.1, 122.8, 92.6, 65.7, 60.5, 59.6, 40.7, 35.1, 34.5, 21.2, 20.7, 20.2, 17.0 ppm. HRMS (NSI) [M+H]⁺ calc. 469.2850, found 469.2839 [C₃₁H₃₇N₂O₂]⁺. IR (neat): 3022, 3007, 2994, 2972, 2936, 1738, 1369, 1217, 1207, 752, 687, 540, 519 cm⁻¹. m.p. = 190 – 193 °C.

3-((4-Chlorophenyl)((2,2,6,6-tetramethylpiperidin-1-yl)oxy)methyl)-2-phenylisoindolin-1-one **178c:**



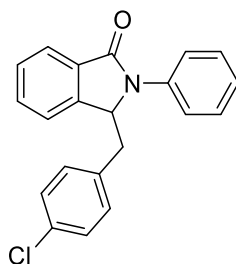
Synthesized according to the general procedure V on a 0.47 mmol scale; **178c** (0.117 g, 56% yield, d.r.: 1.75:1).

Major product: (*R,S*)/(*S,R*)-isomer: colourless solid, 33% yield. ¹H NMR (400 MHz, CDCl₃): δ = 7.72 – 7.65 (m, 3H, Ar*H*), 7.64 – 7.59 (m, 2H, Ar*H*), 7.49 – 7.40 (m, 3H, Ar*H*), 7.28 – 7.21 (m, 1H, Ar*H*), 6.96 (d, *J* = 7.9 Hz, 2H, Ar*H*), 6.58 (d, *J* = 6.8 Hz, 2H, Ar*H*), 6.16 (s, 1H, NCHCH-O), 5.35 (s, 1H, NCHCH-O), 1.70 – 1.41 (m, 6H, NCCH₂CH₂CH₂CN), 1.27 (bs, 3H, NCCH₃), 1.17 (bs, 3H, NCCH₃), 0.73 (bs, 3H, NCCH₃), 0.32 (bs, 3H, NCCH₃) ppm. ¹³C NMR (126 MHz, CDCl₃): δ = 167.8, 142.2, 138.5, 135.2, 133.4, 132.4, 132.1, 129.7, 128.9, 128.5, 127.3, 125.5, 124.5, 124.4, 122.7, 92.4, 65.3, 60.7, 59.7, 40.8, 35.2, 34.8, 20.8, 20.3, 17.1 ppm. HRMS (ASAP) [M+H]⁺

calc. 489.2309, found 489.2304 [C₃₀H₃₄ClN₂O₂]⁺. IR (neat): 2970, 2941, 2920, 1738, 1495, 1368, 1229, 1217, 1207, 752, 739, 687 cm⁻¹. m.p. = 162 – 164 °C.

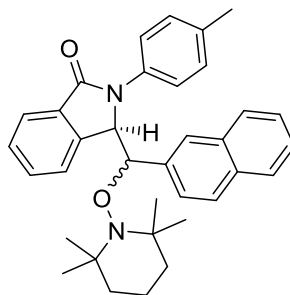
Minor product: (*R,R*)/(*S,S*)-isomer: colourless solid, 23% yield. ¹H NMR (400 MHz, CDCl₃): δ = 8.05 (d, *J* = 7.6 Hz, 1H, Ar*H*), 7.71 (d, *J* = 7.8 Hz, 1H, Ar*H*), 7.64 (t, *J* = 7.3 Hz, 1H, Ar*H*), 7.58 (d, *J* = 7.9 Hz, 2H, Ar*H*), 7.50 (t, *J* = 7.0 Hz, 3H, Ar*H*), 7.26 (t, 1H, Ar*H*), 6.89 (d, *J* = 7.5 Hz, 2H, Ar*H*), 6.39 (d, *J* = 7.7 Hz, 2H, Ar*H*), 6.07 (d, *J* = 4.6 Hz, 1H, NCHCH-O), 5.17 (d, *J* = 3.8 Hz, 1H, NCHCH-O), 1.68-1.55 (m, 6H, NCCH₂CH₂CH₂CN), 1.44 (bs, 3H, NCCH₃), 1.37 (bs, 3H, NCCH₃), 1.06 (bs, 3H, NCCH₃), 0.42 (bs, 3H, NCCH₃) ppm. ¹³C NMR (126 MHz, CDCl₃): δ = 167.0, 141.8, 137.2, 135.3, 133.6, 133.4, 131.8, 129.3, 129.2, 128.9, 127.3, 125.4, 124.6, 124.1, 122.9, 86.0, 61.6, 60.3, 60.3, 40.7, 35.1, 34.4, 21.0, 20.6, 17.1 ppm. HRMS (ASAP) [M+H]⁺ calc. 489.2309, found 489.2311 [C₃₀H₃₄ClN₂O₂]⁺. IR (neat): 3001, 2970, 2945, 1738, 1373, 1366, 1229, 1217, 752, 731, 696, 522 cm⁻¹. m.p. = 162 – 164 °C.

3-(4-Chlorobenzyl)-2-phenylisoindolin-1-one 178cb:



Pale yellow solid, 21% yield. ¹H NMR (400 MHz, CDCl₃): δ = 7.84 (d, *J* = 7.4 Hz, 1H, Ar*H*), 7.64 (d, *J* = 8.1 Hz, 2H, Ar*H*), 7.57 – 7.43 (m, 4H, Ar*H*), 7.31 – 7.27 (m, 1H, Ar*H*), 7.20 (d, *J* = 7.6 Hz, 1H, Ar*H*), 7.09 (d, *J* = 8.0 Hz, 2H, Ar*H*), 6.71 (d, *J* = 8.2 Hz, 2H, Ar*H*), 5.48 (dd, *J* = 6.6, 2.6 Hz, 1H, NCHCH₂), 3.32 (dd, *J* = 13.3, 2.6 Hz, 1H, NCHCH_aH_b), 2.98 (dd, *J* = 13.6, 7.3 Hz, 1H, NCHCH_aH_b) ppm. ¹³C NMR (126 MHz, CDCl₃): δ = 166.9, 143.6, 137.1, 133.4, 132.8, 132.4, 131.7, 130.9, 129.3, 128.7, 128.3, 125.4, 124.2, 123.1, 122.7, 60.8, 37.1 ppm. HRMS (ASAP) [M+H]⁺ calc. 334.0999, found 334.1005 [C₂₁H₁₇ClNO]⁺. IR (neat): 3065, 3048, 2949, 2916, 2855, 1736, 1680, 1491, 1381, 1217, 1209, 812, 752, 733, 692, 513 cm⁻¹. m.p. = 118 – 120 °C.

3-(Naphthalen-2-yl((2,2,6,6-tetramethylpiperidin-1-yl)oxy)methyl)-2-(*p*-tolyl)isoindolin-1-one 178e:



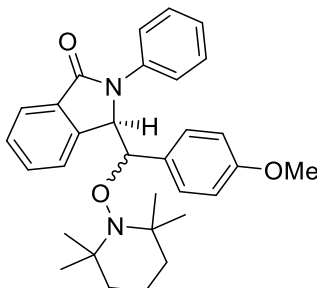
Synthesized according to the general procedure V on a 0.33 mmol scale (0.025 M solution due to low solubility in the solvent mixture used); **178e** (0.135 g, 79% yield, d.r.: 1.57:1).

Major product: (*R,S*)/(*S,R*)-isomer: colourless solid. ^1H NMR (500 MHz, CDCl_3): δ = 7.73 (d, J = 7.5 Hz, 1H, ArH), 7.70 – 7.66 (m, 1H, ArH), 7.63 (td, J = 7.5, 1.0 Hz, 1H, ArH), 7.59 – 7.53 (m, 3H, ArH), 7.53 – 7.46 (m, 2H, ArH), 7.41 – 7.32 (m, 3H, ArH), 7.28 (d, J = 8.2 Hz, 2H, ArH), 7.03 (s, 1H, ArH), 6.89 (s, 1H, ArH), 6.20 (s, 1H, N-CHCH-O), 5.54 (d, J = 1.5 Hz, 1H, N-CHCH-O), 2.43 (s, 3H, ArCH₃), 1.71 – 1.49 (m, 6H, NCH₂CH₂CH₂CN), 1.28 (s, 3H, N-CCH₃), 1.20 (s, 3H, N-CCH₃), 0.81 (s, 3H, N-CCH₃), 0.30 (s, 3H, N-CCH₃) ppm. ^{13}C NMR (126 MHz, CDCl_3): δ = 167.6, 142.4, 135.9, 134.9, 134.4, 132.8, 132.5, 132.3, 131.7, 128.9, 128.6, 127.9, 127.6, 127.4, 126.5, 126.3, 125.7, 125.6, 124.5, 124.1, 122.8, 92.8, 65.8, 60.6, 59.7, 40.7, 35.2, 34.5, 21.2, 20.7, 20.3, 17.0 ppm. IR (neat): 3005, 2970, 2930, 1738, 1699, 1510, 1369, 1366, 1229, 1217, 1207, 818, 808, 745, 689, 503 cm^{-1} . m.p. = 174 – 176 °C. HRMS (NSI) $[\text{M}+\text{H}]^+$ calc. 519.3006, found 519.3001 $[\text{C}_{35}\text{H}_{39}\text{N}_2\text{O}_2]^+$.

Minor product: (*R,R*)/(*S,S*)-isomer: colourless oil. ^1H NMR (500 MHz, CDCl_3): δ = 8.08 (d, J = 7.6 Hz, 1H, ArH), 7.60 (td, J = 7.5, 1.1 Hz, 1H, ArH), 7.57 – 7.51 (m, 2H, ArH), 7.42 – 7.36 (m, 2H, ArH), 7.35 – 7.31 (m, 2H, ArH), 7.30 – 7.22 (m, 5H, ArH), 6.86 (s, 1H, ArH), 6.49 (dd, J = 8.5, 1.7 Hz, 1H, ArH), 6.04 (d, J = 4.8 Hz, 1H, N-CHCH-O), 5.25 (d, J = 4.8 Hz, 1H, N-CHCH-O), 2.37 (s, 3H, ArCH₃), 1.65 – 1.51 (m, 6H, NCH₂CH₂CH₂CN), 1.41 (s, 3H, N-CCH₃), 1.26 (s, 3H, N-CCH₃), 1.02 (s, 3H, N-CCH₃), 0.30 (s, 3H, N-CCH₃) ppm. ^{13}C NMR (126 MHz, CDCl_3): δ = 167.0, 142.2, 135.1, 134.7, 134.2, 133.6, 133.0, 132.4, 131.5, 129.8, 128.7, 128.0, 127.7, 127.6, 126.5, 125.8, 125.8, 125.6, 124.7, 124.0, 123.4, 87.1, 62.1, 60.4, 60.1, 40.7, 35.0, 34.5, 21.2, 21.1, 20.7, 17.2 ppm. IR (neat): 3005, 2970, 2930, 2870, 1738, 1717, 1697, 1510, 1375, 1229, 1217, 1207,

818, 803, 735, 696, 478 cm^{-1} . HRMS (NSI) $[\text{M}+\text{H}]^+$ calc. 519.3006, found 519.2999 $[\text{C}_{35}\text{H}_{39}\text{N}_2\text{O}_2]^+$.

3-((4-Methoxyphenyl)((2,2,6,6-tetramethylpiperidin-1-yl)oxy)methyl)-2-phenylisoindolin-1-one 178g:



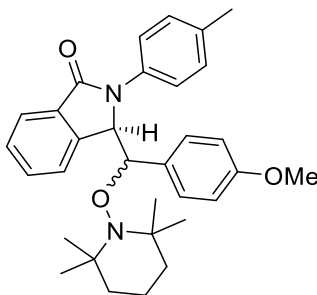
Synthesized according to the general procedure V on a 0.37 mmol scale; **178g** (0.32 g, 18% yield, d.r.: 1.21:1).

Major product: (*R,S*)/(*S,R*)-isomer: colourless solid. ^1H NMR (500 MHz, CDCl_3): δ = 7.73 (d, J = 7.6 Hz, 2H, ArH), 7.65 (d, J = 7.6 Hz, 1H, ArH), 7.63 – 7.56 (m, 2H, ArH), 7.46 (t, J = 7.9 Hz, 2H, ArH), 7.43 – 7.37 (m, 1H, ArH), 7.26 – 7.22 (m, 1H, ArH), 6.60 (d, J = 7.4 Hz, 2H, ArH), 6.52 (d, J = 8.7 Hz, 2H, ArH), 6.13 (d, J = 1.2 Hz, 1H, N-CHCH-O), 5.31 (d, J = 1.6 Hz, 1H, N-CHCH-O), 3.68 (s, 3H, ArOCH_3), 1.70 – 1.45 (m, 6H, $\text{NCH}_2\text{CH}_2\text{CH}_2\text{CN}$), 1.25 (s, 3H, N-CCH₃), 1.15 (s, 3H, N-CCH₃), 0.70 (s, 3H, N-CCH₃), 0.31 (s, 3H, N-CCH₃) ppm. ^{13}C NMR (126 MHz, CDCl_3): δ = 168.0, 158.9, 142.7, 138.7, 132.5, 131.9, 129.7, 128.8, 128.6, 128.4, 125.3, 124.6, 124.2, 122.8, 112.5, 92.3, 65.7, 60.7, 59.6, 55.1, 40.8, 35.1, 34.7, 20.9, 20.3, 17.1 ppm. IR (neat): 2961, 2930, 1701, 1611, 1599, 1512, 1499, 1377, 1250, 1177, 1030, 756, 700, 692 cm^{-1} . m.p. = 150 – 152 °C. HRMS (NSI) $[\text{M}+\text{H}]^+$ calc. 485.2799, found 485.2794 $[\text{C}_{31}\text{H}_{37}\text{N}_2\text{O}_3]^+$.

Minor product: (*R,R*)/(*S,S*)-isomer: colourless solid. ^1H NMR (500 MHz, CDCl_3): δ = 8.07 (d, J = 7.5 Hz, 1H, ArH), 7.70 (d, J = 7.5 Hz, 1H, ArH), 7.64 (t, J = 7.4 Hz, 1H, ArH), 7.56 (d, J = 7.8 Hz, 2H, ArH), 7.51 – 7.45 (m, 3H, ArH), 7.26 – 7.22 (m, 1H, ArH), 6.43 (d, J = 8.6 Hz, 2H, ArH), 6.33 (d, J = 8.5 Hz, 2H, ArH), 6.05 (d, J = 4.7 Hz, 1H, N-CHCH-O), 5.11 (d, J = 4.1 Hz, 1H, N-CHCH-O), 3.66 (s, 3H, ArOCH_3), 1.69 – 1.51 (m, 6H, $\text{NCH}_2\text{CH}_2\text{CH}_2\text{CN}$), 1.44 (s, 3H, N-CCH₃), 1.36 (s, 3H, N-CCH₃), 1.06 (s, 3H, N-CCH₃), 0.42 (s, 3H, N-CCH₃) ppm. ^{13}C NMR (126 MHz, CDCl_3): δ = 167.2, 159.0, 142.3, 137.3, 133.6, 131.6, 129.2, 129.2, 128.8, 128.6, 125.3, 124.7, 124.0, 123.2, 112.4, 86.4, 62.0, 60.3, 60.1, 55.0, 40.7, 35.0, 34.4, 21.0, 20.6, 17.2 ppm. IR (neat): 3003, 2965, 2932,

2870, 1699, 1611, 1597, 1512, 1499, 1379, 1250, 1177, 1034, 912, 831, 752, 733, 696, 550 cm^{-1} . m.p. = 158 – 160 °C. HRMS (NSI) $[\text{M}+\text{H}]^+$ calc. 485.2799, found 485.2793 $[\text{C}_{31}\text{H}_{37}\text{N}_2\text{O}_3]^+$.

3-((4-Methoxyphenyl)((2,2,6,6-tetramethylpiperidin-1-yl)oxy)methyl)-2-(*p*-tolyl)isoindolin-1-one **178h:**



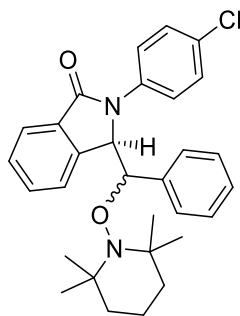
Synthesized according to the general procedure V on a 0.36 mmol scale; **178h** (0.37 g, 21% yield, d.r.: 1.27:1).

Major product: (*R,S*)/(*S,R*)-isomer: colourless solid. ^1H NMR (500 MHz, CDCl_3): δ = 7.64 (d, J = 7.6 Hz, 1H, ArH), 7.63 – 7.54 (m, 4H, ArH), 7.39 (t, J = 7.0 Hz, 1H, ArH), 7.25 – 7.22 (m, 2H, ArH), 6.62 (d, J = 7.5 Hz, 2H, ArH), 6.52 (d, J = 8.6 Hz, 2H, ArH), 6.10 – 6.05 (s, 1H, N-CHCH-O), 5.30 (d, J = 1.1 Hz, 1H, N-CHCH-O), 3.68 (s, 3H, ArOCH₃), 2.39 (s, 3H, ArCH₃), 1.62 – 1.47 (m, 6H, NCH₂CH₂CH₂CN), 1.27 (s, J = 6.2 Hz, 3H, N-CCH₃), 1.14 (s, 3H, N-CCH₃), 0.73 (s, 3H, N-CCH₃), 0.32 (s, 3H, N-CCH₃) ppm. ^{13}C NMR (126 MHz, CDCl_3): δ = 168.0, 158.9, 142.7, 136.2, 134.9, 132.6, 131.7, 129.7, 129.0, 128.5, 124.5, 124.1, 122.8, 114.5, 112.4, 92.2, 65.8, 60.7, 59.6, 55.1, 40.8, 35.1, 34.7, 21.2, 20.8, 20.3, 17.1 ppm. IR (neat): 3017, 2970, 2941, 1738, 1514, 1423, 1366, 1229, 1217, 1206, 1028, 901, 754, 733, 669, 527, 517 cm^{-1} . m.p. = 174 – 176 °C. HRMS (NSI) $[\text{M}+\text{H}]^+$ calc. 499.2955, found 499.2950 $[\text{C}_{32}\text{H}_{39}\text{N}_2\text{O}_3]^+$.

Minor product: (*R,R*)/(*S,S*)-isomer: colourless solid. ^1H NMR (500 MHz, CDCl_3): δ = 8.06 (d, J = 7.6 Hz, 1H, ArH), 7.69 (d, J = 7.6 Hz, 1H, ArH), 7.63 (td, J = 7.5, 1.0 Hz, 1H, ArH), 7.47 (t, J = 7.5 Hz, 1H, ArH), 7.42 (d, J = 8.4 Hz, 2H, ArH), 7.28 (d, J = 8.1 Hz, 2H, ArH), 6.43 (d, J = 8.8 Hz, 2H, ArH), 6.35 (d, J = 8.7 Hz, 2H, ArH), 6.01 (d, J = 4.8 Hz, 1H, N-CHCH-O), 5.09 (d, J = 4.7 Hz, 1H, N-CHCH-O), 3.66 (s, 3H, ArOCH₃), 2.40 (s, 3H, ArCH₃), 1.67 – 1.52 (m, 6H, NCH₂CH₂CH₂CN), 1.43 (s, 3H, N-CCH₃), 1.35 (s, 3H, N-CCH₃), 1.06 (s, 3H, N-CCH₃), 0.41 (s, 3H, N-CCH₃) ppm. ^{13}C NMR (126 MHz, CDCl_3): δ = 167.1, 159.0, 142.3, 135.0, 134.7, 133.7, 131.4, 129.7, 129.2, 128.9, 128.6,

124.6, 123.9, 123.2, 112.4, 86.4, 62.2, 60.3, 60.1, 55.0, 40.7, 35.0, 34.4, 21.2, 21.2, 20.6, 17.2 ppm. IR (neat): 3005, 2970, 2930, 1738, 1512, 1456, 1375, 1366, 1229, 1217, 1207, 1034, 912, 827, 802, 748, 733, 694, 528 cm^{-1} . m.p. = 204 – 206 °C. HRMS (NSI) $[\text{M}+\text{H}]^+$ calc. 499.2955, found 499.2949 $[\text{C}_{32}\text{H}_{39}\text{N}_2\text{O}_3]^+$.

2-(4-Chlorophenyl)-3-(phenyl((2,2,6,6-tetramethylpiperidin-1-yl)oxy)methyl)isoindolin-1-one **178j:**



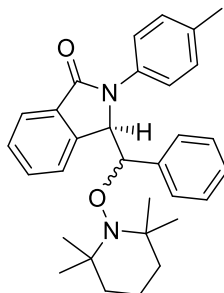
Synthesized according to the general procedure V on a 0.47 mmol scale; **178j** (0.152 g, 66% yield d.r.: 1.06:1 (*R,S/S,R* : *R,R/S,S* in crude ^1H NMR)).

Major product: (*R,R*)/(*S,S*)-isomer: colourless solid, 34% yield. ^1H NMR (400 MHz, CDCl_3): δ = 8.07 (d, J = 7.5 Hz, 1H, ArH), 7.69 – 7.60 (m, 2H, ArH), 7.58 – 7.51 (m, 2H, ArH), 7.50 – 7.42 (m, 3H, ArH), 7.06 – 6.99 (m, 1H, ArH), 6.94 – 6.86 (m, 2H, ArH), 6.47 – 6.40 (m, 2H, ArH), 6.03 (d, J = 4.7 Hz, 1H, N-CHCH-O), 5.16 (d, J = 4.7 Hz, 1H, N-CHCH-O), 1.75 – 1.56 (m, 6H, $\text{NCCCH}_2\text{CH}_2\text{CH}_2\text{CN}$), 1.44 (s, 3H, N-CCH₃), 1.37 (s, 3H, N-CCH₃), 1.06 (s, 3H, N-CCH₃), 0.43 (s, 3H, N-CCH₃) ppm. ^{13}C NMR (126 MHz, CDCl_3): δ = 167.1, 142.0, 136.4, 136.0, 133.1, 131.8, 130.4, 129.3, 128.7, 127.8, 127.8, 127.1, 124.7, 124.0, 123.9, 86.5, 61.8, 60.3, 40.7, 35.2, 34.2, 21.0, 20.6, 17.2 ppm. HRMS (NSI) $[\text{M}+\text{H}]^+$ calc. 489.2303, found 489.2297 $[\text{C}_{30}\text{H}_{34}\text{ClN}_2\text{O}_2]^+$. IR (neat): 3005, 2968, 2936, 2878, 1701, 1493, 1373, 1094, 908, 731, 712, 702, 501 cm^{-1} . m.p. = 150 – 152 °C.

Minor product: (*R,S*)/(*S,R*)-isomer: colourless solid, 32% yield. ^1H NMR (400 MHz, CDCl_3): δ = 7.71 – 7.59 (m, 5H, ArH), 7.46 – 7.39 (m, 3H, ArH), 7.06 (t, J = 7.3 Hz, 1H, ArH), 6.97 (t, J = 7.6 Hz, 2H, ArH), 6.58 (d, J = 6.2 Hz, 2H, ArH), 6.11 (d, J = 1.0 Hz, 1H, N-CHCH-O), 5.37 (d, J = 1.4 Hz, 1H, N-CHCH-O), 1.70 – 1.46 (m, 6H, $\text{NCCCH}_2\text{CH}_2\text{CH}_2\text{CN}$), 1.28 (s, 3H, N-CCH₃), 1.20 (s, 3H, N-CCH₃), 0.80 (s, 3H, N-CCH₃), 0.34 (s, 3H, N-CCH₃) ppm. ^{13}C NMR (126 MHz, CDCl_3) δ 167.7, 142.3, 137.2, 136.4, 132.2, 132.1, 130.4, 128.8, 128.4, 128.1, 127.7, 127.1, 125.4, 124.2, 122.8, 93.0,

65.6, 60.6, 59.7, 40.7, 35.3, 34.5, 20.9, 20.4, 17.1 ppm. HRMS (NSI) $[M+H]^+$ calc. 489.2303, found 489.2296 $[C_{30}H_{34}ClN_2O_2]^+$. IR (neat): 2922, 2874, 1703, 1491, 1369, 816, 712, 683, 615 cm^{-1} . m.p. = 152 – 153 °C.

3-(Phenyl((2,2,6,6-tetramethylpiperidin-1-yl)oxy)methyl)-2-(*p*-tolyl)isoindolin-1-one **178k:**



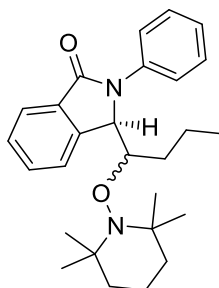
Synthesized according to the general procedure V on a 0.43 mmol scale; **178k** (0.157 g, 78% yield, d.r.: 1.24:1).

Minor product: (*R,R*)/(*S,S*)-isomer: pale yellow oil, 31% yield. 1H NMR (400 MHz, $CDCl_3$): δ = 8.06 (dd, J = 7.6, 0.6 Hz, 1H, Ar*H*), 7.66 (d, J = 7.6 Hz, 1H, Ar*H*), 7.62 (dt, J = 7.5, 3.7 Hz, 1H, Ar*H*), 7.48 – 7.42 (m, 3H, Ar*H*), 7.29 (d, J = 8.1 Hz, 2H, Ar*H*), 7.04 – 6.98 (m, 1H, Ar*H*), 6.93 – 6.86 (m, 2H, Ar*H*), 6.47 (d, J = 7.1 Hz, 2H, Ar*H*), 6.05 (d, J = 4.7 Hz, 1H, N-CHCH-O), 5.18 – 5.14 (m, 1H, N-CHCH-O), 2.41 (s, 3H, ArCH₃), 1.68 – 1.55 (m, 6H, NCH₂CH₂CH₂CN), 1.44 (s, 3H, N-CCH₃), 1.36 (s, 3H, N-CCH₃), 1.07 (s, 3H, N-CCH₃), 0.42 (s, 3H, N-CCH₃) ppm. ^{13}C NMR (126 MHz, $CDCl_3$): δ = 167.1, 142.2, 136.7, 135.0, 134.7, 133.5, 131.5, 129.8, 128.6, 128.0, 127.7, 127.0, 124.6, 123.8, 123.0, 86.6, 62.0, 60.2, 60.1, 40.7, 35.1, 34.2, 21.2, 21.0, 20.6, 17.2 ppm. HRMS (NSI) $[M+H]^+$ calc. 469.2850, found 469.2843 $[C_{31}H_{36}N_2O_2]^+$. IR (neat): 3028, 3001, 2968, 2928, 2862, 1738, 1701, 1508, 1381, 1346, 1217, 1207, 806, 708, 694, 517 cm^{-1} . m.p. = 141 – 143 °C.

Major product: (*R,S*)/(*S,R*)-isomer: pale yellow solid, 47% yield. 1H NMR (400 MHz, $CDCl_3$): δ = 7.68 – 7.52 (m, 5H, Ar*H*), 7.39 (t, J = 7.4 Hz, 1H, Ar*H*), 7.26 – 7.21 (m, 2H, Ar*H*), 7.07 – 7.02 (m, 1H, Ar*H*), 6.98 (t, J = 7.5 Hz, 2H, Ar*H*), 6.68 (d, J = 6.3 Hz, 2H, Ar*H*), 6.11 (d, J = 1.4 Hz, 1H, N-CHCH-O), 5.35 (d, J = 1.7 Hz, 1H, N-CHCH-O), 2.39 (s, 3H, ArCH₃), 1.65 – 1.43 (m, 6H, NCH₂CH₂CH₂CN), 1.28 (s, 3H, N-CCH₃), 1.14 (s, 3H, N-CCH₃), 0.76 (s, 3H, N-CCH₃), 0.32 (s, 3H, N-CCH₃) ppm. ^{13}C NMR (126 MHz, $CDCl_3$): δ = 167.8, 142.5, 136.8, 136.1, 134.9, 132.6, 131.7, 129.0, 128.6, 128.4, 127.5, 127.0, 124.4, 124.1, 122.8, 92.7, 65.7, 60.6, 59.6, 40.8, 35.2, 34.5, 21.2, 20.7, 20.3, 17.1

ppm. HRMS (NSI) $[M+H]^+$ calc. 469.2850, found 469.2845 $[C_{31}H_{36}N_2O_2]^+$. IR (neat): 3001, 2968, 2928, 2870, 1736, 1697, 1514, 1375, 1298, 1207, 1022, 733, 712, 702, 687 cm^{-1} . m.p. = 149 – 151 °C.

2-Phenyl-3-(1-((2,2,6,6-tetramethylpiperidin-1-yl)oxy)butyl)isoindolin-1-one 178m:



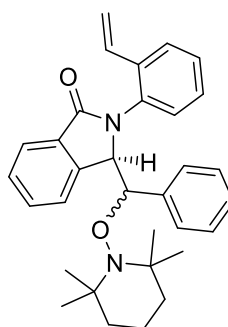
Synthesized according to the general procedure V on a 0.44 mmol scale; **178m** (0.111 g, 75% yield, d.r.: 1.65:1).

Major product: (*R,S*)/(*S,R*)-isomer: 1H NMR (400 MHz, $CDCl_3$): δ = 7.94 (d, J = 7.5 Hz, 1H, ArH), 7.78 (d, J = 7.5 Hz, 1H, ArH), 7.70 (d, J = 8.0 Hz, 2H, ArH), 7.61 (t, J = 7.4 Hz, 1H, ArH), 7.52 (t, J = 7.4 Hz, 1H, ArH), 7.45 (t, J = 7.5 Hz, 2H, ArH), 7.22 (t, J = 7.3 Hz, 1H, ArH), 5.76 (s, 1H, N-CHCH-O), 4.32 – 4.25 (m, 1H, N-CHCH-O), 1.70 – 1.40 (m, 6H, $NCH_2CH_2CH_2CN$), 1.36 – 1.27 (m, 2H, $OCHCH_2CH_2CH_3$), 1.32 (s, 3H, N-CCH₃), 1.24 (s, 3H, N-CCH₃), 1.20 (s, 3H, N-CCH₃), 1.16 – 1.06 (m, 1H, $CH_2CH_2CH_3$), 1.02 (s, 3H, N-CCH₃), 0.92 – 0.79 (m, 2H, $CH_2CH_2CH_3$), 0.56 (t, J = 7.2 Hz, 3H, CH_2CH_3) ppm. ^{13}C NMR (101 MHz, $CDCl_3$): δ = 167.6, 143.1, 137.4, 133.2, 131.8, 129.1, 128.5, 125.4, 124.3, 124.2, 123.4, 80.3, 62.4, 60.7, 60.2, 41.1, 41.0, 35.4, 33.9, 32.1, 20.7, 20.7, 19.7, 17.2, 14.6 ppm. m.p. = 129 – 131 °C. HRMS (NSI) $[M+H]^+$ calc. 421.2850, found 421.2848 $[C_{27}H_{37}N_2O_2]^+$. IR (neat): 3015, 2988, 2970, 2928, 2874, 1738, 1686, 1373, 1229, 1217, 752, 696 cm^{-1} .

Minor product: (*R,R*)/(*S,S*)-isomer: 1H NMR (400 MHz, $CDCl_3$): δ = 7.94 (d, J = 7.4 Hz, 1H, ArH), 7.68 (d, J = 7.9 Hz, 2H, ArH), 7.56 (d, J = 3.3 Hz, 2H, ArH), 7.52–7.46 (m, 1H, ArH), 7.43 (t, J = 7.5 Hz, 2H, ArH), 7.19 (t, J = 7.4 Hz, 1H, ArH), 5.44 (s, 1H, N-CHCH-O), 4.30 – 4.24 (m, 1H, N-CHCH-O), 2.30 – 2.18 (m, 1H, $OCHCH_2CH_2CH_3$), 1.81 – 1.66 (m, 1H, $OCHCH_2CH_2CH_3$), 1.52 – 1.12 (m, 8H, $NCH_2CH_2CH_2CN$, $CH_2CH_2CH_3$), 0.99 (t, J = 7.4 Hz, 3H, CH_2CH_3), 0.95 (s, 3H, N-CCH₃), 0.63 (s, 6H, N-CCH₃), 0.38 (s, 3H, N-CCH₃) ppm. ^{13}C NMR (101 MHz, $CDCl_3$): δ = 167.7, 142.1, 137.7, 133.6, 131.4, 129.0, 128.4, 125.1, 124.1, 123.4, 123.3, 79.4, 63.7, 60.6, 59.2, 40.7, 40.2,

33.9, 33.5, 31.6, 20.4, 19.94, 19.92, 17.2, 14.6 ppm. m.p. = 163 – 166 °C. HRMS (NSI) $[M+H]^+$ calc. 421.2850, found 421.2847 $[C_{27}H_{37}N_2O_2]^+$. IR (neat): 3007, 2970, 2934, 2864, 1738, 1684, 1373, 1366, 1229, 1217, 752, 696 cm^{-1} .

3-(Phenyl((2,2,6,6-tetramethylpiperidin-1-yl)oxy)methyl)-2-(2-vinylphenyl)isoindolin-1-one **178p:**



Performed according to the general procedure V on a 0.37 mmol scale; **178p** (0.150 g, 85% yield d.r.: 2.25:1). The signals in 1H and ^{13}C NMR are broad and difficult to analyse. Running the NMR at 50 °C improved the quality of the spectra, but did not lead to a clean analysis of the product (integration did not match 100% according to the expected product). The compounds were reduced to form the alcohol (compounds **183a** and **183b**), and the structure could be confirmed by X-ray crystallography.

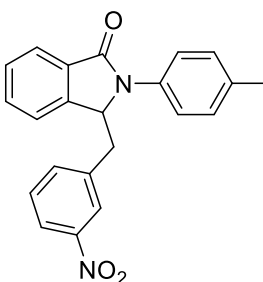
Major product: (*R,S*)/(*S,R*)-isomer (**178pa**): colourless oil, 59% yield. 1H NMR (400 MHz, $CDCl_3$, 50 °C): δ = 7.85 – 7.28 (m, 8H), 7.06 (s, 5H), 6.40 (dd, J = 17.3, 11.0 Hz, 1H), 5.90 (s, 1H), 5.67 (d, J = 17.4 Hz, 1H), 5.33 – 5.18 (m, 2H), 1.51 – 0.32 (m, 18H) ppm. ^{13}C NMR (101 MHz, $CDCl_3$): δ = 143.1, 137.4, 136.6, 135.4, 131.9, 131.2, 128.4, 128.1, 127.8, 127.1, 127.0, 126.7, 124.0, 123.3, 90.5, 66.6, 60.1, 59.8, 40.6, 16.8 ppm. HRMS (ES): $[M-[C_9H_{18}N]]^-$ calc. 339.1239, found 339.1238 $[C_{23}H_{17}NO_2]^-$. IR (neat): 2986, 2931, 1696, 1475, 1461, 1452, 1340, 928, 718 cm^{-1} .

Minor product: (*R,R*)/(*S,S*)-isomer (**178pb**): colourless oil, 26% yield. 1H NMR (400 MHz, $CDCl_3$, 50 °C): δ = 8.14 (d, J = 7.6 Hz, 1H), 7.82 (d, J = 7.6 Hz, 1H), 7.69 (td, J = 7.5, 1.1 Hz, 1H), 7.66 – 7.62 (m, 1H), 7.54 (t, J = 7.5 Hz, 1H), 7.37 – 7.29 (m, 2H), 7.16 – 7.04 (m, 2H), 6.96 (t, J = 7.7 Hz, 2H), 6.62 – 6.52 (m, 2H), 5.98 (d, J = 2.8 Hz, 1H), 5.66 (d, J = 17.4 Hz, 1H), 5.13 (s, 1H), 4.89 (d, J = 4.9 Hz, 1H), 1.80 – 0.80 (m, 18H) ppm. ^{13}C NMR (101 MHz, $CDCl_3$, 50 °C): δ = 167.7, 143.6, 137.1, 135.5, 134.5, 133.8,

133.2, 131.7, 129.7, 128.7, 128.3, 128.1, 127.7, 127.5, 127.1, 125.1, 124.3, 115.6, 115.3, 87.5, 64.2, 60.4, 60.2, 40.8, 34.3, 33.8, 21.1, 20.7, 17.2 ppm. HRMS (ES): $[M+K]^+$ calc. 419.2414, found 419.2428 $[C_{32}H_{36}KN_2O_2]^+$. IR (neat): 2980, 2934, 1701, 1485, 1458, 1364, 908, 718 cm^{-1} .

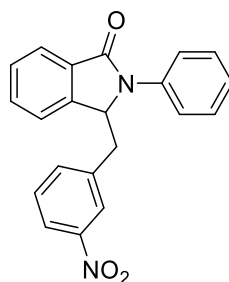
The peaks in 1H NMR and ^{13}C NMR are broad and that makes difficult the analysis. To confirm the structures, the compounds were submitted to a reduction in order to cleave the O-N bond and analyse the product obtained **183**.

3-(3-Nitrobenzyl)-2-(*p*-tolyl)isoindolin-1-one **180:**



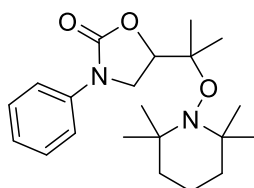
Only product observed when performed according to the general procedure V on a 0.5 mmol scale (0.025 M solution due to low solubility in the solvent mixture used); **180** (0.168 g, 94% yield) was obtained as a colourless solid.

1H NMR (500 MHz, $CDCl_3$): δ = 7.96 (ddd, J = 8.2, 2.2, 1.0 Hz, 1H, ArH), 7.78 (d, J = 7.6 Hz, 1H, ArH), 7.62 – 7.55 (m, 2H, ArH), 7.50 – 7.43 (m, 3H, ArH), 7.37 (dd, J = 7.6, 0.7 Hz, 1H, ArH), 7.31 (d, J = 8.1 Hz, 2H, ArH), 7.23 (t, J = 7.9 Hz, 1H, ArH), 7.01 (d, J = 7.7 Hz, 1H, ArH), 5.54 (dd, J = 6.1, 3.7 Hz, 1H, NCHCH₂), 3.37 (dd, J = 14.1, 3.6 Hz, 1H, NCHCH_aH_b), 3.27 (dd, J = 14.1, 6.2 Hz, 1H, NCHCH_aH_b), 2.40 (s, 3H, ArCH₃) ppm. ^{13}C NMR (126 MHz, $CDCl_3$): δ = 166.9, 147.9, 143.0, 136.8, 135.9, 135.7, 134.3, 132.6, 132.0, 130.1, 129.0, 129.0, 124.8, 124.5, 123.3, 122.6, 122.1, 60.6, 37.3, 21.2 ppm. IR (neat): 3024, 2970, 2945, 1740, 1686, 1524, 1373, 1348, 1229, 1217, 1205, 810, 781, 731, 691, 527, 500 cm^{-1} . m.p. = 132 – 134 °C. HRMS (NSI) $[M+H]^+$ calc. 359.1390, found 359.1392 $[C_{22}H_{19}N_2O_3]^+$.

3-(3-Nitrobenzyl)-2-phenylisoindolin-1-one 181:

Only product observed when synthesized according to the general procedure V on a 0.5 mmol scale (0.025 M solution due to low solubility in the solvent mixture used); **181** (0.157 g, 91% yield) was obtained as a colourless solid.

^1H NMR (500 MHz, CDCl_3): δ = 7.95 (ddd, J = 8.2, 2.2, 1.0 Hz, 1H, ArH), 7.78 (d, J = 7.6 Hz, 1H, ArH), 7.64 – 7.57 (m, 3H, ArH), 7.55 (t, J = 1.9 Hz, 1H ArH), 7.52 – 7.44 (m, 3H, ArH), 7.39 (dd, J = 7.6, 0.7 Hz, 1H, ArH), 7.30 – 7.25 (m, 1H, ArH), 7.22 (t, J = 7.9 Hz, 1H, ArH), 6.99 (d, J = 7.8 Hz, 1H, ArH), 5.58 (dd, J = 6.0, 3.7 Hz, 1H, NCHCH₂), 3.38 (dd, J = 14.1, 3.6 Hz, 1H, NCHCH_aH_b), 3.29 (dd, J = 14.1, 6.1 Hz, 1H, NCHCH_aH_b) ppm. ^{13}C NMR (126 MHz, CDCl_3): δ = 166.9, 147.8, 143.0, 136.9, 136.6, 135.8, 132.5, 132.2, 129.5, 129.1, 129.0, 125.8, 124.7, 124.5, 123.2, 122.6, 122.2, 60.4, 37.2 ppm. IR (neat): 3017, 2970, 2934, 1740, 1680, 1526, 1456, 1373, 1354, 1229, 1217, 1206, 756, 729, 696, 527, 503 cm^{-1} . m.p. = 112 – 114 °C. HRMS (NSI) $[\text{M}+\text{H}]^+$ calc. 345.1234, found 345.1234 $[\text{C}_{21}\text{H}_{17}\text{N}_2\text{O}_3]^+$.

3-Phenyl-5-(2-((2,2,6,6-tetramethylpiperidin-1-yl)oxy)propan-2-yl)oxazolidin-2-one 155:

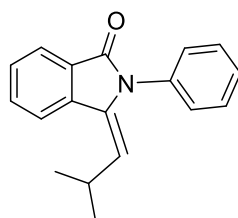
3-Methylbut-2-en-1-yl phenylcarbamate **154** (0.103 g, 0.5 mmol) was dissolved in a mixture of acetonitrile/water (19:1, 10 mL). (2,2,6,6-Tetramethyl-piperidin-1-yl)oxyl (TEMPO) (0.117 g, 0.75 mmol) and benzyltrimethylammonium hydroxide solution (40% w, 0.105 g, 0.25 mmol) were added to the solution, and it was introduced in the electrochemical reactor (0.205 mL inner volume; 128 mA; 4 F/mol, 1–3 V) using a syringe pump (0.4 mL/min). After reaching the steady state, the solution was collected

for 20 min. The outlet was quenched with saturated ammonium chloride aqueous solution, extracted with diethyl ether (3 x 20 mL) and washed with brine. The combined organic layers were dried over anhydrous magnesium sulfate, the solvent was evaporated and the product was purified by column chromatography (*n*-hexane/ethyl acetate, 9:1), giving 0.095 g of pure product **155** as a colourless solid in 66% yield.

^1H NMR (300 MHz, CDCl_3): δ = 7.44 – 7.33 (m, 4H, ArH), 7.25 – 7.17 (m, 1H, ArH), 4.80 – 4.68 (m, J = 7.2 Hz, 2H, N-CHCH₂-O), 4.55 – 4.44 (m, 1H, N-CHCH₂), 1.57 (s, 2H, CH₂CHCH₂), 1.54 – 1.38 (m, 4H, C-CH₂CH), 1.32 (s, 3H, C(CH₃)₃), 1.09 (s, 3H, C(CH₃)₃), 1.08 (s, 3H, C(CH₃)₃), 1.02 (s, 6H, C(CH₃)₃), 0.97 (s, 3H, C(CH₃)₃) ppm. m.p. = 135 – 136 °C (Lit. = 134 – 135 °C).^[16] The spectroscopy data are in agreement with literature.^[16]

6.3.4. Elimination products

3-(2-Methylpropylidene)-2-phenylisoindolin-1-one **185**:

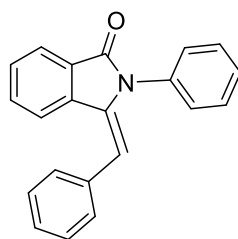


General procedure VI: (*E/Z*)-2-(3-Methylbut-1-en-1-yl)-*N*-phenylbenzamide **164b** (0.133 g, 0.5 mmol) was dissolved in a mixture of acetonitrile/water (19:1, 10 mL). TEMPO (0.117 g, 0.75 mmol) and benzyltrimethylammonium hydroxide solution (40% w/w, 0.418 g, 1.0 mmol) were added to the solution, and it was introduced in the electrochemical reactor (0.205 mL inner volume; 24 mA; 3 F/mol) using a syringe pump (0.1 mL/min). The outlet of the microreactor was connected to a 2.5 mL coil (0.5 mm ID) that was heated to 85 °C using a water bath. The system was pressurised *via* a backpressure regulator (2.8 bar). After reaching the steady state, the solution was collected for 40 min. The outlet was quenched with saturated ammonium chloride aqueous solution, extracted with diethyl ether (3 x 20 mL) and washed with brine. The combined organic layers were dried over anhydrous magnesium sulfate, the solvent was evaporated under reduced pressure and the product was purified by column chromatography (*n*-hexane/ethyl acetate, 9:1), giving 0.040 g of **185** as a diastereomeric mixture (*E/Z* 9:1) in 75% yield.

Major product: *E*-isomer: ^1H NMR (300 MHz, CDCl_3): $\delta = 8.03 - 7.88$ (m, 2H, ArH), 7.65 (t, $J = 7.5$ Hz, 1H, ArH), 7.59 – 7.48 (m, 3H, ArH), 7.44 (d, $J = 6.9$ Hz, 1H, ArH), 7.33 (d, $J = 7.8$ Hz, 2H, ArH), 5.18 (d, $J = 9.7$ Hz, 1H, C=CHCH), 3.47 – 3.22 (m, 1H, CHCH(CH₃)₂), 1.14 (d, $J = 6.7$ Hz, 6H, CH(CH₃)₂) ppm. ^{13}C NMR (126 MHz, CDCl_3): $\delta = 166.2, 135.6, 135.4, 135.0, 134.6, 132.3, 129.5, 129.1, 129.0, 128.2, 126.7, 124.0, 123.5, 121.7, 26.8, 23.4, 23.2$ ppm. m.p. = 106 – 110 °C. IR (neat): 3002, 2967, 2922, 2876, 1730, 1697, 1491, 1377, 1109, 1067, 754, 714, 702, 689, 528, 503 cm^{-1} .

Minor product: *Z*-isomer: ^1H NMR (500 MHz, CDCl_3) $\delta = 7.92$ (d, $J = 7.6$ Hz, 1H, ArH), 7.72 (d, $J = 7.7$ Hz, 1H, ArH), 7.63 (t, $J = 7.5$ Hz, 1H, ArH), 7.53 – 7.49 (m, 3H, ArH), 7.39 (d, $J = 7.4$ Hz, 2H, ArH), 5.46 (d, $J = 10.6$ Hz, 1H, C=CHCH), 2.08 – 1.98 (m, 1H, CHCH(CH₃)₂), 0.87 (d, $J = 7.6$ Hz, 6H, CH(CH₃)₂) ppm.

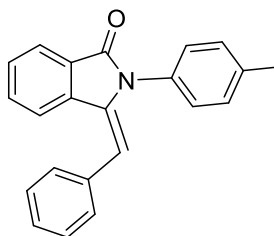
(*E*)-3-Benzylidene-2-phenylisoindolin-1-one **186:**



Performed according to the general procedure VI on a 0.275 mmol scale; **186** (0.050 g, 62% yield, *E/Z* = 19:1).

^1H NMR (400 MHz, CDCl_3): $\delta = 7.96$ (d, $J = 7.5$ Hz, 1H), 7.59 – 7.34 (m, 13H), 6.38 (s, 1H). The spectroscopy data are in agreement with literature.^[17] (*Z*-isomer)^[18]

(*E*)-3-Benzylidene-2-(*p*-tolyl)isoindolin-1-one **187:**

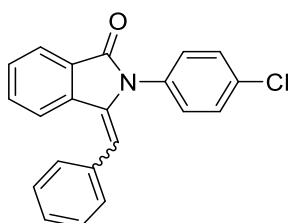


Performed according to the general procedure VI on a 0.313 mmol scale; **187** (0.062 g, 68% yield, *E/Z* = 19:1).

^1H NMR (300 MHz, CDCl_3): $\delta = 7.94$ (d, $J = 7.5$ Hz, 1H), 7.55 – 7.28 (m, 12H), 6.35 (s, 1H), 2.44 (s, 3H) ppm. ^{13}C NMR (126 MHz, CDCl_3): $\delta = 166.5, 138.5, 138.4, 135.4,$

135.1, 132.2, 131.9, 130.3, 130.2, 129.6, 129.6, 128.8, 128.7, 127.9, 123.7, 123.3, 112.3, 21.4 ppm. HRMS (NSI): $[M+H]^+$ calc. 312.1383, found 312.1383 $[C_{22}H_{18}NO]^+$; $[2M+H]^+$ calc. 623.2693, found 623.2685 $[(C_{22}H_{17}NO)_2H]^+$. IR (neat): 3019, 2972, 2914, 1736, 1701, 1512, 1346, 1217, 765, 692 cm^{-1} . m.p. = 113 – 115 °C.

3-Benzylidene-2-(4-chlorophenyl)isoindolin-1-one **188**:

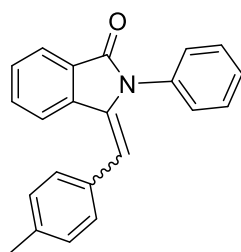


Synthesized according to the general procedure VI on a 0.30 mmol scale; **188** (0.065 g, 66% yield, *E/Z* = 5:1).

Major product: *E*-isomer: colourless oil: 1H NMR (500 MHz, $CDCl_3$): δ = 7.93 (d, J = 7.6 Hz, 1H, *ArH*), 7.54 – 7.48 (m, 3H, *ArH*), 7.45 – 7.35 (m, 9H, *ArH*), 6.36 (s, 1H, $NC=CH$) ppm. ^{13}C NMR (126 MHz, $CDCl_3$): δ = 166.4, 138.0, 135.0, 135.0, 134.4, 133.4, 132.2, 130.4, 129.9, 129.9, 129.8, 129.5, 128.8, 128.1, 123.8, 123.4, 112.4 ppm. IR (neat): 3024, 2970, 2926, 2853, 1736, 1707, 1491, 1472, 1375, 1366, 1348, 1227, 1217, 1088, 1015, 764, 723, 692, 509 cm^{-1} . HRMS (NSI) $[M+H]^+$ calc. 332.0837, found 332.0839 $[C_{21}H_{15}ClNO]^+$.

Minor product: *Z*-isomer: (overlapping with *E* isomer): 1H NMR (500 MHz, $CDCl_3$): δ = 7.95 (d, J = 6.4 Hz, 1H, *ArH*), 7.86 (d, J = 7.8 Hz, 1H, *ArH*), 7.69 (td, J = 7.6, 1.0 Hz, 1H, *ArH*), 7.57 (dt, J = 6.8, 3.4 Hz, 1H, *ArH*), 7.08 – 6.96 (m, 7H, *ArH*), 6.87 (d, J = 7.8 Hz, 2H, *ArH*), 6.86 (s, 1H, $NC=CH$) ppm. ^{13}C NMR (126 MHz, $CDCl_3$): δ = 168.0, 138.7, 134.6, 134.4, 133.5, 132.8, 132.5, 129.5, 129.3, 128.5, 128.4, 127.7, 127.5, 127.1, 124.1, 119.6, 107.9 ppm. Spectra in accordance to literature.^[19]

3-(4-Methylbenzylidene)-2-phenylisoindolin-1-one **189**:

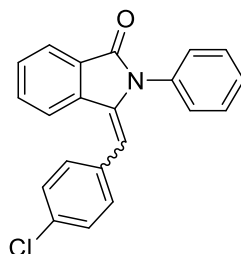


Synthesized according to the general procedure VI on a 0.3 mmol scale; **189** (0.066 g, 71% yield, *E/Z* = 9:1).

Major product: *E*-isomer: colourless oil, ^1H NMR (500 MHz, CDCl_3): δ = 7.94 (dd, J = 7.5, 1.0 Hz, 1H, *ArH*), 7.58 – 7.53 (m, 2H, *ArH*), 7.52 – 7.42 (m, 5H, *ArH*), 7.39 (td, J = 7.6, 1.2 Hz, 1H, *ArH*), 7.30 (d, J = 7.9 Hz, 2H, *ArH*), 7.21 (d, J = 7.9 Hz, 2H, *ArH*), 6.34 (s, 1H, $\text{NC}=\text{CH}$), 2.41 (s, 3H, ArCH_3) ppm. ^{13}C NMR (126 MHz, CDCl_3): δ 166.4, 137.9, 137.8, 135.1, 135.0, 132.2, 131.9, 130.1, 129.6, 129.6, 129.5, 129.4, 129.1, 128.5, 123.7, 123.3, 112.7, 21.5 ppm. IR (neat): 3017, 2970, 2945, 1738, 1724, 1371, 1366, 1354, 1229, 1217, 1206, 756, 694, 538, 527, 517 cm^{-1} . HRMS (NSI) $[\text{M}+\text{H}]^+$ calc. 312.1383, found 312.1384 $[\text{C}_{22}\text{H}_{18}\text{NO}]^+$.

Minor product: *Z*-isomer: (overlapping with *E* isomer) ^1H NMR (500 MHz, CDCl_3): δ = 7.96 – 7.93 (m, 1H, *ArH*), 7.85 (d, J = 7.8 Hz, 1H, *ArH*), 7.67 (td, J = 7.6, 1.1 Hz, 1H, *ArH*), 7.52 (d, J = 0.8 Hz, 1H, *ArH*), 7.12 – 7.07 (m, 6H, *ArH*), 6.81 (s, 1H, $\text{NC}=\text{CH}$), 6.76 – 6.71 (m, 3H, *ArH*), 2.19 (s, 3H, ArCH_3) ppm. ^{13}C NMR (126 MHz, CDCl_3): δ = 168.1, 138.9, 136.7, 136.2, 133.9, 132.5, 130.7, 129.2, 128.3, 128.1, 127.9, 127.3, 126.7, 124.0, 119.4, 108.1, 21.3 ppm. Spectra in accordance to literature.^[19]

3-(4-Chlorobenzylidene)-2-phenylisoindolin-1-one **190**:



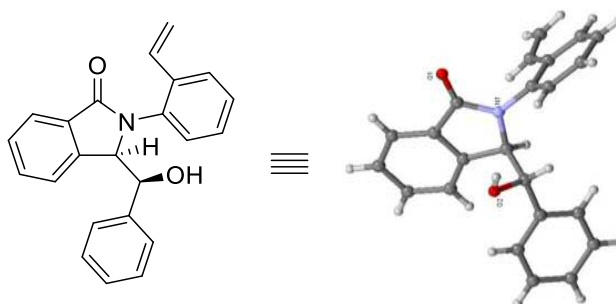
Synthesized according to the general procedure VI on a 0.28 mmol scale; **190** (0.068 g, 73% yield, *E/Z* = 7:1).

Major product: *E*-isomer: colourless oil: ^1H NMR (500 MHz, CDCl_3): δ = 7.97 – 7.91 (m, 1H, *ArH*), 7.59 – 7.32 (m, 12H, *ArH*), 6.27 (s, 1H, $\text{NC}=\text{CH}$) ppm. ^{13}C NMR (126 MHz, CDCl_3): δ = 166.4, 138.8, 134.8, 134.8, 133.8, 133.8, 132.1, 131.0, 130.2, 130.0, 129.7, 129.1, 129.0, 128.7, 123.9, 123.2, 110.8 ppm. IR (neat): 3017, 2970, 2947, 1736, 1717, 1489, 1366, 1354, 1229, 1217, 1206, 1125, 1092, 760, 692, 527, 517 cm^{-1} . HRMS (NSI) $[\text{M}+\text{H}]^+$ calc. 332.0837, found 332.0839 $[\text{C}_{21}\text{H}_{15}\text{ClNO}]^+$.

Minor product: *Z*-isomer: (overlapping with *E* isomer): ^1H NMR (500 MHz, CDCl_3): δ = 7.85 (d, J = 7.8 Hz, 1H, ArH), 7.68 (td, J = 7.6, 1.0 Hz, 1H, ArH), 7.45 – 7.44 (m, 2H, ArH), 7.16 – 7.11 (m, 3H, ArH), 7.10 – 7.04 (m, 2H, ArH), 6.91 – 6.87 (m, 2H, ArH), 6.78 (d, J = 8.3 Hz, 2H, ArH), 6.74 (s, 1H, NC=CH) ppm. ^{13}C NMR (126 MHz, CDCl_3): δ = 168.0, 138.6, 135.9, 135.1, 132.7, 132.6, 132.3, 130.4, 129.6, 128.5, 127.9, 127.5, 127.4, 127.1, 124.1, 119.5, 106.1 ppm. Spectra in accordance to literature.^[19]

6.3.5. Reduction products

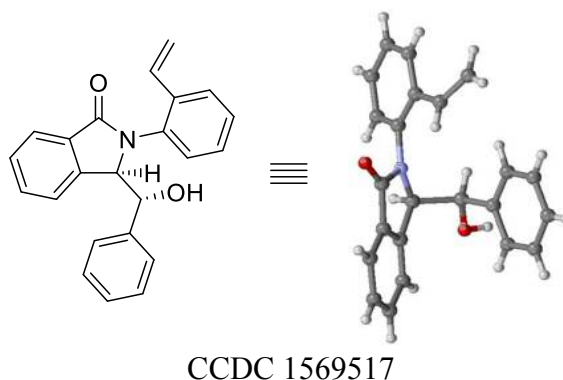
(*R,S/S,R*)-3-(Hydroxy(phenyl)methyl)-2-(2-vinylphenyl)isoindolin-1-one **183a**:



CCDC 1569515

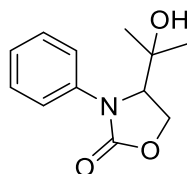
Procedure:^[20] To a solution of 3-(phenyl((2,2,6,6-tetramethylpiperidin-1-yl)oxy)methyl)-2-(2-vinylphenyl)isoindolin-1-one (**178pa**) (0.18 mmol, 84 mg) in THF/AcOH/H₂O (2 mL, 1:3:1 v/v) was added zinc dust (2.16 mmol, 141 mg) at room temperature. The resulting mixture was heated up at 50 °C for 3 h. After that time, the reaction was cooled to room temperature, filtered through a plug of celite, treated with a solution of sodium hydroxide (20 mL, 1 M) and extracted with ethyl acetate (3 x 20 mL). The combined organic layers were dried over MgSO_4 , concentrated *in vacuo* and the product was purified by column chromatography (*n*-hexane/ethylacetate, 7:3), giving 0.026 g of the desired product **183a** in 42% yield as a colourless solid.

^1H NMR (400 MHz, CDCl_3): δ = 7.95 (d, J = 7.5 Hz, 1H), 7.77 – 7.65 (m, 1H), 7.63 – 7.29 (m, 8H), 6.80 – 6.65 (m, 1H), 6.54 – 6.33 (m, 1H), 5.88 – 5.76 (m, 1H), 5.45 – 5.36 (m, 1H), 5.34 – 5.20 (m, 1H), 5.02 – 4.90 (m, 1H) ppm. ^{13}C NMR (126 MHz, CDCl_3): δ = 131.4, 129.2, 129.0, 128.7, 128.66, 128.0, 127.4, 125.8, 124.4, 124.0, 70.7, 68.3 ppm. IR (neat): 3377, 1684, 1485, 1454, 1696, 714, 708 cm^{-1} . HRMS (NSI) $[\text{M}+\text{H}]^+$ calc. 342.1489, found 342.1493 $[\text{C}_{23}\text{H}_{20}\text{NO}_2]^+$. m.p. = 190 – 192 °C.

(*R,R/S,S*)-3-(Hydroxy(phenyl)methyl)-2-(2-vinylphenyl)isoindolin-1-one 183b:

Procedure:^[20] To a solution of 3-(phenyl((2,2,6,6-tetramethylpiperidin-1-yl)oxy)methyl)-2-(2-vinylphenyl)isoindolin-1-one **178pb** (0.06 mmol, 28 mg) in THF/AcOH/H₂O (1 mL, 1:3:1 v/v) was added zinc dust (0.72 mmol, 47 mg) at room temperature. The resulting mixture was heated up at 50 °C for 3 h. After that time, the reaction was cooled to room temperature, filtered through a plug of celite, treated with a solution of sodium hydroxide (10 mL, 1 M) and extracted with ethyl acetate (3 x 20 mL). The combined organic layers were dried over MgSO₄, concentrated *in vacuo* and the product was purified by preparative TLC (*n*-hexane/ethyl acetate, 8:2), giving 0.006 g of the desired product **183b** in 30% yield as a colourless solid.

¹H NMR (400 MHz, CDCl₃): δ = 7.93 – 7.82 (m, 1H), 7.65 – 7.56 (m, 1H), 7.56 – 7.45 (m, 2H), 7.35 – 7.28 (m, 2H), 7.25 – 7.12 (m, 4H), 7.08 – 6.96 (m, 2H), 6.80 – 6.52 (m, 1H), 5.87 – 5.67 (m, 1H), 5.52 – 5.42 (m, 1H), 5.34 – 5.25 (m, 2H), 4.98 – 4.90 (m, 1H) ppm. ¹³C NMR (126 MHz, CDCl₃): δ = 158.5, 142.4, 139.0, 135.7, 132.43, 131.7, 129.0, 128.6, 128.3, 128.0, 127.3, 124.4, 124.3 ppm. IR (neat): 3385, 1680, 1487, 1454, 1389, 756, 710 cm⁻¹. HRMS (NSI) [M+H]⁺ calc. 342.1489, found 342.1491 [C₂₃H₂₀NO₂]⁺.

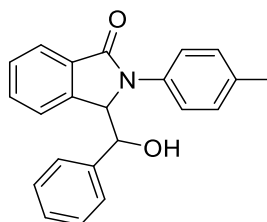
4-(2-Hydroxypropan-2-yl)-3-phenyloxazolidin-2-one 194:

General procedure VII: 3-Methylbut-2-en-1-yl phenylcarbamate **154** (0.133 g, 0.5 mmol) was dissolved in a mixture of acetonitrile/water (19:1 v/v, 10 mL). TEMPO (0.117 g, 0.75 mmol) and benzyltrimethylammonium hydroxide solution (40% w/w, 0.099 g, 0.25 mmol) were added to the solution, and it was introduced in the electrochemical reactor

(0.205 mL inner volume; 24 mA; 3 F/mol) using a syringe pump (0.1 mL/min). The outlet of the microreactor was connected to a T-piece that was connected to a second syringe pump, pumping a mixture of AcOH and water (1:1 v/v, 0.1 mL/min). The resulting mixture was introduced into a cartridge of Zn dust (<10 μm) supported on silica (60-100 mesh, 50% w/w) at 40 °C. After reaching the steady state, the solution was collected for 50 min. The outlet was filtered through a plug of celite, treated with a solution of sodium hydroxide (10 mL, 1M) and extracted with ethyl acetate (3 x 20 mL). The combined organic layers were dried over MgSO_4 , concentrated *in vacuo* and the product was purified by column chromatography (*n*-hexane/ethyl acetate, 6:4), giving 0.049 g of product **194** in 80% yield.

^1H NMR (500 MHz, CDCl_3): δ = 7.46 – 7.36 (m, 4H, ArH), 7.22 (dd, J = 10.3, 4.2 Hz, 1H, ArH), 4.60 – 4.33 (m, 3H, -N-CH-CH₂-O-), 1.15 (s, 3H, CHCH₃), 1.09 (s, 3H, CHCH₃) ppm. ^{13}C NMR (126 MHz, CDCl_3): δ = 156.9, 138.1, 129.4, 126.4, 124.2, 73.1, 64.5, 64.4, 27.0, 25.0 ppm. IR (neat): 3447, 2970, 2940, 1736, 1724, 1501, 1408, 1366, 1217, 1128, 1063, 1045, 953, 762, 694, 677, 419 cm^{-1} . m.p. = 88 – 90 °C. HRMS (NSI) $[\text{M}+\text{H}]^+$ calc. 222.1125, found 222.1124 $[\text{C}_{12}\text{H}_{16}\text{NO}_3]^+$.

3-(Hydroxy(phenyl)methyl)-2-(*p*-tolyl)isoindolin-1-one **195**:

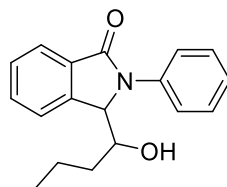


Synthesized according to the general procedure VII on a 0.33 mmol scale; **195** as a colourless solid (0.075 g, 54% yield).

^1H NMR (500 MHz, CDCl_3): δ = 7.79 (d, J = 7.6 Hz, 1H, ArH), 7.66 (d, J = 7.6 Hz, 1H, ArH), 7.58 – 7.49 (m, 3H, ArH), 7.41 (t, J = 7.5 Hz, 1H, ArH), 7.28 (d, J = 8.2 Hz, 2H, ArH), 7.08 (t, J = 7.3 Hz, 1H, ArH), 7.01 (t, J = 7.5 Hz, 2H, ArH), 6.74 (d, J = 7.3 Hz, 2H, ArH), 5.62 (d, J = 4.6 Hz, 1H, N-CHCH-OH), 5.21 (d, J = 4.5 Hz, 1H, N-CHCH-OH), 2.43 (bs, 1H, -OH), 2.40 (s, 3H, ArCH₃) ppm. ^{13}C NMR (126 MHz, CDCl_3): δ = 167.4, 141.4, 137.7, 135.3, 135.0, 132.9, 131.5, 130.0, 128.8, 128.3, 127.8, 126.8, 124.9, 123.8, 123.1, 73.9, 64.5, 21.2 ppm. IR (neat): 3391, 3030, 2970, 2924, 1738, 1670, 1508,

1387, 1366, 1217, 1055, 804, 750, 704, 517 cm^{-1} . m.p. = 198 – 200 °C. HRMS (NSI) $[\text{M}+\text{H}]^+$ calc. 330.1489, found 330.1491 $[\text{C}_{22}\text{H}_{20}\text{NO}_2]^+$.

3-(1-Hydroxybutyl)-2-phenylisoindolin-1-one 196:

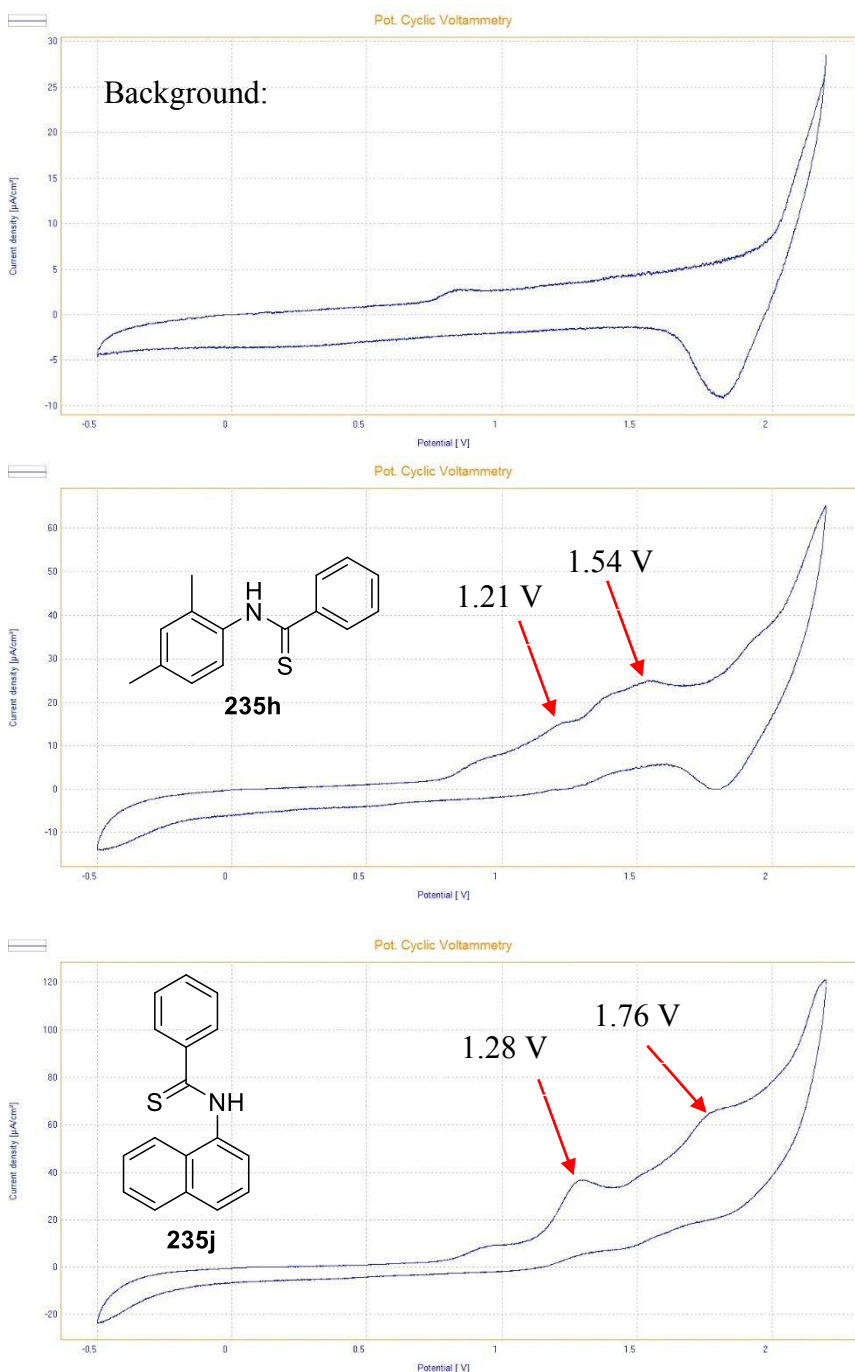


Synthesized according to the general procedure VII on a 0.36 mmol scale; **196** as a colourless solid (0.067 g, 66% yield, d.r.: 2.05:1).

Major product: ^1H NMR (500 MHz, CDCl_3): δ = 7.94 (d, J = 7.5 Hz, 1H, ArH), 7.76 (d, J = 7.6 Hz, 1H, ArH), 7.63 – 7.50 (m, 4H, ArH), 7.47 – 7.41 (m, 2H, ArH), 7.25 – 7.22 (m, 1H, ArH), 5.37 (d, J = 3.9 Hz, 1H, N-CHCH-OH), 4.14 – 4.03 (m, 1H, N-CHCH-OH), 1.90 (s, 1H, -OH), 1.40 – 1.25 (m, 2H, $\text{OCHCH}_2\text{CH}_2\text{CH}_3$), 1.14 – 0.97 (m, 2H, $\text{OCHCH}_2\text{CH}_2\text{CH}_3$), 0.67 (t, J = 7.3 Hz, 3H, $\text{OCHCH}_2\text{CH}_2\text{CH}_3$) ppm. ^{13}C NMR (126 MHz, CDCl_3): δ = 167.8, 142.5, 137.3, 132.9, 132.1, 129.4, 128.8, 126.0, 124.3, 124.1, 123.8, 71.0, 64.6, 32.3, 19.0, 13.9 ppm. IR (neat): 3368, 2957, 2932, 2872, 1736, 1663, 1597, 1499, 1456, 1393, 1217, 1105, 1005, 758, 702, 694, 507 cm^{-1} . m.p. = 148 – 150 °C. HRMS (NSI) $[\text{M}+\text{H}]^+$ calc. 282.1489, found 282.1490 $[\text{C}_{18}\text{H}_{20}\text{NO}_2]^+$.

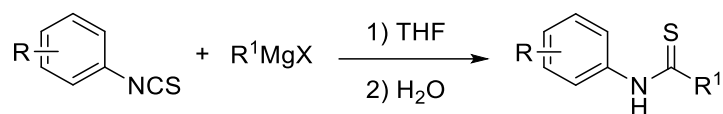
6.4. Experimental data for Chapter 4: Electrochemical synthesis of Benzothiazoles from *N*-arylthioamides in flow

6.4.1. Cyclovoltammetric measurements



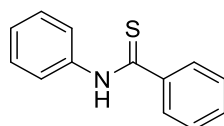
Oxidative cyclic voltammograms of the substrates (1 mM) recorded in 0.075 M $\text{Bu}_4\text{NBF}_4/\text{MeCN}$ electrolyte at 100 mV/s scan rate. Working electrode: glassy carbon electrode tip (3 mm diameter); Counter electrode: platinum wire; Reference electrode: Ag/AgCl in 3 M NaCl .

6.4.2. Synthesis of substrates



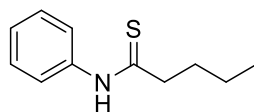
General Procedure VIII: To a solution of phenylisothiocyanate (1.0 equiv) in dry THF (0.8 M) was added dropwise a dry THF solution of Grignard reagent (1.0 equiv) at 0 °C. The reaction mixture was left to warm up to room temperature, and stirred for another 2 h. The reaction was quenched with water (10 mL), extracted with dichloromethane (3 x 10 mL). The combined organic solution was washed with brine and dried over anhydrous MgSO₄. The solvent was evaporated under reduced pressure, and the residue was purified by flash column chromatography (*n*-hexane/ethyl acetate) to give the desired compound.

N-Phenylbenzothioamide (235a):



The title compound **235a** was prepared as a yellow solid in 90% yield (0.924 g) according to the General Procedure VIII on a 4.8 mmol scale using *n*-butylmagnesium bromide solution in THF (2 M, 2.4 mL). ¹H NMR (400 MHz, CDCl₃): δ = 9.02 (br s, 1H), 7.93–7.71 (m, 4H), 7.57–7.38 (m, 5H), 7.35–7.28 (m, 1H) ppm. The spectral data were consistent with those reported.^[21]

N-Phenylpentanethioamide (235b):

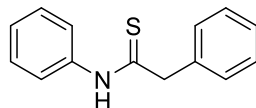


The title compound **235b** was prepared as a yellow solid in 98% yield (0.912 g) according to the General Procedure I on a 4.8 mmol scale using *n*-butylmagnesium chloride solution in THF (2 M, 2.4 mL). The title compound exists as a mixture of rotamers in a ratio of 3:1.

¹H NMR (400 MHz, CDCl₃): δ = 9.39 (br s, 0.25H), 8.67 (br s, 0.75H), 7.66 (d, *J* = 7.9 Hz, 1.5H), 7.49–7.33 (m, 2.25H), 7.30–7.22 (m, 0.71H), 7.16 (d, *J* = 7.6 Hz, 0.5H), 2.86–2.77 (m, 1.5H), 2.66–2.57 (m, 0.5H), 1.92–1.80 (m, 1.5H), 1.80–1.69 (m, 0.5H), 1.50–

1.39 (m, 1.5H), 1.34–1.22 (m, 0.5H), 0.97 (t, $J = 7.4$ Hz, 2.25H), 0.82 (t, $J = 7.3$ Hz, 0.75H) ppm. The spectral data were consistent with those reported.^[22]

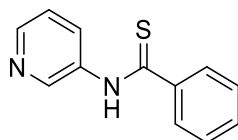
***N*,2-Diphenylethanethioamide (235c):**



The title compound **235c** was prepared as a yellow solid in 73% yield (0.664 g) according to the General Procedure VIII on a 4.8 mmol scale using benzylmagnesium chloride solution in THF (2 M, 2.4 mL). The reaction was stirred at room temperature for 24 h. The title compound exists as a mixture of rotamers in a ratio of 9:1.

¹H NMR (400 MHz, CDCl₃): $\delta = 9.35$ (br s, 0.1H), 8.44 (br s, 0.9H), 7.55 (d, $J = 8.0$ Hz, 1.85H), 7.49–7.41 (m, 1.91H), 7.40–7.32 (m, 4.89H), 7.27–7.16 (m, 0.9H), 7.14–7.05 (m, 0.30H), 7.04–6.96 (m, 0.25H), 4.29 (s, 1.8H), 4.07 (s, 0.2H) ppm. The spectral data were consistent with those reported.^[23]

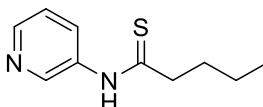
***N*-(Pyridin-3-yl)benzothioamide (235d):**



The title compound **235d** was synthesized as a yellow solid in 91% yield (0.936 g) according to the General Procedure VIII on a 4.8 mmol scale using 3-pyridyl isothiocyanate (0.654 g).

¹H NMR (400 MHz, CDCl₃): $\delta = 9.36$ (br s, 1H), 8.70 (br s, 1H), 8.55–8.47 (m, 1H), 8.45 (d, $J = 4.7$ Hz, 1H), 7.86 (d, $J = 5.9$ Hz, 2H), 7.61–7.34 (m, 4H) ppm. The spectral data were consistent with those reported.^[25]

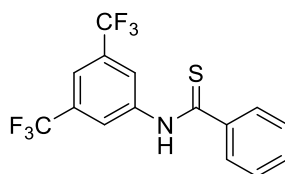
***N*-(Pyridin-3-yl)pentanethioamide (235e):**



The title compound **235e** was synthesized as an orange oil in 99% yield (0.923 g) according to the General Procedure I on a 4.8 mmol scale using 3-pyridyl isothiocyanate (0.654 g). The title compound exists as a mixture of rotamers in a ratio of 9:1.

^1H NMR (400 MHz, CDCl_3): $\delta = 9.44$ (br s, 0.1H), 9.29 (br s, 0.9H), 8.66–8.57 (m, 1H), 8.52 (s, 0.1H), 8.48–8.40 (m, 1.8H), 7.57–7.51 (m, 0.1H), 7.41–7.31 (m, 1H), 2.90–2.81 (m, 1.8H), 2.63–2.56 (m, 0.2H), 1.93–1.82 (m, 1.8H), 1.79–1.69 (m, 0.2H), 1.50–1.38 (m, 1.8H), 1.34–1.26 (m, 0.2H), 0.96 (t, $J = 7.3$ Hz, 2.7H), 0.93–0.87 (m, 0.3H) ppm. ^{13}C NMR (126 MHz, CDCl_3): $\delta = 207.4, 146.4, 144.6, 136.5, 132.2, 123.7, 47.9, 32.0, 22.1, 13.9$ ppm. IR (neat): 3181, 3017, 2970, 2928, 1541, 1456, 1423, 1366, 1217, 901, 719, 527 cm^{-1} . HRMS (ASAP) $[\text{M}+\text{H}]^+$ calc. 195.0956, found 195.0956 $[\text{C}_{10}\text{H}_{15}\text{N}_2\text{S}]^+$.

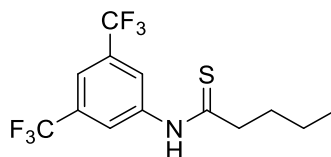
***N*-(3,5-bis(Trifluoromethyl)phenyl)benzothioamide (235f):**



The title compound **235f** was synthesized as a yellow solid in 97% yield (1.63g) according to the General Procedure VIII on a 4.8 mmol scale using 3,5-bis-(trifluoro)phenyl isothiocyanate (1.30 g).

^1H NMR (500 MHz, CDCl_3): $\delta = 9.20$ (br s, 1H), 8.28 (br s, 2H), 7.84–7.74 (m, 3H), 7.57–7.50 (m, 1H), 7.48–7.39 (m, 2H) ppm. ^{13}C NMR (126 MHz, CDCl_3): $\delta = 199.8, 142.5, 140.3, 132.5$ (q, $J = 33.9$ Hz), 132.1, 129.0, 126.8, 123.7, 123.0 (q, $J = 272.9$ Hz), 120.2, ppm. ^{19}F NMR (376 MHz, CDCl_3): $\delta = -63.0$ ppm. m.p. = 90–92 $^\circ\text{C}$. IR (neat): 3131, 3020, 2955, 2889, 1531, 1448, 1375, 1277, 1232, 1128, 1007, 889, 692, 681 cm^{-1} . HRMS (ASAP) $[\text{M}+\text{H}]^+$ calc. 350.0438, found 350.0437 $[\text{C}_{15}\text{H}_{10}\text{F}_6\text{NS}]^+$.

***N*-(3,5-bis(Trifluoromethyl)phenyl)pentanethioamide (235g):**

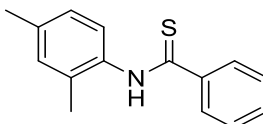


The title compound **235g** was synthesized as a yellow solid in 98% yield (1.55g) according to the General Procedure VIII on a 4.8 mmol scale using 3,5-bis-(trifluoro)phenyl isothiocyanate (1.30 g).

^1H NMR (500 MHz, CDCl_3): $\delta = 8.76$ (br s, 1H), 8.28 (br s, 2H), 7.75 (br s, 1H), 2.89–2.79 (m, 2H), 1.92–1.81 (m, 2H), 1.50–1.40 (m, 2H), 0.97 (t, $J = 7.3$ Hz, 3H) ppm. ^{13}C

NMR (126 MHz, CDCl₃): δ = 206.8, 139.9, 132.4 (q, J = 33.8 Hz), 123.6, 123.0 (q, J = 272.9 Hz), 120.1, 49.2, 31.8, 22.2, 13.9 ppm. ¹⁹F NMR (376 MHz, CDCl₃): δ = -63.0 ppm. m.p. = 36–38 °C. IR (neat): 3146, 3031, 2961, 1533, 1466, 1375, 1275, 1171, 1125, 1078, 895, 725, 700, 681 cm⁻¹. HRMS (ASAP) [M+H]⁺ calc. 330.0751, found 330.0754 [C₁₃H₁₄F₆NS]⁺.

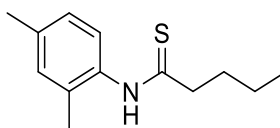
***N*-(2,4-Dimethylphenyl)benzothioamide (235h):**



The title compound **235h** was synthesized as a yellow solid in 67% yield (0.776g) according to the General Procedure VIII on a 4.8 mmol scale using 2,4-dimethylphenyl isothiocyanate (0.784 g). The title compound exists as a mixture of rotamers in a ratio of 9:1.

¹H NMR (400 MHz, CDCl₃) δ 9.23 (br s, 0.1H), 8.76 (br s, 0.9H), 7.97–7.87 (m, 1.8H), 7.77 (d, J = 7.0 Hz, 0.2 H), 7.63–7.38 (m, 4H), 7.18–7.04 (m, 2H), 2.36 (s, 2.7H), 2.32 (s, 0.6H), 2.30 (s, 2.7H). ¹³C NMR (126 MHz, CDCl₃): δ = 199.7, 142.2, 138.1, 134.1, 131.8, 131.4, 128.9, 128.7, 127.6, 126.9, 126.7, 21.3, 17.9 ppm. m.p. = 100–102 °C. IR (neat): 3157, 2961, 2920, 1499, 1450, 1348, 1207, 989, 764, 746, 689, 625 cm⁻¹. HRMS (ASAP) [M+H]⁺ calc. 242.1003, found 242.1006 [C₁₅H₁₆NS]⁺.

***N*-(2,4-Dimethylphenyl)pentanethioamide (235i):**

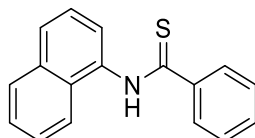


The title compound **235i** was synthesized as an orange solid in 80% yield (0.850g) according to the General Procedure VIII on a 4.8 mmol scale using 2,4-dimethylphenyl isothiocyanate (0.784 g). The title compound exists as a mixture of rotamers in a ratio of 2:1.

¹H NMR (400 MHz, CDCl₃): δ = 8.97 (s, 0.33H), 8.37 (s, 0.67H), 7.26–7.22 (m, 0.67H), 7.13–6.98 (m, 2.33H), 2.87–2.81 (m, 1.34H), 2.49–2.42 (m, 0.66H), 2.36–2.32 (m, 3H), 2.25–2.21 (m, 3H), 1.94–1.83 (m, 1.34H), 1.75–1.65 (m, 0.66H), 1.53–1.41 (m, 1.34H), 1.31–1.19 (m, 0.66H), 0.98 (t, J = 7.4 Hz, 2H), 0.85–0.77 (t, 7.4 Hz, 1H) ppm. ¹³C NMR

(126 MHz, CDCl₃): δ = 210.6, 206.9, 138.9, 138.1, 134.8, 134.3, 134.2 (2C), 131.9, 131.7, 127.7, 127.5, 127.1, 127.0, 47.4, 40.0, 31.9, 31.6, 22.3 (2C), 21.2, 21.1, 18.0, 17.9, 14.0, 13.8 ppm. m.p. = 34–36 °C. IR (neat): 3146, 2961, 2922, 2860, 1522, 1456, 1375, 1227, 1167, 1078, 737, 691, 635 cm⁻¹. HRMS (ASAP) [M+H]⁺ calc. 222.1317, found 222.1317 [C₁₃H₂₀NS]⁺.

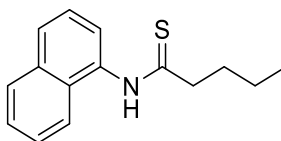
***N*-(Naphthalen-1-yl)benzothioamide (235j):**



The title compound **235j** was synthesized as an orange solid in 89% yield (1.12 g) according to the General Procedure VIII on a 4.8 mmol scale using 1-naphthyl isothiocyanate (0.890 g). The title compound exists as a mixture of rotamers in a ratio of 9:1.

¹H NMR (400 MHz, CDCl₃): δ = 9.67 (br s, 0.1H), 9.20 (br s, 0.9H), 8.06–7.97 (m, 1.8H), 7.96–7.86 (m, 3.3H), 7.78 (m, 1.1H), 7.67–7.44 (m, 5.7H), 7.39–7.34 (m, 0.2H), 7.23–7.17 (m, 0.1H), 7.14–7.05 (m, 0.1H) ppm. ¹³C NMR (101 MHz, CDCl₃): δ = 200.7, 142.2, 135.0, 134.4, 131.7, 129.0, 128.9 (2C), 128.7, 127.1, 127.0, 126.6, 125.6, 124.9, 122.0 ppm. m.p. = 144–146 °C. IR (neat): 3169, 3017, 2970, 2951, 1497, 1445, 1366, 1229, 1217, 980, 766, 692, 523 cm⁻¹. HRMS (ASAP) [M+H]⁺ calc. 264.0847, found 264.0846 [C₁₇H₁₄NS]⁺.

***N*-(Naphthalen-1-yl)pentanethioamide (235k):**

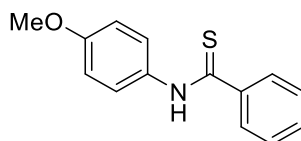


The title compound **235k** was synthesized as an orange solid in 85% yield (0.993g) according to the General Procedure VIII on a 4.8 mmol scale using 1-naphthyl isothiocyanate (0.890 g). The title compound exists as a mixture of rotamers in a ratio of 1.2:1.

¹H NMR (400 MHz, CDCl₃): δ = 9.36 (br s, 0.55H), 8.74 (br s, 0.45H), 7.88 (m, 3H), 7.69 (d, *J* = 7.3 Hz, 0.55H), 7.65–7.49 (m, 3H), 7.38 (d, *J* = 7.1 Hz, 0.45H), 3.05–2.97

(m, 1.1H), 2.49–2.41 (m, 0.9H), 2.06–1.95 (m, 1.1H), 1.69 (m, 0.9H), 1.61–1.51 (m, 1.1H), 1.16 (m, 0.9H), 1.04 (t, $J = 7.4$ Hz, 1.65H), 0.71 (t, $J = 7.3$ Hz, 1.35H) ppm. ^{13}C NMR (126 MHz, CDCl_3): $\delta = 211.9, 208.0, 134.7, 134.4$ (2C), 134.0, 129.9, 129.4, 129.1, 128.9, 128.6 (2C), 127.8, 127.2, 127.0, 126.5, 125.5 (2C), 125.2, 124.9, 122.4, 121.9, 47.8, 40.4, 32.0, 31.9, 22.4, 22.2, 14.1, 13.8 ppm. m.p. = 62–64 °C. IR (neat): 3121, 2955, 2926, 2862, 1508, 1375, 1217, 1088, 760, 733, 706, 511 cm^{-1} . HRMS (ASAP) $[\text{M}+\text{H}]^+$ calc. 245.1160, found 245.1162 $[\text{C}_{15}\text{H}_{18}\text{NS}]^+$.

***N*-(4-Methoxyphenyl)benzothioamide (235I):**

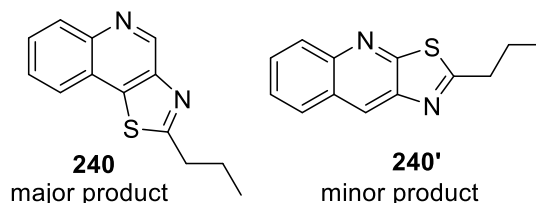


The title compound **235I** was synthesized as a yellow solid in 65% yield (0.759 g) according to the General Procedure VIII on a 4.8 mmol scale using 4-methoxyphenyl isothiocyanate (0.793 g). The reaction mixture was stirred at room temperature for 32 h. The title compound exists a mixture of rotamers in a ratio of 12:1.

^1H NMR (400 MHz, CDCl_3): $\delta = 8.94$ (br s, 1H), 7.92–7.81 (m, 2H), 7.69–7.59 (m, 2H), 7.55–7.49 (m, 1H), 7.47–7.39 (m, 2H), 7.02–6.93 (m, 2H), 3.84 (s, 3H) ppm. The spectral data were consistent with those reported.^[24]

6.4.3. Electrochemical synthesis of benzothiazoles

2-Propylthiazolo[4,5-*c*]quinoline (240) and 2-Propylthiazolo[5,4-*b*]quinoline (240'):



General Procedure IX: A solution of the corresponding thioamide (0.6 mmol) in methanol/acetonitrile (12 mL, 1:1 v/v) was pumped through the electrochemical reactor (0.25 mL inner volume) *via* a syringe pump (0.2 mL min^{-1}), using the corresponding amount of electricity (F). After reaching the steady state, the solution was collected for

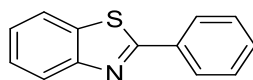
50 minutes. The solvent was evaporated under reduced pressure, and the crude mixture was purified by flash column chromatography.

The title compound was prepared using 2.5 F (53 min collection). Purification using column chromatography (*n*-hexane/ethyl acetate, 9:1) afforded compound **240** as a mixture of regioisomers (0.121 g) in 97% yield.

Major product (0.119 g, 95%): ^1H NMR (400 MHz, CDCl_3): δ = 9.45 (s, 1H), 8.24 (d, J = 8.4 Hz, 1H), 7.98 (d, J = 8.1 Hz, 1H), 7.74 (t, J = 7.3 Hz, 1H), 7.64 (t, J = 7.5 Hz, 1H), 3.21 (t, J = 7.6 Hz, 2H), 2.05–1.91 (m, 2H), 1.10 (t, J = 7.4 Hz, 3H) ppm. The spectral data were consistent with those reported.^[26]

Minor product (0.002 g, 2%): ^1H NMR (400 MHz, CDCl_3): δ = 8.61 (s, 1H), 8.14 (d, J = 8.6 Hz, 1H), 8.01 (d, J = 8.3 Hz, 1H), 7.81–7.73 (m, 1H), 7.62–7.55 (m, 1H), 3.15 (t, J = 7.6 Hz, 2H), 2.04–1.92 (m, 2H), 1.10 (t, J = 7.4 Hz, 3H) ppm.

2-Phenylbenzo[*d*]thiazole (**241a**):

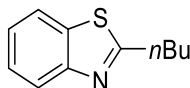


The title compound was prepared according to the General Procedure IX (a small amount H_2O was added as the additive (5.8 mL MeOH, 5.8 mL MeCN and 0.4 mL H_2O)) using starting material **235a** (50 min collection), 2.6 F. Purification using column chromatography (*n*-hexane/ethyl acetate, 9:1) afforded compound **241a** in 96% yield as a colourless solid.

Large-scale reaction: This reaction was run in a 13 mmol scale (2.77 g **235a**, 84 mL MeCN, 84 mL MeOH, 6 mL H_2O) at a flow rate of 0.4 mL min^{-1} . The title compound was obtained in 87% yield, 2.6 F.

^1H NMR (500 MHz, CDCl_3): δ = 8.13–8.05 (m, 3H), 7.91 (d, J = 8.0 Hz, 1H), 7.52–7.47 (m, 4H), 7.39 (t, J = 7.6 Hz, 1H) ppm. ^{13}C NMR (126 MHz, CDCl_3): δ = 168.7, 153.2, 136.8, 133.3, 131.5, 130.0, 129.3, 127.7, 124.5, 124.3, 118.9 ppm. The spectral data were consistent with those reported.^[27]

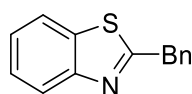
2-Butylbenzo[*d*]thiazole (**241b**):



The title compound was prepared according to the General Procedure IX using starting material **235b**, 2.5 F. Purification using column chromatography (*n*-hexane/ethyl acetate, 9:1) afforded compound **241b** (0.085 g) in 81% yield as a yellow oil.

^1H NMR (400 MHz, CDCl_3): $\delta = 7.97$ (d, $J = 8.1$ Hz, 1H), 7.84 (d, $J = 8.0$ Hz, 1H), 7.45 (t, $J = 7.7$ Hz, 1H), 7.35 (t, $J = 6.5$ Hz, 1H), 3.17–3.09 (m, 2H), 1.92–1.81 (m, 2H), 1.54–1.41 (m, 2H), 0.98 (t, $J = 7.4$ Hz, 3H) ppm. The spectral data were consistent with those reported.^[28]

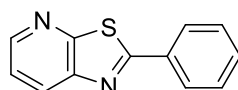
2-Benzylbenzo[*d*]thiazole (**241c**):



The title compound was prepared according to the General Procedure IX using starting material **235c**, 4.0 F. Purification using column chromatography (*n*-hexane/ethyl acetate, 9:1) afforded compound **241c** (0.079 g) in 64% yield as a yellow oil.

^1H NMR (500 MHz, CDCl_3): $\delta = 8.03$ –7.99 (m, 1H), 7.81–7.77 (m, 1H), 7.48–7.43 (m, 1H), 7.41–7.27 (m, 6H), 4.45 (s, 2H) ppm. The spectral data were consistent with those reported.^[29]

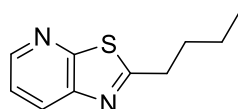
2-Phenylthiazolo[4,5-*c*]pyridine (**241d**):



The title compound was prepared according to the General Procedure IX using starting material **235d**, 3.0 F. Purification using column chromatography (*n*-hexane/ethyl acetate, 8:2) afforded compound **241d** (0.095 g) in 81% yield as a pale yellow solid (mixture of regioisomers, 1:0.07).

^1H NMR (500 MHz, CDCl_3): $\delta = 8.55$ (dd, $J = 4.7, 1.5$ Hz, 1H), 8.26 (dd, $J = 8.2, 1.6$ Hz, 1H), 8.11–8.06 (m, 2H), 7.52–7.47 (m, 3H), 7.42 (dd, $J = 8.2, 4.6$ Hz, 1H) ppm. The spectral data were consistent with those reported.^[32]

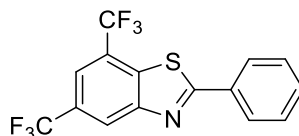
2-Butylthiazolo[4,5-*c*]pyridine (**241e**):



The title compound was prepared according to the General Procedure IX using starting material **235e**, 3.5 F. Purification using column chromatography (*n*-hexane/ethyl acetate, 8:2) afforded compound **241e** (0.092 g) in 87% yield as a colourless oil (mixture of regioisomers, 1:0.08).

^1H NMR (400 MHz, CDCl_3): δ = 8.51 (dd, J = 4.7, 1.5 Hz, 1H), 8.16 (dd, J = 8.2, 1.5 Hz, 1H), 7.37 (dd, J = 8.2, 4.7 Hz, 1H), 3.14–3.07 (m, 2H), 1.92–1.80 (m, 2H), 1.51–1.41 (m, 2H), 0.96 (t, J = 7.4 Hz, 3H) ppm. ^{13}C NMR (126 MHz, CDCl_3): δ = 173.7, 158.7, 146.6, 146.3, 129.5, 121.3, 34.9, 31.6, 22.4, 13.8 ppm. IR (neat): 3026, 2970, 2928, 1506, 1456, 1375, 1217, 1094, 802, 748, 527 cm^{-1} . HRMS (ASAP) $[\text{M}+\text{H}]^+$ calc. 193.0799, found 193.0800 $[\text{C}_{10}\text{H}_{13}\text{N}_2\text{S}]^+$.

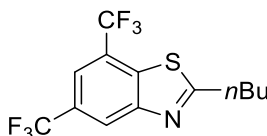
2-Phenyl-5,7-bis(trifluoromethyl)benzo[*d*]thiazole (241f):



The title compound was prepared according to the General Procedure IX using starting material **235f**, 3.0 F. Purification using column chromatography (*n*-hexane/ethyl acetate, 9:1) afforded give compound **241f** (0.145 g) in 76% yield as a colourless solid.

^1H NMR (500 MHz, CDCl_3): δ = 8.49 (s, 1H), 8.15–8.08 (m, 2H), 7.91 (s, 1H), 7.61–7.50 (m, 3H) ppm. ^{13}C NMR (126 MHz, CDCl_3): δ = 171.9, 155.5, 135.3, 132.4, 132.3, 129.5, 129.4 (q, J = 33.8 Hz), 128.0, 125.7 (q, J = 35.1 Hz), 123.7 (q, J = 3.6 Hz), 123.6 (q, J = 272.6 Hz), 123.2 (q, J = 273.0 Hz), 119.3 (hept, J = 4.2 Hz) ppm. ^{19}F NMR (376 MHz, CDCl_3): δ = -62.0, -63.6 ppm. m.p = 104–106 °C. IR (neat): 3026, 2970, 2947, 1483, 1449, 1366, 1269, 1229, 1198, 1117, 984, 883, 764, 685, 633, 600, 527 cm^{-1} . HRMS (ASAP) $[\text{M}+\text{H}]^+$ calc. 348.0282, found 348.0281 $[\text{C}_{15}\text{H}_8\text{F}_6\text{NS}]^+$.

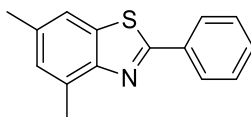
2-Butyl-5,7-bis(trifluoromethyl)benzo[*d*]thiazole (241g):



The title compound was prepared according to the General Procedure IX using starting material **235g**, 4.0 F. Purification using column chromatography (*n*-hexane/ethyl acetate, 9:1) afforded compound **241g** (0.131 g) in 73% yield as a yellow oil.

^1H NMR (400 MHz, CDCl_3): δ = 8.39 (s, 1H), 7.88 (s, 1H), 3.23–3.14 (m, 2H), 1.97–1.85 (m, 2H), 1.49 (dq, J = 14.7, 7.4 Hz, 2H), 0.99 (t, J = 7.4 Hz, 3H) ppm. ^{13}C NMR (101 MHz, CDCl_3): δ = 176.5, 154.7, 135.6, 129.0 (q, J = 33.7 Hz), 125.5 (q, J = 35.0 Hz), 123.7 (q, J = 272.4 Hz), 123.2 (q, J = 272.8 Hz), 123.1 (q, J = 3.5 Hz), 118.9 (hept, J = 3.9 Hz), 34.1, 31.6, 22.4, 13.8 ppm. ^{19}F NMR (376 MHz, CDCl_3): δ = -62.0, -63.7 ppm. IR (neat): 3015, 2970, 2945, 1456, 1364, 1275, 1217, 1128, 978, 895, 527 cm^{-1} . HRMS (ASAP) $[\text{M}+\text{H}]^+$ calc. 328.0595, found 328.0592 $[\text{C}_{13}\text{H}_{12}\text{F}_6\text{NS}]^+$.

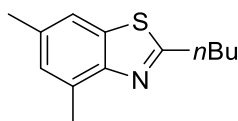
4,6-Dimethyl-2-phenylbenzo[*d*]thiazole (**241h**):



The title compound was prepared according to the General Procedure IX using starting material **235h**, 4.0 F. Purification using column chromatography (*n*-hexane/ethyl acetate, 9:1) afforded compound **241h** (0.088 g) in 67% yield as a colourless solid.

^1H NMR (500 MHz, CDCl_3): δ = 8.13–8.07 (m, 2H), 7.53–7.51 (m, 1H), 7.51–7.43 (m, 3H), 7.12–7.10 (m, 1H), 2.78 (s, 3H), 2.46 (s, 3H) ppm. The spectral data were consistent with those reported.^[33]

2-Butyl-4,6-dimethylbenzo[*d*]thiazole (**241i**):

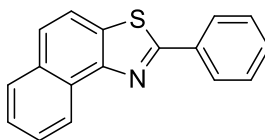


The title compound was prepared according to the General Procedure IX using starting material **235i**, 2.5 F. Purification using column chromatography (*n*-hexane/ethyl acetate, 9:1) afforded compound **241i** (0.096 g) in 80% yield as a yellow oil.

^1H NMR (400 MHz, CDCl_3): δ = 7.45 (s, 1H), 7.06 (s, 1H), 3.15 – 3.07 (m, 2H), 2.70 (s, 3H), 2.42 (s, 3H), 1.91–1.79 (m, 2H), 1.55–1.42 (m, 2H), 0.98 (t, J = 7.4 Hz, 3H) ppm. ^{13}C NMR (126 MHz, CDCl_3): δ = 170.2, 150.8, 135.3, 134.4, 131.9, 128.2, 118.8, 34.3,

32.2, 22.5, 21.5, 18.6, 13.9 ppm. IR (neat): 3015, 2953, 2926, 2858, 1522, 1456, 1366, 1217, 843, 748, 527 cm^{-1} . HRMS (ASAP) $[\text{M}+\text{H}]^+$ calc. 220.1160, found 220.1160 $[\text{C}_{13}\text{H}_{18}\text{NS}]^+$.

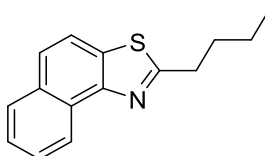
2-Phenylnaphtho[1,2-*d*]thiazole (241j):



The title compound was prepared according to the General Procedure IX using starting material **235j**, 2.5 F. Purification using column chromatography (*n*-hexane/ethyl acetate, 9:1) afforded compound **241j** (0.139 g) in 97% yield as a bright yellow solid.

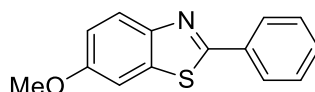
^1H NMR (500 MHz, CDCl_3): δ = 8.96–8.91 (m, 1H), 8.24–8.17 (m, 2H), 7.98–7.94 (m, 1H), 7.92 (d, J = 8.7 Hz, 1H), 7.81 (d, J = 8.7 Hz, 1H), 7.74–7.68 (m, 1H), 7.64–7.57 (m, 1H), 7.56–7.45 (m, 3H) ppm. m.p. = 106–108 °C (lit.^[30] m. p. = 110 °C). The spectral data were consistent with those reported.^[30,31]

2-Butylnaphtho[1,2-*d*]thiazole (241k):



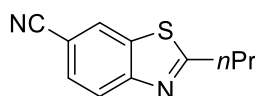
The title compound was prepared according to the General Procedure IX using starting material **235k**, 3.0 F. Purification using column chromatography (*n*-hexane/ethyl acetate, 9:1) afforded compound **241k** (0.123 g) in 93% yield as a red oil.

^1H NMR (400 MHz, CDCl_3): δ = 8.83–8.76 (m, 1H), 7.94 (d, J = 8.1 Hz, 1H), 7.86 (d, J = 7.7 Hz, 1H), 7.77 (d, J = 8.7 Hz, 1H), 7.69–7.64 (m, 1H), 7.60–7.53 (m, 1H), 3.28–3.19 (m, 2H), 1.98–1.88 (m, 2H), 1.59–1.48 (m, 2H), 1.01 (t, J = 7.4 Hz, 3H) ppm. ^{13}C NMR (126 MHz, CDCl_3): δ = 171.6, 149.5, 132.0, 131.6, 128.6, 128.1, 126.9, 125.9, 125.3, 124.0, 119.1, 34.3, 32.3, 22.5, 14.0 ppm. IR (neat): 3026, 2953, 2928, 2859, 1508, 1456, 1364, 1217, 903, 802, 743, 685, 527 cm^{-1} . HRMS (ASAP) $[\text{M}+\text{H}]^+$ calc. 242.1003, found 242.1004 $[\text{C}_{15}\text{H}_{16}\text{NS}]^+$.

6-Methoxy-2-phenylbenzo[*d*]thiazole (2411):

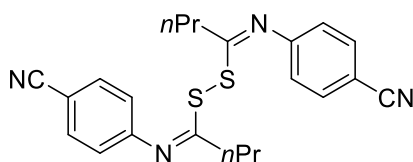
The title compound was prepared according to the General Procedure IX using starting material **235I**, 4.0 F. Purification using column chromatography (*n*-hexane/ethyl acetate, 9:1) afforded compound **2411** (0.109 g) in 82% yield as a colourless solid.

¹H NMR (400 MHz, CDCl₃): δ = 8.07–8.02 (m, 2H), 7.98–7.94 (m, 1H), 7.51–7.45 (m, 3H), 7.35 (d, *J* = 2.5 Hz, 1H), 7.09 (dd, *J* = 8.9, 2.6 Hz, 1H), 3.89 (s, 3H) ppm. The spectral data were consistent with those reported.^[24]

2-Propylbenzo[*d*]thiazole-6-carbonitrile (243):

The title compound was prepared according to the General Procedure IX using starting material **242** (50 min collection), 2.6 F. Purification using column chromatography (*n*-hexane/ethyl acetate, 9:1) afforded compound **7** in 58% yield as a colourless solid.

¹H NMR (500 MHz, CDCl₃): δ = 8.15 (dd, *J* = 1.6, 0.7 Hz, 1H), 7.99 (dd, *J* = 8.5, 0.7 Hz, 1H), 7.67 (dd, *J* = 8.5, 1.6 Hz, 1H), 3.14–3.06 (m, 2H), 1.96–1.84 (m, 2H), 1.04 (t, *J* = 7.4 Hz, 3H) ppm. ¹³C NMR (126 MHz, CDCl₃): δ = 176.9, 155.8, 135.8, 129.2, 126.4, 123.4, 118.9, 108.2, 36.5, 23.0, 13.8 ppm. The spectral data were consistent with those reported.^[22]

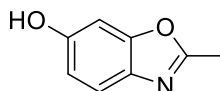
Side product:**(*Z*)-*N*-(4-Cyanophenyl)butyrimidic dithioperoxyanhydride (243b):**

Colourless oil. Yield = 13%. ¹H NMR (500 MHz, CDCl₃): δ = 7.58–7.52 (m, 1H), 6.83–6.73 (m, 1H), 2.70–2.44 (m, 1H), 1.67–1.56 (m, 1H), 0.96–0.86 (m, 1H) ppm. ¹³C NMR (126 MHz, CDCl₃): δ = 167.6, 153.2, 133.6, 120.3, 119.1, 107.9, 37.3, 20.6, 13.8 ppm.

IR (neat): 2963, 2872, 2224, 1638, 1595, 1510, 1375, 849, 552 cm^{-1} . HRMS (ESI) $[\text{M}+\text{H}]^+$ calc. 407.1359, found 407.1359 $[\text{C}_{22}\text{H}_{23}\text{N}_4\text{S}_2]^+$.

6.5. Experimental data for Chapter 5: Electrochemical synthesis of benzoxazoles in flow from resorcinol and nitriles

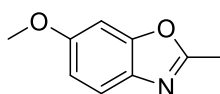
6-Hydroxy-2-methylbenzoxazole (277):



General Procedure X: Resorcinol (0.22 g, 2 mmol) was dissolved in acetonitrile (9.3 mL). Trifluoroacetic acid (0.77 mL, 10 mmol) was added to the solution, and it was introduced in the electrochemical reactor (0.205 mL inner volume; 200 mA; Pt anode / graphite cathode) using a syringe pump (0.16 mL/min). After reaching the steady state, the solution was collected for 56 min. Acetonitrile was evaporated under reduced pressure, and the crude was filtered through a silica plug and purified by column chromatography (hexane/ethyl acetate, 3:1), giving compound **277** as a colourless solid in 23% yield.

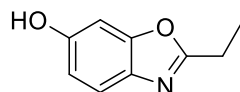
^1H NMR (400 MHz, CDCl_3): δ = 7.47 (d, J = 8.5 Hz, 1H), 6.98 (d, J = 2.3 Hz, 1H), 6.81 (dd, J = 8.5, 2.4 Hz, 1H), 5.42 (bs, 1H), 2.60 (s, 3H) ppm. Spectroscopy data in accordance to the literature.^[34] ^{13}C NMR (126 MHz, CD_3OD): δ = 164.4, 157.1, 153.1, 134.7, 119.6, 113.9, 98.1, 13.9 ppm. m.p. = 198 – 201°C (Lit. = 194 - 196 °C^[34]). IR (neat): 3150-2400 broad m, 1622, 1577, 1485, 1298, 1230, 1195, 1136, 1107, 748, 721, 601 cm^{-1} .

6-Methoxy-2-methylbenzoxazole (286):



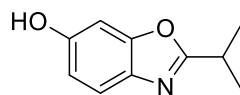
Synthesized according to the general procedure X. Compound **286** was obtained in 7 % yield (^1H NMR yield with ISTD).

^1H NMR (300 MHz, CDCl_3): δ = 7.52 (d, J = 8.8 Hz, 1H), 7.05 (d, J = 2.4 Hz, 1H), 6.94 (dd, J = 8.7, 2.4 Hz, 1H), 3.81 (s, 3H), 2.63 (s, 3H) ppm. Spectroscopy data in accordance to the literature.^[35]

6-Hydroxy-2-ethylbenzoxazole (292):

Synthesized according to the general procedure X. Compound **292** was obtained as a white solid in 34 % yield.

^1H NMR (300 MHz, CDCl_3): δ = 8.53 (s, 1H), 7.40 (d, J = 8.6 Hz, 1H), 7.02 (d, J = 2.2 Hz, 1H), 6.84 (dd, J = 8.6, 2.3 Hz, 1H), 2.92 (q, J = 7.7 Hz, 2H), 1.39 (t, J = 7.6 Hz, 3H) ppm. Spectroscopy data in accordance to the literature.^[36]

6-Hydroxy-2-isopropylbenzoxazole (293):

Synthesized according to the general procedure X. Compound **292** was obtained as a white solid in 34 % yield.

^1H NMR (300 MHz, CDCl_3): δ = 7.67 (bs, 1H), 7.39 (d, J = 8.6 Hz, 1H), 7.02 (d, J = 2.0 Hz, 1H), 6.82 (dd, J = 8.5, 2.1 Hz, 1H), 3.21 (sep, J = 7.0 Hz, 1H), 1.41 (d, J = 7.0 Hz, 6H) ppm. Spectroscopy data in accordance to the literature.^[36]

6.6. References

- [1] S. A. Shahzad, C. Venin, T. Wirth, *Eur. J. Org. Chem.* **2010**, 2010, 3465–3472.
- [2] Y. Yuan, S. A. Zaidi, D. L. Stevens, K. L. Scoggins, P. D. Mosier, G. E. Kellogg, W. L. Dewey, D. E. Selley, Y. Zhang, *Bioorganic Med. Chem.* **2015**, 23, 1701–1715.
- [3] T. Hoshino, Y. Miyahara, M. Hanaoka, K. Takahashi, I. Kaneko, *Chem. Eur. J.* **2015**, 21, 15769–15784.
- [4] P. A. Byrne, K. V. Rajendran, J. Muldoon, D. G. Gilheany, *Org. Biomol. Chem.* **2012**, 10, 3531–3537.
- [5] M. Shimogaki, M. Fujita, T. Sugimura, *Eur. J. Org. Chem.* **2013**, 7128–7138.
- [6] P. Mitra, B. Shome, S. Ranjan De, A. Sarkar, D. Mal, *Org. Biomol. Chem.* **2012**, 10, 2742–2752.
- [7] S. A. Shahzad, C. Vivant, T. Wirth, *Org. Lett.* **2010**, 12, 1364–1367.
- [8] D. Mal, G. Majumdar, P. Ranjan, *J. Chem. Soc., Perkin Trans. 1* **1994**, 1115–1116.
- [9] J. Chen, L. Zhou, C. K. Tan, Y. Y. Yeung, *J. Org. Chem.* **2012**, 77, 999–1009.
- [10] G. Yang, W. Zhang, *Org. Lett.* **2012**, 14, 268–271.
- [11] E. Napolitano, R. Fiaschi, A. Marsili, *Tetrahedron Lett.* **1983**, 24, 1319–1320.
- [12] D. Gauthier, R. H. Dodd, P. Dauban, *Tetrahedron* **2009**, 65, 8542–8555.
- [13] H. Lebel, M. Davi, S. Díez-González, S. P. Nolan, *J. Org. Chem.* **2007**, 72, 144–149.
- [14] X. Zhang, R. Guo, X. Zhao, *Org. Chem. Front.* **2015**, 2, 1334–1337.
- [15] G. D. Vo, J. F. Hartwig, *J. Am. Chem. Soc.* **2009**, 131, 11049–11061.
- [16] F. Xu, L. Zhu, S. Zhu, X. Yan, H. C. Xu, *Chem. Eur. J.* **2014**, 20, 12740–12744.
- [17] C. Kanazawa, M. Terada, *Chem. - An Asian J.* **2009**, 4, 1668–1672.
- [18] L. Li, M. Wang, X. Zhang, Y. Jiang, D. Ma, *Org. Lett.* **2009**, 11, 1309–12.
- [19] A. Gogoi, S. Guin, S. K. Rout, G. Majji, B. K. Patel, *RSC Adv.* **2014**, 4, 59902–59907.
- [20] P. G. M. Wuts, Y. W. Jung, *J. Org. Chem.* **1988**, 53, 1957–1965.
- [21] L. F. Liu, N. An, H. J. Pi, J. Ying, W. Du, W. P. Deng, *Synlett* **2011**, 979–981.
- [22] X.-Y. Qian, S.-Q. Li, J. Song, H.-C. Xu, *ACS Catal.* **2017**, 7, 2730–2734.
- [23] H. Keun Oh, S. Kyung Kim, H. Whang Lee, I. Lee, *J. Chem. Soc., Perkin Trans. 2* **2001**, 1753–1757.
- [24] K. Inamoto, C. Hasegawa, K. Hiroya, T. Doi, *Org. Lett.* **2008**, 10, 5147–5150.
- [25] S. P. Pathare, P. S. Chaudhari, K. G. Akamanchi, *Appl. Catal. A Gen.* **2012**, 425–

- 426, 125–129.
- [26] H. P. Kokatla, E. Yoo, D. B. Salunke, D. Sil, C. F. Ng, R. Balakrishna, S. S. Malladi, L. M. Fox, S. A. David, *Org. Biomol. Chem.* **2013**, *11*, 1179–1198.
- [27] G. Zhang, C. Liu, H. Yi, Q. Meng, C. Bian, H. Chen, J. X. Jian, L. Z. Wu, A. Lei, *J. Am. Chem. Soc.* **2015**, *137*, 9273–9280.
- [28] Y. Cheng, Q. Peng, W. Fan, P. Li, *J. Org. Chem.* **2014**, *79*, 5812–5819.
- [29] R. Shang, Z. Yang, Y. Wang, S. Zhang, L. Liu, *J. Am. Chem. Soc.* **2010**, 14391–14393.
- [30] S. Pal, G. Patra, S. Bhunia, *Synth. Commun.* **2009**, *39*, 1196–1203.
- [31] H. Wang, L. Wang, J. Shang, X. Li, H. Wang, J. Gui, A. Lei, *Chem. Commun.* **2012**, *48*, 76–78.
- [32] K. Inamoto, K. Nozawa, Y. Kondo, *Synlett* **2012**, *23*, 1678–1682.
- [33] S. K. Alla, P. Sadhu, T. Punniyamurthy, *J. Org. Chem.* **2014**, *79*, 7502–7511.
- [34] S. Fujita, Y. Inagaki, *Synthesis* **1982**, 68–69.
- [35] J. J. Lee, J. Kim, Y. M. Jun, B. M. Lee, B. H. Kim, *Tetrahedron* **2009**, *65*, 8821–8831.
- [36] B. M. Bhawal, S. P. Mayabhate, A. P. Likhite, A. R. A. S. Deshmukh, *Synth. Commun.* **1995**, *25*, 3315–3321.